

**VARICOSE/SENZ'ARIA, A MAGUK REQUIRED FOR JUNCTIONAL
ASSEMBLY DURING EPITHELIAL MORPHOGENESIS IN *DROSOPHILA***

**VARICOSE/SENZ'ARIA, A MAGUK REQUIRED FOR JUNCTIONAL
ASSEMBLY DURING EPITHELIAL MORPHOGENESIS IN *DROSOPHILA***

BY

KATHERINE ELLEN MOYER, B.Sc. (Hon.)

A Thesis

Submitted to the School of Graduate Studies

in Partial Fulfillment of the Requirements

for the Degree

Doctor of Philosophy

McMaster University

© Copyright by Katherine Ellen Moyer, October 2008

DOCTOR OF PHILOSOPHY (2008)
(Biology)

McMaster University
Hamilton, Ontario

TITLE: Varicose/Senz'aria, a MAGUK required for junctional assembly during epithelial morphogenesis in *Drosophila*

AUTHOR: Katherine Ellen Moyer, B.Sc. (Hon.) (University of Guelph)

SUPERVISOR: Professor J.R. Jacobs

NUMBER OF PAGES: xvi, 237

ABSTRACT

Scaffolding proteins belonging to the **M**embrane **A**ssociated **G**Uanylate **K**inase (MAGUK) superfamily function as adaptors linking cytoplasmic and cell surface proteins to the cytoskeleton to regulate cell-cell adhesion, cell-cell communication and signal transduction. We have identified a novel *Drosophila* MAGUK member, *Varicose* (*Vari*), the homologue of vertebrate scaffolding protein PALS2. Similar to its vertebrate counterpart, *Varicose* localizes to pleated Septate Junctions (pSJs) of all embryonic, ectodermally derived epithelia and peripheral glia. In *vari* mutants, essential SJ proteins NeurexinIV and FasciclinIII are mislocalized basally and the cells develop a leaky paracellular seal. Localization of SJ protein Discs Large is not affected, indicating *Vari* is not involved in cell polarization. In addition, *vari* mutants display irregular tracheal tube diameters and have reduced luminal protein accumulation suggesting involvement in tracheal morphogenesis. We found that *Vari* is distributed in the cytoplasm of optic lobe neuroepithelium and is required for proper ommatidial patterning. As well, *Vari* is expressed in a subset of neuroblasts and differentiated neurons of the nervous system. We also present a novel MAGUK function in wing hair alignment during adult morphogenesis. We conclude that *Varicose* is involved in scaffold assembly at the SJ and has a role in patterning adult epithelia and in nervous system development.

ACKNOWLEDGEMENTS

To my supervisor, Dr. Roger Jacobs, I thank you most sincerely for your guidance, support and enthusiasm throughout this project. During the times when I thought our path of research had ended, you found alternate routes to take, giving me the hope and motivation needed to continue. Working in your laboratory has strengthened my research, writing and problem solving ability, providing me with valuable skills that will last a lifetime.

To the members of my committee, Dr. Ana Campos and Dr. Juliet Daniel, your supervision throughout this work has been most appreciated. I thank you both for your kindness during troublesome times. You have both helped me to defend my work in the face of reviewers and for that I will be forever grateful.

The journey through graduate school cannot be completed alone. This challenge is conquered through the support and love from friends and family. To members of the Jacobs lab, both past and present, you made coming into the lab everyday an enjoyment. To Leena Patel, Kelly Teal, Dr. Mihaela Georgescu and Verónica Rodríguez Moncalvo, thank you for your guidance and advice both inside the lab and out, and for your friendship. The laughter and stories we have shared will be remembered forever. I cherish each and every one of you and hope I can return to you, the support and encouragement you have given me. To Nancy Tunis, I could not have accomplished this without you. Your friendship has been a foundation of support. To Diana Gavrilovic, thank you for being there at times when I just needed to get away. You were always there, ready for vacation!

Finally, I would like to thank my family for their support and for their understanding on holidays and birthdays, when I had to run into the lab...for just a minute. To my parents, I thank you for encouraging me to work hard and face my challenges head on. My confidence and determination have strengthened because I know I have you to lean on. To JP, through times of stress and times of joy you have been a rock for me to stand on, a shoulder to lean on and a pillar of support, encouraging me to go on. To have you with me throughout this journey means more than I can say.

TABLE OF CONTENTS

	PAGE
Title Page	i
Descriptive Note	ii
Abstract	iii
Acknowledgements	iv
Table of Contents	vi
List of Figures	ix
List of Tables	xi
List of Abbreviations	xii
1.0 <u>CHAPTER ONE:</u> Introduction	1
1.1 Cellularization of the Epithelial Sheet	5
1.2 Cell Polarization	5
1.3 Organization of an Epithelium	8
1.3.1 Apical-Basal Axis	8
1.3.2 Cellular Junctions	11
Zonula Adherens	12
Establishment and Maintenance of Polarized Epithelia	22
Septate Junctions	24
Septate Junctions: A Paracellular Barrier	26
Septate Junctions: Blood Barriers	33
Septate Junctions: Regulating Tube Size	36
1.4 Scaffolding Proteins at Cellular Junctions	39
1.4.1 PDZ Proteins	39
1.4.2 MAGUKs: Membrane Associated Guanylate Kinases	41
1.4.3 PALS: Proteins Associated with Lin-7	48
1.5 Objectives	51
2.0 <u>CHAPTER TWO:</u> Methods and Materials	53
2.1 Fly Maintenance	54
2.2 Genetic Stocks	54
2.3 Single Embryo DNA Extraction	55
2.4 Mutant Viability	57
2.5 Antibody Production	58
2.5a Vari	58
2.5b Vari ^{L27}	58

2.5b.1	Preparation of Vari ^{L27} His Fusion Construct	58
2.5b.2	Induction of Vari ^{L27} His Fusion Protein	61
2.5b.3	Purification of Vari ^{L27} His Fusion Protein	61
2.5b.4	Preparation of Vari ^{L27} Antiserum	63
2.5b.5	Affinity Purification of Vari ^{L27} Serum	64
2.6	Immunohistochemistry	65
2.7	Tissue Dissection	66
2.8	<i>UAS-vari</i> Transgenic Construct	67
2.8.1	RNA Preparation	67
2.8.2	Reverse Transcription and Cloning	68
2.8.3	Expression Analysis of <i>UAS-vari</i>	69
2.9	Scanning Electron Microscopy	71
2.10	Dye Permeability Assay	71
2.11	Electron Microscopy	72
2.12	Library Scale Yeast Two Hybrid System	73
2.12.1	Varicose-GAL4 DNA Binding Domain Fusion Construct	73
2.12.2	Verification of Yeast Strain AH109	73
2.12.3	Verifying Varicose-GAL4 DNA BD Fusion does not Activate Reporter Genes	74
2.12.4	Verifying Varicose-GAL4 DNA BD Fusion Expression by Western Blot	76
2.12.5	<i>Drosophila</i> Adult cDNA Library Screen	78
2.12.6	Identification of Putative Positive Clones	80
2.12.7	Elimination of Duplicate Clones	81
2.12.8	Rescue of Library Plasmids via Transformation of <i>E. coli</i>	82
2.12.9	Verification of Protein Interactions in Yeast	83
2.13	RNA Ligase Mediated Rapid Amplification of cDNA Ends	83
2.13.1	5'RLM-RACE	84
2.13.2	3'RLM-RACE	85
3.0	<u>CHAPTER THREE:</u> Varicose: A novel MAGUK required for the maturation and function of <i>Drosophila</i> septate junctions	87
3.1	ACKNOWLEDGEMENTS	88
3.2	INTRODUCTION	89
3.3	RESULTS	91
3.3.1	Varicose, a Homologue of Vertebrate PALS2/VAM-1	91
3.3.2	Varicose Localizes to Embryonic Epithelial Tissues	91
3.3.3	Varicose Localizes to the Septate Junction During Embryogenesis but not in Imaginal Discs	94
3.3.4	Novel MAGUK Function in the Nervous System	97

3.3.5	Loss-of-Function Varicose Mutants are Embryonic Lethal	101
3.3.6	Septate Junction Assembly Requires Varicose	105
3.3.7	Loss of <i>vari</i> Results in Dilated Tracheal Branches and Reduced Lumenal Staining	111
3.3.8	Varicose is Required for the Development of Adult Structures	112
3.4	DISCUSSION	123
3.4.1	Varicose Plays a Role in Septate Junction Assembly	123
3.4.2	A Novel Role for MAGUKs in the Nervous System	125
3.4.3	Varicose is Involved in Regulating Tube Size	126
3.4.4	MAGUKs are Involved in the Development of Adult Tissues	128
4.0	<u>CHAPTER FOUR:</u> Identification of Varicose Interacting Partners	130
4.1	ACKNOWLEDGEMENTS	131
4.2	INTRODUCTION	132
4.3	RESULTS	134
4.3.1	Varicose-GAL4 DNA-Binding Domain Fusion Protein	134
4.3.2	Varicose is Stably Expressed in Yeast Strain AH109	134
4.3.3	Putative Interacting Partners Identified in cDNA Library Screen	135
4.3.4	Verification of Varicose Interacting Proteins	143
4.3.5	Varicose is Mislocalized in <i>neuroglian</i> Mutants	152
4.4	DISCUSSION	156
4.4.1	Bällchen, A Connection Between Par-1 and Varicose	156
4.4.2	An Interaction Between the Kinase Domain of Awd and Varicose	158
4.4.3	Varicose Associates with a Chitinase-Like Growth Factor	159
4.4.4	Varicose, Egghead and the Visual System	161
4.4.5	Localization of Varicose Requires Neuroglian	162
	CONCLUSIONS	169
	OVERVIEW	172
	REFERENCES	185
	APPENDIX	204

LIST OF FIGURES

Figure 1.1 Nuclear cycles and cellularization during early embryogenesis in *Drosophila melanogaster*

Figure 1.2 Organization of polarized epithelia in *Drosophila* and vertebrates

Figure 1.3 Distribution and activity of polarity complexes in *Drosophila* and vertebrate epithelia

Figure 1.4 Structure and composition of *Drosophila* septate junctions

Figure 3.1 Varicose is a MAGUK family member

Figure 3.2 Varicose is detected at the septate junction in ectodermally-derived tissues

Figure 3.3 Varicose expression is not detected in imaginal discs

Figure 3.4 Varicose nervous system expression is novel for MAGUKs

Figure 3.5 Varicose alleles created by imprecise excision

Figure 3.6 Distribution of septate junction markers and the seal of the transepithelial barrier are compromised in *vari* mutants

Figure 3.7 Varicose is required for tracheal development

Figure 3.8 Examination of cellular ultrastructure in *vari*^{48EP} mutants

Figure 3.9 Ommatidial patterning and wing hair alignment are abnormal in *vari* mutants

Figure 3.10 Expression patterns observed are specific to Varicose

Figure 4.1 Outline of Vari – GAL4 DNA binding domain fusion construct

Figure 4.2 Varicose is expressed in yeast strain AH109

Figure 4.3 Library clones sorted by PCR and restriction digest

Figure 4.4 Rescue of library clone via transformation of *E. coli*

Figure 4.5 Clone 61 but not Clone 9 interacts with Varicose

Figure 4.6 Varicose is mislocalized in *nrg* mutants

Figure A Varicose is present as one predominant transcript in both adult and embryonic CS-P flies

Figure B.1 Map of primers used during imprecise excision mapping

Figure B.2 Varicose expression is not detected in excision alleles

Figure D *pUAS-Vari* transgenic construct

Figure E.1 Loss of Varicose through RNAi disrupts tracheal morphogenesis

Figure E.2 Varicose does not play a role during oogenesis

Figure E.3 Neuroepithelial cells are not affected by loss of Varicose

Figure F.1 Outline of the pET29b(+)-Vari^{L27} construct used to generate our Vari^{L27} antibody

Figure F.2 Comparison of Vari Antibodies, Vari and Vari^{L27}

Figure G PCR amplification of putative positive clones from the yeast two-hybrid adult library screen using Varicose as bait

LIST OF TABLES

Table 2.1 A list of all stocks used in this thesis

Table 2.2 Media requirements for growth of yeast strain AH109

Table 2.3 DNA plasmids required for the yeast two hybrid screen

Table 4.1 A list of the putative interacting clones and the screening steps completed

Table 4.2 Verification of clones interacting with Varicose

Table B Complementation test of *varicose* imprecise excision alleles

Table C Sequence of PCR primers used in the presented thesis

LIST OF ABBREVIATIONS

AD – Activation Domain
Ade – Adenine
AJ – Adherens Junction
aPKC – atypical Protein Kinase C
Arm - Armadillo
ATP α – Na⁺K⁺ATPase
Awd – Abnormal Wing Discs
BD – Binding Domain
Bäll – Bällchen
Baz – Bazooka
BSA – Bovine Serum Albumin
Btsz – Bitesize
CAM – Cell Adhesion Molecule
Cdc – Cell division cycle
CIP – Calf Intestinal Phosphatase
Cmg – Camguk
CNS – Central Nervous System
Cont – Contactin
Cora – Coracle
CS-P – CantonS – P
Crb – Crumbs

Da – Daughterless

DAB – 3,3 diaminobenzidine tetra hydrochloride

DEPC – Diethyl Pyrocarbonate

Dlg – Discs Large

DO - Dropout

DPatj – *Drosophila* PALS1 associated tight junction

DT – Dorsal Trunk

EDTA – Ethylenediamine-tetraacetic acid

Egh – Egghead

FasIII – FasciclinIII

Fz - Frizzled

GAL4 – Galactosidase transgene

GFP – Green Fluorescent Protein

GJ – Gap Junction

Gli – Gliotactin

GUK – Guanylate Kinase

His – Histidine

HRP – Horseradish Peroxidase

IDGF – Imaginal Discs Growth Factor

IOB – Interommatidial Bristles

IPTG – Isopropylthio-beta-D-galactoside

Kkv – krotzkopf verkehrt

L27 – protein-protein interaction domain originally identified in Lin-2 and Lin-7

Lac – Lachesis

LacZ – a reporter gene encoding β -galactosidase

LB – Luria Bertani

Leu – Leucine

Lgl – Lethal Giant Larvae

LT – Lateral Trunk

MAGUK – Membrane Associated Guanylate Kinase

Mega – Megatrachea

Mmy – Mummy

NB – Neuroblast

NE – Neuroepithelia

Nect2 – Nectin-like Molecule 2

NGS – Normal Goat Serum

NMJ – Neuromuscular Junction

nos:VP16 – Nanos promoter fused to potent transcriptional activator VP16

Nrg - Neuroglian

Nrv2 – Nervana 2

NrxIV – NeurexinIV

PAGE – Polyacrylamide Gel Electrophoresis

PALS – Protein Associated with Lin-7

Par – Partitioning Defective

PBS – Phosphate Buffered Saline

PBT – Phosphate Buffered Saline with Triton X-100

PDZ – protein-protein interaction domain named after founding proteins PSD-95/Dlg/ZO-1

PEG – Polyethylene Glycol

PNS – Peripheral Nervous System

PSD – Post-Synaptic Density

pSJ – pleated Septate Junction

Pyd – Polychaetoid

Pygo – Pygopus

QDO – Quadruple Dropout (lacking Adenine, Histidine, Leucine, and Tryptophan)

RACE – Rapid Amplification of cDNA Ends

RLM – RNA Ligase Mediated

RT – Reverse Transcription

sAJ – spot Adherens Junctions

SAP – Synapse Associated Protein

SAR – Sub-Apical Region

Scrib – Scribble

SDS – Sodium Dodecyl Sulfate

Sdt – Stardust

Serp – Serpentine

SH3 – Src Homology 3

Shg – Shotgun

Sinu – Sinuous

SJ – Septate Junction

sSJ – smooth Septate Junction

TAP – Tobacco Acid Pyrophosphatase

TDO – Triple Dropout (lacking Histidine, Leucine, and Tryptophan)

TJ – Tight Junction

Trp – Tryptophan

U1 – Unknown domain 1

UAS – Upstream Activation Sequence

Ura – Uracil

VAM-1 – Veli-Associated MAGUK 1

Vari – Varicose

Verm – Vermiform

Wg – Wingless

X- α -gal – 5-Bromo-4-chloro-3-indoyl α D-galactopyranoside

Y2H – Yeast Two-Hybrid

ZA – Zonula Adherens

ZO-1 – Zona Occludens 1

Introduction

CHAPTER ONE

At an early age, our parents taught us our ABC's, 123's and basic shapes. As we aged, we learned to associate these geometric figures with objects. We knew that a ball is round and a box is square. But did you ever wonder why objects are shaped the way that they are? Take a hexagon for example. Defined as a polygon with 6 sides, this shape has an even number of sides where the opposite sides are parallel. In the 17th century, Polish mathematician Jan Brożek discovered that hexagons can fit together without gaps creating an efficient use of space. It was possible to pack hexagons together using the least amount of material within a given volume and create a minimum surface area. In the 21st century, this work provided scientists and engineers with a useful and efficient building tool. For example, the James Webb Space Telescope has maximized optics from a mirror composed of 18 hexagonal segments. Moreover, nuts and bolt heads have a hexagonal shape allowing a wrench to be placed over three sets of parallel sides providing access in tight spaces. What is most intriguing is the existence of hexagonal structures in naturally occurring environments. An obvious example is the hexagonal composition of the beehive honeycomb. Built by honey bees, this mass of wax contains larvae and stores honey and pollen. Additionally, the hairs on the wing of a fly and cells of the vertebrate lens are hexagonally packed to guide airflow during flight and minimize light scattering, respectively (Wootton, 1992; Hilgenfeldt et al., 2008). It could be hypothesized that the hexagonal shape provides cells with an efficient way to generate the maximum function. It is not so surprising then, that a simple cell type such as an epithelial cell is hexagonally shaped. The ability of these cells to fit together without gaps creates a barrier that protects organisms from environmental harm. The

evolutionary conservation of this cell type from small freshwater organisms to humans is indicative of its functional significance. What is an epithelial cell? What does it do? It is within the following pages that we present our current understanding of epithelial cell formation and the functional importance of this cell type.

Over 1 billion years ago an evolutionary milestone occurred; the emergence of multicellular organisms. This evolutionary change required cells to adhere to one another and act as a unit, adjusting their cellular structure to accommodate animal growth and function (Purves et al., 1998). The attachment between the sides of these cells, or junctions, maintains their unity and together they form a multicellular sheet, or epithelium. From the simple classification of organisms such as sea anemones, jellyfish, and corals to complex higher organisms such as humans, the epithelium is of fundamental importance (Alberts et al., 2002). The health and life advancements of multicellular organisms depended and still depend upon maintaining a stable internal condition, or homeostasis, in response to ever changing environmental climates. The epithelial sheet contributes to the regulation of this homeostatic environment. Through cellular junctions, these cells function as a barrier regulating the movement of chemicals, food, nutrients and foreign substances into the organism's body. In arthropods, the epithelial sheet secretes a cuticle which gives rise to a protective exoskeleton (Payre, 2004). In lower organisms such as *Hydra*, the outer epithelial cells produce a poison capsule that is projected into and kills the animals upon which they feed (Tardent and Holstein, 1982). In humans, the epithelial cells of the skin respond to injury and function in wound healing (Gurtner et al., 2008). It is important to mention that the epithelial sheet, while central to regulating

internal exposure to external substances, is also required for maintaining internal homeostasis and organ morphogenesis. In humans, the internal intestinal wall is lined with epithelia that absorb nutrients. In flies, luminal structures such as the trachea require a proper epithelial seal or barrier to inflate with air. Additionally, epithelial cells require controlled growth and development as perturbations in these processes can lead to cancerous outcomes and ultimately death (Woods and Bryant, 1991). How do epithelial cells distinguish inside from outside environments? How do the cellular attachments regulate the movement of chemicals or absorption of nutrients? We will explore the answers to these questions using *Drosophila melanogaster* as a model system. By examining cell junction components and their interaction at sites of cell contact we will identify fundamental machinery necessary for maintaining internal homeostasis and overall barrier function.

The functional parallels of epithelia between vertebrate and invertebrate systems, in particular humans and flies, and the conservation of cellular components that establish epithelia suggest that epithelial arrangement is evolutionarily conserved. *Drosophila melanogaster*, the fruit fly, is a relatively simple and a well studied model organism. The life cycle, developmental events and genomic structure have been extensively characterized. Furthermore, the technical advances of molecular and genetic tools enable the manipulation of genes and proteins to elucidate their functional role during cellular processes (Venken and Bellen, 2005). The conservation of molecular and genetic pathways between humans and flies permits the exploration of human disease and possible therapeutic targets for the treatment of those diseases.

We will revisit the conservation of these pathways in the latter part of this work, but for now it is best to begin at...well, just that...the beginning. We will outline how the epithelial sheet is established and focus upon the maintenance and functional roles of this tissue within *Drosophila*.

1.1 Cellularization of the Epithelial Sheet

Drosophila embryonic development begins upon fertilization of the female egg. This event triggers zygotic nuclei to rapidly divide 13 times in the absence of cytokinesis creating a multinucleated mass of cytoplasm. Initiation of the 14th cleavage is concurrent with a dramatic remodeling of the plasma membrane such that over 5000 nuclei are packaged by invaginating membrane in a process termed cellularization (Foe and Alberts, 1983; Foe et al., 1993). This hybrid mechanism of cytokinesis and polarization gives rise to a single layer of epithelia ready to undergo rearrangement and eventual tissue morphogenesis (Fig. 1.1).

1.2 Cell Polarization

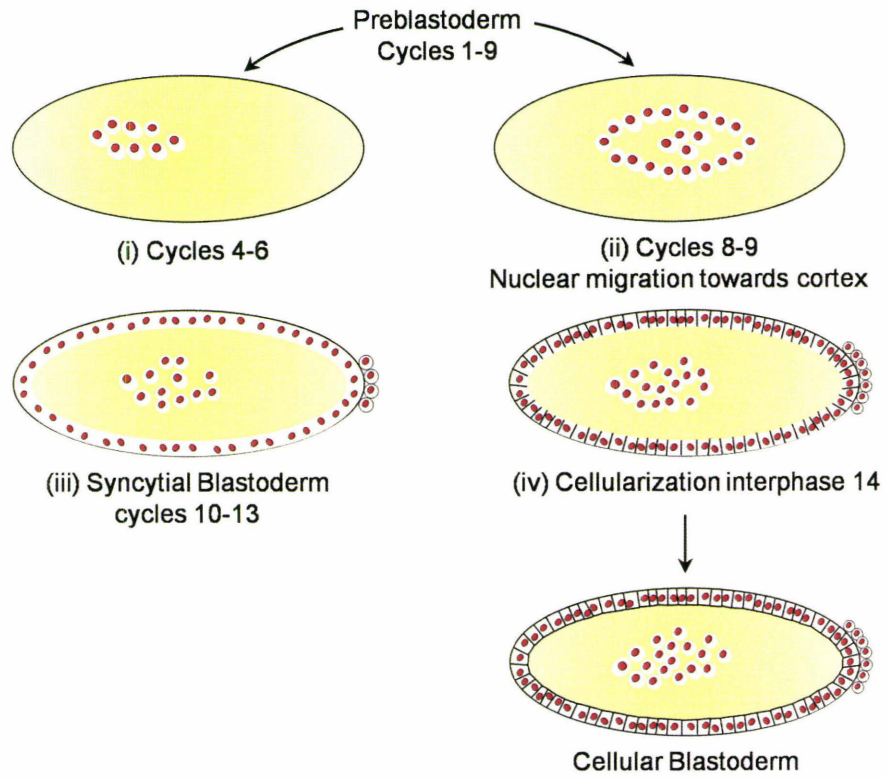
Cell polarization refers to the asymmetry of cell shape, cell function and distribution of cellular components such as proteins. Polarization is evident in cell types such as neurons and epithelia and is fundamental for proper function. For example, the directional regulation of epithelial vectorial functions such as secretion, absorption and protection depend upon polarized organization (Simons and Fuller, 1985). Polarization is also reflected in the asymmetric distribution of cellular components. In the early stages of studying polarization, the directed trafficking of membrane components was observed in epithelial cells infected with enveloped viruses. The polarized release of virions from

Figure 1.1: Nuclear cycles and cellularization during early embryogenesis in *Drosophila melanogaster*.

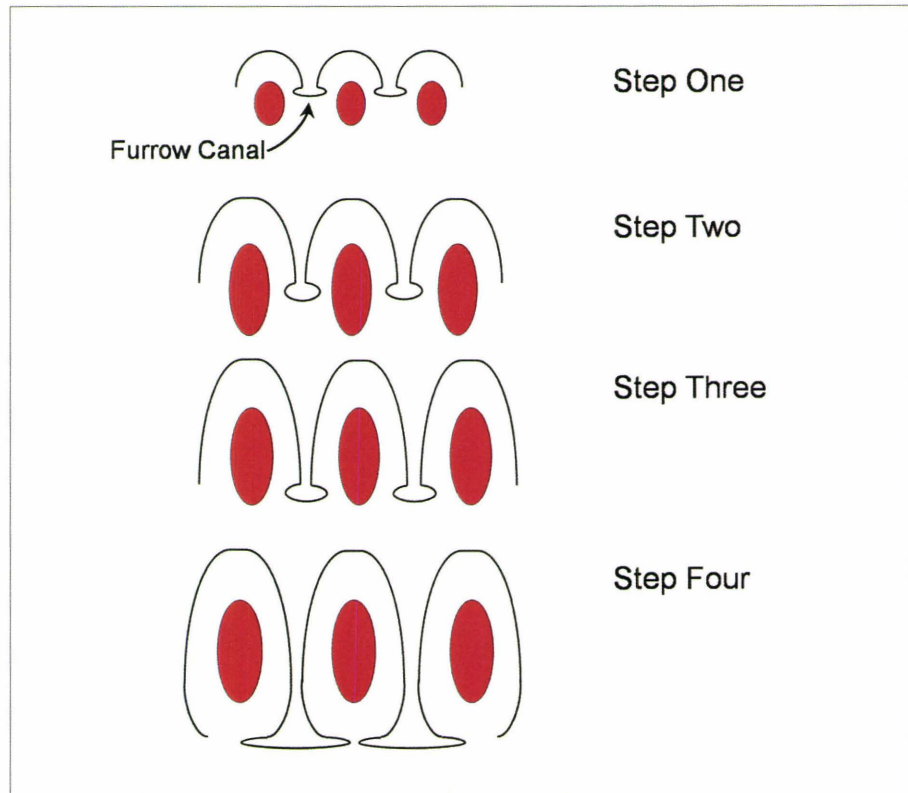
(A) Prior to cellularization, nuclei undergo 13 rounds of division. **(i-iii)** While the first seven divisions occur synchronously in the egg interior, over the next three divisions nuclei start to move toward to egg surface, leaving few nuclei in the interior. **(iv)** Following three more synchronous divisions, mitosis is halted at interphase of cycle 14.

(B) The onset of cellularization is characterized by dome-like plasma membrane invaginations that umbrella over each individual nuclei. A series of four phases complete the cellularization process. During step one, the leading edge of each membrane invagination forms a bulbous structure called the furrow canal and marks the invagination front. Step two coincides with nuclei elongation and a slow ingression of the membrane front until the furrow canals reach the basal end of the nuclei, marking the end of step three. Step four and completion of cellularization involves and increase in the speed of ingression and establishing individual epithelial cells with defined membrane regions (Adapted from BioEssays, Vol. 24, Mazumdar, A., Mazumdar, M., How one becomes many: blastoderm cellularization in *Drosophila melanogaster*, 2002, with permission pending from Wiley Periodicals, Inc., October 27th, 2008).

A



B



these cells was reflected in changes of the cell surface by the incorporation of glycoproteins to specific membrane domains. This phenomenon enabled scientists to explore the biogenesis and transport of proteins to the cell surface (Rodriguez-Boulant and Sabatini, 1978). In addition to membrane specific proteins, lipids and organelles including Golgi, nuclei and centrioles are also polarized (reviewed in Fristrom, 1988) (Fig. 1.2A). Moreover, establishing polarized membrane regions involves sorting of components, a role suspected to be attributed to the Golgi apparatus. While membrane proteins are transported through a common Golgi, they become segregated and are finally inserted into opposing membrane domains (Matter and Mellman, 1994).

1.3 Organization of an Epithelium

Extensive work has focused upon epithelial architecture and ultrastructure. Two fundamental structural features have emerged, an apical-basal axis of polarity and the assembly of intercellular junctions connecting the cells as a sheet (Fristrom, 1988).

1.3.1 Apical-Basal Axis

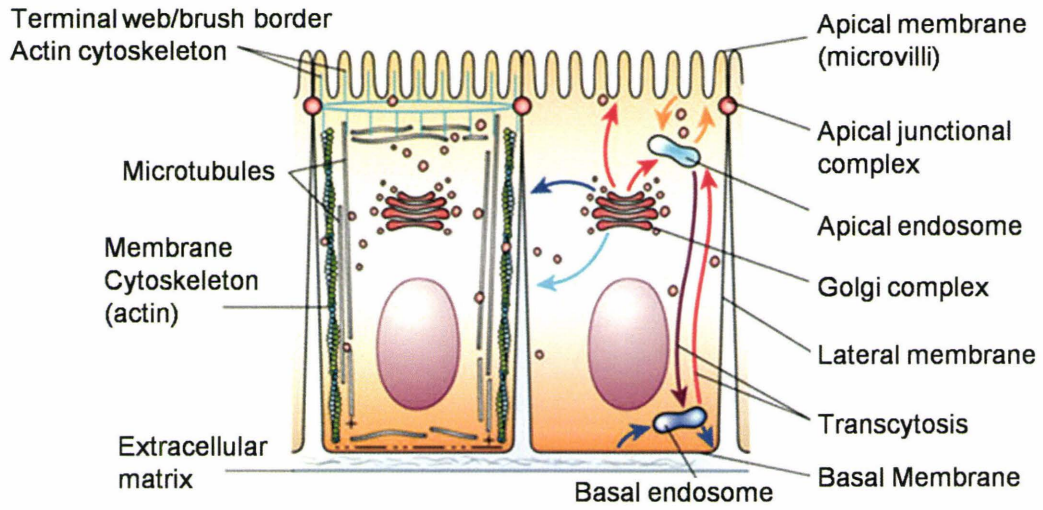
The typical monolayered epithelium is divided into functionally and biochemically distinct but physically continuous domains; apical, lateral and basal (Müller, 2000) (Fig. 1.2A). The apical plasma membrane is a specialized surface that is not usually in contact with other cells (Fristrom, 1988). This surface often faces the external environment, or the lumen of tubular structures such as the trachea, hindgut and salivary glands. Microvillous projections covering the apical surface increase the surface area of these cells and enhance the secretory and absorptive functions (Matter and Mellman, 1994). The basal surface secretes an extracellular basal lamina which, in

Figure 1.2: Organization of polarized epithelia in *Drosophila* and vertebrates.

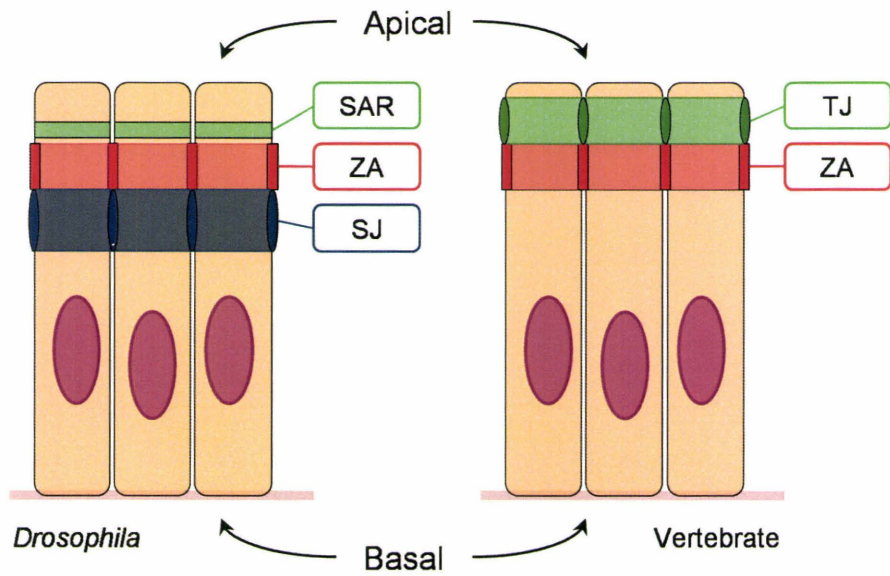
(A) Schematic representation of polarized epithelial cells. Left, organization of the actin and microtubule cytoskeletons; right, organization of vesicle transport pathways to different plasma membrane domains either directly from the Golgi complex, or indirectly via apical or basal endosomes through endocytic or transcytotic pathways (Reprinted from Nature, Vol.422, Nelson, W.J., Adaptation of core mechanisms to generate cell polarity, 766-774, 2003, with permission from Elsevier).

(B) Comparison of cell junctions in *Drosophila* and vertebrate epithelia. In both *Drosophila* and vertebrates, the apical and basal domains remain distinctly segregated by cellular junctions organized along the lateral domain. The adherens junctions, which form the mature Zonula Adherens (ZA) (red), predominantly regulate the adhesive properties between cells. Both Septate Junctions (SJ) (blue) in *Drosophila* and Tight Junctions (TJ) (green) in vertebrates, regulate trans-epithelial movement between cells. However, TJs lie apical to the ZA whereas in *Drosophila*, SJs lie basal to the ZA. In *Drosophila*, the Sub-Apical Region (SAR) (green) lies apical to the ZA, in a position analogous to the TJ. (Reprinted with minor modification from Current Opinion in Cell Biology, Vol.15, Gibson, M.C., Perrimon, N., Apicobasal polarization: epithelial form and function, 747-752, 2003, with permission from Elsevier).

A



B



vertebrates contacts neighbouring mesenchyme or in invertebrates faces the fluid body cavity.

The apical and basal domains remain distinctly segregated by cellular junctions organized along the lateral domain. These junctional organizations wrap circumferentially around each epithelial cell like a belt and form connections with neighbouring epithelial cells. The assembly of cellular junctions is pivotal for metazoans to maintain a homeostatic environment. Through these junctions, cells strongly adhere to one another, are able to communicate, synchronize function and modify the paracellular flow of molecules (Erez et al., 2005; Knust and Bossinger, 2002; Tsukita et al., 2001; Rodriguez Boulan and Nelson, 1989). Furthermore, junctional structures appear to mediate epithelial polarity and control cell proliferation (Woods and Bryant, 1993).

1.3.2 Cellular Junctions

Functional characterization of cellular junctions has revealed an important role for each junction type. Adherens Junctions (AJs), as the name suggests, predominantly regulates adhesive properties between cells. Actin microfilaments associated with these junctions primarily regulate membrane shape and movement (Ebnet, 2008; Niessen and Gottardi, 2008). Tight Junctions (TJs) and Septate Junctions (SJs) function as permeability barriers regulating the movement of molecules across epithelial sheets and prevent the mixing of molecules from apical and basal membrane domains (Banerjee et al., 2006; Tsukita et al., 2001). Gap Junctions (GJs) couple cells both chemically and electrically and may regulate choreographed morphogenetic events by controlling the transfer of ions and small molecules from one cell to another. In this manner, GJs can act

as communication devices for patterning (see Prochnow and Dermietzel, 2008; Phelan, 2005 for reviews). AJs are the structural landmark for polarization, providing signaling cues for multi-protein complex assembly whereas SJs are not required for initial polarization (Banerjee et al., 2006). This is evidenced by the absence of SJs during early stages of development and normal polarization in several SJ mutants such as *neurexinIV* and *coracle* (Tepass and Hartenstein, 1994; Baumgartner et al., 1996; Lamb et al., 1998). We will discuss these genes, the functional importance of the SJ and more in the sections to come.

The composition of junctional structures differs between vertebrate and invertebrate species. In vertebrates, several epithelial intercellular junctions exist, the two most widely studied being TJs and AJs (D'Souza-Schorey, 2005; Matter and Balda, 2003). Invertebrate species also possess AJs and although they lack TJs, invertebrates assemble a functionally analogous junction, the septate junction (Tepass and Hartenstein, 1994) (Fig. 1.2B). Despite a difference in lateral membrane location, TJs (apical to AJs) and SJs (basal to AJs) both form an intercellular barrier to regulate the trans-epithelial diffusion of solutes (Tepass et al., 2001). The establishment and maintenance of septate junctions is of great significance to this work, however before we begin our exploration of the septate junction, we will first provide a brief overview of adherens junction assembly and the junctional involvement in establishing polarization.

Zonula Adherens

The adherens junctions appear as a dense network of fibres adjacent to the cytoplasmic surface. This dense specialization is referred to as the undercoat which

connects to the microfilament network. The spot AJ (sAJ) is commonly observed in epithelia and is the first and only known junction to appear as early as cellularization (Tepass and Hartenstein, 1994). sAJs coalesce into a belt-like structure that surrounds the cell apex forming the mature zonula adherens (ZA) (Tepass, 1997). The establishment of ZA defines the apical and basolateral domains, and as a result, epithelial polarization (Tepass, 2002).

When visualized by electron microscopy, it is suggested that junctions are an assembly of multiprotein complexes including transmembrane and cytoskeletal proteins that perform adapter functions and organize signaling centres. Pioneering genetic screens performed by Nüsslein-Volhard, Wieschaus and Jürgens in the early 1980's involved mutagenesis induced lesions to identify genes involved in pattern formation. From these early genetic works, several zygotic mutants showed strong defects in the surface of the ectodermal epithelium. Of these mutants, six appeared to be involved in the maintenance of the surface epithelium including *shotgun* (*shg*), *crumbs* (*crb*), *stardust* (*sdt*), *bazooka* (*baz*), *lethal giant larvae* (*lgl*) and *discs large* (*dlg*). Research over the past several years has identified three major protein complexes that contribute to the overall establishment of polarization, the Crb complex, the Baz complex and the Lgl complex. We will take a moment to briefly introduce each complex followed by a short summary of how these complexes intertwine to establish a polarized epithelial cell (Fig. 1.3).

Shotgun. The adhesive function of AJs is in part regulated by cell adhesion molecules (CAMs). Cadherins are adhesion molecules that localize to sites of cell-cell contact. Cadherins are transmembrane proteins that are able to link adjacent cells

through homophilic interactions. Additionally, the cytoplasmic tail of cadherins binds to catenins which associate with F-actin forming a link between the cell surface and the cytoskeleton. This multiprotein association creates a filamentous connection through the entire epithelial sheet (Ebnet, 2008). In *Drosophila*, the cadherin protein complex is composed of epithelial cadherin, encoded by the *shotgun* gene (DE-cadherin), α -catenin and Armadillo (Arm), the *Drosophila* homologue of β -catenin (Pai et al., 1996), localizes to the ZA. In the absence of *shotgun*, epithelial cells undergoing morphogenetic rearrangement lose integrity and breakdown however epithelial polarity may still be established (Harris and Peifer, 2004). Although the role of cadherins may indirectly regulate polarization by maintaining mature ZA, the primary role of this complex appears to involve cell adhesion and signaling (Le Bivic, 2005). Cadherin-mediated adhesion and signalling are not the focus of this work, and therefore will not be discussed further.

The Crumbs Complex. For nearly two decades, the role of the transmembrane protein Crumbs (Crb) in epithelial polarity has been extensively studied. The onset of Crumbs expression is first detected at the apical membrane during gastrulation and regulates cell polarization through characterization of the apical membrane and regulating epithelial organization (Patthy, 1991; Tepass et al., 1990). Although not a component of ZA, Crb localizes to the lateral membrane apical of ZA, a region known as the Sub-Apical Region (SAR) (Fig. 1.3A) (Tepass, 1996). In the absence of *crb*, epithelial cells of ectodermal origin become severely disorganized and eventually undergo cell death (Tepass et al., 1990). Moreover, sAJs fail to accumulate at the apical cell surface and as a consequence, ZA fail to develop (Grawe et al., 1996). Overexpression of *crb* results in

Figure 1.3: Distribution and activity of polarity complexes in *Drosophila* and vertebrate epithelia.

(A) *Drosophila* epithelial cells exhibit two principal sets of junctions: adherens junctions, which form the ZA (red), and SJs (blue). Proteins of the Lgl group localize at or below the level of the SJ. The SAR (green) lies apical to the ZA in a position analogous to the vertebrate TJ. Proteins of the *Drosophila* Crb and Baz/Par3 complexes localize to the SAR, or marginal zone.

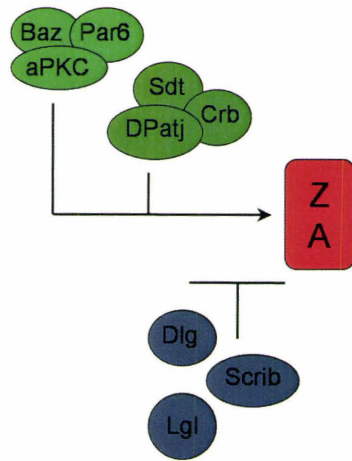
(B) (i) Model for the activity of polarity protein complexes in *Drosophila* epithelial polarization and ZA morphogenesis. (ii) Model for the activity of polarity protein complexes in mammalian epithelia. Here, mammalian Lgl binds and inactivates Par6/aPKC in the lateral plasma membrane domain, but dissociates upon phosphorylation by aPKC. Par6/aPKC is then free to bind Par3 and form an active complex that mediates TJ morphogenesis through interactions between Par6 and PALS1 of the Crb complex (Reprinted with minor modification from Current Opinion in Cell Biology, Vol.15, Gibson, M.C., Perrimon, N., Apicobasal polarization: epithelial form and function, 747-752, 2003, with permission from Elsevier).

A



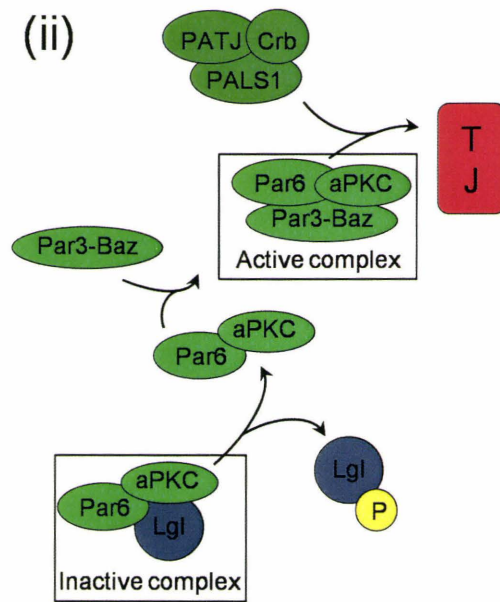
B

(i)



Insect (*Drosophila*)

(ii)



Vertebrate

the expansion of the apical surface and concurrent reduction in the basal surface (Wodarz et al., 1995). However, deletion of the cytoplasmic tail leads to a complete loss of function and loss of cell polarity, suggesting that the tail end of Crb is vital for proper function (Wodarz et al., 1995). The C-terminal portion of Crb contains two important binding motifs. The first motif may recognize protein 4.1 family member *Drosophila* Moesin (DMoesin) and through this association is able to recruit β_{Heavy} -Spectrin. It is speculated that Crumbs may play a role in the redistribution of actin, a process required during the maturation of sAJs to ZA (Médina et al., 2002). The second motif characteristically binds PDZ domains (named after founding proteins Post-Synaptic Density 95 (PSD95)/Discs-large (Dlg)/Zona Occludens 1 (ZO-1)) (Klebes and Knust, 2000) and has been shown to interact with the PDZ domain of Stardust, a Membrane Associated GUanylate Kinase (MAGUK) family member (Bachmann et al., 2001; Hong et al., 2001). Studies have shown that these two proteins function in the same genetic pathway to regulate epithelial organization (Tepass and Knust, 1993).

Stardust. Scaffolding proteins such as Stardust (Sdt) consist of multiple protein-protein interaction domains. Based on the composition of interaction domains encoded within the Stardust protein [two L27 domains (L27N and L27C, named after founding proteins Lin-2 and Lin-7), one PDZ, one src homology 3 (SH3) and one guanylate kinase (GUK) domain], Stardust is classified as a MAGUK family member (Bachmann et al., 2001; Hong et al., 2001). A detailed look at the MAGUK family will be provided in later sections. In *Drosophila*, the absence of *sdt* results in ectodermally-derived epithelial breakdown during organogenesis whereby cells cluster into multilayers and finally

undergo extensive cell death (Tepass and Knust, 1993). This phenotype is almost identical to that of *crb* and through genetic manipulation it has been shown that these two proteins function in the same genetic pathway. Sdt has been shown to co-localize with Crb at the SAR in ectodermal epithelia and both proteins are interdependent in their localization suggesting that together they form a complex regulating epithelial organization (Hong et al., 2001). Moreover, *Drosophila* Pals1 Associated TJ (DPatj) protein directly interacts with Sdt (Bulgakova et al., 2008; Wang et al., 2004) and together these three proteins form a complex and are mutually dependent for their localization and stability (Fig. 1.3A). The interaction between Crb, Sdt and DPatj is now well known as the Crumbs complex and is conserved among vertebrate systems (Roh et al., 2002). During embryogenesis, the absence of *sdt* also affects the accumulation of Bazooka (Baz), a PDZ protein found to regulate epithelial organization (Wieschaus et al., 1984). Mutations in both *sdt* and *baz* result in phenotypes more severe than single mutants suggesting these proteins function in separate pathways (Müller and Wieschaus, 1996). Additionally, Sdt is able to interact with *Drosophila melanogaster* Par6 (DmPar6), a member of the Bazooka complex (Bulgakova et al., 2008; Wang et al., 2004). Similarly, DmPar6 directly interacts with DPatj which is suggested to mediate its apical localization. These interactions serve as possible links connecting two multiprotein complexes to regulate polarity (Hutterer et al., 2004).

The Bazooka Complex. Partitioning-defective or Par genes were originally characterized in *C. elegans* and functionally elucidated for their role in asymmetric polarization during several stages of development. The association between Par-3, Par-6

and a seventh *par* gene, PKC3 (atypical protein kinase C), was necessary for their asymmetric localization to the apical cortex and proper cell division (reviewed in Nance, 2005). Homologues of the Par proteins have been identified in *Drosophila* and function in the polarization of epithelial cells and neurons (Ohno, 2001). Par-3, known as Bazooka in *Drosophila*, localizes to the apical surface in epithelia and to the apical cytocortex in neuroblasts. Mislocalization of *baz* disrupts axis polarity in both tissue types (Kuchinke et al., 1998) and severe malformations of the embryonic epidermis develop (Wieschaus et al., 1984). As seen in *crb* and *sdt* mutants, *baz* mutants fail to accumulate sAJs along the apex of the cell surface and do not develop ZA. Although similar to *crb* and *sdt* mutations, Baz has been shown genetically to function in a parallel yet different pathway (Müller and Wieschaus, 1996). Similar to the tripartite complex found in *C. elegans*, Baz has been shown to directly associate with *Drosophila* atypical protein kinase C (DaPKC) and DmPar6 at the SAR (Wodarz et al., 2000; Petronczki and Knoblich, 2001) (Fig. 1.3A). Proper localization and maintenance of epithelial architecture and polarity is mutually dependent within this protein complex (Petronczki and Knoblich, 2001). A fourth member of the Bazooka complex has recently been introduced (Hutterer et al., 2004). Binding of DmPar6 to Cell division cycle 42 (Cdc42) is a requirement for proper DmPar6 apical targeting. In the absence of this interaction neither Baz nor DPatj accumulate apically and thus polarity is not established. The apical localization of DmPar6 and the subsequent association of DaPKC results in the phosphorylation of Lethal giant larvae (Lgl) which is suggested to facilitate its targeting

to the lateral membrane. In turn, phosphorylated Lgl repels DmPar6 from the basolateral membrane and helps to maintain polarization (Hutterer et al., 2004).

The Lethal Giant Larvae Complex. The curious phenotype associated with the loss of the *lethal giant larvae (lgl)* gene has received much attention. In the 1930s, it was discovered that *lgl* was required for normal growth of brain and imaginal disc tissue and it soon became well known for its noninvasive neoplasms resulting from a loss of epithelial architecture and cell shape (Gateff, 1978). These cellular properties were similar to characteristics of human tumors and as such, Lgl was classified as a neoplastic tumor suppressor (Gateff, 1978). Besides acting as a tumor suppressor protein, Lgl was also found to play a role in the development of other tissues (Strand et al., 1994a; Wirtz-Peitz and Knoblich, 2006). Subcellularly localized in the cytoplasm and on the inner surface of the lateral membrane, Lgl is also able to interact with the cytoskeleton (Strand et al., 1994b). During embryogenesis, loss of *lgl* results in cell shape changes (Manfruelli et al., 1996) suspected to be brought about by the failure of *lgl* mutant cells to establish apical-basal polarity. In addition, the plasma membrane fails to segregate into distinct apical and basal domains and apical determinants leak into basolateral domain (Hutterer et al., 2004). Prior to the establishment of polarity, Lgl can be detected at the apical surface. It is proposed that through the interaction between Lgl and DmPar6, Lgl is brought into close proximity of DaPKC and undergoes phosphorylation in a DaPKC-dependent manner (Betschinger et al., 2003). The phosphorylated form of Lgl is prevented from associating with the Par complex in the apical domain and facilitates its targeting to the lateral membrane. In response to the lateral localization, DmPar6 is

repelled from the basolateral membrane and maintains apical-basal segregation (Hutterer et al., 2004) (Fig. 1.3B). The idea that Lgl helps to maintain apical-basal segregation is supported by the aberrant distribution of Crb in the absence of *lgl*. Moreover, AJs are fragmented and do not develop belt-like characteristics (Bilder et al., 2000). Dosage sensitive experiments indicate that *lgl* and *crb* function in separate genetic pathways (Tanentzapf and Tepass, 2003). It is well established that a tumor suppressor protein, Discs Large (Dlg) (Woods and Bryant, 1991), multi-PDZ protein Scribble (Scrib) (Bilder and Perrimon, 2000) and Lgl colocalize at the lateral membrane and together function in a common pathway to organize epithelial architecture (Bilder et al., 2000) (Fig. 1.3A).

Discs Large. Similar to the tumorous outgrowths seen in *lgl* mutants, imaginal discs in *discs large* (*dlg*) mutants produce a neoplastic overgrowth phenotype whereby larval brains and discs grow beyond normal size and fuse with each other (Stewart et al., 1972). In addition to cell proliferation, cellular events such as establishing cell polarity, cell adhesion and cell differentiation depend on Dlg. Depletion of *dlg* from imaginal epithelia results in columnar cells losing their cellular architecture by rounding up and detaching from neighbouring cells (Woods and Bryant, 1993a). Similar to Sdt, Dlg is a MAGUK family member that possesses three PDZ domains, an SH3 domain, a HOOK motif and an inactive GUK domain (Woods and Bryant, 1993b). The potential for Dlg to connect the cell surface to the cytoskeleton is directed by this domain composition. In *dlg* mutants, actin, tubulin, transmembrane proteins FasciclinIII (FasIII) and Neuroglian (Nrg), in addition to membrane cytoskeletal protein Coracle (Cora) (Fig. 1.4), are aberrantly organized resulting in abnormally developed epithelia (Woods and Bryant,

1996). Furthermore, SJ structure is lost (Bryant, 1997). Epithelial defects observed in *dlg* mutants during embryogenesis occur before SJs form suggesting that this abnormality might be the result of polarity disruption (Perrimon, 1988). Dlg localizes to a small apical belt at the lateral membrane corresponding to the SJ in imaginal epithelia (Woods and Bryant, 1991). Dlg and Lgl colocalize at the lateral membrane although the expression of Lgl is broader along the lateral surface. A more distinct overlap in expression pattern is seen between Dlg and Scrib (Bilder et al., 2000). Mutant *scrib* phenotypes are consistent with those of *dlg* and *lgl*. Epidermal cells are disrupted into multilayered strips which are frequently interrupted by rounded up cells that are separating from one another. The effects of *scrib* on epithelial polarity are observed prior to the emergence of SJs. Apical markers Crb and Arm show an unrestricted localization and AJs form at ectopic basolateral positions (Bilder and Perrimon, 2000). In addition, Dlg and Lgl fail to target to the lateral surface. Moreover, evidence suggests that Dlg is required for a stable association of Scrib at SJ, while Scrib is required for cortical association of Lgl, and all three genes are required to localize Dlg and Scrib to the SJ (Bilder et al., 2000).

Establishment and Maintenance of Polarized Epithelia

Over the last decade, studies have focused on how the Baz, Crb, and Lgl complexes work together to yield polarized epithelia (Fig. 1.3). Analysis of double mutants in all three complexes has revealed that the Baz complex is epistatic to both the Crb and Scrib complexes and that the Scrib complex is epistatic to the Crb complex. Since *baz*-mutants display a more severe phenotype than *crb*-mutants and *scrib*-mutants,

it is hypothesized that the Baz complex plays a role in the stability of adherens junctions whereas the Crb and Scrib complexes play a role in assembling the ZA from sAJs (Tanentzapf and Tepass, 2003). Live imaging data has revealed that Baz may initially be positioned apically by cytoskeletal cues and dynein-mediated transport. This positioning promotes the apicalization of DaPKC and DmPar6, triggering the formation of the apical domain (Harris and Peifer, 2005). Bitesize (Btsz), a synaptotagmin-like protein may be recruited apically by Baz. Together with DMOesin, Btsz could spatially define the SAR through actin organization (Pilot et al., 2006; Fehon, 2006). The localization of the Lgl complex denotes the basolateral domain and restricts the Baz and Crb complexes to the apical domain. Recruitment of the Crumbs complex to the apical domain counteracts the function of the Lgl complex (Bilder et al., 2003; Hurd et al., 2003; Tanentzapf and Tepass, 2003). Yurt, a protein 4.1 family member is also proposed to negatively regulate Crb activity in the SAR (Laprise et al., 2006). Crb and its complex partners are recruited by Baz to the SAR. It is proposed that DaPKC-dependent phosphorylation of Crb is necessary to maintain apical Baz (Sotillos et al., 2004). The antagonistic relationship between apical and basal complexes prevents apical proteins from expanding into the basolateral domain. Together these scaffolding protein complexes, in addition to novel proteins effecting polarity, provide the boundaries of the apical and basal membrane domains. It remains unclear however, what cues are required for localization of Lgl and its partners to the basolateral membrane and future site of the SJ.

Septate Junctions

The Septate Junction is common to all epithelia (Tepass and Hartenstein, 1994). From an evolutionary perspective, SJs have progressed from appearing as straight shelves across the lateral cell surface, to pleated shelves and finally developed into hexagonal arrangements that are seen in insects such as *Drosophila* (Banerjee et al., 2006; Gilula et al., 1970). Early electron microscopy work revealed an electron-dense material between neighbouring cells, within the interseptal space. Combined with freeze-fracture analysis, this dense material was resolved into rows of septa that are continuous with the junctional membrane, traverse the intercellular space and join adjacent cells (Gilula et al., 1970). Rows of septa are arranged perpendicular to the cell membrane separating the apical and basal intercellular space (Noirot-Timotheé et al., 1982; Fristrom, 1982). Ultrastructure and additional freeze-fracture analysis of cell junctions reveal that SJs maintain a constant distance between epithelial cells through ladder-like septa that spiral on the outside of the cell and fill the intermembrane space (Tepass and Hartenstein, 1994). These encircling septa extend the travel distance for molecules to traverse the paracellular path, thereby regulating the flow of material (Carlson et al., 2000). Functionally analogous to the SJ, the tight junction (TJ), also known as the occluding junction, functions as a permeability barrier regulating the diffusion of small molecules through the intercellular space and across the epithelium (Fristrom, 1988). Unlike the ladder organization of the SJ, TJs appear as a series of contact points, or ‘kissing sites’. Opposing membranes are held together by rows of proteinaceous adhesive elements that bridge the width of the junctional membrane. Freeze-fracture analysis reveals that TJs

consist of interconnecting mesh-works of fibrils forming a band-like structure around the cell and in turn an epithelial seal (Staehelin, 1973). In spite of a diverged morphology, globular and transmembrane proteins are suspected to form the bridge between cells filling the intermembrane space of TJs and SJs, respectively (Staehelin, 1973; Tepass et al., 2001). In *Drosophila*, SJs first appear during stage 14 of embryogenesis. Septa appear as individual strands or as small groups of septae. Septa are continuously added until the SJ covers one to two thirds of the lateral surface. The late emergence of the SJ suggests it is involved structurally and/or physiologically in epithelia rather than in epithelial morphogenesis (Tepass and Hartenstein, 1994).

Two types of SJs have been observed in *Drosophila*, smooth (sSJs) and pleated (pSJs). Smooth SJs, which lack ladder-like septae are found in tissues such as the midgut and malpighian tubules and cover the apical 20% of the lateral surface (Tepass and Hartenstein, 1994). The septa of the sSJ are arranged in closely packed parallel rows that are not clearly seen until larval stages (Graf et al., 1982; Tepass and Hartenstein, 1994). Septa of the sSJ may be positively charged allowing the permeability of a variety of substances that are uncharged or negatively charged and of relatively small diameter creating an electrical potential difference between the lumen and hemolymph (Skaer et al., 1987)

Pleated SJs are found in all ectodermally derived epithelial tissues such as trachea, salivary glands, hindgut and epidermis as well as in glial cells and are proposed to play a role in the formation of barriers, maintenance of cell polarity, mediating cell-cell interactions and regulating tube size (Tepass et al., 2001; Wu and Beitel, 2004).

Septate Junctions: A Paracellular Barrier

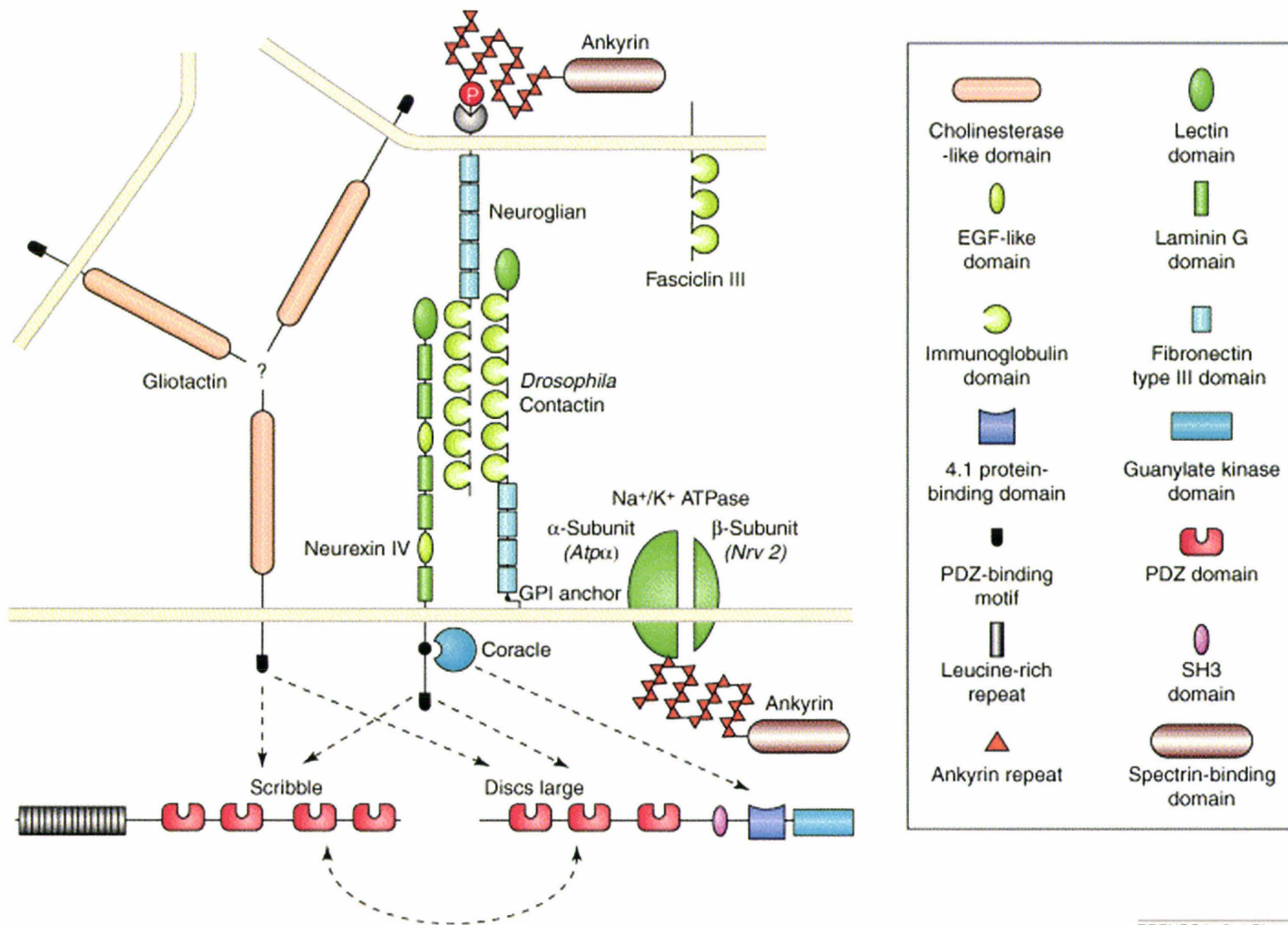
The SJ is thought to act as an impermeable obstacle within the paracellular route creating a ‘collective detour effect’ (Kukulies and Komnick, 1983). As such, SJs have been thought to enforce impenetrable permeability barriers (Noirot-Timothee and Noirot, 1980). Paracellular barrier function has been evidenced by the injection of tracer dyes showing an exclusion of dye at the SJ (Carlson et al., 2000).

Within the last decade key molecular elements of pSJs have been identified and shown to be involved in this barrier process. Through genetic analysis, various transmembrane and membrane-associated proteins have been identified as vital components in the formation of the SJ (Fig. 1.4). The two most widely studied SJ components are NeurexinIV (NrxIV) and Coracle (Cora) (Baumgartner et al., 1996; Fehon et al., 1994). Additional constituents including Neuroglian (Nrg), Na⁺/K⁺ ATPase (ATPα), Nervana 2 (Nrv2), Gliotactin (Gli), Contactin (Cont), Sinuous (Sinu), Megatrachea (Mega), Lachesin (Lac), Moody and Discs Large (Dlg) have also been implicated in regulating SJ formation and/or function (Genova and Fehon, 2003; Paul et al., 2003; Faivre-Sarrailh et al., 2004; Wu et al., 2004; Behr et al., 2003; Llimargas et al., 2004; Schwabe et al., 2005; Woods and Bryant, 1991).

NeurexinIV. Among the first identified SJ components was NeurexinIV (NrxIV), a member of the neurexin gene family and transmembrane protein encoding a large extracellular domain and transmembrane-spanning domain. The earliest detection of NrxIV occurs during embryogenesis one hour prior to the emergence of SJs. NrxIV is expressed in all ectodermally-derived epithelia and glial cells of the central nervous

Figure 1.4: Structure and composition of *Drosophila* septate junctions.

A simplified, schematic representation of septate junction components of *Drosophila* and their interactions. The diagram incorporates aspects of both epithelial and glial–axonal septate junctions. Several of the septate junction components might be required on both cellular sides of the junctional complex, e.g. Neuroglian and FasciclinIII might participate in homophilic, adhesive contacts. The molecular interactions between the *Drosophila* septate-junction proteins NeurexinIV, Coracle and the two Ig-domain cell-adhesion molecules (CAMs) Neuroglian (NRG) and Dcontactin have either been experimentally demonstrated or can be deduced from their vertebrate homologs. Postulated interactions between the cytoplasmic PDZ-binding domains of Gliotactin and NeurexinIV with the PDZ domains of the Scribble or the DLG protein, as well as interactions between the Coracle protein and the 4.1-protein-binding domain of DLG, are indicated by broken arrows. An extracellular ligand of Gliotactin, as well as heterophilic extracellular interactions involving the septate junction markers FasciclinIII and the Na⁺/K⁺ ATPase, are currently unknown. All of the depicted molecules, with the exception of FasciclinIII and the *Drosophila* ankyrins, have now been demonstrated to be essential for the function of septate junctions in the epithelia or the nervous system of *Drosophila* (Reprinted from TRENDS in Cell Biology, Vol.13, Hortsch, M., Margolis, B., Septate and paranodal junctions: kissing cousins, 557-561, 2003, with permission from Elsevier).



system (CNS) and peripheral nervous system (PNS). Localizing adjacent to apical marker Crumbs, NrXIV was found to accumulate at the SJ and suspected to play a role in SJ formation and function in both epithelia and glia. This hypothesis was evidenced by the absence of ladder-like septa in *nrxIV* mutants (Baumgartner et al., 1996). The cytoplasmic portion of NrXIV shares 68% similarity with the cytoplasmic domain of Glycophorin C, a transmembrane binding partner for the N-terminus of Protein 4.1 (Anderson and Lovrien, 1984). The *Drosophila* homologue of Protein 4.1, Coracle, colocalizes with NrXIV in epithelial pSJs (Fehon et al., 1994; Ward et al., 1998). In *nrxIV* mutants, Coracle expression at the lateral membrane becomes unrestricted. Localization of Dlg remains unaffected suggesting a possible interaction between NrXIV and Cora (Baumgartner et al., 1996).

Coracle. *Drosophila* Coracle, a member of the Protein 4.1 family, is expressed shortly before the appearance of pSJs in epithelia derived from the ectoderm but is absent from pSJs in the CNS and its derivatives (Fehon et al., 1994; Ward et al., 1998). Unlike vertebrate Protein 4.1, Cora does not encode a spectrin/actin binding site suggesting the interaction with the cytoskeleton is not conserved (Fehon et al., 1994). Cora interacts however, with transmembrane proteins forming a link to the cytoplasmic surface of the plasma membrane (Lamb et al., 1998). Cora binds to the C-terminus of NrXIV *in vitro* and this interaction is necessary in order to maintain their proper SJ localization (Ward et al., 1998). The interdependent localization of these proteins suggests that a third protein member is involved this complex. It is predicted that a PDZ containing protein may be an appropriate candidate. Initial thoughts of Dlg as a third party member were discarded

based on a failure to detect any interactions between these proteins and dissimilarity in mutant phenotypes (Ward et al., 1998). As it stands, the third party protein is still unknown. As in *nrxIV* mutants, *cora* mutants lack intermembrane septa. The effectiveness of the paracellular seal was tested by injecting 10 kDa rhodamine-conjugated dextran into late stage embryos. Unlike wildtype embryos, where dye was excluded from lumenal spaces for up to one hour, dye could be detected in the lumenal space of the salivary gland in the absence of *cora*. This result implied that the intermembrane septa may be responsible for ensuring an effective paracellular seal and Cora is required to maintain this barrier function (Lamb et al., 1998).

Neuroglian, Na⁺K⁺ATPase and Gliotactin. Cora and NrxIV have been found to interact with Nrg at the pSJ as well as form a complex independently with ATP α (Genova and Fehon, 2003). Nrg is an integral membrane glycoprotein that localizes to the lateral membrane of epithelial cells such as the trachea, salivary gland and hindgut, in addition to the surface of glial cells, regulating the adhesion between neurons and glial cells (Bieber et al., 1989; Dubreuil et al., 1997). The Na⁺K⁺ATPase is an α/β heteromultimer that creates an electrochemical gradient across the plasma membrane (Paul et al., 2003). Two subunits of Na⁺K⁺ATPase, ATP α and Nrv2 (a β subunit) were identified as essential SJ components. Mutations in *ATP α* , *nrv2* or *nrg* results in mislocalization of Cora and NrxIV and disrupts SJ structure by depleting the number of septa arrays. Although fewer septa are observed, regular spacing between plasma membranes is maintained (Genova and Fehon, 2003).

Gliotactin, a transmembrane protein, belongs to a class of adhesion molecules called electrotactins (Auld et al., 1995). Gli colocalizes with Nr x IV at pSJs but shortly after becomes restricted to a specialized region, the tricellular junction. Septa number is unaffected in *gli* mutants, however septa fail to compact and remain loosely arrayed, a phenotype distinct from *cora* and *nrxIV* (Schulte et al., 2003). Disruption of SJ structure in *nrg*, *ATP α* , *nrv2*, and *gli* mutants facilitates a paracellular seal leaky to tracer dyes (Genova and Fehon, 2003). However, FasciclinIII, an adhesion and transmembrane molecule associated with the SJ (Woods and Bryant, 1993a; Patel et al., 1984), is properly localized suggesting that part of the SJ remains intact (Genova and Fehon, 2003). This also suggests that protein mislocalization is a consequence of the independent relationship required for proper localization and not a result of junctional breakdown. It is important to note that in the above mutants, epithelial integrity, apico-basal polarization and the localization of SJ protein Dlg were unaffected suggesting Dlg plays a broader role in establishing epithelial morphology (Hortsch and Margolis, 2003; Lamb et al., 1998). Dlg localization is disturbed however in *gli* mutants suggesting a possible physical association between Gli and SJ strands. The restriction of Gli to the tricellular plug suggests that it plays a role in the maturation of pSJ, not the development septa strands as seen in *cora* and *nrxIV* (Schulte et al., 2003).

Contactin. Organization of SJ strands requires Contactin (Cont), a glycosphosphatidylinositol (GPI)-anchored membrane-associated cell adhesion molecule (Faivre-Sarrailh et al., 2004). Cont interdependently localizes with Nr x IV and Nrg at the SJ in all epithelia derived from the ectoderm and in glia of the PNS suggesting these three

proteins may form a complex. Nr_xIV has been shown to be responsible for targeting Cont to the plasma membrane and a heterophilic cis-interaction between these proteins has been proposed. It is unknown if this protein pair interacts with Nrg within the same cell or between cells. In the absence of *cont*, SJ strands are clustered into small groups suggesting that, like Gli and claudin-like protein Sinuous, Cont functions in organizing interseptal strands and facilitates their lateral position. A leaky paracellular barrier in *cont* mutants further supports the necessity of this protein within the SJ (Faivre-Sarrailh et al., 2004). It appears as though some SJ components are required for SJ strand formation while others are required for strand organization. It will be interesting to discover if distinct multiprotein complexes are needed to fulfill each step in strand synthesis and how these complexes intertwine to form the mature SJ.

Claudin Proteins: Megatrachea and Sinuous. The presence of claudin-like proteins in *Drosophila* further supports the functional analogy between TJs and SJs. Claudins are localized to the TJs in vertebrates and function in regulating paracellular diffusion (for a comprehensive review see Ebnet, 2008). Sinuous (Sinu) and Megatrachea (Mega) are two claudin-like proteins composed of four transmembrane domains and cytoplasmic N- and C-terminal domains. Both proteins contain PDZ domain-binding motifs capable of binding proteins such as MAGUKs. Each protein localizes to pSJs in ectodermally-derived epithelia and fails to overlap with apical markers such as Armadillo. This is reminiscent of Cora and Nr_xIV expression. Both Cora and Nr_xIV are mislocalized in *sinu* and *mega* mutants and in turn, both require the presence of Cora and Nr_xIV for localization (Wu et al., 2004; Behr et al., 2003).

Overexpression of *mega* can mislocalize Cora and NrXIV suggesting a direct or indirect connection between these three proteins (Behr et al., 2003). In addition, Mega is required for proper Sinu localization but it is unknown if Sinu is required for Mega localization (Wu et al., 2004). The claudin-like proteins differ however in their mutational effect on SJ strands. While septa number is reduced in *sinu* mutants reminiscent of *gli* mutants, a lack of ladder-like septa are seen in *mega* mutants reminiscent of *cora* and *nrXIV* mutants. Dye permeability assays however show that both *sinu* and *mega* are required for a proper paracellular seal. Although the expression of Sinu and Mega may be redundant, both proteins are essential for the barrier function of SJs (Wu et al., 2004; Behr et al., 2003).

Collectively, these studies have shown that the SJ is composed of multiprotein complexes that are mutually dependent. These complexes function together, either within or between epithelial cells, to assemble the protein scaffold regulating paracellular movement.

Septate Junctions: Blood Barriers

Insects such as *Drosophila* possess an open circulatory system whereby the surrounding hemolymph, with a high concentration of potassium ions and low concentration of sodium ions, permeates the entire animal. *Drosophila* have evolved complex barriers that block the passage of blood-borne elements from coming in contact with underlying neuronal surfaces of the peripheral (blood-nerve barrier) and central nervous systems (blood-brain barrier) as well as the visual system (blood-eye barrier) (Carlson et al., 2000).

Glia provide a plethora of functions during nervous system development such as cues for migrating neurons, axonal conduction and neurotransmitter uptake in addition to providing nutrients for neurons. Consequently, glia provide an environment fundamental for normal functioning of neurons (Stork et al., 2008). SJs have been detected between ensheathing glial membranes providing the first line of ionic permeability barrier (Banerjee et al., 2008). Neurons are surrounded by several glial types that form a diffusion barrier between neurons and hemolymph (Hortsch and Margolis, 2003; Parker and Auld, 2006; Carlson et al., 1997). A compromised barrier prevents action potential propagation resulting in paralysis of the animal (Schwabe et al., 2005).

Neurons of the larval CNS are covered by two layers of glial cells, an outer layer (perineurium) and an inner layer (subperineurium). The subperineurium develops by early stage 17 and contains maturing pSJs (Tepass and Hartenstein, 1994). Glia are differentially organized in the PNS and CNS. In the PNS, glia wrap around individual axons of nerves and contain autocellular SJs. In the CNS, neuropile glia are located below the subperineurial glial layer where they cover neuronal cell bodies, axon tracts and dendritic compartments (Stork et al., 2008). SJs exist between glial membranes and may also provide an adhesive function in addition to its barrier properties. This is evidenced by an increase in the spacing between outer and inner glial layers in *nrg* mutants (Banerjee et al., 2006b). Glial cells ensheathing peripheral nerves are derived from the ectoderm and are continuous with the subperineurium of the CNS (Tepass and Hartenstein, 1994).

The SJ is considered the structural basis of the blood barriers as proved by kinetic studies using injection of tracer dyes. These experimental studies have shown that barrier function is mostly attributed to the subperineurial cells (Stork et al., 2008). Similar to the composition of SJs in epithelia, SJ components of glia include *NrxIV*, *Cont* and *Nrg*. These proteins, in addition to *Gli* are found at the SJ in subperineurial cells whereas novel components such as *Moody* are expressed at the SJ in the perineurium of the CNS (Stork et al., 2008; Banerjee et al., 2006b). *Moody* is a G-coupled receptor that upon ligand binding catalyzes GDP to GTP. Loss of *moody* disrupts cortical actin which may cause a shortening of the SJ resulting in a greater permeability of the barrier (Schwabe et al., 2005). *nrxIV* and *moody* mutants both display a leaky barrier to 10 kDa dyes. For larger molecular weight dyes, penetration of the barrier was significantly reduced suggesting that are other mechanisms besides the subperineurium regulating barrier function. *cora*, *nrv2*, *nrg* and *cont* mutants produced similar phenotypes as *nrxIV* (Stork et al., 2008).

Loss of any gene essential in the formation of SJs may lead to embryonic paralysis (Banerjee et al., 2006). A severe reduction in coordinated muscle propagation waves was observed in *nrxIV* mutants and animals appear paralyzed. The reduced ability to propagate action potentials under high K^+ conditions is consistent with observations of *gliotactin* mutants (Baumgartner et al., 1996; Auld et al., 1995). Muscular contractions are also severely diminished during late embryogenesis in *cora*, *nrv2*, *Atpa*, and *nrg* mutants (Ward et al., 1998; Genova and Fehon, 2003). It is proposed then, that *NrxIV* and in turn the SJ, is required for proper axonal insulation and blood barrier formation (Baumgartner et al., 1996).

The *Drosophila* eye is a characteristic hexagonal array of nearly 800 ommatidia. Each ommatidium is composed of eight photoreceptor cells, four cone cells and three types of pigment cells all housed in a cylindrical cassette that maximizes the amount of light absorbing membranes. Protection of photoreceptors from the surrounding hemolymph is necessary for phototransduction processes. Banerjee and colleagues (2008) have identified apical and basal SJs between cone cells, pigment cells, and cone/pigment cells of the adult eye. Compromising junctional structure disrupts a blood-eye barrier. These studies showed that NrXIV localizes to the SJ in the larval and pupal discs and the mature adult eye. Loss of *nrXIV* results in the absence of septa strands between the cone cells and lack of exclusion of dextran dye into the adult eye.

The blood-brain barrier, blood-nerve barrier and blood-eye barrier share a common fundamental junction, the septate junction. The consistent inability to exclude permeable dyes in flies with mutant components of the SJ provides additional validation to the idea that SJs regulate permeability barriers.

Septate Junctions: Regulating Tube Size

Tubular organs require tightly regulated processes to guide tube formation and growth in order to sufficiently transport gases and liquids necessary to support an organism's needs (Beitel and Krasnow, 2000). The *Drosophila* tracheal system is a developmentally regulated and highly organized tubular network that allows easy dissection of pathways regulating tube formation. The system arises from ectodermal clusters of cells that invaginate to form 10 bilateral epithelial sacs which undergo extensive sprouting and extension and interconnect forming a ramifying network of

approx 10,000 oxygen transporting tubes (Ghabrial et al., 2003). The simplicity of this monolayered epithelial tube structure provides an eloquent system for studying tube size regulation (Beitel and Krasnow, 2000). During embryonic stages 11 to 13, a period where primary branching and growth are occurring, epithelial tube size remains constant. However, during stages 14 to 16, tube diameter almost triples (Cabernard et al., 2004; Myat, 2005). Tube length, in contrast to tube dilation, increases steadily from embryonic to larval stages implying that these developmental mechanisms are independent (Beitel and Krasnow, 2000).

A trend has emerged linking SJ components to the regulation of tracheal tube size. By the end of embryogenesis, trachea of *nrxIV*, *cora*, *nrv2*, *Atpa*, *nrg* and *gli* mutants fail to inflate with air (Baumgartner et al., 1996; Ward et al., 1998; Genova and Fehon, 2003). Genetic studies have shown that *sinu* may function in the same genetic pathway as *nrxIV* and *scrib* to regulate tube length, but not *nrv2*. *sinu* mutants also display an irregular folded pattern of taenidium implying defective luminal cuticle secretion leading to elongated and tortuous tracheal trunks (Wu et al., 2004). Studies have shown that the increase in tube size is a result of the expansion of the epithelial apical surface. While the apical surface enlarges, little change is occurring at the basal surface (Beitel, and Krasnow, 2000). The apical surface acts as an independent structure isolated from other parts of the cell and enlargement is necessary for the proper secretion of luminal proteins. Secretion, assembly and growth of a chitin cylindrical matrix within the tracheal lumen coordinates radial expansion, while modifications of chitin structure terminate tube elongation (Wang et al., 2006). Vermiform (Verm) and Serpentine (Serp) are

extracellular matrix proteins required to preserve the tight texture of the chitinous luminal cylindrical cable, regulating tube length (Luschnig et al., 2006; Beitel and Krasnow, 2000). Luminal accumulation of Verm, by a pathway that may be regulated by SJ components, is reduced in *Atpα* and *sinu* mutants possibly resulting in the observed elongated tracheal trunks (Wang et al., 2006). In addition, increasing tube diameter requires formation of luminal chitin-based matrix and in its absence, β_{Heavy} -spectrin is disrupted indicating that the chitin matrix signals cells to reorganize their cytoskeleton (Swanson and Beitel, 2006). SJ machinery may functionally regulate both tube length and tube diameter as mutations in these genes cause tracheal length or diameter defects (Wu and Beitel, 2004). However, the role of the SJ in paracellular barriers and tube size expansion may operate by separate mechanisms. This is evidenced by abnormal tracheal cell shape in *mega* and *lachesin (lac)* mutants with no prominent cytoskeletal organization defects (Behr et al., 2003; Llimargas et al., 2004). Lachesin is a cell surface immunoglobulin adhesion molecule and component of pSJs. It is also possible these two proteins point to a novel role for SJs in morphogenesis (Llimargas et al., 2004). Additionally, the presence or absence of septa is not responsible for tracheal tube size defects (Wu et al., 2004). It is hypothesized that SJ mediate the secretion of structural components, such as enzymes involved in chitin matrix modification (Kerman et al., 2006). Taken together, it appears that the size of epithelial tubes in the *Drosophila* tracheal system depend heavily upon the SJ and its constituents.

A common core connection between junctional components of epithelia is the accumulation and association of multiple proteins collectively functioning to assemble

structures necessary for completing a variety of cellular processes. It is still unknown however, how these membrane proteins are maintained within their surface domain. It is hypothesized that scaffolding proteins such as those belonging to the MAGUK superfamily are responsible for maintaining polarity and cell junction structure (Caruana, 2002).

1.4 Scaffolding Proteins at Cellular Junctions

Generating distinct membrane domains requires trafficking of scaffolding proteins (Tanentzapf et al., 2000). Scaffolding proteins ensure the localization of specific protein complexes to regions of the cell where signal transduction is required or subcellular domains need to be defined. Scaffolding proteins are typically characterized by modular structures that function in protein-protein interactions. These modular structures comprise domains such as the PDZ and SH3 domains, among others. A protein is often referred to as a scaffolding protein when more than one of these domains are present within a single polypeptide (Sierralta and Mendoza, 2004).

1.4.1 PDZ Proteins

The PDZ domain is a common motif encoded in a variety of signaling molecules found at the plasma membrane. Proteins such as Bazooka, Stardust and Discs Large contain PDZ domains leading to the speculation that these domains function in the clustering of signaling complexes at particular plasma membrane domains (Fanning and Anderson, 1996). The number of PDZ domain containing proteins has increased with multicellularity suggesting this domain has prevailed throughout evolution to accommodate the signaling demands of multicellular animals (Zimmermann, 2006).

PDZ domain. The domain was originally named DHR (Discs-large Homology Region) for a series of three GLGF repeats within the N-terminus of Post-Synaptic Density-95 protein (PSD-95) (Cho et al., 1992). The discovery of two additional proteins, *Drosophila* Dlg and vertebrate tight junction protein ZO-1, were found to encode the repeated GLGF series (Woods and Bryant, 1991; Willott et al., 1993). To reflect the origin of the domain, the more suitable name PDZ (PSD-95/Dlg/ZO-1) was chosen (Kennedy, 1995). PDZ domains are small, approximately 80-100 amino acids, and fold into a globular shape with the N and C- termini in close proximity (Sierralta and Mendoza, 2004). The binding site of these proteins resides in the carboxy tail of its target ligand with overlapping promiscuity between domain and target ligands (Sierralta and Mendoza, 2004; Jemth and Gianni, 2007). The domain has a globular structure consisting of six β strands (β A-F) and two α helices (α A-B). The C-terminus of the ligand docks in the cavity of the PDZ domain between strands β B and α B and a 'carboxylate-binding loop' connecting β A and β B strands. The first residue of the α B strand (α B1) confers some specificity for the last four amino acids (-3 to 0) in the C-terminus of the target ligand and the basis for domain classification (Zimmermann, 2006). The classification presented here is an oversimplified explanation that needs revisiting, which is beyond the scope of this work. The side chain at position -2 in the target ligand comes into direct contact with α B1 providing the basis of PDZ grouping. For example, the α B1 residue in class I PDZ domains is a Histidine that recognizes a Serine/Threonine at -2 position of the ligand. Class II PDZ domains are characterized by a hydrophobic residue at both the -2 and α B1 positions. An α B1 Tyrosine residue in

nNOS (neuronal nitric oxide synthase) PDZ domains prefers negatively charged amino acids in the ligand. It may also be possible for PDZ domains to dimerize as well as interact with internal sequences that are structurally mimicking a free C-terminus (Zhang and Wang, 2003; Hung and Sheng, 2002).

PDZ proteins located in the cytoplasm thus have the ability to connect the cell surface to the cytoskeleton and to cytosolic signaling proteins. Typically PDZ proteins contain multiple protein interacting domains, either as additional PDZ domains or domains like SH3 and LRR (leucine rich repeats) allowing these proteins to form large multiprotein complexes at the cell membrane (Bilder, 2001).

1.4.2 MAGUKs: Membrane Associated Guanylate Kinases

PDZ proteins are often found in multiprotein complexes with a family of proteins called **M**embrane **A**ssociated **G**Uanylate **K**inases, MAGUKs. MAGUKs are a class of scaffolding proteins that tether adhesion molecules at sites of cell-cell contact, such as septate and tight junctions (reviewed in Funke et al., 2005). Large protein complexes assembled on MAGUK scaffolds are implicated in maintaining cell junction structure, apical-basal polarity, cell adhesion, targeting of proteins to the membrane, and polarizing signaling cascades (reviewed in Funke et al., 2005). Disruption of these processes results in developmental defects such as multi-layered epithelia, cell overproliferation, and cell invasion (Caruana, 2002). Moreover, MAGUKs have been extensively studied for their role in targeting proteins in polarized cells such as neurons and epithelia. MAGUK members are not found in protozoans, fungi and plants but throughout animal phyla and encode a heterologous group with diverse biological functions. In vertebrates, 22

MAGUK proteins have been identified whereas only five have been discovered in *Drosophila* including Stardust, Discs-large, Polychaetoid (Pyd), Camguk (Cmg) and Skiff (te Velthuis et al., 2007). In the previous sections we have detailed the importance of MAGUK members Sdt and Dlg in the regulation of epithelial morphogenesis. Other members, with the exception of the uncharacterized gene *skiff*, regulate different biological functions such as cell fate specification and synaptic transmission during *Drosophila* development.

Polychaetoid. The PNS is composed of several types of sensory organs including mechanosensory (bristles) and touch receptors. The sensory organ develops from a sensory precursor cell which is singled out from the imaginal disc. Mutations in *Pyd/tamou* display extra mechanosensory organs possibly due to extra precursor cells (Chen et al., 1996; Takahisa et al., 1996). Localizing to sites of cell-cell contact, Pyd partly overlaps with DE-cadherin and also extends slightly basal (Takahisa et al., 1996; Wei and Ellis, 2001). Pyd associates with PDZ protein Canoe at the adherens junction, a requirement for correct dorsal closure (Takahashi et al. 1998). Additionally, the C-terminus of Pyd is involved in associating with the actin cytoskeleton (Katusbe et al., 1998). Cell fate and cell specification in the imaginal disc and trachea, respectively, require functional Pyd (Chen et al., 1996; Jung et al., 2006). Moreover, Pyd was recently shown to regulate patterning of the adult eye by modulating levels of AJ-proteins and adhesive properties (Seppa et al., 2008).

Camguk. This unique MAGUK encodes a calcium/calmodulin-dependent protein kinase catalytic domain (CaMK) and calmodulin binding domain. Also known as

Caki, Camguk (Cmg) plays a role in synaptic plasticity (Dimitratos et al., 1997). In the absence of *cmg*, adult flies have reduced walking speeds, impaired flight ability and altered courtship conditioning indicative of defects in associative learning (Martin and Ollo, 1996; Zordan et al., 2005; Lu et al., 2003). Cmg is expressed almost exclusively in the ventral nerve cord and brain. More specifically, Cmg has been detected at pre- and post-synaptic membranes of the neuromuscular junction (NMJ) (Zordan et al., 2005). Nurse cells and tissues such as malpighian tubules and the hindgut also express Cmg (Martin and Ollo, 1996; Lopes et al., 2001). Defective synaptic transmission of *cmg* mutants (Martin and Ollo, 1996) suggests a role in regulating neurotransmitter release at the synapse (Zordan et al., 2005).

We have presented here, evidence that MAGUKs are involved in a plethora of cellular events that require the propagation of cell signals. It is perhaps through the multiple protein – protein interaction domains encoded within MAGUKs that they are able to regulate the flow of communication between cells as well as between external and internal environments.

MAGUK proteins contain a core domain structure consisting of 1-3 PDZ domains, an SH3 domain and a GUK (Dimitratos et al., 1999). In addition, some MAGUK members encode an N-terminal L27 domain which functions in protein-protein interactions (Kaech et al., 1998). This multi-domain composition allows MAGUKs to function as the backbone onto which protein complexes can assemble (Caruana, 2002). These complexes then bring together functionally dissimilar proteins to link transmembrane proteins with the cytoskeleton (González-Mariscal et al., 2000). A

number of subfamilies make up the MAGUK protein family including Dlg, Lin-2, ZO-1 and palmitoylated membrane protein 55 (p55). The Dlg subfamily, consisting of Dlg, Synapse Associated Protein 97 (SAP 97), PSD-95, SAP 102 and p-Dlg, contains the core MAGUK protein made up of the PDZ/SH3/GUK domains, plus two more PDZ domains. The Lin-2/CASK/Camguk subfamily contains the MAGUK core along with an N-terminal calcium/calmodulin-dependent protein kinase and a repeated L27 domain (Caruana, 2002). The ZO-1 family members (Pyd/ZO-1, 2, 3) consist of 3 PDZ domains, SH3 and GUK domains along with C-terminal proline-rich regions. The p55 subfamily, is made up of the MAGUK core plus a repeated L27 domain, excluding p55. Members of this family include p55, Dlg2, Dlg3, Protein Associated with Lin-7 1 (PALS1) and PALS2/Veli-Associated MAGUK 1 (VAM-1). Several MAGUK proteins also contain a HOOK/4.1 binding domain, which binds actin-associated proteins, linking MAGUKs to the cytoskeleton (Caruana, 2002).

L27 Domain. The L27 domain is named from a pair of *C. elegans* proteins Lin-2 and Lin-7. Lin-2, homologous to *Drosophila* Camguk, and Lin-7, a small PDZ protein, homologous to *Drosophila* Lin-7 (DLin-7) (Dimitratos et al., 1997; Bachmann, 2004) share a small region of homology at their N-terminus (Doerks et al., 2000). Together with Lin-10, these three proteins function as a complex to target LET-23, a receptor tyrosine kinase to the basolateral domain of epithelia cells in turn regulating vulval induction (Simske et al., 1996). L27 domains are ~50 amino acids long and have a regular folding pattern despite low sequence identity. The sequence differences are suspected to prevent incorrect association and avoid self-association between L27

domains (Li et al., 2004). It was proposed that the L27 domains of Lin-2 and Lin-7 form a heterodimer interaction, suggesting this protein-protein interaction domain may facilitate the assembly of scaffolding complexes (Doerks et al., 2000; Harris et al., 2002; Li et al., 2004). Such a case is observed in the assembly of the Crumbs complex in which Stardust interacts with DPatj through heterodimerizing L27 domains (Wang et al., 2004). Individual L27 domains appear to have an unfolded structure which becomes rigid upon heteromultimerization (Harris et al., 2002). Each domain is composed of three helices which upon dimerization create a tetrameric or four-helical bundle (Li et al., 2004; Feng et al., 2004). The C-terminal helix is critical in choosing its binding partner and specificity in complex assembly (Feng et al., 2005). Furthermore, L27 domains can be categorized into A and B types where an A/B pair heterodimerizes whereby their specificity is optimized by negative design such that A/A and B/B pairs are repulsed. Two keystone positions in each L27 domain, (α B3 and α C2) determine domain type. Positively and negatively charged amino acids at α B3 determine A and B types, respectively. In addition a hydrophobic and polar amino acid at α C2 determines A or B type, respectively. This finding is supported by the interaction between Lin-7 and Lin-2 L27 domains, which are type A and B, respectively, and between Stardust and DPatj which have type B and type A L27 domains, respectively (Petrosky et al., 2005).

SH3, HOOK and GUK Domains. The Src homology 3 domain is ~50-70 amino acids in length and is noncatalytically active (González-Mariscal et al., 2000). It is suggested that this domain mediates protein-protein interactions targeting signaling components to the plasma membrane (González-Mariscal et al., 2000; Hough et al.,

2007). Canonical ligands for the SH3 domain are a minimum of seven residues in length and contain polyproline (PXXP) motifs, however the domain structure is unique in MAGUK proteins. Typically, SH3 domains are composed of five β strands (A-E) whereas in MAGUKs, the domain is composed of six β strands (A-F) (McGee et al., 2001). Analysis of functional domains in *dlg* revealed that the SH3 domain is not required for proper SJ localization but is required for SJ formation (Hough et al., 1997). A single amino acid substitution (Leu632 to Pro) causes a loss of SJs in imaginal discs and results an overgrowth phenotype (Woods et al., 1996; Hough et al., 1997). In MAGUKs the canonical SH3 hydrophobic binding surface required to bind polyproline motifs is replaced by a large hinged region that occludes the polyproline binding site (McGee et al., 2001). Once thought of as an independent domain, the hinged region or HOOK domain, is now known as a part of the SH3 domain. The HOOK domain, including characterized amino acid sequence KKKK (Tseng et al., 2001), is able to bind members of protein 4.1/ERM family of actin-associated proteins. The HOOK domain of *dlg* is required as a membrane targeting signal where *dlg*, in the absence of the HOOK, is not associated with the membrane but found in the nucleus (Hough et al., 1997). β strands E and F of the SH3 domain are separated by the GUK domain (McGee et al., 2001). The GUK domain shares sequence homology with *S. cerevisiae* guanylate kinase, an enzyme that catalyzes the conversion of GMP to GDP using ATP. GUK domains of MAGUKs typically lack the key residues necessary for ATP binding and are therefore assumed to be catalytically inactive (te Velthuis et al., 2007; González-Mariscal et al. 2000). *dlg* function was not affected in the absence of the GUK, however a *dlg* allele

truncating the protein just prior to the GUK domain appears to play a negative regulatory role in imaginal discs, possibly through binding of another protein (Hough et al., 1997). The SH3 and GUK domains of MAGUKs have surpassed their canonical function and interact with each other to form a super domain (te Velthuis et al., 2007). The two domains form an integrated structural unit that can potentially occur intermolecularly as well as intramolecularly, however, intramolecular interaction is favoured preventing intermolecular interactions (McGee and Brecht, 1999). The SH3/GUK interaction appears vital for MAGUK function (Reese et al., 2007). Genetic mutations of the SH3 and GUK domain of *dlg* complement each other by rescuing viability suggesting that the SH3/GUK interaction may oligomerize MAGUK scaffolds (Woods et al., 1996; Olsen and Brecht, 2003).

Splice Variations. The function of many scaffolding proteins includes regulating more than a single process. Oftentimes the same protein may be expressed in different tissues and participate in very different processes. The diversity of such proteins may sometimes be attributed to variations in protein composition due to alternative splicing. This mechanism promotes altered protein composition, localization and function (Funke et al., 2005). The best example can be provided by the well known and extensively studied protein, Dlg. The *dlg* gene has at least 23 exons that give rise to several different mRNAs and is expressed in both epithelia and neurons where it interacts with a variety of proteins such as ion channels, cell adhesion molecules and other scaffolding proteins. One Dlg splice variant includes the addition of an N-terminal region encoding a domain homologous to the N-terminus of vertebrate SAP97. This variant is expressed in neuropil

regions of the CNS and at NMJs of late embryos and larvae and is referred to as Dlg-S97 (Mendoza et al., 2003). SAP97 localizes to the presynaptic nerve termini, along bundles of unmyelinated axons, and along the basal lateral membrane in epithelial cells. Moreover, SAP97 is classified as a vertebrate homologue of *Drosophila* Dlg (Müller et al., 1995). During early stages of *Drosophila* embryogenesis, both Dlg and Dlg-S97 are expressed in the blastoderm however Dlg-S97 has a more diffuse expression. By stage 11, Dlg-S97 is found predominantly in the nervous system followed by the developing muscle at stage 15 and is no longer detected in epithelial cells (Mendoza et al., 2003). Dlg and DLin-7 segregate to different membrane domains in epithelia, however Dlg-S97 and DLin-7 form a complex at the post-synaptic membrane at NMJs. It has also been shown that localization of DLin-7 requires the N-terminal S97 domain of Dlg-S97 (Bachmann, 2004). Other MAGUK members, such as Sdt and Pyd also produce alternately spliced isoforms. Several isoforms of Sdt exist, two of which are expressed during embryogenesis and two are expressed during development of the adult eye (Berger et al., 2007). Two isoforms of Pyd, produced from alternate splicing of a 78 amino acid exon differentially control protein localization and the addition of this exon may on its own function in protein-protein interactions. The Pyd isoform containing the spliced exon tightly localizes to AJ whereas without the exon, Pyd is more loosely distributed along cell membrane (Wei and Ellis, 2001).

1.4.3 PALS: Proteins Associated with Lin-7

Two novel MAGUK proteins were identified in a far western overlay assay designed to isolate interacting partners of mouse Lin-7 (Kamberov et al., 2000). These

proteins, PALS1 and PALS2, which make up the PALS (**P**roteins **A**ssociated with **L**in-7) subfamily of MAGUK proteins anchor scaffolding complexes at junctional regions (Funke et al., 2005; Kamberov et al., 2000). Both proteins contain the core MAGUK structure but differ in the N-terminal region. PALS1 contains a repeated L27 domain as well as an unknown domain (U1) whereas PALS2 lacks the U1 domain (Roh et al., 2002). It is believed that these MAGUKs interact with the L27 domain located in the N-terminal region of Lin-7 (Roh et al., 2002; Kamberov et al., 2000).

Studies using vertebrate models have shown that PALS1 localizes to tight junctions where it functions as an adaptor protein linking together Crumbs and PATJ (Roh et al., 2002). It was further demonstrated that the U1 domain interacts with Par6, a member of the PAR3/Bazooka complex (Wang et al., 2004). More recently, PALS1 was shown to bind Ezrin, a band 4.1 protein, providing a direct link to the cytoskeleton (Cao et al., 2005). Similarly, in *Drosophila*, the PALS1 orthologue Stardust, functions as an adaptor protein joining Crumbs and DPatj (Bachmann et al., 2001; Hong et al., 2001). As was previously mentioned, Stardust interacts with DmPar6 through similar mechanisms (Wang et al., 2004). These findings provide a connection between two major scaffolding complexes involved in epithelial polarity as well as demonstrate an evolutionary conservation of function between vertebrates and invertebrates.

Studies using vertebrate models to elucidate the function of PALS2 remain limited. PALS2 has been shown to localize below tight junctions, at spot-like adhesion sites along the lateral plasma membrane, however protein function remains unclear (Roh et al., 2002). In 2003, Shingai and colleagues demonstrated that PALS2 interacts with

Nectin-like molecule 2 (Necl-2). Nectins, a subfamily of four, are cell-cell adhesion molecules involved in the organization of cell-cell junctions functioning with or independently of Cadherins. Nectins are Ca^{+} -independent proteins that link to the cytoskeleton through Afadin, which directly binds the C-terminal four amino acids of each Nectin (Ogita and Takai, 2008). Five Nectin-like molecules (Necl) were identified based on domain structures similar to those of nectin. Each Necl contains an extracellular region with three immunoglobulin-like loops, a transmembrane domain and a cytoplasmic region unable to bind Afadin (Takai et al., 2003). Necl-2 is a Ca^{+} -independent cell-cell adhesion molecule with both homophilic and heterophilic properties binding to Necl-1 and Nectin-3 (Shingai et al., 2003). In addition, Necl-2 binds MAGUK member PALS2. The interaction between Necl-2 and PALS2 has been localized to the extra-junctional regions of the basolateral surface of epithelial cells and is mediated through the C-terminal four amino acid residues of Necl-2 (EYFI) and the PDZ domain of PALS2 (Shingai et al., 2003). It is speculated that Necl-2 is recruited to Nectin-3 sites of cell-cell adhesion during the formation of AJs and is then relocated to the basolateral surface. Necl-2 also binds band 4.1 protein DAL-1, implicating PALS2 in membrane organization and scaffold assembly (Shingai et al., 2003).

Veli-Associated MAGUK 1 (VAM-1), a homolog of PALS2, has been identified in humans. VAM-1 was mapped to human chromosome 7p15-21, a region reported to show alterations in malignant peripheral nerve sheath tumors and in certain tumors such as Wilm's tumors. This altered chromosomal region suggests the presence of a tumor suppressor gene in kidney epithelial cells (Tseng *et al.*, 2001).

Identifying PALS1 and PALS2 as interactors of Lin-7 was an intriguing finding as characterizing the function of *Drosophila* Lin-7 has been one of the major areas of study in our laboratory. As the homology between PALS1 and *Drosophila* Stardust is well established, we focused our efforts toward investigating PALS2 in *Drosophila*. The evolutionary conservation of vertebrate and invertebrate junctional proteins prompted our search for the invertebrate homologue of PALS2 to elucidate its molecular and genetic function. Our search identified *Drosophila* CG9326, also reported recently as the gene interrupted in the *varicose* (*vari*) mutation (Beitel and Krasnow, 2000; Wu et al., 2007; Bachmann et al., 2008). Our previously reported *senz'aria* (*szar*) alleles (Moyer and Jacobs, 2006) are thus renamed as alleles of *vari*. We propose that Vari, based on our knowledge of characterized MAGUKs, tethers adhesion molecules in-turn organizing cell junctions and specializing regions of the epithelial cell surface.

1.5 Objectives

Our experimental approach was designed to address three major questions. Where is Varicose expressed throughout the *Drosophila* life cycle? What happens when Varicose expression is depleted? What proteins interact with Varicose, either directly or indirectly? To answer our first question, we focused on the expression pattern of Varicose in a variety of embryonic tissues in addition to larval, pupal and adult tissues. We were able to identify the specific membrane domain and cell junction to which Varicose was targeted. P-element mutagenesis was performed to generate mutant alleles of Varicose and elucidate the answer to our second question. Characterization of these

mutant alleles was carried out to determine the breakpoints associated with each allele and to examine the domains required for proper Varicose function. We then investigated the phenotypic effects associated with each allele. To determine if these phenotypic effects were attributed solely to the absence of Varicose we engineered transgenic *varicose* genes to rescue the observed phenotypic effects. Employing yeast two-hybrid and genetic screening approaches we have begun to explore possible Varicose interaction partners. We discuss the results of these experiments in regards to epithelial morphogenesis and conclude with how this work has provided novel insights into the conservation of invertebrate and vertebrate scaffolding complexes.

Methods and Materials

CHAPTER TWO

2.1 Fly Maintenance

All fly stocks were maintained at room temperature, approximately 21-23°C. Flies were housed in large fly vials (Fisher, AS519) plugged with rayon rope (Fisher, 12 640 41). Weaker stocks and/or small crosses (2-10 flies) were raised in 16 x 100 mm glass tubes (Fisher, 14-961-29). All flies were fed a basic yeast/sugar agar medium made as follows: a 1.8% agar solution was supplemented with final concentrations of 10% sucrose, 0.8% sodium potassium tartrate, 0.1% di-potassium hydrogen orthophosphate (dibasic) and 0.05% of each sodium chloride, calcium chloride, magnesium chloride and ferric sulfate. In a separate flask, a solution of 5% dry yeast in deionized and distilled water (ddH₂O) was mixed. Food and yeast solutions were autoclaved, combined, cooled to 54°C and treated with 7% methyl 4-hydroxybenzoate (tegosept – 10% stock solution in ethanol) and 0.5% acid mix solution [42% propionic and 4.2% phosphoric acid in ddH₂O]. Flies were transferred to fresh food vials every 14 days. Adult flies were cleared from vials one week after transfer.

2.2 Genetic Stocks

The following table is a list of all fly stocks used in this thesis. All imprecise excision stocks were outcrossed to ensure clean backgrounds. *vari*^{48EP}, *vari*^{B4}, *vari*^{K4}, *vari*^{L4} and *vari*^{B5} were generated by imprecise excision of GE13049 (Appendix B). *Df(2L)Exel*⁷⁰⁷⁹ deficiency deletes genomic region 38E6-38F3 which includes 19 genes in addition to *vari*; Caudal (CG1759), CG9324, CG9328, CG9329, CG14405, CG9331, CG31673, CG31674, CG9333, CG9334, CG31676, CG14402, CG9335, CG14400, CG9336, CG9337, CG9338, CG31675, and CG14401.

Table 2.1: A list of all stocks used in this thesis

Stock	Stock Number	Source
Canton-S P (CS-P)		Jacobs lab central stocks
<i>P-element insertion GE13049</i>	13049	GenExel, Inc.
<i>w-; vari^{48EP}/CyO</i>		This thesis
<i>w-; vari^{B4}/CyO</i>		This thesis
<i>w-; vari^{K4}/CyO</i>		This thesis
<i>w-; vari^{L4}/CyO</i>		This thesis
<i>w-; vari^{B5}/CyO</i>		This thesis
<i>w-; vari^{-03953b}/CyO</i>	11359	Bloomington <i>Drosophila</i> Stock Centre
<i>P{UAS-vari^{RNAi}}</i>	24156	Vienna <i>Drosophila</i> RNAi Centre
<i>w-; Df(2L)Exel⁷⁰⁷⁹/CyO</i>	7852	Bloomington <i>Drosophila</i> Stock Centre
<i>w-; wee/CyO, {Actin GFP}</i>		Shelagh Campbell
<i>w-; Sco/CyO, {Engrailed LacZ}</i>		Corey Goodman Lab
<i>Nrg¹⁴/FM7c</i>	5708	Bloomington <i>Drosophila</i> Stock Centre
<i>Nrg¹⁷/FM7c</i>	5595	Bloomington <i>Drosophila</i> Stock Centre
<i>y¹; ry⁵⁰⁶ P{SUPor-P}KG04161/TM3, Sb¹, Ser¹</i>	14591	Bloomington <i>Drosophila</i> Stock Centre
<i>ru¹h¹Nrx-IV⁴³⁰⁴st¹ry⁵⁰⁶e¹/TM6B, Tb¹</i>	4380	Bloomington <i>Drosophila</i> Stock Centre
<i>y¹w[*]; P{lacW}awd^{2A4}/TM3, Sb¹</i>	12167	Bloomington <i>Drosophila</i> Stock Centre
<i>Dlg^{XI-2}/Basc</i>		Vivian Budnik
<i>w[*]; P{neoFRT}82Bpygo^{S123}/TM6B, P{Ubi-GFP.S65T}PAD2, Tb¹</i>	7209	Bloomington <i>Drosophila</i> Stock Centre
<i>w[*]; P{neoFRT}82Bpygo^{S28}/TM3, Sb¹Ser¹</i>	7208	Bloomington <i>Drosophila</i> Stock Centre
<i>Bällchen⁴³/TM3</i>		Maria Leptin
<i>Bällchen⁵³/TM3</i>		Maria Leptin
<i>y¹w^{67c23}; P{lacW}cora^{k08713}/CyO</i>	10801	Bloomington <i>Drosophila</i> Stock Centre
<i>y[1]w[*]; CyO, H{w[+mC]=PDelta2-3}HoP2.1/Bc[1]</i>	2078	Bloomington <i>Drosophila</i> Stock Centre
<i>w[*]; P{w[+mC]=GAL4-Hsp70.PB}89-2-1</i>	1799	Bloomington <i>Drosophila</i> Stock Centre
<i>P{Single minded GAL4}</i>		John Nambu
<i>w[*]; P{w[+mC]=GAL4-btl.S}2, P{w[+mC]=UASp-Act5C.T;GFP}2</i>	8807	Bloomington <i>Drosophila</i> Stock Centre
<i>w[1118]; P{da-GAL4.w[-]}3</i>	8641	Bloomington <i>Drosophila</i> Stock Centre
<i>P{GAL4::VP16-nos.UTR}MVD1</i>	4937	Bloomington <i>Drosophila</i> Stock Centre
<i>P{GawB}C855a</i>	6990	Bloomington <i>Drosophila</i> Stock Centre
<i>w[*]; L[2]Pin[1]/CyO, P{w[+mC]=GAL4-Kr.C}DC3, P{w[+mC]=UAS-GFP.S65T}DC7</i>	5194	Bloomington <i>Drosophila</i> Stock Centre
<i>w-; Sco/CyO</i>		Jacobs Lab Central Stocks
<i>w-; D/TM3, Sb¹</i>		Jacobs Lab Central Stocks
<i>y¹w[*]; P{UAS-mCD8::GFP.L}LL5</i>	5137	Bloomington <i>Drosophila</i> Stock Centre

2.3 Single Embryo DNA Extraction

These experiments were used to isolate DNA from homozygous embryos for imprecise excision mapping. Stocks were maintained over a green fluorescent protein

(GFP) balancer, and homozygous embryos were selected by the absence of GFP. Each embryo was placed in a single 0.2 mL microfuge tube (DiaMed, AD0210-FCN) and 50 μ L of squishing buffer [10 mM Tris-HCl pH 8.2, 2 mM Ethylenediamine-tetraacetic acid (EDTA), 0.2% Triton X-100, 100 μ g/mL Proteinase K, fresh] was added. Each embryo was homogenized several times, vortexed and incubated at 37°C for 30 minutes (vortexing every 10 minutes). Following incubation, the embryo extract was heated to 95°C for 5 minutes and cooled on ice for 2 minutes. The extract was centrifuged for 5 minutes at 4°C at 14,000 rpm. The supernatant was transferred to a fresh microfuge tube and stored at 4°C for up to one week.

3 μ L of DNA extraction was used per polymerase chain reaction (PCR). The reagent mix was prepared for 50 μ L reactions and kept on ice until placed in the thermocycler (Biometra, T Personal-48). Each reaction included a final concentration of 2.5 μ M forward and reverse primers, 1X PCR buffer (supplied with taq DNA polymerase), 0.3 mM MgCl₂, 5 mM dNTP mix (Invitrogen, 18427-013) and 0.5 μ L (2.5 U) of taq DNA polymerase (Invitrogen, 18038-042). Sterile ddH₂O was used to complete the 50 μ L volume. PCR reactions were completed using hot-start conditions; the thermocycler was preheated to 94°C before adding the reactions. 30 PCR cycles were carried out as follows, denaturing 94°C for 30 seconds, annealing 60°C for 30 seconds, extension 72°C for 1 minute 30 seconds. PCR products were stored at 4°C until examination by electrophoresis.

PCR products were analyzed on a 0.8% agarose gel. Products required for sequencing were purified using phenol:chloroform. Products were excised from the

agarose gel using a scalpel blade (MAGNA, No. 11) and placed in a 1.5 mL microfuge tube (DiaMed, DPE155-N) at -20°C overnight. The tubes were centrifuged at 14,000 rpm for 30 minutes at 4°C. The supernatant was transferred to a fresh 1.5 mL tube and an equal volume of phenol:chloroform, 1:1, was added. Each tube was vortexed briefly and centrifuged for 10 minutes at 10,000 rpm at 4°C. The upper layer was transferred to a fresh 1.5 mL tube and the DNA was ethanol precipitated using 1/10 volume of 3 M sodium acetate, pH 5.2 and 2.5 volumes of cold 100% ethanol. The tubes were mixed by inversion and placed at -80°C for 15 minutes. DNA was pelleted by centrifugation for 30 minutes at 14,000 rpm at 4°C and washed with 100 µL of 70% ethanol in sterile ddH₂O. The pellets were dried at room temperature for 10 minutes and resuspended in 5 µL of sterile ddH₂O at 37°C for 5 minutes. DNA concentration was determined by mass gel electrophoresis. 0.5 µL of purified DNA was run alongside a low DNA mass ladder (Invitrogen, 10068-013) on a 0.8% agarose gel. DNA concentration was determined by comparison of band intensity against the known ladder standards. Samples were prepared for sequencing on an Applied Biosystems 3730 DNA Analyzer using ABI BigDye Terminator Chemistry (MOBIXlab, McMaster University). Using ClustalW online software, sequence results were aligned to the extended gene region of *varicose* (Crosby et al., 2007). Excision breakpoints were determined by the absence of genomic DNA and documented.

2.4 Mutant Viability

All *vari* alleles generated by imprecise excision are homozygous lethal. To determine the stage of lethality, *vari* alleles were crossed to wildtype, Canton S-P (CS-P).

Trans-heterozygotes (*w*-; *vari*/+) were crossed and embryos were collected on apple juice agar plates [apple juice agar – a flask of 3% agar in ddH₂O, and a flask of 10% sucrose in apple juice were autoclaved, combined, cooled to 45°C and supplemented with 1% tegosept (10% stock solution in ethanol)]. 50 embryos were aligned on a fresh apple juice agar plate, incubated at room temperature and monitored for 24-48 hours. The number of hatched embryos was recorded. Embryos that failed to hatch were placed on a microscope slide covered in double-sided tape. Using fine forceps, embryos were unrolled from their chorion layer. The number of fertilized unhatched embryos and unfertilized unhatched embryos were recorded. 600 embryos were scored for each *vari* allele and % viability was calculated.

$$\% \text{ Viability} = \frac{\# \text{ of Fertilized Unhatched Embryos}}{\text{Total number of embryos} - \# \text{ of Unfertilized Unhatched embryos}} \times 100$$

2.5 Antibody Production (*Vari* and *Vari*^{L27})

2.5a *Vari*

Rat polyclonal antibody, *Vari*, was generated and purified by Kelly Teal (Teal, 2005).

2.5b *Vari*^{L27}

*2.5b.1 Preparation of *Vari*^{L27} Histidine (*His*) Fusion Construct*

Rat polyclonal antibody, *Vari*^{L27} was designed to the full-length sequence of *varicose* transcript B. EST clone RE31492, corresponding to transcript B was obtained from the *Drosophila* Genomics Resource Centre. The plasmid DNA was received on a Whatman FTA disc placed within a microfuge tube, requiring transformation into

bacterial cells. To remove the DNA from the disc, 50 μ L of sterile 1X TE [0.1 M Tris-HCl, 10 mM EDTA, pH 8.0] was added to the tube, pipetted up and down twice quickly and completely removed from the tube. 50 μ L of chemically competent DH5 α cells (Invitrogen, 18265-017) were added and the tube was placed on ice for 30 minutes. The cells and disc were heat shocked for 2 minutes at 37°C and cooled on ice for 2 minutes. Bacterial cells (not the disc) were transferred to 1 mL of Luria Bertani (LB) medium [10 g tryptone, 5 g yeast extract, 10 g NaCl, 20 g agar (for plates), 950 mL ddH₂O per 1 L of medium] and incubated for 1 hour at 37°C with shaking. Transformed cells were spread evenly onto LB plates containing 10 mg/mL of ampicillin, inverted and incubated for 16-18 hours at 37°C. Successful transformants were isolated and stock plates were generated. Colonies containing clones with the appropriately sized insert were screened by restriction digest and electrophoresis followed by sequencing. DNA was extracted from several clones using GenElute Plasmid Miniprep kit (Sigma, PLN350-1KT) or QIAprep Spin Miniprep kit (Qiagen, 27104). DNA was digested with 1 μ L of REact 3 and 1 μ L (10 U) of *Bam*H I at 37°C overnight and heat inactivated at 65°C (Invitrogen, 15201-023). Digests were analyzed on a 0.8% agarose gel. Positive clones were sequenced using gene specific primers ML3746 and ML1508 and vector specific primers T7 Promoter and T7 Terminator.

Vari^{L27B} was PCR amplified from an RE31492 clone using sense primer ML16977, antisense primer ML15551 and platinum taq DNA polymerase high fidelity (Invitrogen, 11304-011). The reaction mix was prepared as previously described. PCR was performed using a hot-start and 30 cycles as follows, denaturing 94°C for 30

seconds, annealing 60°C for 30 seconds, extension 72°C for 2 minutes. The amplified product was immediately used for ligation into vector pCR2.1. The ligation reaction was performed using 1 µL of PCR product, 50 ng of vector pCR2.1, 1X ligation buffer, 1 µL (4 U) of T4 DNA ligase and sterile ddH₂O to a final volume of 10 µL. The reaction was incubated overnight at 15°C (TA Cloning[®] Kit, Invitrogen, K2020-20). The ligation was transformed into DH5α cells and selected on LB plates containing 33 mg/mL of kanamycin, 40 µL of 100 mM Isopropylthio-beta-D-galactoside (IPTG) and 40 mg/mL of 5-Bromo-4-chloro-3-indolyl β-D-galactopyranoside (X-Gal). Colonies were screened by blue/white selection where colonies containing an insert remain white due to disruption of the lacZ gene. White colonies were restriction digested and sequenced using vector specific primers M13 forward and M13 reverse.

The Vari^{L27B} insert was shuttled from pCR2.1 into expression vector pET29b(+). DNA was digested with 1 µL of REact 4 buffer and 1 µL (10 U) of restriction enzyme *Kpn* I at 37°C for 3 hours (Invitrogen, 15232-010), heat inactivated at 65°C for 15 minutes and briefly centrifuged. DNA was ethanol precipitated and digested with 1 µL of REact 10 buffer and 1 µL (10 U) of restriction enzyme *Sal* I at 37°C overnight (Invitrogen, 15217-011). The cut DNA was purified by phenol:chloroform and ligated overnight at 15°C using 2 µL of 5X ligation buffer and 1 µL (5 U) of T4 DNA ligase (Invitrogen, 15224-041). Ligations were transformed and positive colonies were sequenced. Results confirmed the Vari^{L27B} insert was in-frame for fusion with a C-terminal histidine tag in vector pET29b(+).

2.5b.2 Induction of Vari^{L27} His Fusion Protein

Vari^{L27B} cDNA in pET29b(+) was transformed into bacterial strain BL21λDE3 (Invitrogen, C6000-03) and inoculated into 10 mL of LB containing kanamycin and grown for 16-18 hours at 37°C with shaking. This culture was used to inoculate 500 mL of LB containing kanamycin and incubated at 37°C with shaking until the cells reached an OD₆₀₀ ~ 0.4. The culture was then induced with 0.5 mM IPTG and incubated at 37°C for 3 hours with shaking. Cells were harvested by centrifugation at 6,500 rpm for 10 minutes at 4°C and the supernatant was removed. The cell pellet was dried and stored at -20°C until protein purification.

2.5b.3 Purification of Vari^{L27} His Fusion Protein

The fusion protein was purified from inclusion bodies by affinity chromatography using His-Select Nickel Affinity Gel (Sigma, P 6611) under denaturing conditions. Harvested cells were resuspended in 200 mL of binding buffer [50 mM Na₂PO₄, 300 mM NaCl, 20 mM imidazole, pH 8.0] and sonicated for 5 minutes with a 30 second pause between each minute. Inclusion bodies and cellular debris were separated from proteins in solution by centrifugation at 5,000 g for 15 minutes at 4°C. The supernatant was discarded and the pellet was resuspended in 100 mL of binding buffer followed by 3 minutes of sonication with 30 second breaks between each minute. The pellet was collected through centrifugation at 5,000 g for 15 minutes at 4°C and resuspended in 25 mL of binding buffer containing 8 M urea. Protein was dissolved on ice for one hour. Insoluble material was removed by centrifugation at 16,000 g for 30 minutes at 4°C. Prior to affinity chromatography, the supernatant was loaded into a 60 mL syringe with a

luer-lok tip (BD, REF 309653) and filtered through a 0.45 μm acrodisc syringe filter (Pall Life Sciences, PN4614).

A column was prepared by adding His-Select Nickel Affinity Gel to a chromatography column and allowed to settle under gravity flow until a resin bed volume of 1.5 mL was reached. The column was washed with 3 volumes of ddH₂O followed by 3 volumes of binding buffer containing 8 M urea. The filtered supernatant was loaded into the column and eluted at a rate of 10 volumes per hour. The flow-through was run through the column a second time and then washed with 30 mL of wash buffer [50 mM Na₂PO₄, 300 mM NaCl, 20 mM imidazole, pH 6.3]. Protein was eluted in 12 mL of elution buffer [50 mM Na₂PO₄, 300 mM NaCl, 500 mM imidazole, pH 5.0] containing 8 M urea, collected in 1.5 mL fractions and stored at -20°C until dialysis.

Dialysis was used to remove urea from the solution of purified protein. Dialysis tubing was cut in 20 cm lengths and boiled for 10 minutes in 500 mL of 2% w/v sodium bicarbonate containing 1 mM EDTA, pH 8.0. The tubing was rinsed thoroughly with distilled water and boiled again for 10 minutes in 1 mM EDTA, pH 8.0. The tubing and solution were allowed to cool and stored at 4°C. Before use, the tubing was rinsed inside and out with distilled water.

Eluted fractions were combined and dialyzed overnight at 4°C with stirring in 1X phosphate buffered saline (PBS) [0.256% Na₂H₂PO₄*H₂O, 1.194% Na₂HPO₄, and 10.22% NaCl in ddH₂O, pH 7.4 adjusted with 10 N NaOH] containing 6 M urea. The next day, the dialysis solution was substituted for 1X PBS containing 4 M urea and once again with 1X PBS containing 2 M urea for overnight. On the third day, the dialysis

solution was changed every 3 hours to fresh 1X PBS and dialyzed in fresh 1X PBS overnight at 4°C. Dialyzed protein was transferred to a 1.5 mL centrifuge tube and the concentration was determined by Sodium Dodecyl Sulfate Polyacrylamide Gel Electrophoresis (SDS-PAGE).

Protein samples (1 µL dialyzed protein, and known concentrations of protein standard Bovine Serum Albumin (BSA) – 1 µg, 5 µg, 10 µg) were mixed with an equal volume of 2X Laemli buffer in ddH₂O [5X stock – 60 mM Tris-HCl (pH 6.8), 25% glycerol, 2% SDS, 14.4 M 2-mercaptoethanol, 0.1% bromophenol blue], heated for 5 minutes at 95°C and centrifuged for 10 minutes at 10,000 rpm. Samples were loaded onto a 10% resolving gel (BioRad, 161-1101) for PAGE. Proteins were identified by coomassie staining [0.03% coomassie brilliant blue, 50% methanol, 10% acetic acid] followed by destaining [10% methanol, 10% acetic acid]. The dialyzed protein concentration was estimated against the protein standards.

2.5b.4 Preparation of Vari^{L27} Antiserum

Purified Vari^{L27} His fusion protein in 1X PBS (final concentration 100 µg/mL) was mixed with an equal volume of Freund's complete adjuvant (Sigma, F5881) using an 18 gauge needle. The mixture was injected into 3 white male Wistar rats 3 months of age. Each rat was subjected to 3 subcutaneous injections, 0.1 mL per site. All injections were performed by the Central Animal Facility, McMaster University. To optimize immunization, rats were given booster shots every 14 days for a period of 8 weeks. Booster shots contained Freund's incomplete adjuvant (Sigma, F5506) instead of complete. A tail bleed of 0.5 mL was taken prior to the first injection and 3rd booster

shots. Sera was prepared by incubating the bleeds at 37°C for 1 hour to enhance clotting, then placed on ice at 4°C for overnight. Blood samples were centrifuged at 13,000 rpm for 10 minutes and the supernatant was collected. Samples were frozen at -20°C until affinity purification.

2.5b.5 Affinity Purification of Vari^{L27} Serum

Vari^{L27} post-immune serum was affinity purified using CNBr activated sepharose 4B (Amersham Biosciences, 17-0430-01). Sepharose beads (330 mg=1 mL) were washed with 1 mM HCl for 15 minutes (70 mL HCL for 1 mL beads). The amount of sepharose required depends upon the amount of protein to be coupled (5-10 mg protein/mL gel). The swollen sepharose beads were transferred to a sintered glass funnel, washed with 200 mL of 1 mM HCl followed by 5 mL of coupling buffer [0.1 M NaHCO₃, pH 8.3, 0.5 M NaCl, 2 M urea].

Vari^{L27} antigen was dialyzed in 0.1 M NaHCO₃, pH 8.3, 0.5 M NaCl and 2 M urea. The sepharose beads were transferred to the antigen solution (1 mg protein in 5 mL coupling buffer) and mixed gently overnight at 4°C. To remove unbound antigen, the beads were washed with 5 volumes of coupling buffer. The conjugated protein beads were incubated in 0.1 M Tris, pH 8.0 for 2 hours at room temperature to block the remaining active groups. Beads were washed 3 times with alternating pHs [0.5 M NaCl, 0.1 M NaAc, pH 4.0 and 0.5 M NaCl, 0.1 M Tris, pH 8.0] followed by 10 mL of PBS.

The conjugated beads were combined with Vari^{L27} post-immune serum, 4 volumes of PBS and incubated overnight at 4°C on a roller. Beads were washed with 10 mL of PBS and packed into a chromatography column. Purified antibody was eluted

with 0.1 M glycine, pH 2.4, neutralized by the addition of 30 μ L of 3 M Tris, pH 8.8 and 20 μ L of 5 M NaCl and then dialyzed in 1X PBS.

2.6 Immunohistochemistry

Embryos were collected on apple juice agar plates and aged at 25°C for 8 hours followed by 16 hours at 18°C to stage embryos from mid to late embryogenesis. Embryos were dechorionated in 50% bleach in ddH₂O and incubated in fixative [4.5 mL of 1X PBS, 0.5 mL of 37% formaldehyde, 5 mL of heptane] on a rotator for 30 minutes. Vitelline membranes were cracked with 100% methanol and washed with methanol several times to remove traces of fixative. Immunohistochemistry techniques were adapted from Patel (Patel, 1994). Prior to antibody labeling, embryos were washed 5 times in 0.1% PBT [1X PBS, 0.1% Triton X-100] and washed on a rotator for 20 minutes in 0.1% PBT. Embryos were allowed to settle by gravity flow and blocked in 0.5% PBT and 10% normal goat serum (NGS) on a shaker for 40 minutes. Primary antibody was added at the appropriate dilution and incubated overnight on a shaker at 4°C. Primary antibodies were used at the following dilutions: rat anti-Vari (1:15), rat anti-Vari^{L27} (1:15), rabbit anti-NrxIV (1:300) (gift from H.J. Bellen, Baylor College of Medicine, Houston, TX), chicken anti- β -galactosidase (β -Gal) (1:150) (MacMullin and Jacobs, 2006), and anti-Phosphotyrosine (1:300) (Millipore). The following monoclonal antibodies were obtained from the Developmental Studies Hybridoma Bank: Crumbs (1:30), α -Spectrin (1:30), Dlg (1:30), Na⁺K⁺ATPase (1:300), MAb2A12 (1:30), Repo (1:7), Elav (1:75), Prospero (1:4), and FasIII (1:30). Embryos were washed for 4-8 hours in 0.1% PBT, changing 0.1% PBT every hour. Embryos were blocked as above and

incubated in secondary antibody (1:150) for 2 hours at room temperature on a shaker. Embryos were washed several times in 0.1% PBT and reacted according to secondary antibody type. Embryos labeled with fluorescent secondary antibodies, Alexa 488 and Alex 594 (Molecular Probes) were protected from light using tinfoil and stored in 70% glycerol in 1X PBS at 4°C. Embryos were mounted in 70% glycerol on microscope slides and coverslips were sealed with nail polish 1 hour prior to visualization by confocal microscopy using Zeiss LSM510. MAb2A12 was detected using secondary antibody goat anti-mouse conjugated to horseradish peroxidase (HRP) (Jackson ImmunoResearch Laboratories, Inc.) and 3,3-Diaminobenzidine Tetra hydrochloride (DAB, Gibco-BRL). Anti- β -Gal was detected using biotinylated secondary antibody (Vector Laboratories) followed by incubation with Vector Laboratories Elite ABC and DAB. Embryos were dehydrated using an ethanol gradient (30, 50, 70, 80, 90, 95% ethanol in ddH₂O and 100% ethanol) and stored at room temperature in methyl salicylate (Fisher, 03695-500). Embryos were mounted in D.P.X neutral mounting medium (Sigma, 31,761-6) and visualized using Zeiss Axioskop microscope. Images were processed using OpenLab, ImageJ and Adobe Photoshop[®] 7.0.

2.7 Tissue Dissection

Larvae – wandering third instar larval brains were dissected in cold 1X PBS using 2 sets of forceps. The posterior end of the larva was held steady with one set of forceps while the other was used to pull gently on the mouth hooks, separating the mouth hooks, brain and imaginal discs from the larval body. Brains were cleared away from the extra tissue and fixed in 4% paraformaldehyde [4 g of paraformaldehyde, 50 mL of ddH₂O, 1

mL of 1 M NaOH, 10 mL of 10X PBS, pH 7.4 adjusted with 1 M HCl, 0.45 μ m filter sterilized]. Following several washes in 0.3% PBT, the brains were incubated in primary and secondary antibody as described above.

Pupae – embryos were collected on apple juice agar plates and aged at 25°C until 48-50 hours after pupal formation (APF). To dissect pupal brains, the pupal case was removed and the pupal head was separated from the body using iradectomy scissors (F.S.T, 15008-08). Brains were removed by gently turning the pupal head inside out and clearing away extra tissue from the brain. Pupal brains were fixed and labeled as per larval brains. FasII antibody was diluted 1:30 in 0.5% PBT and 10% NGS.

Ovaries – immunohistochemical labeling of ovaries was adapted from the Spradling Lab (Lin and Spradling, 1993). Females were fed a high yeast diet for 3-5 days. Ovaries were dissected in 1X Ringers Solution (130 mM NaCl, 4.7 mM KCl, 1.9 mM CaCl₂, 10 mM Hepes, pH 6.9) (Goldstein and Fyrberg, 1994). Ovaries were fixed and labeled as outlined above.

2.8 *UAS-vari* Transgenic Construct

2.8.1 *RNA Preparation*

All solutions used were prepared with Diethyl Pyrocarbonate (DEPC) (Sigma, D5758) treated water. DEPC was added to ddH₂O to a final concentration of 0.1%, incubated at 37°C overnight and autoclaved. Total RNA was extracted from Canton-S P adults using TRIzol (Invitrogen, 15596-018). Approximately 200 adult flies were collected and stored in a foodless fly vial for 1-2 hours to minimize ingested yeast. Flies were stored at -20°C until use.

Flies were ground in liquid nitrogen with a pre-cooled mortar and pestle and transferred to a cooled dounce homogenizer containing 2 mL of TRIzol. Fly carcasses were homogenized to free cells and nuclei. The extraction was transferred to a 1.5 mL microfuge tube and centrifuged at 4,000 rpm for 4 minutes at 4°C. Cellular debris was pelleted and the supernatant was transferred to a clean tube. Chloroform was added (0.2 mL per 1 mL TRIzol) and the tube contents were briefly vortexed and centrifuged at 10,000 rpm for 10 minutes at 4°C. The upper aqueous layer was transferred to a clean tube with an equal volume of isopropyl alcohol, mixed by inversion and stored at -80°C for 15 minutes. The RNA was pelleted by centrifugation at 14,000 rpm for 30 minutes at 4°C and washed with 70% ethanol. The pellet was air dried for 5 minutes and resuspended in DEPC-ddH₂O. RNA concentration and purity was determined by absorbance at 260 nm and 260/280 nm, respectively.

2.8.2 Reverse Transcription and Cloning

cDNA was generated from total RNA by reverse transcription (RT). In a 0.2 mL microfuge tube, 1 µg of total RNA, 1 µL of M-MLV Reverse Transcriptase, 1 µL (1 U) of RNase inhibitor and final concentrations of 1X RT buffer and 0.2 µM random decamers were added. Nuclease-free water was added to adjust the reaction volume to 20 µL (First Choice RLM-RACE kit, Ambion, 1700). The reaction was mixed gently and spun briefly to pool the contents. The reverse transcription was carried out at 42°C for 1 hour and then stored at -20°C until PCR amplification.

Full-length *vari* transcript C was amplified from the above cDNA template using the sense primer ML3596 and the antisense primer ML3033. The reaction mix is

described in 'Single Embryo DNA Extraction' and PCR was performed using a hot-start and 30 cycles were completed as follows, denaturing 94°C for 30 seconds, annealing 60°C for 30 seconds, extension 72°C for 1 minute and 30 seconds. This PCR product was ligated into vector pCR2.1, and sequenced. The cDNA insert was shuttled into the transformation vector pUAS_t (Brand and Perrimon, 1993). DNA was digested using 1 µL REact 2 buffer and 1 µL (10 U) of restriction enzyme *Xba* I (Invitrogen, 15226-012). Insert and vector pUAS_t were ligated, transformed into DH5α, and insert orientation was determined by sequencing using ML5220, a primer designed to the *hsp70* TATA region. The transgenic construct and helper vector DNA (a gift from G. Boulianne) were prepared for microinjection using an EndoFree Plasmid Maxi Kit (Qiagen, 12362). Plasmid DNA was injected into *yw*- embryos by Xiao-Li Zhao using standard techniques (Roberts, 1986).

2.8.3 *Expression Analysis of UAS-vari*

Heat Shock

To ensure transgenic expression of full-length Vari protein, 1 day old adult flies *w*-; *heat shock GAL4* or *w*-; *UAS-vari* or *w*-; *heat shock GAL4; UAS-vari* were subjected to heat shock at 37°C for 45 minutes. Flies were recovered at room temperature for 1 hour and the heat shock and recovery treatments were repeated. Adults were homogenized in cold RIPA buffer [150 mM NaCl, 1% Nonidet P-40, 0.5% deoxycholate, 0.1% SDS, 50 mM Tris-HCl, pH 8.0] supplemented with protease inhibitor cocktail tablets (1/50 mL) (Roche Diagnostics, 11 873 580 001) and incubated on ice for 10 minutes. Fly carcasses were pelleted by centrifugation at 10,000 rpm for 10 minutes at 4°C. The supernatant

was collected and protein concentration was determined by Bradford assay. All steps were performed on ice and samples were stored in 50 µg aliquots at -80°C until western blot analysis.

Western Blot

Protein samples were thawed in an equal volume of 2X Laemli buffer and heated at 95°C for 5 minutes. Samples were spun at 10,000 rpm for 10 minutes, loaded onto a 10% resolving gel, separated by PAGE and transferred to PVDF membrane (Pall Life Sciences, 30718) at 100 V for 1 hour at 4°C in transfer buffer [200 mL of methanol, 3 g Tris, 14.4 g glycine, 0.75 g SDS per 1 litre]. The membrane was washed 2 times for 10 minutes each in TTBS [25 mM Tris-HCl, pH 7.4, 150 mM NaCl, 0.5% Tween 20], blocked for 30 minutes in TBS [no Tween 20] with 5% milk powder and incubated overnight in a 1:1000 dilution of Vari antibody in 2% milk powder in TBS. The membrane was washed 3 times for 10 minutes each in TTBS followed by 2 hours of incubation in a 1:5000 dilution of goat anti-rat-HRP conjugated secondary antibody (Jackson ImmunoResearch Laboratories, Inc.) in TBS with 2% milk powder. Following 3 more 10 minute washes with TTBS, the tagged antibody was reacted with ECL western blotting detection reagents (Amersham, RPN2106) and detected on hyperfilm (Amersham, 28-9068039).

UAS-vari Rescue of *vari*^{48EP} Null Embryos

Embryonic lethality of homozygous null embryos is rescued by ubiquitous expression of *UAS-vari* by *daughterlessGAL4*. *w-; vari*^{48EP}/*CyO*, *Actin-GFP*; *UAS-vari* flies were crossed to *w-; vari*^{48EP}/*CyO*, *Actin-GFP*; *daGAL4* flies and viability was

calculated as described in ‘Mutant Viability’. Crosses were raised at 25°C. Phenotypes were only assessed in adults fully hatched from their pupal casings. To visualize defects in wing and leg hairs, whole flies were dehydrated using an ethanol gradient. Flies were washed in 30%, 50%, 70%, 80%, 90%, 95% and 3X in 100% ethanol and stored in methyl salicylate. Wings and legs were dissected from fly bodies using spring scissors (F.S.T., 91500-09), mounted in D.P.X. on microscope slides and sealed with coverslips. Hairs were visualized on Nikon SMZ1500 and Zeiss Axioskop microscopes. Adult eyes were imaged as described below in ‘Scanning Electron Microscopy’. Images were processed using OpenLab, Nikon Coolpix-990 and Adobe Photoshop® 7.0.

2.9 Scanning Electron Microscopy

Adult flies were frozen at -20°C within 3 days of eclosion. Several flies were mounted on each stub with a graphite/white glue mixture, and viewed at 0.3 Torr in a Philips Electroscan 2020 Environmental Scanning Electron Microscope (ESEM). At least 10 female eyes from each genotype were imaged at 140X and 300X, and 200 dpi images were recorded as TIFF files. The images were processed with Adobe Photoshop® 7.0.

2.10 Dye Permeability Assay

Fluorescent dye injection was performed as described (Lamb et al., 1998). Embryos were collected every 2 hours and aged at room temperature. Dechorionated stage 17 embryos were mounted on double sided tape, and immersed in Volatef halocarbon oil. Embryos were visualized on an inverted microscope. Employing a micromanipulator, a glass microelectrode filled with Rhodamine-labeled dextran (10,000

mol wt; Invitrogen, D-1817) reconstituted to 3 mM in embryo injection buffer [5 mM KCl, 0.1 mM phosphatase buffer, pH 6.8: 0.074 g KCl, 10 mL stock phosphatase buffer, pH 6.8, 190 mL H₂O – Stock Phosphatase Buffer, pH 6.8: 46.3 mL of 1 M Na₂HPO₄, 53.7 mL of 1 M NaH₂PO₄ (Schulte et al., 2003)], was used to pierce the posterior end of the embryo and dye was injected by air pressure (from building compressed air). Stage 17 embryos were examined within 30 minutes of injection on a Zeiss LSM510. Mutants were identified by lack of GFP expression from the balancer (*CyO*, *Kr-GAL4*, *UAS-GFP*).

2.11 Electron Microscopy

Stage 17 embryos were mounted on double sided tape, and immersed in primary fixative [5% glutaraldehyde in 0.05 M Cacodylate buffer, pH 7.2]. Embryos were visualised on an inverted microscope. Employing a micromanipulator, a glass microelectrode filled with primary fixative was used to pierce the posterior end of the embryo as described (Prokop et al., 1998), and fixative was injected by air pressure (from building compressed air). After 60 minutes of fixation, embryos were washed in Cacodylate buffer, post-fixed in 1.0% Osmium tetroxide in cacodylate buffer for 60 minutes, washed in ddH₂O and stained *en bloc* with aqueous 2% uranyl acetate. Embryos were dehydrated in an ethanol series, and infiltrated with Epon plastic in a 1:1, 1:3 and 100% series. Plastic was cured, trimmed, sectioned and post-stained with Sato's Lead Citrate with established methods (Jacobs and Goodman, 1989). Semi-serial sections were visualised on a Jeol 120CX electron microscope (Sato, 1967).

2.12 Library Scale Yeast Two Hybrid Screen

2.12.1 *Varicose-GAL4 DNA-Binding Domain Fusion Construct*

Full-length *varicose* transcript C was PCR amplified from a cDNA template generated from total RNA as described above. PCR was performed using sense primer ML3746 and antisense primer 'Y2H bait construct' following the same conditions described in 'Transgenic Construct'. The PCR product was ligated into pCR2.1 then shuttled into yeast two-hybrid (Y2H) vector pGBKT7 (MATCHMAKER GAL4 Two-Hybrid System 3, Clontech, PT3247-1). Insert and Y2H vector were digested with 1 μ L of REact 6 buffer and 1 μ L (5 U) of *Nde* I (Invitrogen, 15426-018) followed by digestion with *Sal* I. Digested DNA was ligated, transformed and clones were screened for the appropriate insert by restriction digest and sequencing using T7 promoter primer. Results verified the insert was in-frame with the GAL4 DNA-binding domain (BD) and an N-terminal c-Myc epitope tag.

2.12.2 *Verification of Yeast Strain AH109*

To become familiar with the yeast strain and to verify its phenotype and nutritional requirements, strain AH109 was streaked on adenine supplemented YPD (YPDA) plates [20g difco peptone, 10 g yeast extract, 20 g agar (for plates), 15 mL of 0.2% adenine hemisulfate per litre of medium, adjusted to pH 6.5, autoclaved and cooled to 55°C before adding a final concentration of 2% dextrose] and incubated at 30°C for 3-5 days. Using isolated colonies, 3-4 colonies were streaked onto plates containing minimal SD base (Clontech,8602-1) and the appropriate drop-out (DO) supplement and incubated at 30°C for 4-6 days. Stock plates were sealed with parafilm and stored at 4°C for up to 4

weeks. The following table depicts the conditions required for growth (+) or no growth (-) of strain AH109.

Table 2.2: Media requirements for growth of yeast strain AH109

Strain	SD/-Leu	SD/-Trp	SD/-Ade/-His/-Leu/-Trp	SD/-Ura	YPDA
AH109	-	-	-	+	+

2.12.3 Verifying *Varicose-GAL4 DNA-BD Fusion does not Activate Reporter Genes*

Each Y2H construct was transformed into strain AH109 and selected using the appropriate DO supplement. Transformations were performed using small scale conditions. The following table lists the vectors used throughout the Y2H screen along with their antibiotic resistance marker, nutritional marker and epitope tag.

Table 2.3: DNA plasmids required for the yeast two hybrid screen

Vector	Fusion	Antibiotic Resistance	Nutritional Marker	Epitope Tag
pGBKT7-Vari	BD-bait	Kanamycin ^r	TRP1	c-Myc
pACT2-library clone	AD-library (prey)	Ampicillin ^r	LEU2	HA
pGBKT7-p53	BD-p53	Kanamycin ^r	LEU2	c-Myc
pGADT7-SV40 T antigen	AD-T antigen	Ampicillin ^r	LEU2	HA
pCL1	GAL4	Ampicillin ^r	LEU2	
pGBKT7-lam	BD-lamin C	Kanamycin ^r	TRP1	c-Myc

Small Scale Yeast Transformation

To transform yeast strain AH109, 1-3 week old colonies were used to inoculate liquid culture. Using a sterile toothpick, a single colony was resuspended in 1 mL of YPDA medium by vortexing and transferred to a flask containing 50 mL of YPDA. The inoculated culture was incubated at 30°C for 16-18 hours with shaking or until stationary phase was reached ($OD_{600} > 1.5$). The culture was transferred to 300 mL of YPDA (to produce $OD_{600} = 0.2-0.3$) and incubated at 30°C for another 3 hours or until an $OD_{600} =$

0.5±0.1 was obtained. Cells were split into 50mL tubes and centrifuged at 1,000 g for 5 minutes at room temperature. Pelleted cells were resuspended by vortexing in 25-50 mL of 1X TE, pH 7.5. The resuspensions were pooled and centrifugation was repeated. The supernatant was decanted and the cells were resuspended in 1.5 mL of freshly prepared sterile 1X TE/LiAc solution [made from 10X TE and 10X LiAc (1 M lithium acetate, Sigma, L-6883, adjusted to pH 7.5 with dilute acetic acid)]. For the highest transformation efficiency, cells were transformed within 1 hour of preparation.

In a separate 1.5 mL microfuge tube, 0.1 µg of transforming plasmid DNA and 0.1 mg of herring testes carrier DNA (10 mg/mL, Clontech, K1606-A) were mixed. 0.1 mL of yeast competent cells and 0.6 mL of freshly prepared sterile PEG/LiAc solution [40% PEG 4000, 1X TE, 1X LiAc] were added. The tube contents were mixed by vortexing at high speed and incubated at 30°C for 30 minutes with shaking. 70 µL of dimethyl sulfoxide (DMSO) was added and the tube was mixed by gentle inversion. Transformation was performed in a 42°C water bath for 15 minutes and the cells were chilled on ice for 2 minutes. The transformed cells were collected by centrifugation at 14,000 rpm for 5 seconds at room temperature. The supernatant was discarded and the cells were resuspended in 0.5 mL of YPDA.

Transformants were selected on DO supplemented media lacking tryptophan (Clontech, 8604-1), a nutritional marker for pGBKT7 plasmids, or leucine (Clontech, 8605-1), a nutritional marker for pGADT7, pCL1 and library vector pACT2. To obtain even growth, cells were spread by shaking the plate back and forth, not round and round. To verify that the plasmids do not activate the histidine, adenine and *MEL1* reporter

genes in the AH109 strain, plates were spread with 100 μ L of 5-Bromo-4-chloro-3-indolyl- α -D-galactosidase (*X- α -Gal*, Clontech, PT3353-2) [4 mg/mL in dimethylformamide, DMF] to assay for *MEL1* activation. α -galactosidase is taken up by the yeast and cleaves *MEL1* producing blue colonies. Colonies lacking *MEL1* expression remain white (Aho et al., 1997). Transformation of pCL1, was used as a positive control. Similarly, to test for activation of histidine and adenine reporter genes, transformants were plated onto quadruple DO media (QDO) [SD media with leucine, tryptophan, histidine and adenine DO supplement, Clontech, 8619-1] or onto triple DO media (TDO) [SD media with leucine, tryptophan and histidine DO supplement, Clontech, 8610-1].

2.12.4 Verifying Varicose-GAL4 DNA-BD Fusion Expression by Western Blot

Protein Preparation

To ensure our fusion protein was expressed in the AH109 yeast strain, a western blot was prepared and probed with an antibody to the c-Myc epitope tag. To prepare protein from yeast, 5 mL of SD/-TRP medium was inoculated with transformed yeast and incubated for 16-18 hours at 30°C with shaking to reach an $OD_{600} > 1.5$. As a negative control, a 10 mL culture of untransformed yeast was inoculated into YPD medium. Using the overnight cultures, 50 mL aliquots of YPD medium were inoculated and incubated at 30°C until the OD_{600} was reached 0.4-0.6. The cultures were quickly chilled by pouring them into a precooled 100 mL centrifuge tube halfway filled with ice. The cells were placed in a prechilled rotor and centrifuged at 1,000 g for 5 minutes at 4°C. The supernatants were decanted and the cells were resuspended in 50 mL of ice-cold H₂O.

The pellets were recovered by repeating the centrifugation. The pellets were frozen in liquid nitrogen and stored at -80°C until protein preparation.

Cell pellets were resuspended in complete cracking buffer prewarmed to 60°C [Complete cracking buffer: 1 mL of cracking buffer, 10 μL of β -mercaptoethanol, 70 μL of protease inhibitor solution, 50 μL of 100X phenylmethyl-sulfonyl fluoride (PMSF) stock in isopropanol – Cracking buffer: 50 g urea, 2.5 g SDS, 2 mL of Tris-HCl pH 6.8, 10 μL of 0.5 M EDTA, 20 mg bromophenol blue, ddH₂O to total 50 mL – Protease Inhibitor Solution: 0.1 mg/mL pepstatin A, 0.03 mM leupeptin, 145 mM benzamidine, 0.37 mg/mL aprotinin]. 100 μL of cracking buffer was used per 7.5 OD₆₀₀ units of cells (OD₆₀₀ units of cells = OD₆₀₀ of a 1 mL sample X total culture volume). The cell suspension was transferred to a 1.5 mL screw-cap microfuge tube (DiaMed, SSI2220-00 and TEC052SSC-N) containing 80 μL of glass beads (Sigma, G-8772) per 7.5 OD₆₀₀ units of cells. The tube was heated to 70°C for 10 minutes to free membrane-associated proteins. The heated tubes were vortexed vigorously for 1 minute and cellular debris and unbroken cells were pelleted by centrifugation at 14,000 rpm for 5 minutes at 4°C . The supernatant was transferred to a clean 1.5 mL screw-cap tube and boiled at 100°C for 3-5 minutes. Vortexing and centrifuging were repeated and the supernatants were pooled. Protein concentration was determined by Bradford assay and stored at -80°C until western analysis.

Western Blot

20-30 μg of protein lysate was prepared as previous described. Samples were loaded onto a 12% resolving gel (BioRad, 161-1102), separated by PAGE and transferred

to PVDF membrane. The membrane was washed in TTBS and blocked prior to incubation in a 1:5000 dilution of c-Myc monoclonal antibody (a gift from J.A. Hassell) and tagging with a 1:5000 dilution of goat anti-mouse-HRP conjugated secondary antibody. The tagged antibody was reacted with ECL western blotting detection reagents and detected on hyperfilm.

2.12.5 Drosophila Adult cDNA Library Screen

Library Amplification

A pACT2 *Drosophila Melanogaster*, adult MATCHMAKER cDNA library (Clontech, IL4002AH) was titred to $>1.05 \times 10^7$ cfu/mL. To obtain enough plasmid library for screening (100-500 μ g screens $\sim 1 \times 10^6$ independent clones) the plasmid library was amplified. The number of plates needed to screen 3X the size of the original library, plated with 20,000 cfu/plate was determined using calculations outlined in the user manual (Clontech, PT3247-1).

(# of independent clones x 3) = # clones to screen
of clones to screen/ colonies per plate = # of 150 mm plates
clones to screen/ library titre = μ Ls of library to plate
plates x 150 μ L = volume of media required to plate 150 μ L on each plate

Therefore, 35 μ L of our cDNA library was added to 78.75 mL of LB containing ampicillin and spread onto 525 plates (Fisher, 08-757-14). The inoculum was spread over LB containing ampicillin plates (dried at room temperature for 2-3 days prior to plating) until all visible liquid was absorbed. Plates were incubated at room temperature for 20 minutes then inverted and moved to 30°C for 36-48 hours. To each plate, 5 mL of LB containing ampicillin was added and colonies were scraped into the liquid using a spatula. The resuspended colonies were pooled in a flask, incubated at 30°C with shaking

for 2-4 hours and mixed with a final concentration of 25% glycerol. One-third (1 L) of the library culture was set aside for plasmid preparation. Five 1 mL aliquots of library culture were stored at -80°C for re-amplification of the library. The remainder of the library was divided into 50 mL aliquots and stored at -80°C .

Large-Scale Plasmid Preparation

The library cell culture was divided into four-250 mL centrifuge tubes and pelleted at 5,000 rpm for 10 minutes at 4°C . A total of 36 mL of solution I [50 mM glucose, 25 mM Tris-HCl, pH 8.0, 10 mM EDTA, pH 8.0] was used to resuspend the pellets which were then combined into one tube. 80 mL of solution II [0.2 M NaOH, 1% SDS] was added and the tube was mixed gently for 1-2 minutes. 40 mL of cold solution III [3 M K^{+} /5 M Ac^{-}] was added and the tube was mixed gently, placed on ice for 10 minutes and then centrifuged at 9,000 rpm for 15 minutes at 4°C . The pellet was rinsed with 70% ethanol, dried at 37°C for 10 minutes and resuspended in 10 mL of sterile ddH₂O with 20 μL of RNase A (10 mg/mL). The resuspension was incubated at 37°C for 20 minutes, added to 0.5 volumes of PEG [20% PEG 6000, 2.5 M NaCl] and incubated on ice for 60 minutes. The precipitated DNA was collected by centrifugation at 12,000 rpm for 15 minutes at 4°C . The pelleted DNA was dissolved in 10 mL of ddH₂O and purified using an equal volume of phenol:chloroform followed by 2 volumes of chloroform. Purified DNA was ethanol precipitated, rinsed with 70% ethanol, dried and dissolved in 1 mL of TE (Sambrook and Russell, 2001).

Library Scale Yeast Transformation

Yeast strain AH109 transformed with our Vari-GAL4 DNA-BD fusion construct was used to generate competent cells for our screen of the adult cDNA library.

Competent cells were prepared as previous described with the following changes. The overnight culture was inoculated into 150 mL of YPDA media, grown to an $OD_{600} 0.5 \pm 0.1$ and the pellet was resuspended in 500 mL of sterile 1X TE followed by resuspension in 8 mL of freshly prepared 1X TE/LiAc solution.

In a separate tube, 1 mg of library plasmid DNA was mixed with 20 mg of herring testes carrier DNA and transformed into 8 mL of competent cells by heat shock. The transformed cells were resuspended in 12 mL of YPDA medium and plated in 200 μ L aliquots on 35 TDO plates and 25 QDO plates containing X- α -Gal.

As a positive control, pGBKT7-53 was transformed with 1 μ g of pGADT7-SV40 (a fusion protein containing SV40 T-antigen, a protein known to interact with p53, and the activation domain of GAL4). Similarly, as a negative control, pGBKT7-lam was transformed with 1 μ g of pGADT7-SV40 (a protein which does not interact with lamin C). All transformations were plated on both SD/-TRP/-LEU (Clontech, S1913) and QDO plates to assay for successful transformation of the prey protein and protein-protein interactions, respectively.

2.12.6 Identification of Putative Positive Clones

The initial library transformants may contain more than one library plasmid per colony and this would complicate the analysis of positive clones. Each of the 142 potential positive clones were restreaked onto SD/-TRP/-LEU/X- α -Gal plates 3 times to

reduce the number of library plasmids. Plates were incubated at 30°C for 4-6 days. Clones were then restreaked onto QDO/X- α -Gal plates to verify a protein-protein interaction between the Vari and the library clone. A ‘working’ plate containing all interacting clones was streaked and freezer stocks were made for long-term storage. A single colony from each putative clone was inoculated into 500 μ L of YPD medium, vortexed vigorously and supplemented with a final concentration of 25% glycerol. Stocks were stored at -70°C.

2.12.7 Elimination of Duplicate Clones

Plasmid Prep from Yeast

To eliminate any duplicate colonies, plasmid DNA was isolated from yeast. 2-4 day old colonies were inoculated into 0.5 mL of QDO media. The inoculum was vortexed to break up the colony and to resuspend the cells and grown overnight at 30°C in QDO media. Cells were pelleted at 14,000 rpm for 5 minutes. The supernatant was decanted and the cells were resuspended in the residual liquid (~50 μ L). Yeast cells were lysed by incubating cells with 10 μ L of lyticase solution [5 U/ μ L in TE buffer] for 60 minutes at 37°C followed by the addition of 10 μ L of 20% SDS and vigorous vortexing for 1 minute. To ensure complete lysis of the cells, samples were frozen at -20°C, thawed and vortexed again. The sample volume was adjusted to 200 μ L using TE buffer, pH 7.0. An equal volume of phenol:chloroform:isoamyl alcohol (25:24:1) was added and the samples were vortexed and centrifuged at 14,000 rpm for 10 minutes. The upper phase was transferred to a fresh tube and 8 μ L of 10 M ammonium acetate and 500 μ L of 100% ethanol were added. The DNA was precipitated at -80°C for 1 hour and centrifuged at

14,000 rpm for 10 minutes. The supernatant was removed, the pellet dried and resuspended in 20 μL of ddH₂O.

Sorting Colonies by PCR and Restriction Digest

Library inserts were amplified by PCR using the purified plasmid DNA from yeast. The PCR reaction mix was prepared using 2 μL of plasmid DNA and 2.5 μM of each AD-insert screening primer. PCR was performed using 30 cycles as follows, denaturing 94°C for 30 seconds, annealing 59°C for 30 seconds, extension 68°C for 3 minutes. PCR products were run on a 0.8% agarose gel and separated by electrophoresis. To eliminate duplicate clones, each PCR product was digested with 1 μL of REact 2 buffer and 1 μL (10 U) of *Hae*III (Invitrogen, 15205-016). Fragment sizes were analyzed by gel electrophoresis on a 1.2% agarose gel and duplicate clones were eliminated.

2.12.8 Rescue of Library Plasmids via Transformation of *E. coli*

Library plasmids were rescued by transformation into bacterial cells. 40 μL of KC8 electrocompetant cells (Clontech, C2023-1) were added to a prechilled electroporation cuvette (VWR Scientific, 47727-640). To the cuvette, 2 μL of library plasmid DNA was added and mixed by gently tapping. Electroporation was performed at 1.8 kV with 10- μF constant capacitance and 600-Ohm resistance (Bio-Rad Gene Pulser® II). Electroporated cells were transferred to 1 mL of SOC medium [20 g tryptone, 5 g yeast extract, 0.5 g NaCl, 10 mL of 250 mM KCl, pH adjusted to 7.0] and incubated at 37°C for 1 hour. Cells were pelleted at 2,500 rpm for 5 minutes. The supernatant was removed and the cells were resuspended in 100 μL of LB containing ampicillin, plated on LB containing ampicillin and incubated at 37°C for 24 hours. DNA was prepared from

successful transformants using QIAprep Spin Miniprep kit (Qiagen, 27104). To verify that the same library plasmid was obtained, the DNA was used as a PCR template. The PCR cycles used above for plasmid DNA isolated from yeast were repeated for plasmid DNA isolated from bacteria. PCR products were analyzed by agarose gel electrophoresis and compared against the PCR products amplified from yeast plasmid DNA. Clones with the appropriately sized insert compared to the yeast clones were stored at -80°C.

2.12.9 Verification of Protein Interactions in Yeast

Interactions between Vari-GAL4 DNA-BD fusion and library clones were verified by small-scale transformation into AH109. To select for both plasmids, transformants were selected on SD/-TRP/-LEU. To verify an interaction, colonies were restreaked onto QDO media containing X- α -Gal. As a negative control, transformations were also completed using empty vector pGBKT7. As a positive control, pGBTK7-p53 and pGADT7-T antigen were transformed into AH109. Library clones that interact with Vari-GAL4 DNA-BD fusion but not the empty vector were sequenced. Results were used in a BLAST search of the *Drosophila* genome to identify the interacting protein.

2.13 RNA Ligase Mediated Rapid Amplification of cDNA Ends (RLM-RACE)

Total RNA was extracted from embryonic and adult CS-P flies using TRIzol as previously described. Embryos were collected on apple juice agar plates, incubated in 50% bleach for 5 minutes and collected on a sieve. Embryos were scrapped into a prechilled mortar and pestle and RNA was extracted with TRIzol. The total RNA extracted was used for both 5' and 3' RACE experiments using a First Choice RLM-RACE kit (Ambion, 1700).

2.13.1 5'RLM-RACE

10 µg of total RNA was treated with 2 µL of calf intestinal phosphatase (CIP), 1X CIP buffer and nuclease-free water to 20 µL. The contents were mixed, centrifuged briefly and incubated at 37°C for 1 hour. CIP was added to remove the 5'PO₄ from degraded mRNA, rRNA, tRNA and DNA. To stop the reaction, 15 µL of ammonium acetate solution was added and the RNA was extracted using 150 µL of phenol:chloroform. The reaction was vortexed thoroughly and centrifuged for 5 minutes at room temperature at 14,000 rpm. The top aqueous phase was transferred to a new tube and 150 µL of chloroform was added. The tube was vortexed and centrifuged again. Similarly, the top layer was transferred to a new tube, mixed with an equal volume of isopropanol, vortexed and incubated on ice for 10 minutes. Following incubation, the tube was spun at 14,000 rpm for 20 minutes. The pellet was washed with 0.5 mL of 70% ethanol, centrifuged for 5 minutes at maximum speed and the ethanol was discarded. The pellet was dried and resuspended in 11 µL of nuclease-free water.

5 µL of CIP'd RNA was treated with 2 µL of tobacco acid pyrophosphatase (TAP) to remove the 5' cap from full-length mRNA, and 1X TAP buffer. Nuclease-free water was added to a final volume of 10 µL. The reaction was mixed and incubated for 1 hour at 37°C. Using 2 µL of CIP/TAP-treated RNA, 1 µL of a 5'RACE adapter [5'GCUGAUGGCGAUGAAUGAACACUGCGUUUGCUGGCUUUGAUGAAA3'] was ligated to the 5' end of the decapped mRNA using 1X RNA ligase buffer, 2 µL (5 U) of T4 RNA ligase and 4 µL of nuclease-free water. Again the reaction was mixed and incubated at 37°C for 1 hour. RT was performed as previously described using 2 µL of

ligated RNA and 1 μ L of M-MLV reverse transcriptase. The cDNA generated was used as a template for Outer 5' RLM-RACE PCR analysis. 1 μ L of the RT reaction was amplified using 2.5 μ M of a sense primer designed to the outer adaptor region and 2.5 μ M of an antisense gene specific outer primer ML816, 1.25 mM dNTP mix, 1X PCR buffer, 1.25 U of thermostable DNA polymerase and nuclease-free water to 50 μ L. PCR was performed using a hot-start and 35 cycles as follows: denaturing 94°C for 30 seconds, annealing 60°C for 30 seconds, extension 72°C for 1 minute 45 seconds. Inner 5' RLM-RACE PCR was performed using the same reaction mix and cycles as above with the following changes: 1 μ L of Outer PCR products was used as a template, 2.5 μ M of a sense primer designed to the inner adaptor region and 2.5 μ M of an antisense gene specific inner primer ML817. 5' RACE was also performed in the absence of TAP treatment to test for DNA contamination. PCR products were analyzed by 2% agarose gel electrophoresis, gel extracted using phenol:chloroform, and sequenced. Results were aligned with the predicted varicose transcripts using ClustalW and documented.

2.13.2 3'RLM-RACE

Total RNA (1 μ g) was reverse transcribed using 2 μ L of a 3' RACE adapter primer 5'-GCGAGCACAGAATTAATACGACTCACTATAGGT₁₂VN-3', 1.25 mM dNTP mix, 1X RT buffer, 1 μ L of M-MLV Reverse Transcriptase and nuclease-free water to 10 μ L. The adapter primer adds an additional 32 nucleotides to the 3' end of the mRNA transcripts. The RT reaction (1 μ L) was used as a template for Outer 3' RLM-RACE PCR analysis and amplified using a sense gene specific outer primer ML1341 and an antisense primer designed to the outer adaptor region. The same reaction conditions as

Outer 5' RLM-RACE were applied. Inner 3' RLM-RACE was performed using 1 μ L of Outer 3' RACE PCR products as a template, a sense gene specific inner primer ML1342 and an antisense primer designed to the inner adaptor region. PCR products were analyzed by 2% agarose gel electrophoresis, gel extracted using phenol:chloroform and sequenced. Results were compared against the predicted *varicose* transcripts using ClustalW and documented.

**Varicose: A Novel MAGUK Required for the Maturation and
Function of *Drosophila* Septate Junctions**

CHAPTER THREE

3.1 ACKNOWLEDGEMENTS

A special thanks to Kelly Teal for generating our Vari antibody. Xiao-Li Zhao helped generate our transgenic stocks. We thank Hugo Bellen for providing Nr_xIV antibody. Noor Hossain generated the compound eye micrographs. Leena Patel, Allison MacMullin and Verónica Rodríguez Moncalvo provided technical assistance. Thanks to Dr. Juliet Daniel and Dr. Ana Campos for their helpful suggestions and encouragement. Antibodies obtained from the Developmental Studies Hybridoma Bank: Cq4 (Crumbs, provided by E. Knust), 3A9 (α Spectrin, provided by D. Branton and R. Dubreuil), 4F3 (Discs Large, provided by C. Goodman), α 5 (Na⁺K⁺ATPase, provided by D. Fambrough), MAb2A12 (provided by M. Krasnow), 8D12 (Repo, provided by C. Goodman), 9F8A9 (Elav, provided by G.M. Rubin), MR1A (Prospero, provided by C. Doe), 7G10 (FasIII, provided by C. Goodman). This work supported by NSERC.

CONTRIBUTIONS

Dr. R. Jacobs performed dye injections and electron microscopy.

3.2 INTRODUCTION

Membrane **A**ssociated **G**uanylate **K**inases (MAGUKs) are a family of scaffolding proteins that regulate multiple cellular mechanisms such as cell polarity, adhesion, proliferation and synapse transmission. The multidomain composition of MAGUKs enable them to interact with receptors, ion channels, cytoskeletal proteins and other MAGUK members facilitating their ability to connect the cell surface to the cytoskeleton and cytosolic signaling proteins (te Valhuis et al., 2007). 22 MAGUK family members have been identified in vertebrates, 6 of which have invertebrate homologues.

Drosophila MAGUKs, Stardust and Discs Large regulate cellular processes such as cell polarization and proliferation (Bachmann et al., 2001; Woods et al., 1996) while Pyd and Camguk have a neurological function in sensory organ development and long-term potentiation, respectively (Hodge et al., 2006; Takahisa et al., 1996). The functional role of two novel MAGUK members, Skiff and Varicose remains unclear.

The objective of this chapter is to characterize the expression and function of *Drosophila* Varicose. To elucidate the role of Varicose during development, it is important to identify the tissues in which Varicose is localized. Employing dissection and immunohistochemical techniques, we have examined the expression pattern of Varicose from embryogenesis to adulthood and present our results in the first part of this chapter. The second part of this chapter focuses on the functional role of Varicose.

The genetic and molecular techniques developed to characterize *Drosophila* gene function are well established. These strategies enable functional targeting of a specific gene in order to dissect its role in developmental processes. Genetic tools such as P-

element excision are used to discover gene function from loss-of-function phenotype (reviewed by Adam and Sekelsy, 2002). Through imprecise excision, we have created 5 *varicose* alleles and identified phenotypic effects due to the loss of *varicose*. Moreover, the UAS-GAL4 system provides temporal and spatial control over the expression of a target gene. Using a gene specific promoter to regulate the expression of transcriptional activator GAL4, a target gene under UAS control can be expressed in a manner that reflects the GAL4 pattern (reviewed by Duffy, 2002). We were able to engineer a transgenic stock whereby Varicose is under UAS control. Misexpression of our Varicose transgene provided insights into Varicose function and are presented in the latter part of this chapter.

3.3 RESULTS 3

3.3.1 *Varicose, a Homologue of Vertebrate PALS2/VAM-1*

Our search for the invertebrate homologue of mammalian PALS2 identified *Drosophila* CG9326 as a candidate, sharing 39% amino acid identity to PALS2/VAM-1. Like its vertebrate counterparts, CG9326 encodes a MAGUK protein possessing PDZ, SH3 and GUK domains. The genomic sequence of CG9326 is 8381 bp in length and is composed of 10 introns and 11 exons (Crosby et al., 2007). Genome annotations predict that CG9326 may generate three transcripts, denoted B, C and D, which would encode three proteins, Vari^{L27B}, Vari^{L27D} and Vari, respectively (Fig. 3.1A). Transcripts B and D, but not C give rise to products encoding an N-terminal L27 domain (Fig. 3.1B). Two L27 domains interact heterophilically to link scaffolding proteins, for example Lin-2 (CASK) and Lin-7 (Veli) (Lee et al., 2002). CG9326-B differs from CG9326-D by a 21 amino acid insertion, as vertebrate PALS2 β differs from PALS α by a 14 amino acid insertion (Kamberov et al., 2000).

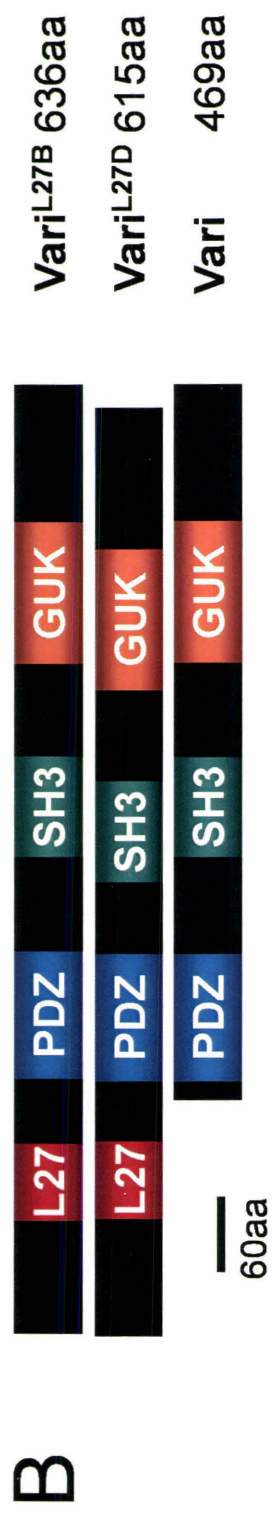
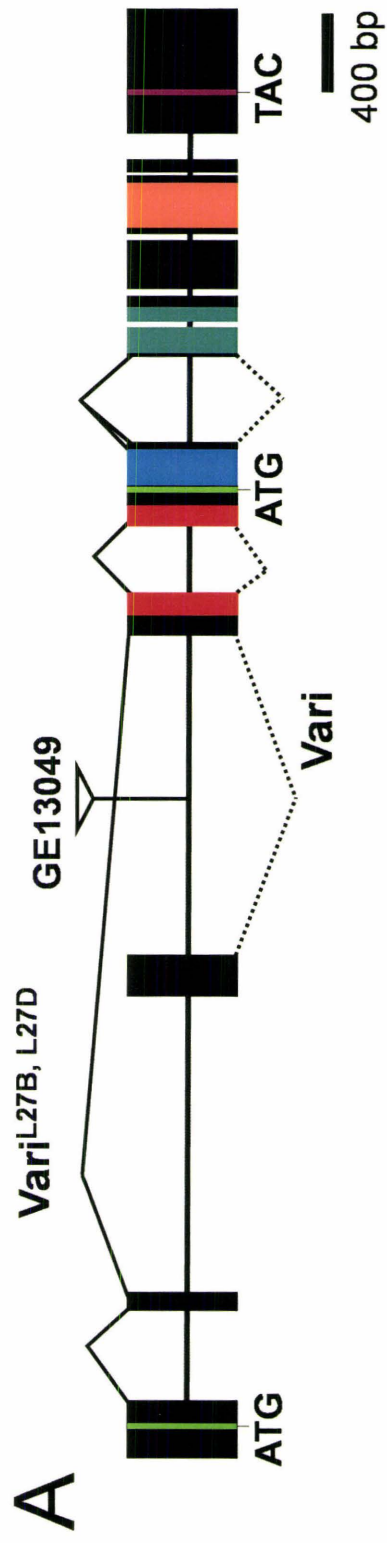
3.3.2 *Varicose Localizes to Embryonic Epithelial Tissues*

We have examined the transcript and protein expression of Varicose using *in situ* hybridization and immunohistochemistry, respectively. Varicose transcripts were detected from early stage 10 of embryogenesis until hatching (Teal, 2005). Protein expression was first detected during stage 13 of embryogenesis by immunolabeling with anti-Vari, and until late stage 17.

Varicose expression was restricted to epithelial tissues such as the epidermis, trachea, proventriculus, salivary gland, and hindgut (Fig. 3.2A).

Figure 3.1: Varicose is a MAGUK family member.

Vari has 3 predicted transcript isoforms, Vari, Vari^{L27B}, and Vari^{L27D} [A]. Each isoform encodes a protein possessing PDZ, SH3, and GUK domains, while Vari^{L27B} and Vari^{L27D} include an additional N-terminal L27 domain. Vari^{L27B} differs from Vari^{L27D} by a 21 amino acid insertion between the PDZ and SH3 domain [B].



Subcellularly, expression was restricted to the lateral membrane in the trachea (arrow, Fig. 3.2B), hindgut (Fig. 3.2C) and epidermis (Fig. 3.2D). We did not detect expression in non-ectodermal epithelia of the amnioserosa, in mesodermal/ectodermal epithelia of the malphigian tubules (Denholm et al., 2003), or in any epithelial tissues in our null allele, *vari*^{48EP} (Fig. 3.2E, Fig. 3.10A).

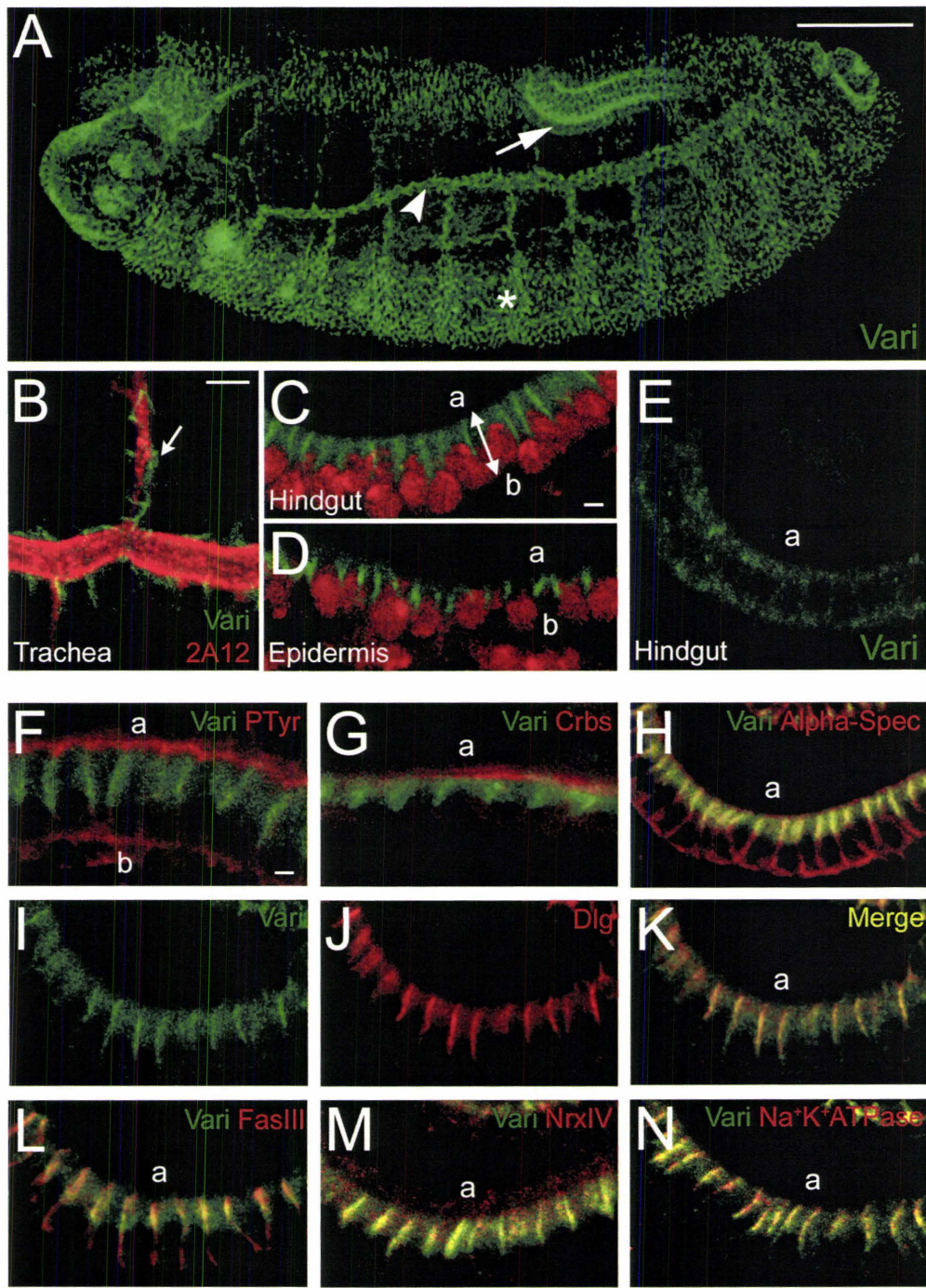
3.3.3 Varicose Localizes to the Septate Junction During Embryogenesis but not in Imaginal Discs

In *Drosophila*, MAGUKs typically function as scaffolding proteins upon which multiprotein complexes form to regulate cell polarization and adhesion (reviewed in Funke et al., 2005). The restricted membrane localization of Vari suggested to us that it may act similarly. We compared Varicose expression with various lateral membrane markers in the hindgut of stage 15 embryos (Fig. 3.2F-N). Vari localizes adjacent to, yet fails to co-localize with, the sub-apical marker Crumbs (Tepass, 1996) and the adherens junction marker Phosphotyrosine (Woods et al., 1997). Co-localization of Varicose and plasma membrane marker α -Spectrin (Dubreuil et al., 1997) is seen in the apical region of the lateral membrane but Vari is not seen in the basal region, indicating Vari localizes to the apicolateral membrane, a region corresponding to the SJ. Septate junctions are characterized by the localization of proteins such as Discs-large, Coracle and NeurexinIV (Baumgartner et al., 1996; Fehon et al., 1994; Woods and Bryant, 1991). Double-labeling experiments with Varicose and SJ markers Dlg, FasIII, NrXIV and Na⁺K⁺ ATPase (Fig. 3.2I-N) reveal a complete overlap of expression, suggesting that Varicose is localized solely in the septate junction. Co-localization of Vari and Dlg is also seen in

Figure 3.2: Varicose is detected at the septate junction in ectodermally-derived tissues.

[A-E] Whole-mount wildtype embryos labeled with Vari were visualized by confocal microscopy. All images are of stage 15 embryos. [A] Vari is detected in epithelial cells of the trachea (arrowhead), hindgut (arrow) and epidermis (*). Expression is also found in the salivary gland (not shown). [B] WT embryos stained with Vari (green) and tracheal antibody, 2A12 (red). Vari is restricted to epithelial cells and is excluded from tracheal lumen (arrow). [C-D] WT embryonic hindgut [C] and epidermis [D] labeled with Vari (green) and nuclear stain, propidium iodide (red). Vari is limited to the basolateral region of the plasma membrane in both tissues. [E] Vari was not detected at the SJ in the null allele, *vari*^{48EP}. Calibration: 50µm, A; 5µm, B; 2µm, C-E.

[F-N] Whole-mount stage 15 wildtype embryos. Hindguts were labeled with Vari (green) and lateral membrane markers (red). [F, G] Vari localizes basal to the subapical region, shown by the lack of overlap with Phosphotyrosine (F) and Crumbs (G). [H] Vari overlaps at the apical membrane with α -Spectrin (yellow) but is excluded from the basal membrane. Vari [I] is restricted to SJs, shown by co-localization with SJ markers Dlg [J, merge K; yellow], FasIII [L], NrXIV [M], and Na⁺K⁺ATPase [N]. Apical membrane faces are indicated (a) and basal (b). Calibration: 2µm, F-N.



the trachea, salivary gland and proventriculus (data not shown). We conclude that Varicose expression is restricted to the SJ region in all embryonic ectodermally-derived epithelial tissues.

Unlike MAGUK proteins Dlg and Sdt, Varicose expression was not detected in imaginal discs (Fig. 3.3). Vari is the first SJ protein not detectable in third instar imaginal discs. It is possible that polarization, proliferation and development of these tissues do not require Vari. Alternatively, Vari expression levels may be below the threshold of antibody detection.

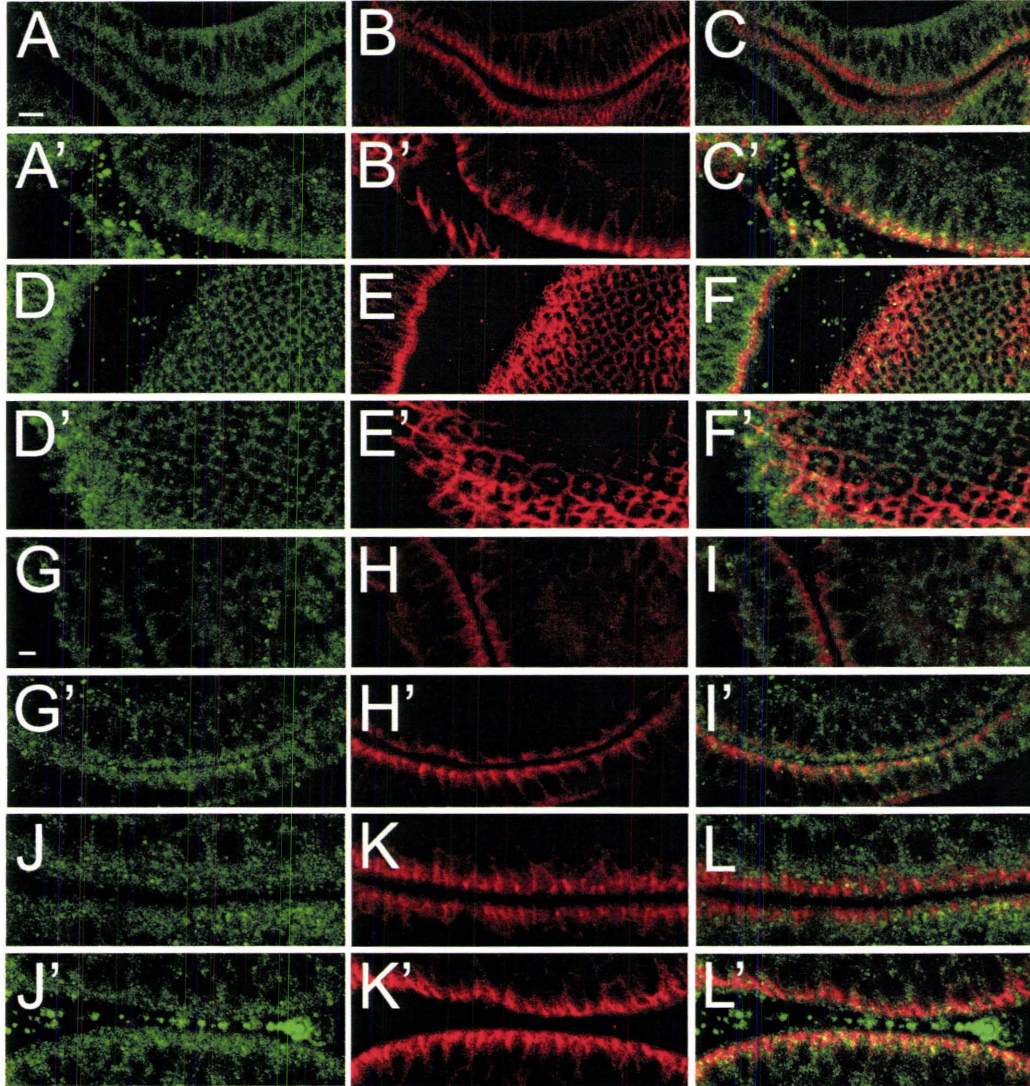
3.3.4 Novel MAGUK Function in the Nervous System

Pleated SJs are found in glial cells of the peripheral nervous system (PNS). For this reason we immunolabeled wildtype embryos for Vari and a glial cell marker Repo (Xiong et al., 1994). Varicose is localized to cell junctions in Repo positive cells in the embryo (arrow, Fig. 3.4A). To determine if Varicose localization was restricted to the SJ, we double-labeled embryos with Vari and NrxF, a known SJ marker of glial cells (arrow, Fig. 3.4B). We observed colocalization of Vari and NrxF (arrow, Fig. 3.4C) in peripheral nerves but unlike NrxF, Vari was not detected in midline glia (asterisk, Fig. 3.4C). We did not observe Vari expression within synaptic junctions (arrow, Fig. 3.4D) nor in the CNS (asterisk, Fig. 3.4D). Thus, in the embryo, Varicose expression is restricted to pSJs.

Varicose expression was observed in the neuroepithelium of the developing optic lobe. The optic lobe consists of two populations of cells, symmetrically dividing lateral

Figure 3.3: Varicose expression is not detected in imaginal discs.

Third instar larval discs were dissected and double immunolabeled with Vari post-immune serum (green) and Dlg (red) [A-L] or pre-immune serum (green) and Dlg (red) [A'-L']. We did not detect expression differences between and pre and post-immune sera in antennal [A-C], eye [D-F], leg [G-I] or wing [J-L] discs. It is possible that Varicose expression may be weak in the eye discs [D-F], however, characteristic SJ expression pattern is not observed. Images are a single section, visualized by confocal microscopy. Gain levels for images A'-L' were increased in order to visualize possible immunolabeling. Calibration: 5 μ m, A-F; 2 μ m, G-L.



neuroepithelial (NE) cells and asymmetrically dividing medial neuroblasts. NE cells possess similar properties as embryonic epithelial cells and express junctional markers at similar locations (Egger et al., 2007). To determine if Varicose localized to SJs in postembryonic epithelia, we labeled third instar larvae brains with Vari and Dlg. Dlg localizes to the SJ in NE cells (arrow, Fig. 3.4F) and to the cortex in neuroblasts (left of arrowheads, Fig. 3.4E-G). In contrast to what we observed in embryonic epithelia, Varicose has limited colocalization with Dlg (Fig. 3.4G). Varicose expression is found in the apical cytoplasm of NE cells (arrow, Fig. 3.4E) but is not found in neuroblasts (left of arrowheads, Fig. 3.4E). We were unable to detect neuroepithelial labeling with pre-immune sera suggesting the observed pattern is due to Varicose expression (Fig. 3.10B-D). If this expression pattern is true for other SJ markers, we would expect to see NrxFIV at the SJ of NE cells. We did not observe any NrxFIV expression in NE cells or in neuroblasts; we however did detect expression in neuroblast progeny (not shown). Expression of Varicose restricted to the neuroepithelium of the optic lobe suggests a role in the symmetrically dividing cell pool. Moreover, we have identified a MAGUK member that does not always associate with the plasma membrane, suggesting a novel role for this protein in the neuroepithelium.

Central neuroblasts found in third instar larvae brains also express Varicose. We performed various double-labeling experiments using several neuroblast markers (Fig. 3.4H-K). Varicose did not colocalize with Dlg, a cortex marker, Prospero, a ganglion mother cell marker, or Repo, a glial cell marker (Doe et al., 1991; Peng et al., 2000; Xiong et al., 1994). Weak Varicose expression was observed in differentiated neurons

labeled with Elav (Fig. 3.4I) (Berger et al., 2007). We concluded that Varicose expression at this stage remains in the cytoplasm of neuroblasts.

Identifying Varicose expression in neuroblasts prompted us to characterize Varicose expression in the adult nervous system. We immunolabeled pupal brains 50 hours after eclosion with Vari and either Dlg (Fig. 3.4L), FasII (Fig. 3.4M), Elav (Fig. 3.4N) or Repo (Fig. 3.4O). We did not observe Varicose expression in the mushroom bodies or in the antennal lobes. Varicose however, colocalized with Dlg in the cell bodies of neurons surrounding these neuropile regions (yellow; Fig. 3.4L). We deduced that these cell bodies belong to differentiated neurons as opposed to glial cells by localization of Vari to Elav (Fig. 3.4N) and not Repo labeled cells (Fig. 3.4O). Although Elav has been shown to be transiently expressed in neuroblasts and glioblasts during embryogenesis, Elav expression was not detected in late embryonic glial cells or in postembryonic NBs (Berger et al., 2007). Therefore, Varicose localizes to a subset of differentiated neurons surrounding neuropile regions of the adult nervous system.

3.3.5 Loss-of-Function Varicose Mutants are Embryonic Lethal

We have created a loss-of-function allelic series, *vari*^{48EP}, *vari*^{K4}, *vari*^{L4}, *vari*^{B4}, and *vari*^{B5}, to determine whether Vari plays a role in septate junction assembly. The embryonic lethal P-element insertion line GE13049 (GenExel, Inc), contains an EP insertion 3507 bp downstream of the translation start site of Vari^{L27B} and Vari^{L27D}, and 1731 bp upstream of the translation start site of Vari (Fig. 3.1A). Using standard procedures, we mobilized GE13049 and generated 5 mutant alleles by imprecise excision (Figure 3.5). Here we present allele *vari*^{48EP}, an excision allele which removed 4717 bp

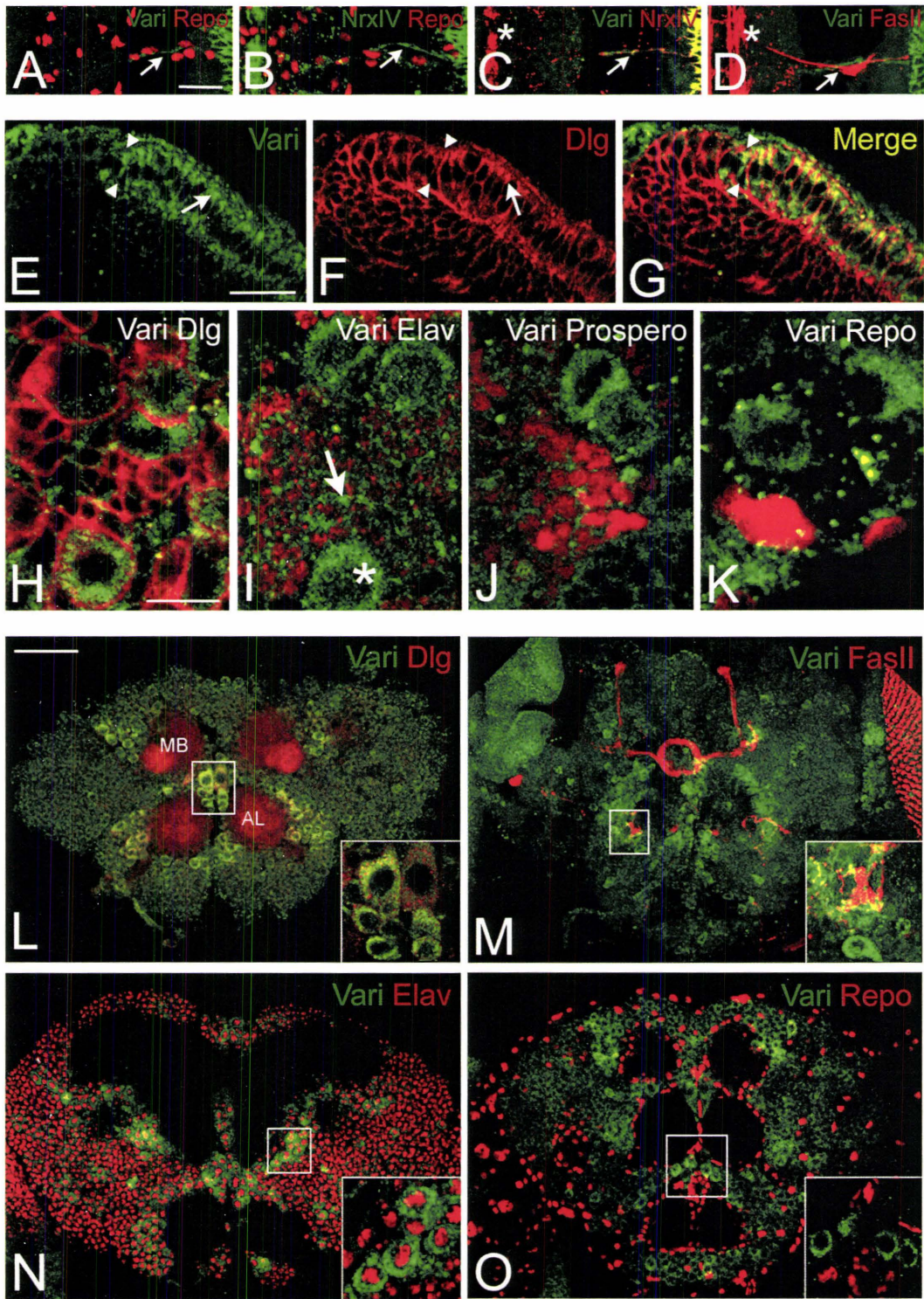
Figure 3.4: Varicose nervous system expression is novel for MAGUKs.

[A-D] Stage 16-17 wildtype embryos were stained with Vari and a glial cell marker, Repo. Vari localizes with Repo in peripheral glial cells (arrow, A) in a similar pattern to NrxF, a known pSJ marker of PNS glia (arrow, B). Double-labeled embryos with Vari and NrxF show colocalization of these proteins in peripheral glia (arrow, C) but not in midline glia (asterisk, C). No Vari labeling was found in the CNS (at left of A, asterisk, C-D). FasciclinII antibody labeled motor axons and synaptic terminations (D), demonstrating that Vari does not label developing synapses (arrow, D). Images A-D are a ventral view of a single confocal section. Anterior at top; ventral midline at left. Calibration: 20µm, A-D.

[E-G] Brains from late 3rd instar larva were labeled with Vari and Dlg. Images are a dorsal view of a single confocal section. (E) Vari expression is restricted to the apical region (arrow) of symmetrically dividing epithelial cells of the neuroepithelium (NE) (right of arrowheads) and excluded from the asymmetrically dividing neuroblasts (NBs) (left of arrowheads). (F) Dlg is detected at the SJ of NE cells (arrow) and distributed cortically in NBs. Colocalization of Dlg and Vari is limited along the lateral membrane of the NE (G). [H-K] Varicose is expressed in the cytoplasm of a subset of NBs in third instar larvae. Vari (green) expression is detected throughout the cytoplasm in a subset of central brain neuroblasts. Vari fails to co-localize with Dlg (H), which outlines the cell cortex and appears to have low levels of expression in differentiated neurons (arrow, Elav, I). Vari is excluded from ganglion mother cells that label for Prospero (red, J), and

glial cells that label for Repo (red, K) (NBs denoted by asterisk). Calibration: 20 μ m, E-G; 10 μ m, H-K.

[L-O] Pupa brains stained with Vari (green) and Dlg (L), FasII (M), Elav (N) or Repo (O) (red). (L, N, O) Single cross sections visualized by confocal microscopy. Vari and Dlg co-localize in cell bodies (inset, L) but fail to co-localize in the antennal lobes (AL) and mushroom bodies (MB). (M) A projection of sections visualized by confocal microscopy. Vari is excluded from the mushroom bodies and axon tracts labeled by FasII. Vari expression appears to concentrate in areas surrounding the axon tracts (inset, M). Vari localizes to cells expressing Elav, representing a subset of differentiated neurons (inset, N) but is not expressed in glial cells labeled with Repo (inset, O). Calibration: 50 μ m, L-O.



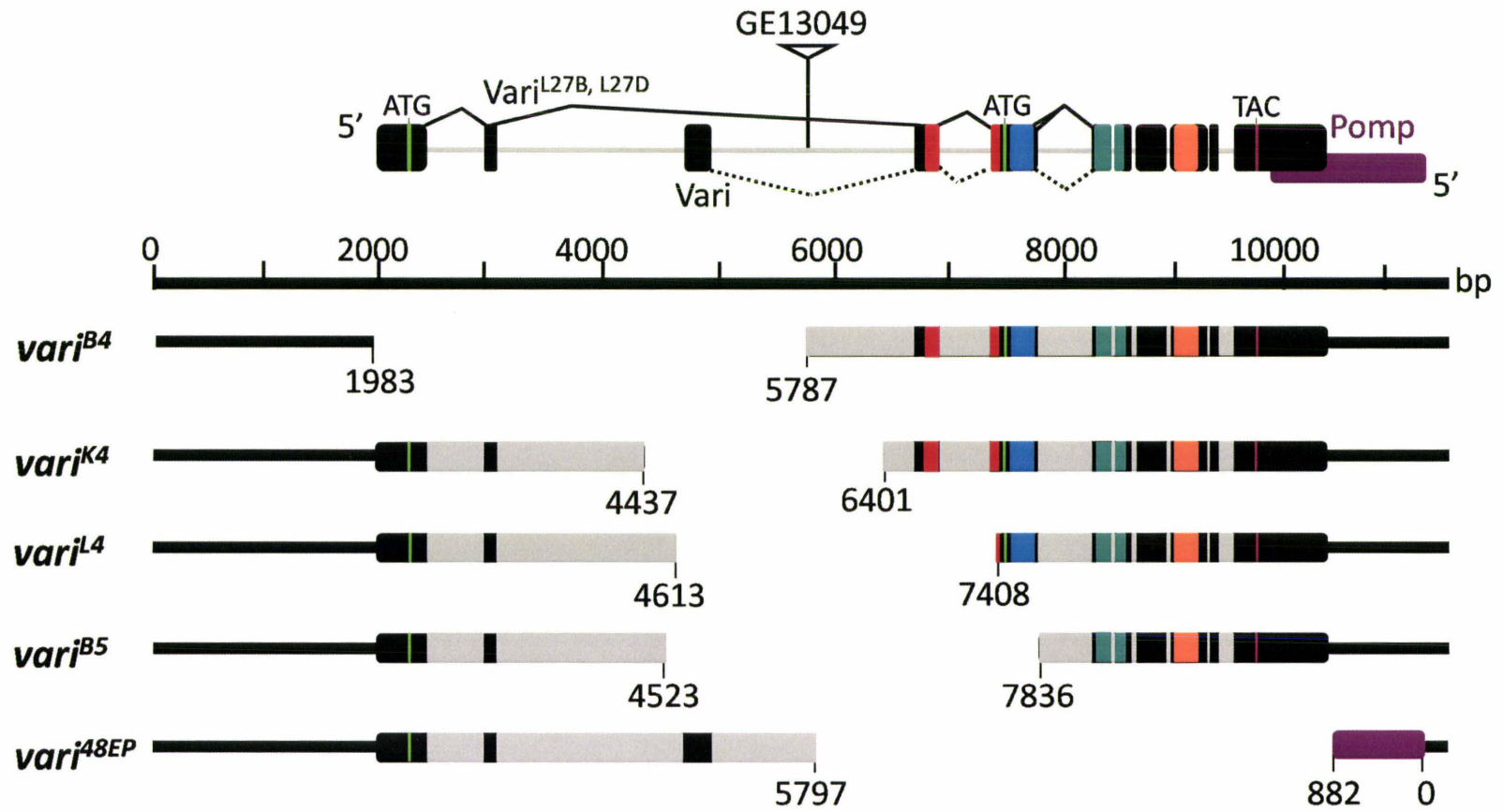
of genomic sequence (20792456...20797173) leaving behind 416 bp of the P-element. Our other alleles, *vari*^{K4} and *vari*^{L4} are clean excisions that removed 1964 bp and 2795 bp of genomic sequence, respectively. In addition, *vari*^{B4} removed 3806 bp leaving behind 27 bp of P-element sequence, while *vari*^{B5} removed 3313 bp of genomic sequence leaving 216 bp of P-element sequence behind. All *vari* alleles are late embryonic lethal, however *vari*^{K4} has few larval escapers that are second instar lethal stage and all fail to complement the lethality of GE13049 or the *Df(2L)Exel*⁷⁰⁷⁹ deficiency. We also consider GE13049 a null allele as its phenotypes are indistinguishable from mutant *vari*^{48EP} or transheterozygotes. *Df(2L)Exel*⁷⁰⁷⁹ is a molecularly characterized deficiency deleting chromosomal region 38E6-38F3. All 7 alleles are phenotypically null for *varicose* function, however the 3' UTR of both *varicose* and *CG9324/pomp*, a 20S maturase, overlap (Lundgren et al., 2005). Our *vari*^{48EP} excision removed the 3' UTR of *pomp* as well as 3 carboxy-terminal amino acids. This *vari* allele complements a lethal allele, *pomp*^{EY06518}, indicating that our lethal phenotype is a result of disruption of *vari*. In addition, our sequenced revertant, *vari*^{34P}, restores viability.

3.3.6 Septate Junction Assembly Requires Varicose

Septate junction assembly begins during stage 14 of embryogenesis (Tepass et al., 2001; Tepass and Hartenstein, 1994), a time that corresponds to the onset of Varicose expression. To determine if Varicose is required for the assembly of septate junctions, we assessed the subcellular localization of SJ markers in *vari*^{48EP} mutants. Proteins normally enriched at the septate junction, such as NrXIV, FasIII and Na⁺K⁺ATPase are mislocalized basally in the absence of Varicose function (arrows, Fig. 3.6A-D). These

Figure 3.5: Varicose alleles created by imprecise excision.

Imprecise excision of P-element insertion line GE13049 generated an allelic series of *vari*. Five *vari* alleles were produced, *vari*^{B4}, *vari*^{K4}, *vari*^{L4}, *vari*^{B5} and *vari*^{48EP} removing 3806 bp, 1964 bp, 2795 bp, 3313 bp and 4717 bp of genomic sequence, respectively. Excision *vari*^{48EP} generated a protein null allele. The 3'UTR of *vari* overlaps with the 3'UTR of the adjacent *CG9324/pomp*. The *vari*^{48EP} excision removes the 3'UTR's of both genes, and three terminal amino acids of CG9324. Start/stop codons and protein domains are colour coded as follows: start sites (green), L27 domains (red), PDZ domain (blue), SH3 domain (teal), GUK domain (orange), stop codon (purple), introns (grey).



data are consistent with the findings of Wu et al., (2007). However, localization of SJ marker Dlg was unaffected (not shown). Discs-large is a tumor suppressor that acts to regulate cell polarization, proliferation and adhesion (Woods and Bryant, 1991). It is possible that multiple protein complexes function at the septate junction in independent pathways. These data suggest that Varicose may play a role in the assembly of septate junctions but is not required for the establishment of cell polarity.

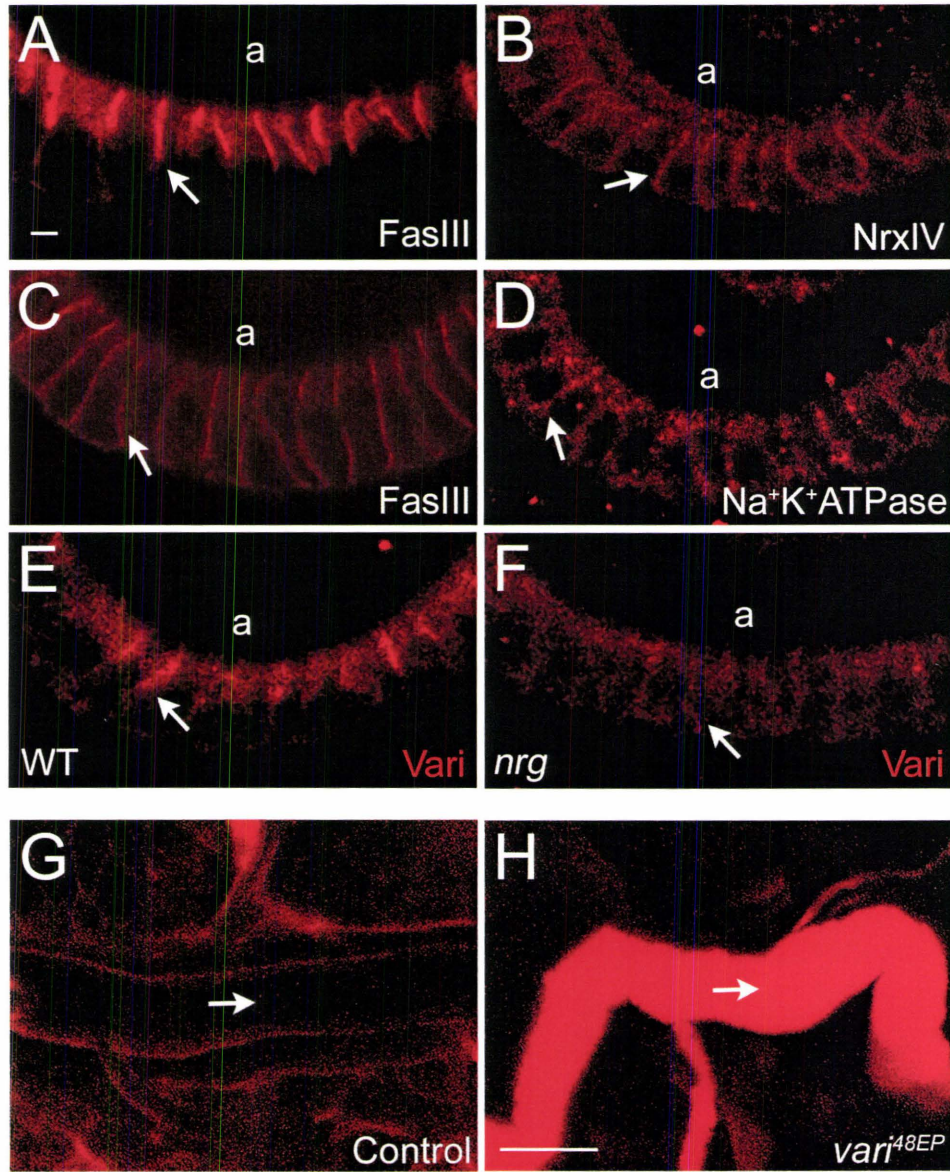
As previously mentioned, proper localization of SJ components is interdependent. We assessed the proper localization of Vari in several SJ mutants including *dlg^{X1-2}*, *nrg¹⁴*, *nrx⁴³⁰⁴*, and *cora^{K08713}*. Unexpectedly, Vari was properly localized in all SJ mutants examined, except *nrg¹⁴*. Varicose expression is severely reduced and mislocalized basally along the lateral membrane (Fig. 3.6E, 3.6F). While *nrg¹⁴* mutants display reduced or absent transverse septae, the spacing between epithelial plasma membranes is maintained (Genova and Fehon, 2003). It is unknown whether the interaction between Vari and Nrg occurs within the same cell or between cells however, this data supports the interplay between SJ proteins and its necessity for their proper localization.

Septate junctions are the structural basis of the paracellular barrier in insect epithelia (Fristrom, 1982). To determine whether the transepithelial barrier was compromised in *vari* mutants we performed dye exclusion assays, as described by Lamb et al., (1998). Rhodamine- conjugated dextran was injected into late stage wildtype embryos and dye was excluded from the lumens of the salivary glands and trachea beyond 90 minutes (Fig. 3.6G). In contrast, within 30 minutes of injection, dye could be detected in the tracheal lumen of *vari^{48EP}* mutants (Fig. 3.6H).

Figure 3.6: Distribution of septate junction markers and the seal of the transepithelial barrier are compromised in *vari* mutants.

[A-D] We examined the distribution of SJ markers in *vari* mutants. [A] Balancer LacZ control. [B, C] *vari*^{GE13049}. [D] *vari*^{48EP}. Mutant embryos were stained with NrXIV, FasIII or Na⁺K⁺ATPase. Homozygous embryos were selected by absence of balancer lacZ and whole-mount stage 15 embryos were visualized by confocal microscopy. FasIII [A], NrXIV, and Na⁺K⁺ATPase (q.v. Fig. 2L-N) localize to hindgut epithelial SJs in lacZ control embryos and are excluded more basally (arrow, A). In *vari* mutants, when compared to controls, NrXIV, FasIII, and Na⁺K⁺ATPase are mislocalized basally along the lateral plasma membrane (arrows B, C, and D, respectively). [E, F] We assessed the distribution of Vari in the SJ mutant, *nrg*. Mutant embryos were stained with Vari antibody and homozygous embryos were selected by absence of a balancer GFP expression. In stage 15 control embryos, Vari localizes to the SJ of epithelial hindgut cells (arrow, E), however accumulation of Vari is greatly reduced and mislocalized basally in *nrg* mutants (arrow, F). Apical denoted by (a). Calibration: 2µm, A-F.

[G, H] The integrity of the transepithelial barrier in *vari*^{48EP} mutants was determined by permeability assay as described by Lamb et al. (1998). Following injection of rhodamine-conjugated dextran, dye was detected within the tracheal lumen of mutants (arrow, H) but excluded from the lumen in controls (arrow, G), indicating disruption in barrier function. Dye remained undetectable in the lumen of controls 90 minutes post-injection. Calibration: 10µm, G and H.



In order to gain insight into the structural underpinnings of barrier establishment, we examined the ultrastructure of cell junctions in *vari*^{48EP} mutants through semi-serial electron microscopy. We observed no structural differences between wildtype (Fig. 3.8C) and *vari*^{48EP} (Fig. 3.8D) septate junctions or lateral membranes. We did not observe pleated junctions characteristic of SJs in either group. Ladder-like septa found in pleated sheets typical of mature SJs (Tepass and Hartenstein, 1994) do not appear in wildtype until stage 17, and at this stage, signs of necrosis indicate that *vari* homozygotes are dying. Taken together, these observations support a requirement for *varicose* in septae formation, and establishing the seal of the transepithelial barrier.

3.3.7 Loss of vari Results in Dilated Tracheal Branches and Reduced Luminal Staining

Previous reports suggest that a disruption of septate junction assembly also reduces the efficiency of apical secretion into the tracheal lumen. This generates abnormal fibrillar structures in the lumen and distorted and tortuous tracheal trunks (Luschnig et al., 2006; Wang et al., 2006). If *Varicose* is required for septate junction assembly, then tracheal development should also require *Vari*. To address this possibility, we labeled the tracheal lumen of all *vari* mutant alleles with the luminal marker MAb2A12 (Fig. 3.7). Tracheal abnormalities were found in homozygotes of these alleles and all hetero-allelic combinations. However, tracheal morphology reverted to wildtype in *Drosophila* carrying a precise excision of *vari*^{GE13049}, *vari*^{34P}, and in transheterozygotes, *vari*^{GE13049}/*vari*^{34P} (Fig. 3.7C), indicating that the genetic background of the original insert did not contribute to the phenotype. Overexpression of *UAS-vari*

using *breathlessGAL4* fails to rescue the tracheal phenotype (data not shown). However, ubiquitous expression using *daughterlessGAL4* rescues the tracheal phenotype of *vari*^{48EP} null embryos (Fig. 3.7I) in addition to rescuing lethality. Furthermore, the mutant tracheal phenotype was evident in transheterozygotes from different genetic backgrounds (Fig. 3.7K and 3.7L). Tracheal branches exhibit a balloon-like appearance, representing large dilations. However, tube-length was not dramatically affected. In addition, luminal stain was reduced in all *vari* mutants (Fig. 3.7B, 3.7D-H) when compared to the controls (Fig. 3.7A and 3.7C). This is consistent with earlier findings of reduced levels of Vermiform and no Serpentine labeling in *vari* mutants (Wu et al., 2007).

To further understand the tracheal dilations, we examined tracheal cell ultrastructure using electron microscopy. Although *vari* mutants have abnormally large lumen diameters (arrow, Fig. 3.8B) compared to controls (Fig. 3.8A), the overall cell morphology is similar to wildtype (Fig. 3.8A and 3.8C). In addition, cuticle secretion was similar in both mutants and wildtype controls. Proper cuticle secretion, tanideal folds and normal cell morphology in *vari* mutants suggest that its role may be independent of apical secretion.

3.3.8 *Varicose is Required for the Development of Adult Structures*

Absence of Vari from SJs of imaginal discs suggests an alternate role for Varicose during pupal and adult development. Rescue experiments of our *vari*^{48EP} null allele provided insight into the possible role of Varicose during the development of adult structures. Ubiquitous expression of *UAS-vari* using *daGAL4* rescues lethality of null embryos. Viability of the rescued animals ranges from late pupation (80%, n=73) to

Figure 3.7: Varicose is required for tracheal development.

[A-L] The tracheal lumen of early stage 16 *vari* mutant embryos were labeled with MAb2A12. In both wildtype [A; magnified A'] and in embryos heterozygous for the original EP insert and a precise excision of that insert [C], the diameter of the Dorsal Trunk (DT) is uniform, and the Lateral Trunk [LT] is continuous with the DT. All *vari* mutants [B, D-H, J, and heteroallelic K and L] share similar tracheal defects. Mutants exhibit large dilations along the DT (arrowhead, H) and LT (*, H). Some LT branches appear disconnected from the DT (arrow, H). Irregular branch diameters are also seen in 2° branches. Luminal staining is reduced in all *vari* alleles in comparison to wildtype and control. Tracheal phenotypes of null *vari*^{48EP} embryos are restored upon ubiquitous expression of *UAS-vari* by *daGAL4* [I]. Lateral view: anterior to the left, dorsal is up. Calibration: 20µm, A, A', and C.

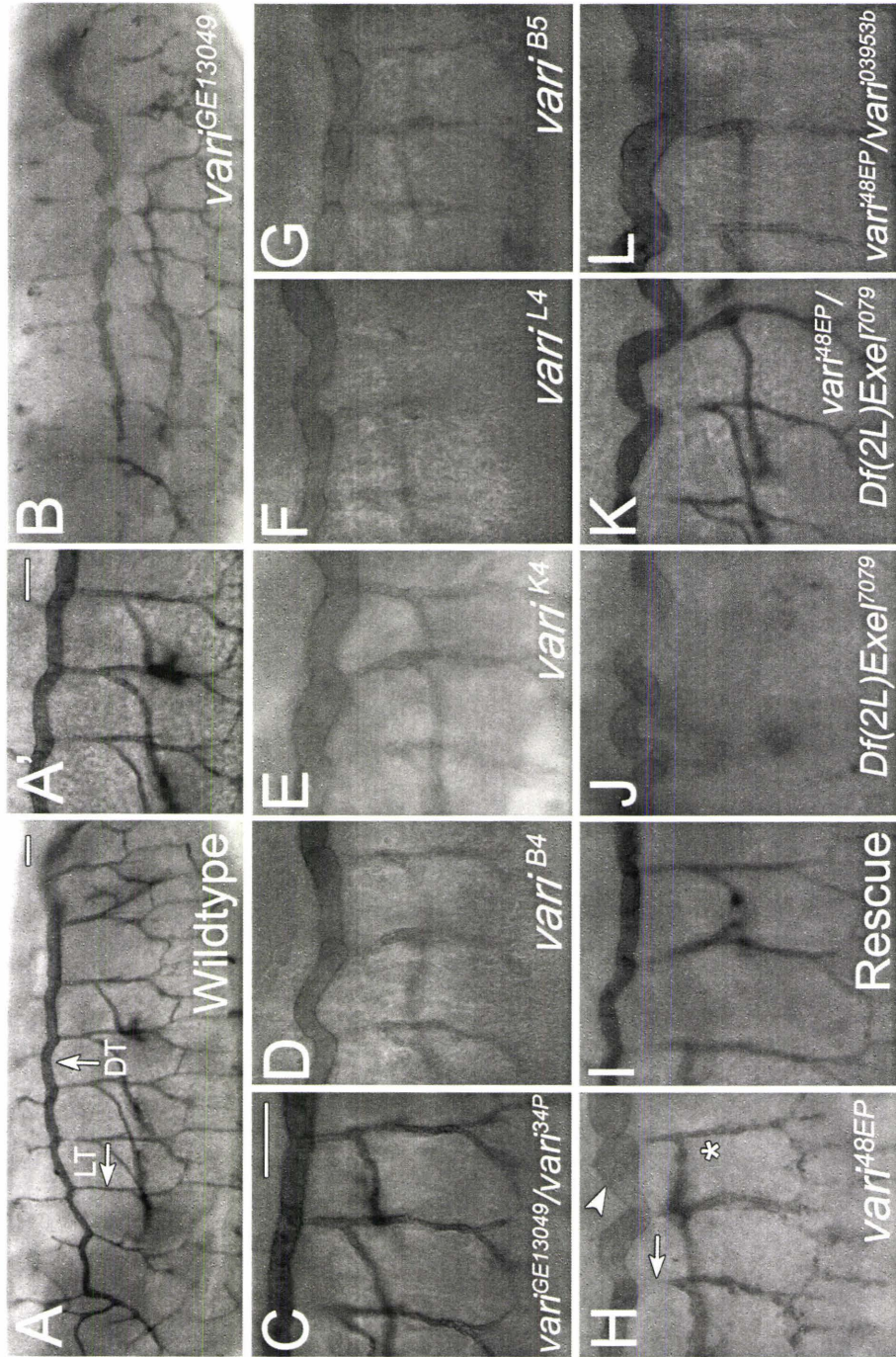
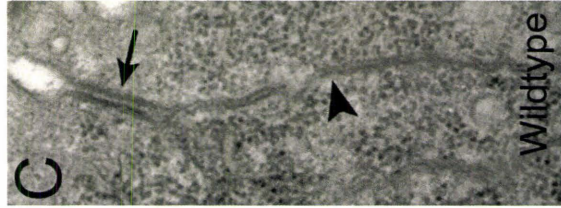
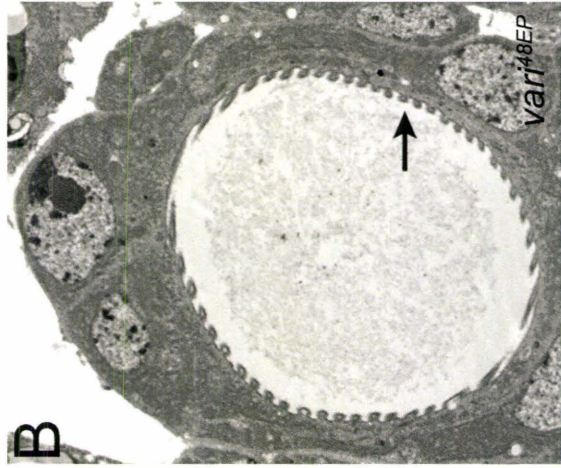
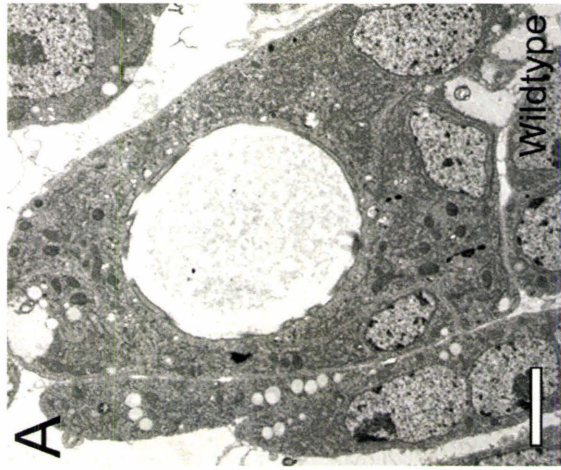


Figure 3.8: Examination of cellular ultrastructure in *vari*^{48EP} mutants.

[A-D] We have compared the ultrastructure of the cells of stage 16 trachea and hindgut between wildtype [A, C] and *vari*^{48EP} mutants [B, D]. The lumen of *vari* trachea could be significantly dilated relative to wildtype, but the structure of luminal cuticle and tanideal ridges were not affected (arrow B). We also examined the ultrastructure of epithelial cell junctions from semi-serial sections of the hindgut. Relative to wildtype [C], apposed lateral membranes (arrows) and septate junctions (arrowheads) were similar in *vari* mutants [D]. Calibration: 2 microns A, B and 200 nm C and D.



viable adults (20%). Viable adults are weak, fail to fly or walk, and have a life span averaging 3 days. While grooming habits are attempted, lack of coordination appears to prevent the rescued adult from performing these activities. In addition, adults are unable to move/raise their legs, although the action seems to be attempted. The ability to rescue null embryos with a *Vari* transgene lacking the L27 domain suggests that its role during development is not necessary for viability.

We examined adult epithelial structures for developmental abnormalities and found disruption in ommatidial patterning and wing hair alignment. Overexpression of *UAS-vari* in both a heterozygous mutant (Fig. 3.9A) and wildtype background (Fig. 3.9C) show a mild phenotype where interommatidial bristles (IOBs) are missing (arrowhead, Fig. 3.9A'-C') and few are misaligned (asterisk, Fig. 3.9A'-C'). This phenotype is also seen in the parental *daGALA* control (data not shown). However, overexpression in a null mutant background results in missing ommatidia or extra IOBs (arrow, Fig. 3.9B') in addition to missing and irregular bristle patterns.

SJ components Gliotactin (Gli) and Cora are required for proper hair alignment in the adult wing (Venema et al., 2004). We examined overall wing morphology of adult flies overexpressing *Vari* in a null mutant background (inset, Fig. 3.9E) and found it to be similar to the controls (inset, Fig. 3.9D). Although morphology is unaffected the wing hair alignment is abnormal. Unlike the control wing (Fig. 3.9D), rescued adults show patches of wing hairs with abnormal alignment compared to their neighbouring hairs (arrowheads, Fig. 3.9E). The abnormal hair alignment was observed in unmounted wings eliminating the possibility of a mounting artifact. This phenotype is unlike that of

Frizzled pathway mutants where wing hairs largely retain parallel alignment in relation to their neighbouring hairs but are incorrectly polarized (Wong and Adler, 1993). We examined the polarity of bristles on the thorax, abdomen and legs of rescued adults (data not shown) and did not detect abnormal polarization. Furthermore, we did not detect any multiple hairs per cell. From these results, we suspect that the misalignment phenotype is not due to a disruption in planar cell polarity.

Figure 3.9: Ommatidial patterning and wing hair alignment are abnormal in *vari* mutants.

[A-C] Ubiquitous overexpression of *UAS-vari* using *daGAL4* in heterozygous *vari*^{48EP} null mutant (A), homozygous *vari*^{48EP} null mutant (B) and wildtype backgrounds (C). [A'-C'] Magnified images of A-C. Overexpression results in a mild phenotype where interommatidial bristles (IOBs) are missing (arrowheads) and few as misaligned (below the asterisk). Overexpression in a null mutant background results in missing ommatidia and extra bristles (arrows, B'). In addition, IOBs are missing and irregularly patterned (asterisk, B'). [D-E] No phenotypic effects are observed in the wing by overexpression of *UAS-vari* in a wildtype background. Wing hairs retain a parallel alignment while pointing distally (E) and overall wing morphology remains wildtype (inset, E). In a null mutant background, overexpression results in abnormal wing hair alignment (arrowheads, D). While some hairs point distally, patches of hairs point in random directions with irregular alignments when compared with neighbouring hairs. Overall wing morphology is similar to the control (inset, D). A-C: 140X magnification. A'-C': 300X magnification. D, E: 20X magnification.

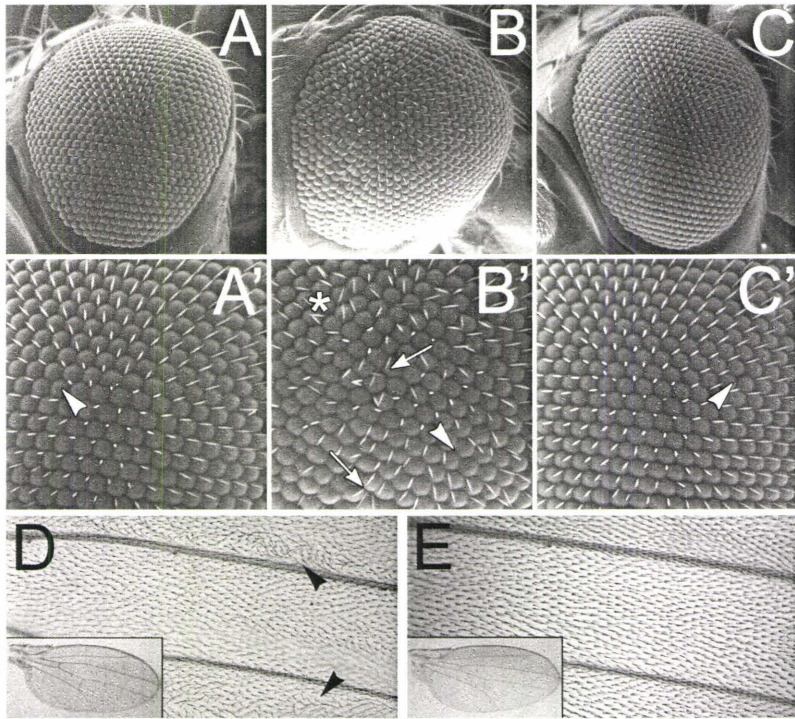
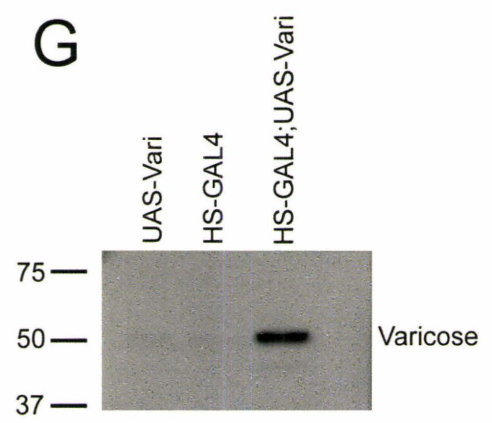
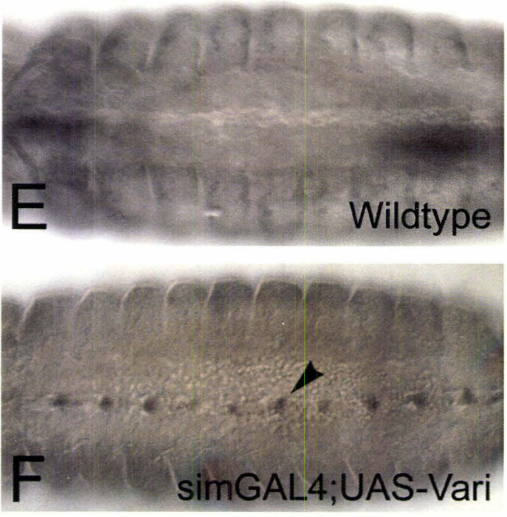
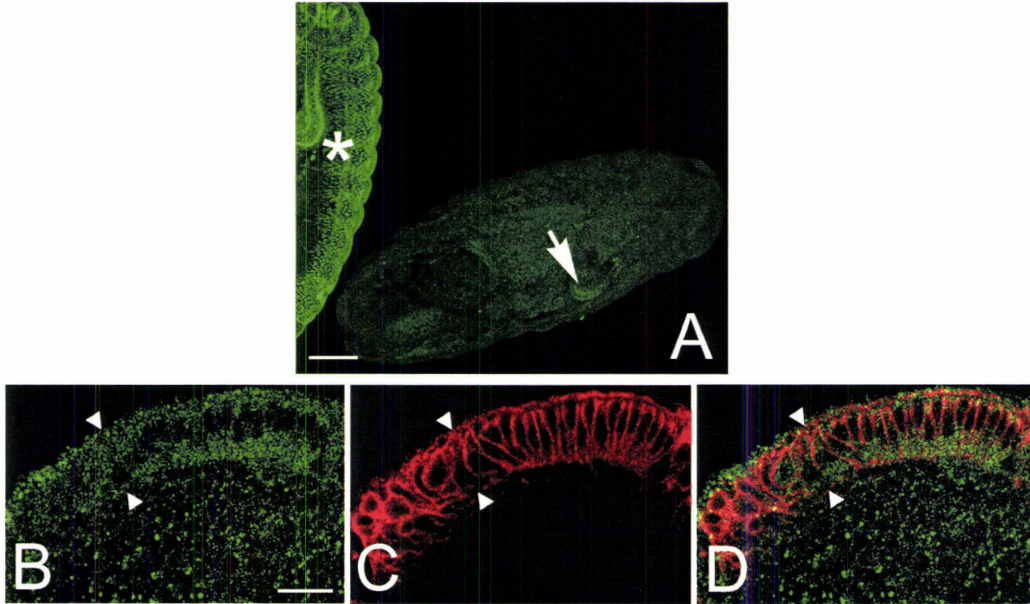


Figure 3.10: Expression patterns observed are specific to varicose.

To ensure specificity of anti-Vari, whole-mount *vari*^{48EP} null embryos were labeled, mounted and visualized by confocal microscopy. Homozygous embryos were selected by the absence of balancer GFP expression. [A] The wildtype Varicose expression pattern seen in the balancer controls (asterisk) was not observed in embryos homozygous for null allele *vari*^{48EP} (arrow). Similarly, Varicose expression is not detected in neuroepithelial cells immunolabeled with pre-immune sera (B) and Dlg (C; merge, D). To further establish antibody specificity, we misexpressed *UAS-vari* in the mesectoderm, using *single-mindedGAL4*. Embryos were collected and labeled using anti-Vari. When misexpressed, Varicose was seen in the embryonic ventral midline [arrowhead, F] whereas midline expression is absent in wildtype embryos labeled with anti-Vari [E]. Ventral view, anterior to the left. [G] In addition, we overexpressed *UAS-vari* using *heat-shockGAL4* to visualize *varicose* protein levels by Western blotting. In contrast to low protein levels in wildtype embryos, overexpression provides sufficient protein levels to detect Varicose. Calibration: 50µm, A; 10µm, B-D.



3.4 DISCUSSION 3

Our studies have identified a novel MAGUK family member encoded by *Drosophila* CG9326, *Varicose*. We have shown that *Varicose* localizes to pSJs of all embryonic ectodermally-derived epithelial tissues as well as the pSJs of the PNS. We have detected *Vari* expression in the neuroepithelium of the developing optic lobe in a non-junction associated pattern, which is unique for a MAGUK member. Expression of *Varicose* in a subset of central brain neuroblasts and differentiated neurons of the adult nervous system emphasizes the importance and versatility of its function throughout development. Mutations in *vari* result in mislocalized SJ markers and disruption of the paracellular seal. Loss-of-function *vari* alleles display dilated and contorted tracheal tubes implicating *vari* in tracheal morphogenesis. Furthermore, expression of *Vari* during the development of adult tissues regulates ommatidial patterning and wing hair alignment.

3.4.1 *Varicose Plays a Role in Septate Junction Assembly*

We have presented here several lines of evidence suggesting *Varicose* is required for septate junction formation. First, *Varicose* colocalizes with known SJ protein *NrxIV* in all embryonic pSJs and *NrxIV* is mislocalized in the absence of *varicose* activity. Second, ladder-like septa do not develop in *vari* mutants. Third, the transepithelial barrier of *vari* mutants is ‘leaky’ to tracer dyes.

Embryos mutant for *varicose* show mislocalization of SJ proteins like *NrxIV*, *FasIII* and the Na^+K^+ ATPase basally along the plasma membrane of epithelia (this thesis and Wu et al., 2007). The localization of SJ protein *Dlg* was not affected however, indicating *Vari* is not required to establish and maintain epithelial polarity. This is not a

surprising result as the onset of Varicose expression appears midway through embryogenesis, a time when polarity has already been established and SJs begin to assemble (Tepass et al., 2001).

SJ proteins such as FasIII and Na⁺K⁺ATPase are mislocalized in *vari* mutants. It is possible that in the absence of *vari*, the assembly of key proteins is interrupted, disrupting the architecture of the junctional region and creating a cascade of mislocalized proteins. Proper localization of Vari requires Neuroglian. It is probable that the mislocalization of Vari is secondary to a disruption in SJ structure caused by the mutation in *nrg*. Although Varicose has been shown to interact with NrXIV (Wu et al., 2007), our studies show that Varicose localization is independent of this function.

Interestingly, Varicose was not detected in third instar imaginal discs. This is the first recorded junctional protein found in embryonic epithelia and absent in imaginal disc epithelia. These results could suggest that the mechanisms regulating junction structure during embryonic and larval development differ. Identifying other junctional players will be necessary to dissect the structural differences between these junctions.

Our ultrastructural analysis suggests that *vari* mutant embryos die before intermembrane septa develop. *nrxIV* and *cora* mutants lack septa, which are proposed to have a sealing function in the transepithelial barrier (Baumgartner et al., 1996; Lamb et al., 1998). An affinity approach has identified NrXIV as a potential Vari binding partner (Wu et al., 2007). These data are consistent with the failure to exclude dye in embryonic trachea. In contrast, SJ mutants, *gliotactin* and *sinuous* (*sinu*) show defects in septa array and septa number, respectively (Schulte et al., 2003; Wu et al., 2004). Mutations in *vari*

enhance the *sinu* phenotype (Wu et al, 2004). Together these results suggest Vari, like NrxF and Cora, functions in assembling septa strands. Further, the low levels of Vari in larvae, and their absence from imaginal discs suggest that Vari is not essential to maintain SJ.

SJ integrity in *Drosophila* requires Megatrachea (Mega), a claudin that has a C-terminal PDZ binding domain (Behr et al., 2003). It has been suggested that a MAGUK member may act to tether Mega to the NrxF/Cora complex to assemble the SJ (Behr et al., 2003; Ward et al., 1998). We propose Vari as a candidate for this function.

3.4.2 A Novel Role for MAGUKs in the Nervous System

Expression of Vari in peripheral glia, but not the perineural sheath or midline glia of the embryonic nervous system is consistent with function in the establishment of ectodermally-derived pSJs. Neural expression was not detected in embryos. However, the distribution of Vari in the late larval and adult central nervous system suggests non-junctional roles for this MAGUK. In the optic lobe NE, which does express Dlg, Vari expression overlaps, and extends into the apical cytoplasm. Vari is not expressed in NBs of the embryo and medial optic lobe, yet is expressed in the cytoplasm of some central NBs of late third instar, and in low levels in the soma of differentiated neurons. This pattern of expression is not typical of other junctional or cell polarity markers like Bazooka, Glaikit or Miranda (Dunlop et al., 2004; Kuchinke et al., 1998; Shen et al., 1997), or of MAGUKs in general and must be clarified by further study. As a result, specificity of our antibody must be further examined. Several independent lines of evidence suggest that our serum is specific to Varicose. First, our epithelial expression

pattern observed during embryogenesis is consistent with previous reports on *varicose* (Wu et al., 2007). Second, a null allele, *vari*^{48EP}, lacks all wildtype varicose expression patterns. Third, the NE expression pattern is absent when third instar larval brains are labeled with pre-immune sera. Fourth, our antibody detects Varicose expression in the ventral midline when *UAS-vari* is misexpressed in the midline using *single-mindedGAL4* (Nambu et al., 1990). Fifth, although protein levels are at the threshold of detection, over-expression of *UAS-vari* using *heat-shockGAL4* provides ample protein to be detected by western blotting. Collectively, these data show our antibody is specific to Varicose.

3.4.3 *Varicose is Involved in Regulating Tube Size*

The *Drosophila* tracheal system is a well developed model for the dissection of pathways regulating tube formation (Beitel and Krasnow, 2000). pSJ components are implicated in the regulation of tubule size. Genes regulating tube size fall into two phenotypic categories; those required to regulate tube length and those required for normal tube diameter (reviewed in Kerman et al., 2006). Several lines of evidence have suggested that pSJ components are involved in regulating tube length. Mutations in SJ proteins like *mega*, *sinu* and the Na⁺K⁺ATPase β subunit, *nrv2* cause tortuous and elongated tracheal trunks without affecting tube diameter (Behr et al., 2003; Paul et al., 2003; Wu et al., 2004). In contrast, mutations in *vari* do not appear to affect tube length. Tracheal tubes in *vari* mutants have irregular and enlarged tube diameters reminiscent of mutations affecting *mummy (mmy)/cystic* and *krotzkopf verkehrt (kkv)*, enzymes required for chitin synthesis (Araújo et al., 2005; Moussian et al., 2005). Epistatic analysis of *vari*

and *sinu* reveals a tracheal phenotype in double mutants that is worse than either single mutant, suggesting these proteins function in different pathways (Wu et al., 2004).

The chitin matrix is secreted from the apical surface of tracheal cells and synthesis of the matrix has been linked to controlling tube diameter. The chitin matrix is a fibrillar cylinder that forms inside the tracheal lumen. During expansion of the dorsal trunk, the cylinder expands as the lumen dilates (Luschnig et al., 2006). *mmy/cystic* mutants lack secreted chitin resulting in a luminal envelope detached from the tracheal cell membrane. It is suggested that formation of the chitin matrix is needed for the organized radial expansion of tracheal tubes (Araújo et al., 2005). The tracheal phenotype of *vari* is similar to *cystic* and *kkv* mutants, and all three have reduced deposition of 2A12 antigen (Araújo et al., 2005). Wu and colleagues (2007) further show that *vari* mutants fail to secrete apical protein Serpentine and secrete variable amounts of Vermiform. Nevertheless, cuticle ultrastructure appears normal in *vari* mutants. In addition, taenidial ridges form normally in *vari* mutants. This result is unlike tracheal mutants affecting tube length, such as *sinu*, where taenidial folds are irregular suggesting *vari* is not involved in this process (Wu et al., 2004). However, normal taenidial ridges are an uncharacteristic result suggesting that the role of Varicose during morphogenesis is unique at the septate junction during tube expansion. Our data suggests that luminal protein secretion in *vari* mutants is sufficient to produce cuticle and regulate tube length, and that the SJ may also play a role in regulating tube diameter.

3.4.4 *MAGUKs are Involved in the Development of Adult Tissues*

As septate junctions play such a vital role in maintaining a homeostatic environment, it would seem logical that this structure is necessary throughout the *Drosophila* life cycle. Studies pertaining to the function of septate junctions during late stages of adult development are limited. Recently, the identification of SJs in the adult ommatidium supports this hypothesis. SJ component, Nr x IV was shown to localize to these junctional regions in the pupal and adult eye. Loss of *nrxIV* disrupts SJ function which leads to structural disorganization resulting from a loss of adhesion between cells of the adult ommatidia (Banerjee et al., 2008). Varicose is expressed during pupal development although expression in the eye remains unknown. We do know that loss of *vari* during the development of adult tissues results in missing ommatidia and irregular bristle patterning. As Nr x IV is a proposed interacting partner of Vari, we could speculate that Vari plays an adhesive role during this developmental process, where loss of *vari* results in loss of adhesion and loss of cellular organization.

The involvement of SJs during wing imaginal disc to adult wing morphogenesis is unclear. However, two known SJ components, Gli and Cora are required for proper alignment of adult wing hairs (Venema et al., 2004). Here we present another SJ component, and the first MAGUK family member also involved in wing hair morphogenesis. Similar to mutations in *gli* and *cora*, *vari* mutants display patches of wing hairs that fail to point distally. Although reminiscent of a *frizzled* (*fz*) planar cell polarity phenotype, the mechanism regulating hair alignment seems to act independent of *fz*. While *fz* mutants disrupt the polarity of the wing hairs, this act is not random. Patches

of wing hairs, although not pointing distally retain a parallel alignment with their neighbouring hair (Adler, 2002). This is unlike the random alignment seen in *vari*, *gli*, and *cora* mutants where polarity of neighbouring wing hairs is different. During pupal development, the position and orientation of wing prehair are determined and then stabilized during later stages (Venema et al., 2004). Whether Vari plays a role in prehair positioning or wing hair stability is unclear. The involvement of MAGUKs during this developmental mechanism is unique and needs to be resolved.

The MAGUK protein PALS2 has been proposed to act in scaffold formation at the basolateral membrane of mammalian epithelia (Shingai et al., 2003). Here we show that a *Drosophila* homologue, Vari, is similarly distributed, and is required in ectodermally-derived epithelia to elaborate pSJs and establish a paracellular barrier. Embryos lacking *vari* function display mislocalization of essential pSJ membrane proteins, including NrXIV, Na⁺K⁺ATPase and FasIII, and are unable to control the permeability of the tracheal membrane. As a result, the trachea fail to fill with air, and the embryos die in early stage 17. Vari is not expressed in the embryonic central nervous system, but is expressed apically in the neuroepithelium of the optic lobes and in neuronal cell bodies. These structures do not have pSJs, and indicate that there are uncharacterized functions of Vari, distinct from a role in the assembly of cell junctions.

Identification of Varicose Interacting Partners

CHAPTER FOUR

4.1 ACKNOWLEDGEMENTS

Library amplification was performed with the help of Breanna Ireland. 70 putative clones were screened for duplicates by Faiza Upal. In addition, Faiza performed all library plasmid rescues via transformations of *E. coli* as well as performed the verification of protein interactions.

4.2 INTRODUCTION

Protein-protein interactions are essential to cellular biology. The two-hybrid system is a rapid, powerful and sensitive technique to detect and characterize the interaction of proteins (Young, 1998). Most importantly, this technique enables the identification of novel interacting partners of a single protein or domain by screening a protein library (Miller and Stagljar, 2004). We have employed a two-hybrid method that requires the expression of fusion proteins in the yeast cell nucleus so that protein-protein interactions are detected by reporter gene expression. The endogenous yeast transcriptional activator, GAL4, is composed of a DNA-binding domain (BD) and an activation domain (AD), both of which are required for activator function. If interacting proteins were synthesized as fusion proteins with either the DNA-BD or the -AD, the interaction of these proteins would bring the GAL4 domains in close proximity and reconstitute a functional transcriptional activator that could drive expression of reporter genes (Fields and Song, 1989; Chein et al., 1991).

Our knowledge of proteins that interact with Varicose is limited. However, the vertebrate homologue of Varicose, PALS2 was identified as an interacting partner of mammalian Lin-7 (Kamberov et al., 2000). Loss of mammalian Lin-7 from epithelial cells disrupts TJ formation and results in reduced levels of PALS2 (Straight et al., 2006). The similarity between *Drosophila* and vertebrate membrane components and cell junctions suggests evolutionarily conserved mechanisms regulating epithelial architecture (Bryant, 1997; Hortsch and Margolis, 2003).

A two-hybrid based protein map was presented for the *Drosophila* genome (Giot et al., 2003). These studies identified multiple Varicose binding partners including Cdc37, a protein required for cell growth and viability; bric á brac 1, a morphogenic regulator of imaginal development; a mitochondrial ribosomal protein and an uncharacterized gene CG5273 (Lange et al., 2002; Couderc et al., 2002; Crosby et al., 2007). In addition, Varicose was found to interact with *Drosophila* Lin-7, supporting evolutionary conservation.

To identify additional Varicose interacting partners, we attempted a yeast two-hybrid screen using a Varicose-GAL4 DNA-BD fusion. Our screen of a *Drosophila* adult cDNA library resulted in 142 putative positive clones. This chapter will outline our screening process and present our preliminary results. Moreover, we will discuss the possible functional role(s) of Varicose and its interacting partners.

4.3 RESULTS 4

4.3.1 *Varicose-GAL4 DNA-Binding Domain Fusion Protein*

Early computational predictions of the *varicose* transcript sequence suggested that the translated protein encoded PDZ, SH3 and GUK domains. At the time of our yeast two hybrid screen, we used this data to generate a Varicose protein fused to the DNA-binding domain of GAL4. The full-length *varicose* transcript (C) was amplified by PCR and cloned into vector pGBKT7 (Fig. 4.1). Sequencing confirmed the in-frame fusion between Varicose and the DNA-BD however two amino acid substitutions were detected in the Varicose sequence. A threonine to serine amino acid substitution was identified at position 22. This position also coincides with the 16th amino acid of the PDZ domain. Both amino acids are hydrophilic with polar side groups (Snustad and Simmons, 2000). The second substitution occurs at position 463 where valine is substituted for alanine. Both amino acids are hydrophobic with nonpolar side groups (Snustad and Simmons, 2000). As both substitutions may be due to polymorphisms between the predicted and CS-P *varicose* sequences (Crosby et al., 2007), we opted to continue our two-hybrid screen with the Varicose fusion. These sequence polymorphisms were not seen in the wildtype strain, Oregon R.

4.3.2 *Varicose is Stably Expressed in Yeast Strain AH109*

Yeast strain AH109 contains three engineered reporter genes ADE2, HIS3 and MEL1. Each gene is under the control of UAS and TATA boxes and yields a strong response to GAL4 (James et al., 1996). To ensure the Varicose fusion did not autoactivate these reporter genes, the fusion construct was transformed into AH109. The

transformants were selected on media lacking nutritional supplement tryptophan (SD/-TRP) and we assayed for the expression of MEL1 using X- α -Gal (Aho et al., 1997). In parallel, control plasmids pGBKT7-p53 and pCL1, were transformed into AH109. The Varicose fusion and pGBKT7-p53 transformants were selected on SD/-TRP. All colonies remained white indicating that neither plasmid autoactivates the reporter gene. Control plasmid pCL1 transformants were selected on media lacking leucine (SD/-LEU) and containing X- α -Gal. pCL1 encodes the full-length GAL4 protein and was a positive control for our X- α -Gal assay. All selected transformant colonies were blue.

The yeast model system is advantageous for two-hybrid screening as many proteins are stably expressed in yeast (Sudbery, 1996). To ensure that our Varicose fusion was expressed in yeast we performed western blot analysis. While Varicose is a 54 kDa protein, the addition of the DNA-BD and epitope tag increases the protein molecular mass to ~70 kDa. We extracted protein from transformed AH109 and detected fusion protein expression using a c-Myc antibody. A protein product corresponding to the predicted molecular weight of the Varicose fusion was detected in transformed AH109 but was not seen in the negative control, untransformed AH109. Additionally, control plasmids expressing p53 and lamin C proteins were detected at ~56 kDa and 41 kDa, respectively (Fig. 4.2).

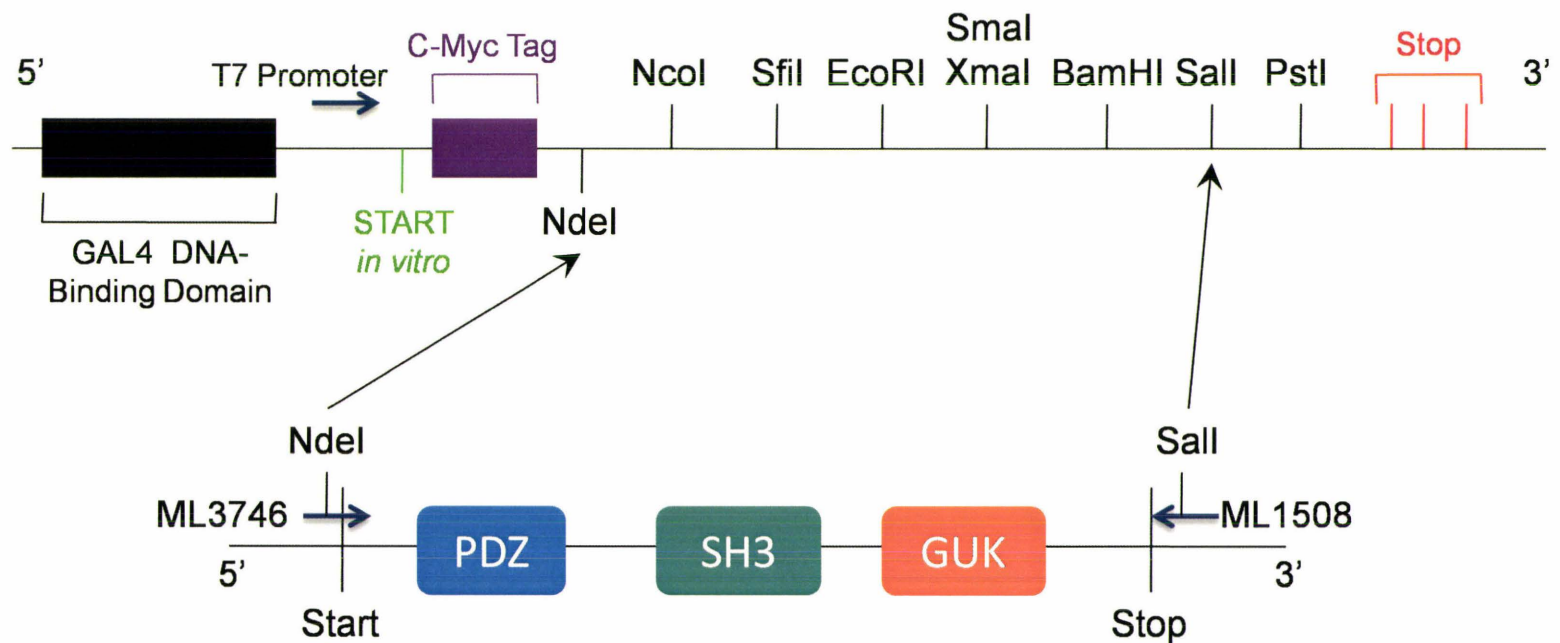
4.3.3 Putative Interacting Partners Identified in cDNA Library Screen

The interaction between Varicose and DLin-7 has been identified in both vertebrate and invertebrate systems. To identify additional binding partners and/or confirm previous results, we screened a *Drosophila* adult cDNA library for candidate

Figure 4.1: Outline of Vari – GAL4 DNA-binding domain fusion construct.

Our bait construct for yeast two hybrid screening was created by cloning cDNA corresponding to *varicose* transcript C into vector pGBKT7. This construct creates a fusion between Varicose and the GAL4 DNA-binding domain (BD) allowing for screening of library plasmids containing a fusion with the GAL4 activation domain (AD).

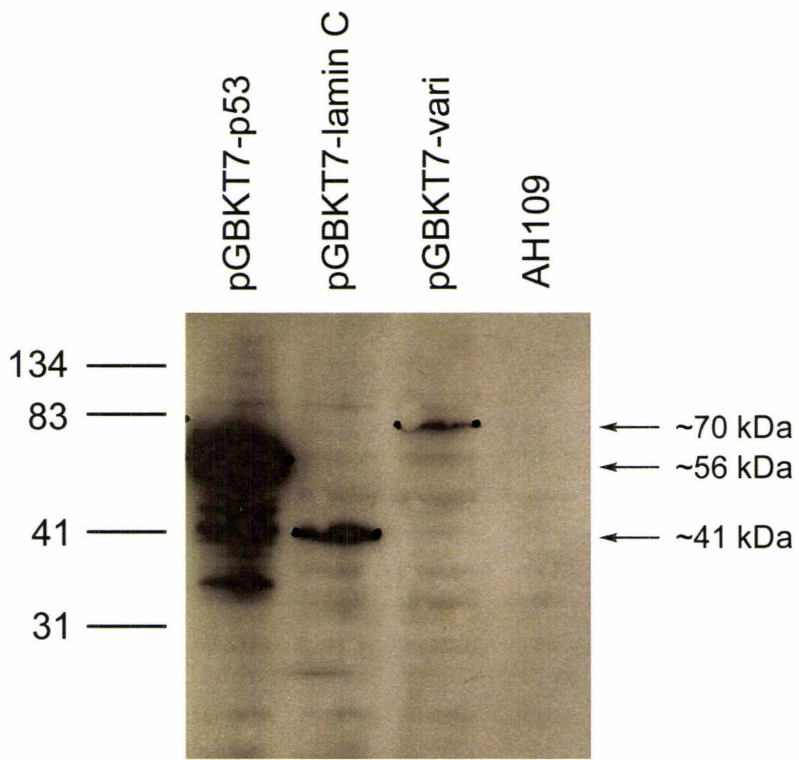
pGBKT7 – Vari



This construct was sequenced to ensure the insert was in-frame with the GAL4 DNA-Binding Domain

Figure 4.2: Varicose is stably expressed in yeast strain AH109.

Bait fusion constructs, Varicose, p53 and lamin C were transformed into yeast strain AH109. Protein prepared from transformed yeast was separated by SDS-PAGE, transferred to PVDF membrane and immunoblotted with c-Myc antibody. Expression of a 56 kDa protein, a 70 kDa protein and a 41 kDa protein were detected corresponding to p53, Varicose and Lamin C, respectively. The approximate weight of each fusion construct was determined by adding the weight of the protein to the weight of the DNA-BD (16.7 kDa) plus the epitope tag (1.2 kDa). Protein prepared from untransformed yeast strain AH109 was used as a negative control.



interactors using the Varicose-GAL4 DNA-BD fusion. The library consists of cDNAs cloned into vector pACT2 creating a fusion with the GAL4 AD. Transformants containing both the Varicose fusion and the library fusion were selected on media lacking tryptophan and leucine, to select for both fusion plasmids, as well as lacking adenine and histidine, to select for expression of reporter genes. X- α -Gal was added to select for MEL1 expression. Blue colonies selected on quadruple dropout media (QDO) were isolated. In addition to this highly stringent method of plating, transformants were selected on medium stringency media lacking tryptophan, leucine and histidine (triple dropout, TDO). Colonies were replica plated onto QDO media with X- α -Gal and blue colonies were isolated. A total of 142 colonies were isolated as putative positive clones.

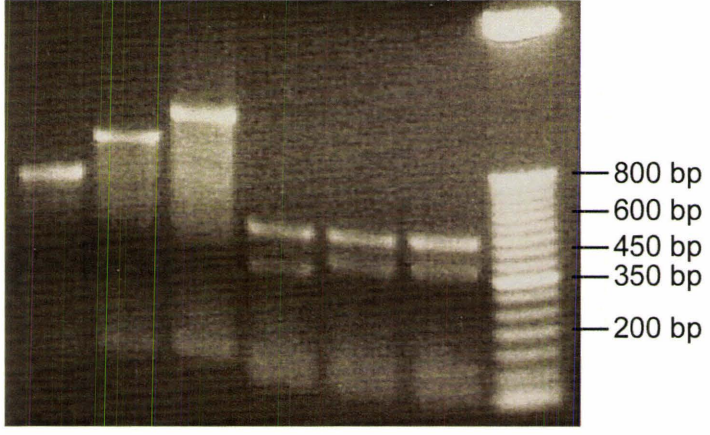
Analysis of the putative clones was carried out in several steps. To begin, each clone was streaked onto SD/-TRP/-LEU media several times to reduce the presence of multiple plasmids. The phenotypes were verified by a final streak onto QDO media with X- α -Gal. Each library clone was then screened by PCR for a single library insert (Fig. 4.3, Appendix G). We were unable to PCR amplify inserts from the following yeast clones 12, 39, 41, 93, 94, 95, 96, 103, and 132. The PCR products from the remaining 133 clones were digested with a frequently cutting restriction enzyme, *HaeIII*. Digested fragments were analyzed and clones exhibiting similar patterns were eliminated as duplicates. To confirm this method of elimination, we sequenced three clones with identical digestion patterns, clones 117, 127 and 128 (Fig. 4.3). All three clones contained an identical sequence and as a result, clones 127 and 128 were eliminated as duplicates. In addition, clones 6, 23, 42, 107, and 111 were also eliminated as duplicates.

Figure 4.3: Library clones sorted by PCR and restriction digest.

Yeast DNA preparations were used as a template for PCR analysis. PCR products were analyzed by gel electrophoresis to check for multiple library inserts (Clones 66, 70, 106). To characterize each PCR product and eliminate duplicate clones, amplified inserts were digested with a frequent cutter restriction enzyme, *Hae*III. Digestions were analyzed by gel electrophoresis. Clones exhibiting the same digest characteristics (Clone 117, 127, 128) were eliminated as duplicates. Sequencing of clones 117, 127, and 128 confirmed each plasmid was the same. Clones 127 and 128 were eliminated as duplicates.

Clone 66
Clone 70
Clone 106
Clone 117
Clone 127
Clone 128
50 bp Ladder

Yeast DNA Prep *Hae*III Digests



Our final step rescued the library plasmids by transformation of *E. coli*. Out of 126 clones, 113 were successfully transformed into bacteria. To verify the same library plasmid was obtained in bacteria, plasmid inserts were amplified by PCR and compared against the amplified products from yeast (Fig. 4.4). The results of these analyses are summarized in Table 4.1.

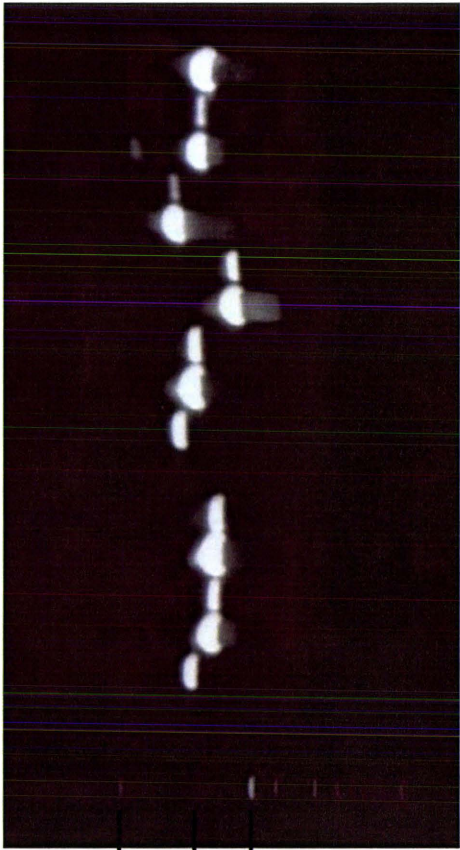
4.3.4 Verification of Varicose Interacting Proteins

To ensure the protein interactions identified prior to bacterial transformation were due to an interaction with Varicose and not an autoactivation of reporter genes, library plasmids were transformed into AH109 with either the Vari fusion or empty pGBKT7 vector as a negative control. Transformants were selected on SD/-TRP/-LEU to select for both plasmids. To retest the protein-protein interaction, colonies were restreaked onto QDO media. Interactions between library clones and both the Vari fusion (Fig. 4.5B) and the negative control (Fig. 4.5A) were eliminated as autoactivating clones. Library clones that interacted with the Vari fusion (Fig. 4.5D) but failed to interact with the negative control (Fig. 4.5C) were sequenced. Out of 18 library clones tested, 9 clones were autoactivating (4, 9, 14, 18, 20, 21, 40, 45, 51) while 9 clones verified an interaction with Varicose (5, 11, 15, 26, 37, 38, 54, 61, 62). The remaining 95 clones are still to be tested. These results are summarized in Table 4.2. All verified library clones were sequenced, with the exception of clone 38 which was not sequenced due to time constraints. Candidate proteins were identified through a BLAST search of the *Drosophila* genome.

A 286 bp cDNA fragment corresponding to CG2210, or abnormal wing discs (awd) was identified from clone 5. This fragment aligns with the nucleoside diphosphate

Figure 4.4: Rescue of library clone via transformation of *E. coli*.

Each library clone was transformed into bacteria for further analysis and verification of positive clones. Bacterial DNA preparations were used as a template for PCR to amplify the library insert. PCR products were compared against the PCR profiles from yeast to ensure the same library plasmid was obtained.



Yeast Clone 36
Bacterial Clone 36
Yeast Clone 51
Bacterial Clone 51
Yeast Clone 62
Bacterial Clone 62
Yeast Clone 66
Bacterial Clone 66
Yeast Clone 70
Bacterial Clone 70
Yeast Clone 74
Bacterial Clone 74
Yeast Clone 106
Bacterial Clone 106
Yeast Clone 117
Bacterial Clone 117
Yeast Clone 140
Bacterial Clone 140
H₂O control
1Kb ladder

500bp
1000bp
1600bp

Table 4.1: A list of the putative interacting clones and the screening steps completed

	Number of Clones	Clone Number
Clones isolated in screen	142	
No yeast DNA prepared	9	12, 39, 41, 93, 94, 95, 96, 103, 132
Incomplete bacterial transformations	13	85, 130, 135, 140, 10, 17, 27, 63, 65, 74, 75, 78, 79
Duplicate clones eliminated	7	6, 23, 42, 107, 111, 127, 128
Clones to be verified	113	
Clones Sequenced (prior to verification)	9	36, 51, 62, 66, 70, 74, 106, 117, 140

kinase domain encoded by *Awd*. Growth and differentiation of imaginal discs require *Awd* function and the nucleoside diphosphate kinase activity has been shown to have tumor metastasis suppressing activity by regulating cell motility (Timmons and Shearn, 2000; Nallamotheu et al., 2008; Dammai et al., 2003).

CG6386, a gene encoding *bällchen* (*bäll*) was identified from a 494 bp cDNA fragment encoded in clone 11. This protein encodes a nucleosomal histone kinase-1 proposed to be involved in mitotic and meiotic progression (Cullen et al., 2005). Loss of *NHK-1* results in female sterility (Ivanovska et al., 2005). In addition, *Bällchen* was identified as an interacting partner of *Par-1* in germ cell development (Klinge et al., 2004). *Par-1* is well characterized and plays a dynamic role in cell polarization. It is possible that an interaction between *Varicose* and *Bällchen* is necessary for the establishment of cellular architecture.

BLAST alignment of cDNA encoded in clone 15 identified CG11518, a gene also known as *pygopus* (*pygo*). This cDNA fragment corresponds to the 3'UTR, suggesting this interaction may not be a true positive. We were unable to identify an open reading frame within the cDNA sequence supporting a false positive hypothesis. *Pygo* is a nuclear protein that functions in *Wingless* (*Wg*) – dependent signalling (Jessen et al., 2008; Parker et al., 2002). On the other hand, *Pygo* mediates chromatin remodelling to regulate target gene expression, a role independent of *Wg* (Parker et al., 2002; Thompson et al., 2002). The current research has focused upon the nuclear expression of *Pygo*, a cellular compartment devoid of *Varicose*. The absence of an open reading frame and the non-overlapping expression of these two proteins suggest that the putative interaction is

false. During our experimental design, we regrettably failed to determine if an interaction exists between our Varicose-GAL4 DNA-BD fusion and empty GAL4 AD vector (pACT2). An interaction between the two could lead to false positive results.

A new five member family of polypeptide growth factors have been identified in *Drosophila*, Imaginal Disc Growth Factors (IDGFs) (Hipfner and Cohen 1999; Kawamura et al., 1999). These factors, although possessing chitinase-like properties (Zhu et al., 2004) are catalytically inactive and have evolved to acquire a growth-promoting function (Kawamura et al., 1999). Clone 62 encodes one member of the five member family, IDGF4. Expression of IDGF4 has been identified in embryonic epithelia as well as in the larval optic lobe and central brain; however, its functional role has not yet been addressed.

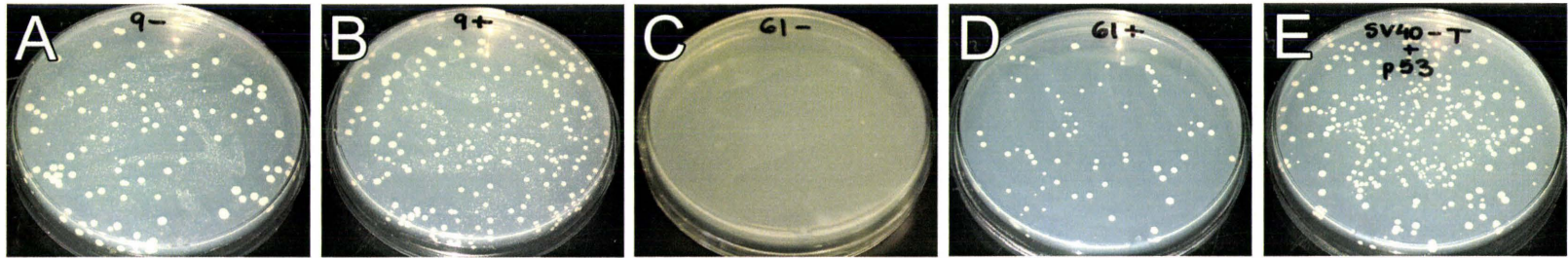
Egghead (Egh), a glycosyltransferase encoded by *Drosophila* gene CG9657 and clone 61, functions in the establishment and maintenance of epithelial architecture by regulating oocyte-follicle cell adhesion. Moreover, loss of *egh* results in follicle cells exiting the epithelium and losing apical-basal polarity (Goode et al., 1996). Disrupted *egh* function leads to disorganized lamina glial cells in the developing optic lobe suggesting Egghead plays a role in visual system development (Fan et al., 2005).

Three clones are suspected false positives. Two clones, 26 and 37, were identified as gene CG6779 which encodes Ribosomal protein S3 (RpS3). RpS3 functions in DNA damage repair (Deutsch et al., 1997). Clone 54 encodes two potential genes, mitochondrial large ribosomal RNA and Porin, a mitochondrial voltage-gated anion

Figure 4.5: Clone 61 but not Clone 9 interacts with Varicose.

Each library plasmid was verified for an interaction with Varicose. Yeast strain AH109 was transformed with the Varicose fusion construct and the putative positive library clone. As a negative control, empty pGBKT7 vector was transformed with each library clone. To screen for protein interactions that activate reporter genes, transformants were selected on supplemented dropout media lacking tryptophan, leucine, adenine and histidine. An interaction was detected between Clone 9 and the Varicose fusion (B) as well as with the negative control (A) suggesting this clone autoactivates the reporter genes. An interaction was detected between Clone 61 and the Varicose fusion (D) but not with the negative control (C) suggesting this clone may be a true interacting partner of Varicose. As a positive control p53 fusion construct and SV40 T-antigen fusion construct were transformed into strain AH109 (E).

SD/-TRP/-LEU/-ADE/-HIS



pGBKT7 +
library clone #9

Vari +
library clone #9

pGBKT7 +
library clone #61

Vari +
library clone #61

Positive
Control

Table 4.2: Verification of clones interacting with Varicose

	Number of Clones	Clone Number
Clones to be verified	113	
Autonomously activating clones	9	4, 9, 14, 18, 20, 21, 40, 45, 51
Verified Positive Clones	9	5, 11, 15, 26, 37, 38, 54, 61, 62
Sequenced Positive Clones	7	5, 11, 15, 26, 37, 54, 61
Clones to be sequenced	1	38
Transformed Bacterial Clones requiring verification	95	1, 2, 3, 7, 8, 13, 16, 19, 22, 24, 25, 28-36, 43, 44, 46-50, 52, 53, 55-60, 64, 66-73, 76, 77, 80-84, 86-92, 97-102, 104-106, 108-110, 112- 126, 129, 131, 133, 134, 136-139, 141, 142

channel (Lee et al., 2007). Based on our expression data and phenotypic analysis of Varicose (Chapter 3), it is unlikely that Varicose interacts with these identified proteins.

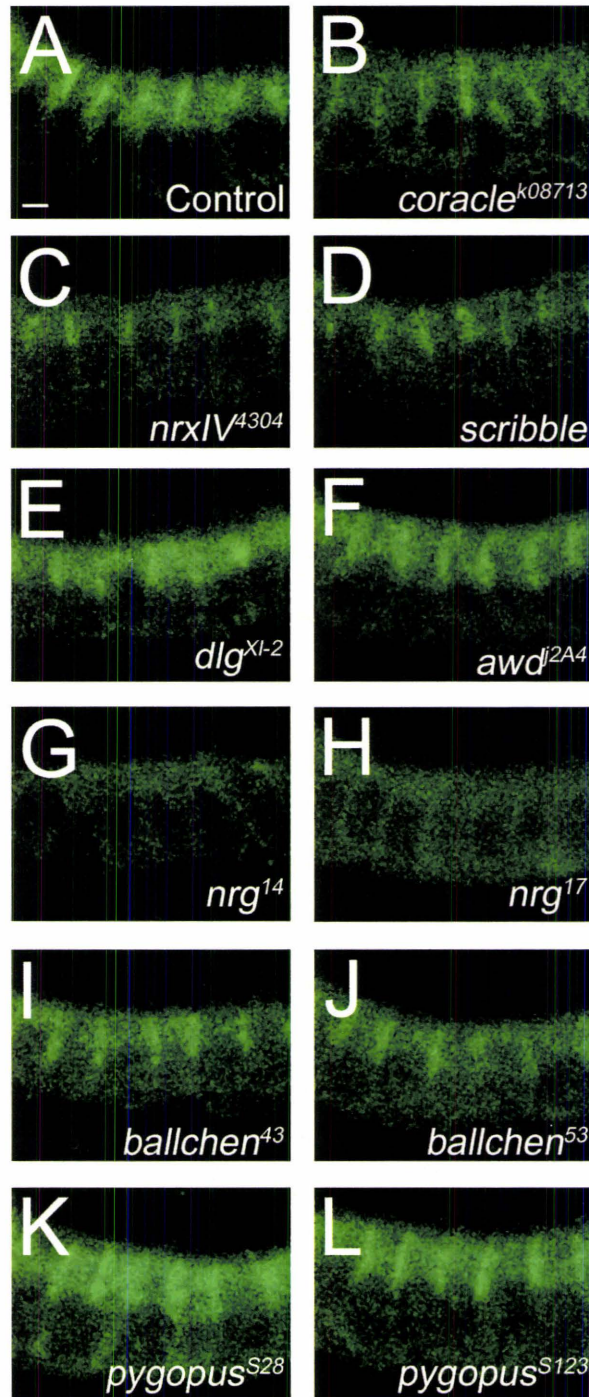
4.3.5 *Varicose is Mislocalized in neuroglial Mutants*

One of the objectives of our yeast two-hybrid screen was to identify novel interacting partners of Varicose. Identification of these proteins would enable us to hypothesize a functional role(s) for Varicose during *Drosophila* development. We wanted to genetically verify the interaction between Varicose and our novel interacting partners, *awd*, *bäll* and *pygo* within the *Drosophila* system. Moreover, knowing that Varicose localizes to the SJ of all ectodermally-derived epithelial tissues, we wondered if there could be an interaction between Varicose and other SJ components. To test this, we examined the localization of Varicose at the lateral membrane of hindgut epithelial cells in all yeast two-hybrid candidates and several SJ mutants. In the control, Varicose expression is localized to the lateral membrane of the epithelial cells (Fig. 4.6A). When compared to the controls, Varicose expression in our yeast two-hybrid mutants *awd*^{j2A4} (Fig. 4.6F), *bällchen*⁴³ and *bällchen*⁵³ (Fig. 4.6I, 4.6J), *pygopus*^{S28} and *pygopus*^{S123} (Fig. 4.6K, 4.6L) is indistinguishable suggesting Varicose localization is independent of these proteins. Varicose expression is also similar to the controls in *coracle*^{k08713} (Fig. 4.6B), *neurexin*⁴⁰³⁴ (Fig. 4.6C), *scribble* (Fig. 4.6D), and *discs large*^{XL-2} (Fig. 4.6E). These results differ from those observed by Wu et al. (2007) where Vari levels are reduced and mislocalized basally in *nrx*⁴⁸⁴⁶ and *cora*⁵ mutants. However, it is important to note that in these separate studies, different alleles were used. Unique to our study, we found that Varicose is not properly localized in *neuroglial* mutants (Fig. 6G, 6H). In both alleles

examined *nrg*¹⁴ and *nrg*¹⁷, Varicose expression levels are severely reduced and in *nrg*¹⁷, mislocalized basally. Similar results are also observed at the lateral membrane in tracheal epithelial cells (data not shown). It is possible that the interaction between Varicose and Neuroglian may be indirect, but our results suggest that proper localization of Varicose requires proper Neuroglian function.

Figure 4.6: Varicose is mislocalized in *nrg* mutants.

Varicose expression was examined in various SJ mutants. Whole-mount early stage 16 embryos were immunolabeled with anti-Vari and visualized by confocal microscopy. Mutant stocks were maintained over GFP balancers and homozygous mutant embryos were selected by absence of GFP. Varicose expression was detected at the SJ in hindgut epithelial cells of *cora* (B), *nrxIV* (C), *scrib* (D), *dlg* (E), *awd* (F), *bäll* (I and J) and *pygo* (K and L) mutants, which is consistent with controls (A). Varicose was mislocalized in both *nrg* alleles (G and H). Expression levels are severely reduced and expression appears more basal (H). Each image is a single confocal section. Calibration: 2 μ m, A-L.



4.4 DISCUSSION 4

We have employed a yeast two-hybrid screen to identify proteins that interact with Varicose. The Vari isoform, lacking the L27 domain, isolated 142 putative interacting partners from an adult cDNA library. Verification of 18 clones identified 9 autonomously activating clones and 9 putative protein partners. Four partners appear to be false positives while 4 appear to be novel interactors: Bällchen, Abnormal Wing Discs, Imaginal Disc Growth Factor 4 and Egghead. One protein remains to be sequenced. We screened putative interacting protein mutant alleles and several SJ mutant alleles to determine which proteins are required for proper Vari SJ localization. In the absence of *neuroglian*, Vari levels were reduced and in some cases mislocalized basally along the lateral membrane. Although the other proteins do not appear to be required for Varicose sublocalization, their interaction with Vari may be required for other cellular processes. We discuss below some putative functional roles for Varicose and its novel interacting partners.

4.4.1 *Bällchen, A Connection Between Par-1 and Varicose*

We have identified a novel interaction between Varicose and CG6386, Bällchen proteins. Recent studies have focused upon the nucleosomal histone kinase (NHK) function of this protein. Bäll has been isolated from nuclear extracts and shown to phosphorylate Thr 119 on histone H2A (Aihara et al., 2004) where it functions to hold non-homologous chromosomes together during meiosis and is responsible for maintaining chromosomal alignment during mitosis (Cullen et al., 2005). As a result, *bäll* mutants have a reduced testis and recessive male sterility (Arguello et al., 2006;

Klinge et al., 2004). Expression studies have not identified Varicose as a nuclear protein, suggesting that a nuclear interaction between Bällchen and Varicose is unlikely.

Bällchen is expressed throughout embryonic development and ubiquitously expressed in the head, thorax and testes of adult flies (Arguello et al., 2006; Klinge et al., 2004). *bäll* mutants display no tracheal or mesodermal developmental defects and have no effect on growth and survival of imaginal discs (Zhu et al., 2005). The expression pattern of Bällchen throughout embryonic development has yet to be determined, however these mutants properly localize Varicose to the SJ, implying Varicose localization is not dependent on Bällchen expression. It is unknown whether these two proteins have overlapping expression patterns during embryogenesis and the possible interaction during this stage of development needs to be further explored.

Overexpression of Bällchen results in a rough eye phenotype possibly by functioning through the platelet-derived growth factor/vascular endothelial growth factor (PDGF/VEGF or PVR) signalling pathway (Zhu et al., 2005). This pathway is also involved in germ cell development. Bällchen was isolated in a yeast two-hybrid screen as a putative interactor of a *Drosophila* kinase, Par-1 (Klinge et al., 2004) and in this study as a putative interactor of Varicose. In the germline, Par-1 functions to determine oocyte polarity through protein phosphorylation (Benton and St Johnston, 2003). Expression of Varicose has not been explored in the female germline and therefore a role during oogenesis cannot be excluded.

Par-1 also functions in embryonic epithelia where it localizes to the lateral membrane and restricts subapical and adherens junction proteins to the apicolateral

region of the plasma membrane (Bayraktar et al., 2006; Benton and St Johnston, 2003). The Dlg/Scrib complex also restricts apical proteins from the lateral membrane; however the mechanisms regulating Par-1 and Dlg/Scrib functions are obligatory (Bayraktar et al., 2006). As seen with Varicose, depletion of Par-1 does not result in an expansion of the apical membrane into the basal region. It is proposed that Par-1 functions to specify the basolateral region by establishing a barrier to prevent the lateral movement of proteins (Bayraktar et al., 2006). Based on these correlations, it is realistic to propose the hypothesis that Vari may function with Par-1 to establish the basolateral membrane, through an interaction between Vari and Bällchen.

4.4.2 An Interaction Between the Kinase Domain of Awd and Varicose

One might propose that the interaction between Awd and Vari implies these proteins participate in a similar cellular process, yet Varicose was properly localized to the SJ of epithelial cells in *awd* mutants. Awd is expressed at low levels in all embryonic cells and at high levels in tracheal cells (Dammai et al., 2003). During embryogenesis, Awd is required for tracheal branch migration and is necessary for directing tubes, not their development. Although *awd* mutants display ectopic tracheal branching and looping, late stage developing organs such as the gut are properly formed (Dammai et al., 2003). Varicose is also required for tracheal morphogenesis (Chapter 3) however, expression is required during later stages of embryogenesis. As the critical roles of Awd and Vari occur during different developmental stages, it is possible to eliminate an interactive role for these proteins during embryogenesis.

The Vari/Awd interaction was obtained using an adult cDNA library suggesting their role during later developmental stages is more likely. *Drosophila* Awd encodes a subunit of a 100 kDa Nucleoside DiPhosphate kinase (NDP) (Biggs et al., 1988) and through its kinase activity regulates cell proliferation/differentiation, a requirement for the growth and formation of metastatic tumors (Timmons et al., 1993; Zinyk et al., 1993). Importantly, Awd kinase activity is not sufficient for biological function suggesting that the role may be independent of enzymatic activity (Timmons and Shearn, 2000; Xu et al., 1996). Awd is detected at 3rd larval instar in all imaginal discs, salivary glands, brain lobes, lymph glands and fat bodies (Timmons and Shearn, 2000). Awd is weakly expressed during early 3rd larval instar wing discs with increasing expression until puparium formation (Timmons et al., 1993). Our studies have shown that Vari is required for proper adult wing and eye development (Chapter 3). Moreover, these results were recently confirmed by western blotting and RNAi (Bachmann et al., 2008). Larval brains in *awd* mutants are small comparable to wild type as mitosis is arrested in proliferating neuroblasts (Timmons et al., 1993). Knowing that Varicose is expressed in a subset of neuroblasts and in the proliferating neuroepithelium, it is possible that these proteins may function together. Although much work is needed to dissect this protein interaction, one potential role for these proteins is in the development of larval imaginal discs and optic lobes of the adult brain.

4.4.3 Varicose Associates with a Chitinase-Like Growth Factor

Imaginal disc growth factors (IDGF) are an emerging family of proteins with chitinase-like properties. Each of the five family members (IDGF1-4 and DS47) encodes

an N-terminal signal sequence proposed to regulate extracellular location and a consensus motif for N-linked glycosylation (Kawamura et al., 1999). In addition, each protein consists of a chitinase catalytic domain, however a glutamine to glutamate substitution at a key enzymatic residue renders these proteins catalytically inactive (Zhu et al., 2004). As a result, these chitinase-like growth factors are suspected carbohydrate binding proteins (lectins or lectin-like proteins) (Zhu et al., 2004) which are found intracellularly in luminal compartments or extracellularly and localized to the plasma membrane (Dodd and Drickamer, 2001). Moreover, these proteins have been linked to functional roles in cell proliferation and/or cell-cell communication (Zhu et al., 2004; Hipfner and Cohen, 1999).

An interaction between Varicose and IDGF4 is very intriguing. The potential for these proteins to functionally interact is probable in several tissues. First, IDGF4 is found in embryonic epithelia such as the salivary glands, a tissue in which Varicose is also expressed. Second, IDGF4 is expressed in the trachea at the end of embryogenesis. As a possible lectin or lectin-like protein, IDGF4 would be capable of binding to chitin (Kawamura et al., 1999). We have shown previously that Varicose also plays a role in regulating tube size, a process thought to involve chitin secretion. Absence of Serpentine and variable amount of secreted Vermiform in *vari* mutants suggests Vari plays a role in cuticle secretion (Wu et al., 2007), however ultrastructural analysis of *vari* tracheal lumens shows cuticle secretion is unaffected (this work). We could suggest then that Vari and IDGF4 function to adhere to the chitin matrix to the surrounding cells regulating tube size. Third, IDGF4 is expressed at 3rd larval instar in two parallel lines in the optic

lobe (Kawamura et al., 1999). Although this pattern has not been characterized, it appears similar to the expression pattern of the proliferating centres of the optic lobe (Egger et al., 2007). IDGFs are proposed to have acquired growth promoting activity with local control of cell proliferation (Hipfner and Cohen, 1999). We have also shown that Varicose is expressed in the outer proliferation centre of the optic lobes, a region corresponding to the neuroepithelium. We are tempted to speculate that Varicose and IDGF4 could function together to regulate proliferation of the neuroepithelial cell pool which gives rise to neurons of the adult eye.

4.4.4. *Varicose, Egghead and the Visual System*

Egghead, a glycosyltransferase, plays a role in the biosynthesis of glycosphingolipids (Chen et al., 2007). These lipids are necessary structural components of cellular membranes and help maintain a homeostatic environment by associating with proteins to modulate cell adhesion and signal transduction (Chen et al., 2007). What possible role could Varicose and a glycosyltransferase have in common? Egghead has been implicated in the organization of lamina glia. In the absence of *egh*, photoreceptor axons project aberrantly through the lamina/lobula complex boundary of the developing optic lobe (Fan et al., 2005). This projection phenotype can be rescued by expressing Egghead in the optic lobe using a tissue specific driver, *c855aGAL4* (Fan et al., 2005). Reducing Varicose levels by RNAi, using the same driver is lethal suggesting that both Varicose and Egghead are required for development of the optic lobe. *c855aGAL4* drives expression in cells of the developing lobula and lamina including inner proliferating cells (IPCs) and outer proliferating cells (OPCs) (Egger et al., 2007; Hrdlicka et al., 2002; Fan

et al., 2005). While Egh appears to play a more specific role in the lobula and IPCs, Varicose is expressed in the OPCs suggesting the expression link between these proteins may be a red-herring. In the adult visual system, we have observed Varicose expression in the sheath-like glia of lamina neurons. It is possible that an interaction between the glia of lamina neurons and the lamina/lobula complex glia function together to regulate axon projections. A more in-depth analysis of this protein interaction is required.

Egghead is also required in the oocyte-follicle cell adhesion system. Without *egh* expression, epithelial cells fail to maintain their columnar characteristics and lose apical-basal polarity resulting in the accumulation of several epithelial layers (Goode et al., 1996). We have been unable to detect Varicose expression in the female germline, however recent experiments by Bachmann et al. (2007) have shown by western blotting that Varicose is expressed in the ovary. An alternative interaction between Egghead and Varicose could occur during oogenesis.

4.4.5 Localization of Varicose Requires Neuroglian

We have previously shown that Varicose is required for proper subcellular localization of several SJ proteins such as NeurexinIV, FasciclinIII and Na⁺K⁺ATPase. Additionally, Varicose is required for proper targeting of Coracle to the septate junction (Wu et al., 2007). Varicose however, was not required for proper localization of Dlg. We determined whether the localization of Varicose and these SJ proteins was interdependent. Varicose was properly localized in both *dlg* and *scribble* mutants. This is expected as both proteins function in regulating cell polarity, an event that does not require Vari. While all three proteins localize to the same submembrane domain, it

appears that several multidomain complexes assemble at the septate junction and regulate different cellular mechanisms.

Localization of Varicose to the SJ was unaffected in our *coracle* mutant. This is contradictory to previous results (Wu et al., 2007). We expect that the difference in our findings is due to the alleles examined. While our studies involved *coracle* allele, *cora*^{k08713}, which contains a P-element insertion in the 5' region of *coracle*, other studies have utilized allele, *cora*⁵, a null allele that disrupts SJ barrier function (Genova et al., 2003). Although *cora*^{k08713} is considered a phenocopy of the *cora*⁵ allele and a zygotic null, this P-element insertion line is described as a protein hypomorph (Chen et al., 2005) and could possibly be accountable for the discrepancies observed in Varicose distribution.

It is well known that Coracle and NeurexinIV are interdependent in their localization at the SJ junction. Both proteins are required for SJ barrier function and are thought to exist as a complex (Baumgartner et al., 1996; Fehon et al., 1994). It would be expected that if Coracle is required for expression of Vari at the SJ, that Neurexin would also be required. Varicose was properly localized in our *nrx*⁴³⁰⁴ allele. Contradictory results were observed using the *nrx*⁴⁸⁴⁶ allele (Wu et al. 2007). We could again speculate that the difference in results is due to a difference in alleles. *nrx*⁴³⁰⁴, an ethyl methanesulfonate induced mutation, is described as a hypomorphic or null allele. This allele is associated with SJ defects including disrupted septae and a defective paracellular barrier. The source of the *nrx*⁴⁸⁴⁶ mutation and resulting phenotypes have not been described. Precipitation assays have identified a physical interaction between the PDZ

domain of Varicose and the C-terminal domain of Nr_xIV (Bachmann et al., 2008; Wu et al., 2007). While this interaction may likely exist at the SJ, it does not imply that Nr_xIV is required for Varicose localization. Our results suggest that Vari localization is independent of Coracle and Neurexin and we suspect that Varicose plays a role in tethering these proteins to the SJ.

Proper localization of Vari requires Neuroglian, a glycoprotein belonging to the immunoglobulin (Ig) superfamily. Nrg is expressed on the surface of glia in the PNS and CNS and in non-neuronal tissues including the trachea, hindgut, and salivary gland (Bieber et al., 1989). Nrg has been isolated in a complex with Cora and Nr_xIV and all three are interdependently localized (Genova et al., 2003). The depletion and mislocalization of Varicose in *nrg* mutants suggests that Vari may also belong to this interdependent complex. We do not know if Vari is required for Nrg localization but based on previous findings with other SJ proteins, we speculate that there is a co-dependency between Vari and Nrg for proper SJ localization. It remains possible that the mislocalization of Vari is secondary to a disruption in SJ structure caused by the mutation in *nrg*. Ankyrin, a membrane skeletal component, interacts with the C-terminus of Nrg at sites of cell-cell contact (Genova et al., 2003). It is proposed that the Cora/Nr_xIV/Nrg complex assembles on ankyrin, however other scaffold proteins may be involved in this complex assembly. Vari may act in such a role.

The family of MAGUK proteins contains multiple protein-protein interaction domains which allow them to function as a protein scaffolds upon which many proteins assemble. Through our yeast two-hybrid screen we have identified multiple proteins

proposed to interact with Varicose. While some proteins are transmembrane proteins and others function as kinases, we have identified novel putative functions for Varicose during development. We have previously shown Varicose is expressed in the proliferating centres of the optic lobe. A role for Varicose in this tissue is supported by the identification of potential interacting partners that also regulate these proliferating centres.

Currently, our identified interacting proteins lack the L27 domain. It is possible that proteins containing L27 domains, such as D Lin-7 remain in the group of uncharacterized clones. Identifying Lin-7 as a partner of Vari would further support the evolutionary conservation of protein complexes between vertebrate and invertebrate systems.

The PDZ domain of Varicose has been shown to interact with the C-terminal EIFI sequence of transmembrane protein NrxIV (Wu et al., 2007). This sequence is similar to the C-terminal EYFI sequence of Necl-2 shown to interact with the PDZ domain of PALS2 (Shingai et al., 2003). Both Varicose and PALS2 contain a Proline residue at position αB1 of the PDZ domain which typically interacts with hydrophobic residues at position -2 of the peptide ligand. However, the -2 residue of Necl-2 is hydrophilic suggesting other properties of this ligand influence PDZ binding. Similarly, we have shown that Vari localization depends on transmembrane protein Nrg, yet the C-termini of both Nrg isoforms, ATYV and RKGL fail to interact with the PDZ domain of Vari (Wu et al., 2007). This indicates that the interaction between Nrg and Vari is not direct. Our recently identified transmembrane protein IDGF4 ends in amino acid sequence KSKL, a

probable PDZ binding ligand. Although serine is a hydrophilic residue, it is not unlikely that these two proteins may physically interact. Further studies are required for clarification of this matter.

The SH3 domain has been implicated in targeting signaling components to the plasma membrane by interacting with polyproline rich motifs within the peptide ligand (Yu et al., 1994). Through an interaction between the SH3 domain of α -spectrin and a proline motif encoded within epithelial Na⁺ channel α ENaC, the channel is properly localized to the apical membrane (Rotin et al., 1994). Additionally, the SH3 domain has been shown to regulate enzymatic activities. For example, the SH3 domain in ZO-1 binds to a serine protein kinase that phosphorylates a C-terminal region to the SH3 domain. The significance of this interaction is unclear (Balda et al., 1996). Polyproline motifs PFFP and PVVP have been identified in Awd as well as PQTP, PRTP and PKGVPPP motifs in Bällchen. Perhaps the SH3 domain of Varicose is able to interact with the proline-rich motifs identified within these kinases.

Little is known about the consensus motif required for GUK interactions (Reese et al., 2007). Studies in vertebrate systems have shown that the GUK domain is able to interact with proteins such as microtubule associated protein 1a (MAP1a) and guanylate kinase associated protein (GKAP) linking MAGUKs to the neuronal cytoskeleton and to glutamate receptor scaffolds, respectively (Brenman et al., 1998; Kim et al., 1997). It is not clear if these interactions are conserved in *Drosophila*. We have been unable to detect Varicose at the synapse and the interaction between these GUK associated proteins

does not seem probable. It seems more likely that scaffold assembly occurs through the SH3/GUK intramolecular interactions of MAGUKs and other multidomain proteins.

Our recent introduction to the use of hydrophobicity plots to predict biological roles or characteristics of proteins, has aided in our ability to elucidate the likelihood of a protein-interaction between Varicose and our candidate proteins. In general, the distribution of hydrophobic and hydrophilic residues along a protein sequence may be used to predict protein membrane-spanning segments (hydrophobic) or protein regions likely to be exposed (hydrophilic) (Kyte and Doolittle, 1982). A hydropathy plot for each of our candidate proteins was generated (courtesy of Dr. Michael Hortsch). The presence of a hydrophobic region (ie. a hydrophobicity score greater than 2.0) at the N-terminus of IDGF4 is suggestive of a signal sequence indicating this protein is likely to be secreted. Moreover, a similar pattern was seen in the protein sequence of Egh. In addition, hydrophobic regions within the C-terminus are potential transmembrane segments. The short sequence following these transmembrane segments is not expected to interact with other proteins such as Varicose. Therefore, based on Kyte-Doolittle hydrophobicity plots, IDGF4 and Egh are unlikely candidates for Varicose-interacting proteins. On the other hand, hydrophobic regions are not observed in Bällchen suggesting it is a cytoplasmic protein. As well, a potential N-terminal hydrophobic region of Awd suggests this protein may function cytoplasmically. This data therefore indicates that unlike IDGF4 and Egh, Bäll and Awd may be potential interacting proteins of Varicose.

We have only begun to examine the yeast two-hybrid interacting clones and look forward to identifying the remaining Varicose putative partners. We anticipate this work

will provide a better understanding for the role of Varicose during septate junction organization, tracheal morphogenesis and optic lobe development as well as identify novel Varicose functions.

CONCLUSIONS & PROSPECTS

The data we have presented here supports a role for MAGUK member Varicose in cell junction assembly. Varicose is expressed in all ectodermally-derived epithelial cells including the epidermis, trachea and hindgut but excluding the malpighian tubules. The region of expression is detected along the lateral plasma membrane corresponding to the septate junction. Neuroglian is required for localization of Varicose to the SJ, which in turn, is necessary for the proper localization of other SJ proteins such as NeurexinIV, Na⁺K⁺ATPase and FasciclinIII. Discs large is properly targeted to the SJ in the absence of *varicose* and cell polarity is unaffected. This data correlates with the late on-set of Varicose expression at the SJ, a time when cell polarization has already been established. We do not know if Varicose directly associates with other SJ proteins, however, one could suggest that based on the numerous protein-protein interaction domains encoded in this MAGUK that Varicose serves as a scaffold upon which other junction-associated proteins assemble. Transgenic overexpression in *vari* mutants partially restores the targeting of NrXIV to the lateral membrane suggesting Vari may regulate the proper localization of SJ components. Additionally, the HOOK domain of Varicose has the potential to bind members of the band 4.1 protein family which could link Varicose to the cytoskeleton and consequently tether NrXIV to the SJ.

We have shown that Varicose is fundamental in establishing a paracellular seal. Failure to exclude tracer dyes from the tracheal lumen suggests Varicose participates in the assembly of SJs. One might expect that trans-epithelial diffusion of the tracer dye may be due to disruption in the assembly of septa strands. Our ultrastructural data

suggests that septa strands do not develop in *vari* mutants and as result, the seal is compromised. Taken together, our findings suggest that Nrg, NrXIV and Varicose function together during SJ assembly to develop septa strands necessary for intracellular regulation.

Scaffolding proteins often regulate more than a single process, mediated by the multiple protein-protein interactions. The pattern of Varicose expression and additional phenotypes associated with *vari* mutants suggest that this MAGUK plays a role in several processes which may or may not be associated with the SJ. Our findings suggest that Varicose is involved in regulating tube size during tracheal morphogenesis. Tracheal development appears normal in *vari* mutants; however, the mechanism(s) of tube expansion appear unregulated. While tube length does not appear to be dramatically affected, the dorsal trunk exhibits extreme dilations. This phenotypic effect can be rescued with *vari* transgenics. Regulation of tube diameter involves secretion of an apical chitin matrix. It would be expected then, that the chitin matrix is disrupted in *vari* mutants; however the ultrastructural data indicates that the chitinous taenidial folds form properly. How Varicose is involved in tube size regulation is currently unknown.

We have also identified potential roles for Varicose in the peripheral nervous system and during the development of adult structures such as the wing and eye. We have not observed Varicose labelling in larval third instar imaginal discs leading us to speculate that the role of Varicose during development of these tissues occurs during pupal stages. We have unveiled a novel role for MAGUKs in the late larval and adult central nervous system which is independent of membrane junctions. Our knowledge of

how Varicose participates in these processes remains limited. Future work in identifying Varicose interacting partners and dissecting the role of Varicose in these post-embryonic tissues will provide insight into the junctional regulation of cellular processes and elaborate on the extensive roles of MAGUK members.

OVERVIEW

During the course of this work several labs have independently reported on the role of Varicose at the septate junction. These works, in combination with our own have enabled us to build a model involving Varicose in septate junction maturation.

Varicose and Nr_xIV have overlapping expression patterns in all ectodermally-derived epithelial tissues. Mutational analysis of these genes suggests an interdependent relationship for proper SJ localization. Mutations in both genes result in a defective paracellular seal due to the absence of intercellular septa strands (this work; Baumgartner et al., 1996). These findings support the idea of a potential interaction between Vari and Nr_xIV. The C-terminus of Nr_xIV is highly similar to the C-terminus of vertebrate Glycophorin C, which binds to cytoskeletal-associated Protein 4.1 and the PDZ domain of MAGUK palmitoylated membrane protein 55 (p55) to regulate erythrocyte cell membrane structure (Anderson and Lovrien et al., 1984; Kusunoki and Kohno, 2007). Similarly, in *Drosophila*, the C-terminus of Nr_xIV binds to the Protein 4.1 ortholog, Coracle, and has the potential to interact with type II PDZ domains (Baumgartner et al., 1996). The interdependent colocalization of Cora and Nr_xIV, in addition to their role in the formation of septa strands is well established (Ward et al., 1998; Lamb et al., 1998), however the protein(s) required for the initial targeting of this protein pair to the membrane surface is unknown. It was not surprising that, like Glycophorin C, the C-terminal amino acid sequence of Nr_xIV binds the PDZ domain of Vari, which has high sequence similarity with the p55 subfamily of MAGUKs (Wu et al., 2007). This interaction is further supported by misexpression studies of Nr_xIV whereby

misexpression of *nrxIV* is followed by accumulation of Vari to the sites of misexpression (Bachmann et al., 2008). Unlike Coracle, Vari encodes a HOOK domain which has the potential to associate with cytoskeletal-associated proteins. It is likely that through the HOOK domain, Vari tethers NrxIV and Coracle to the lateral membrane regulating the formation of septa strands.

An interdependent localization of Nrg and Vari has also been observed in embryonic epithelia (this work; Laval et al., 2008). Vari, however, is unable to bind to the C-terminus of Nrg (Wu et al., 2007). This raises the question, how are Vari and Nrg connected at the SJ? Nrg has been found to form a protein complex with NrxIV and Cora at the SJ (Genova and Fehon, 2003). Although NrxIV appears to function as a heterophilic cell adhesion molecule (Baumgartner et al., 1996), Nrg favours strong homophilic interactions (Hortsch et al., 1995). A third transmembrane protein, Cont, has been found to associate with NrxIV and Nrg at the SJ. Cont interacts with NrxIV in *cis* and forms a biochemical complex with Nrg. It is unclear if the NrxIV/Cont pair interacts with Nrg within the same cell or between cells (Faivre-Sarrailh et al., 2004). Unlike *nrxIV* mutants, *cont* and *nrg* mutants have a reduced number of septa suggesting that NrxIV acts upstream in the formation of strands whereas Cont and Nrg are involved in strand organization (Faivre-Sarrailh et al., 2004; Genova and Fehon, 2003). To complicate matters, claudin-like transmembrane protein Mega depends upon NrxIV and Cora for proper membrane localization and is involved in the formation of septa strands (Behr et al., 2003). Like NrxIV, the C-terminus of Mega possesses a PDZ binding motif (QGYI) of the type II class and could potentially bind Vari.

Lateral mobility studies have shown that mutations in transmembrane proteins such as *NrxIV* and *Nrg* increase the mobility of other transmembrane proteins along the lateral membrane. What is more intriguing is the greater effect that mutations in scaffolding proteins have on transmembrane mobility. Depletion of *vari* from the SJ increases the ability of both *NrxIV* and *Nrg* to laterally move along the membrane suggesting that this scaffolding protein may cross-link scaffold or transmembrane proteins (Laval et al., 2008). One might propose that *Vari* binds the C-terminus of both *NrxIV* and *Mega*. Binding of the PDZ domain to its ligand may release the intramolecular inhibition of the GUK domain (Bachmann et al., 2008) and allow the oligomerization with itself or other MAGUK members. The C-terminus of *Vari* encodes a potential PDZ binding motif (NWIY) (Wu et al., 2007) providing an additional method by which cross-linking may occur. How *Nrg* is targeted to the cell surface is unknown. The C-terminus of *Nrg* is capable of binding ankyrin (Hortsch et al., 1998), a linker protein that connects the actin-spectrin network to various membrane proteins (Bouley et al., 2000) and type I PDZ domains such as those found in *Dlg*. It is possible that *Cont* and *Nrg* are recruited to the SJ by *NrxIV* and *Dlg*, respectively, and as an ensemble these proteins organize septa strands. These strands may be stabilized by *Vari* through the association with cytoskeleton via ankyrin. Although this model requires extensive exploration, the lateral mobility studies performed by Laval and colleagues (2008) support a role for *Varicose* at the SJ as the backbone for multiprotein scaffold assembly.

A more speculative role for Varicose may involve regulation of the blood-nerve barrier. Peripheral axons are wrapped in a layer of subperineurial glia which in turn is wrapped by larger perineurial glial cells (Tepass and Hartenstein, 1994). Cell junctions, such as the SJ can be found between glial layers as well as between the axons and glia (Banerjee et al., 2006b). These junctions form the blood-nerve barrier that protects axons from the surrounding high potassium hemolymph (Carlson et al., 2000). Both Vari and Nr_xIV colocalize at the SJ of peripheral glia. Additionally, the Nr_xIV/Cont/Nrg complex is conserved at peripheral SJs (Banerjee et al., 2006b; Faivre-Sarrailh et al., 2004). Both Nr_xIV and Cont localize to the glial membrane whereas Nrg localizes to both glial and axonal membranes. As seen in epithelial cells, these three proteins form a complex that is interdependent for their localization to peripheral nerves. Loss of either of these proteins results in disruption of the SJ and a leaky blood-nerve barrier. Further examination of *nrxIV* mutants has revealed a reduction in coordinated muscle propagation leading to embryonic paralysis. It is proposed that loss of *nrxIV* disrupts glial-glial SJs. Junctional breakdown results in the disruption of action potential propagation and perturbation of the blood-nerve barrier exposing peripheral nerves to the hemolymph (Baumgartner et al., 1996). Similar paralysis phenotypes are seen in *nrg* mutants (Genova and Fehon, 2003). Is it possible that the association of Vari with Nr_xIV and Nrg is conserved in the peripheral nervous system? Our preliminary data suggests that this might be the case. Transgenic rescues of *vari* mutants restore adult viability however these animals experience little movement and an inability to walk. Is it possible that severely reduced walking coordination is resultant of blood-nerve barrier breakdown? Further examination

of SJ ultrastructure and permeability of tracer dyes across the blood-nerve barrier will help to support this hypothesis.

Flies and humans are more than 500 million years apart on the evolutionary scale. We have consistently observed an evolutionary conservation of protein complexes across vertebrate and invertebrate species, for example, the Crumbs/Bazooka/Lgl pathways. However, we question the evolutionary conservation of Varicose. The following section compares the similarities and differences between Vari and vertebrate homologue, PALS2, in addition to addressing the question of whether Vari/PALS2 regulate similar cellular processes through conserved protein complexes.

In *Drosophila*, the SJ regulates the paracellular movement of molecules between epithelial sheets and acts as a barrier to protect peripheral nerves from the hemolymph (Noirot-Timothee and Noirot, 1980; Carlson et al., 1997). In vertebrates, paracellular regulation is maintained by TJs (Tsukita et al., 2001). While SJs and TJs seem to provide an analogous function, the molecular components are not easily comparable. Vari, as we have shown, localizes to the SJ and is necessary for barrier establishment. The proposed vertebrate homologue of Vari, PALS2, as previously mentioned in the introduction, is not associated with cellular junctions and appears to bind Necl2 at the basolateral region of the epithelial membrane (Shingai et al., 2003). Searching the *Drosophila* genome for a homologue of Necl2 identified several cell adhesion molecules with 25% amino acid identity to Necl2. These CAMs play a role in myoblast fusion (Kocherlakota et al., 2008; Dworak et al., 2001), a process that does not seem to involve Vari. One particular CAM,

Hibris, associates with DE-Cadherin at AJs in the eye (Carthew, 2007). Vari has been implicated in eye development (this work; Bachmann et al., 2008), however in an AJ-independent manner. The functional importance of the Necl2/PALS2 interaction has yet to be determined. It is unknown if a *Drosophila* homologue of Necl2 exists, however, it seems clear that PALS2 does not play a role in paracellular regulation implying that the functional roles of Vari and PALS2 in epithelia have diverged evolutionarily.

To date, SJs appear absent from vertebrate epithelia, however septate-like junctions can be found in the nervous system. In the PNS, Schwann cells (myelin) are a type of glial cell that wraps long segments of axons and exposes small segments of axons, the nodes of Ranvier (Susuki and Rasband, 2008) which are advantageous for achieving rapid action potential propagation. Voltage-gated Na⁺ channels cluster at the nodes of Ranvier to facilitate saltatory conduction (Bellen et al., 1998). Concurrent with axonal myelination, several polarized domains are formed around the nodes of Ranvier (Banerjee et al., 2006b). The paranodal regions flank the nodes (Susuki and Rasband, 2008). Septate-like junctions are found in these regions where ladder-like septa form between myelin loops and axolemma (Banerjee et al., 2006b). The paranodal region is characterized by a tripartite complex consisting of Contactin-associated protein (Caspr), a homologue of *Drosophila* NrXIV (Peles et al., 1997a), Contactin (CONT) and Neurofascin 155 (NF155). Caspr is expressed on the axonal membrane where it *cis*-interacts with Contactin (Peles et al., 1997b) which in turn, interacts with glial surface cell adhesion molecule Neurofascin 155 (Poliak et al., 2001; Bonnon et al., 2007). Protein 4.1B interacts with both actin and spectrin to link the Caspr complex to the

axonal cytoskeleton (Susuki and Rasband, 2008). This Caspr/CONT/NF155 complex is highly similar to the NrXIV/Cont/Nrg complex found at invertebrate SJs and is thought to serve as a diffusion barrier to the leakage of ions and small molecules (Faivre-Sarrailh et al., 2004). Additionally, this complex may function as a physical barrier to separate the Na⁺ channels of the node from the K⁺ channels (Kv1 channels) of the juxtaparanode (Banerjee et al., 2006), which are thought to help maintain internodal resting potential and stabilize conduction (Poliak et al., 1999). The juxtaparanode is a polarized domain that flanks the paranode and also associates with the cytoskeleton whereas the internode flanks the juxtaparanode, with slight overlap, and is located beneath the myelin sheath (Susuki and Rasband, 2008).

The evolutionary conservation of the Caspr and NrXIV complexes raises the question of whether it is possible that the Vari/NrXIV interaction is conserved between PALS2/Caspr. Although experimental studies aimed to address this question have not been conducted, it is probable that PALS2 does not interact with Caspr at the paranode, but rather associates with a highly related protein, Caspr2 at the juxtaparanode (Poliak et al., 1999). Unlike Caspr, which lacks a C-terminus capable of binding PDZ domains (Arroyo et al., 1999), Caspr2 binds protein 4.1B, and in addition, is capable of binding type II PDZ domains, such as that found in PALS2. It is suspected that Caspr2 localizes K⁺ channels to the juxtaparanode via a PDZ-containing protein, implicating PALS2 as a probable candidate (Poliak et al., 1999). It is possible that PALS2 may serve this function suggesting that the invertebrate NrXIV/Cora/Vari association may be conserved complex of Caspr2/4.1B/PALS2. Alternatively, Necl2 has been found along the

internodal region of myelinated nerves (Maurel et al., 2007). While the role of Necl2 in this region has not been explored and the expression of PALS2 along myelinated nerves has not been determined we open the door to the possibility that PALS2 may associate with Necl2 at the internode but make no further assumptions.

The septate-like paranodal regions provide a barrier for the diffusion of small ions and passage of larger molecules between the node and juxtaparanode (Bellen et al., 1998) similar to glial SJs of the *Drosophila* PNS. Absence of PALS2 from this region would indicate that PALS2 does not play a role in barrier formation or establishment. It is clear that pinpointing the membrane localization of PALS2 in the nervous system is a necessary step in the exploration of its functional significance and conservation with Vari. The current data suggests that the both Vari and PALS2 may bind NrxF and Caspr2, respectively, through conserved mechanisms yet the functional roles of these MAGUK proteins appear to have diverged over time.

PALS2 was originally identified as an interacting partner of mLin-7. Studies to elucidate how these proteins interact *in vivo* remain limited. Several independent lines of evidence suggest that mLin-7, also known as Veli, may associate with PALS2 to properly target inwardly rectifying potassium channels. (1) PALS2 and mLin-7/Veli are expressed in the brain and (2) are thought to interact through their L27 domains (Kamberov et al., 2000). (3) Veli directly associates with channel Kir2.2 in brain extracts and has been shown to target Kir2.2 to the basolateral plasma membrane of Madin-Darby Canine Kidney (MDCK) epithelial cells in coordination with MAGUK member CASK, the

vertebrate homologue of *Drosophila* Camguk (Leonoudakis et al., 2004a). (4) PALS2 was identified as a Kir2.2-associated protein in whole brain extracts (Leonoudakis et al., 2004b). Kir2 channels are a family of strong inwardly-rectifying potassium channels, meaning they have a stronger ability to pass K^+ current in the inward direction than the outward (Leonoudakis et al., 2004a). The polarized localization of these transport proteins are necessary for vectorial functions such as the transport of water and ions across epithelia as well as cellular processes such as cell excitability and repolarization of action potentials (Olsen et al., 2002). Trafficking of these ion channels to polarized subcellular domains is regulated by interactions with MAGUK family members (Leonoudakis et al., 2004b). Once the channels have reached their target membrane, they may be anchored through interactions with the cytoskeleton or other membrane-associated proteins. The C-terminus of Kir2 channels encode a type I PDZ ligand suggesting asymmetric distribution is directed by PDZ-containing proteins (Olsen et al., 2002). It is not likely that PALS2 directly associates with the PDZ ligand of Kir2.2, but rather is recruited by Veli, which directly associates with the channel to ensure proper subcellular localization (Leonoudakis et al., 2004b). The precise role of PALS2 in potassium channel targeting is not yet clear. Whether PALS2 is involved in targeting of the channel to specific domains or is involved in anchoring the channel to the membrane remains to be resolved.

The limited exploration of the Vari/DLin-7 interaction in *Drosophila* has revealed that these proteins are able to physically interact (Bachmann et al., 2008). In 2003, a genome-wide protein interaction map isolated DLin-7 and Vari as interacting proteins,

providing additional verification of this interaction (Giot et al., 2003). However, in epithelia, Vari localizes to the SJ whereas DLin-7 has been found to associate with Sdt at the SAR (this work; Bachmann et al., 2004). Is it possible that Vari and DLin-7 function together in non-epithelial tissues? DLin-7 was shown to be enriched postsynaptically at the NMJ, yet we were unable to detect Vari expression at these sites. As well, DLin-7 is observed in larval neuropile regions of the CNS (R.J, personal communication), another region devoid of Vari expression. *Drosophila*, like vertebrate systems, possesses inwardly rectifying potassium channels which are found in the malpighian (renal) tubules (Döring et al., 2002; Evans et al., 2005). Unfortunately, neither Vari nor DLin-7 expression is observed in these tissues. The evidence would imply that Vari and DLin-7 do not associate functionally, yet the evolutionary conservation of this protein interaction cannot be ignored suggesting this interaction is of unknown functional significance.

Varicose has also been shown to play a role in tubulogenesis. Major organs such as the lung and kidney are mainly composed of tubes that facilitate the transportation of fluids or gases (Behr et al., 2007). Although these tubes arise through different mechanisms, they are initially small and experience periods of growth to achieve their mature size. Defects in respiratory tube diameter may compromise the rate of gas exchange. In both *Drosophila* and vertebrates, biogenesis of the apical membrane and secretion are critical in determining tube size (Lubarsky and Krasnow, 2003). We know that apical secretion of chitinous material into the lumen contributes to tube size regulation. Reduction in apically secreted chitin modifying enzymes and luminal antigen

suggests that Vari is involved in apical secretion of an unknown mechanism to regulate tube size. The means of regulating tube growth in vertebrates is less understood. Individuals with polycystic kidney disease (PKD) are plagued with fluid-filled cysts that arise from focal expansions along the renal tubule. Cilia protruding from the apical surface of renal epithelial cells may regulate a tube-size sensor signaling pathway that arrests tube growth (Lubarsky and Krasnow, 2003). Even though *Drosophila* tracheal tubes lack cilia, both invertebrates and vertebrates encompass sensor mechanisms to halt expansion when the lumen has reached its mature size. Wu and Beitel (2004) propose SJs may regulate an apical extracellular matrix that controls tracheal cell shape. Similarly, polycystin 1, a gene mutated in ~85% of PKD cases, is capable of cell-matrix interactions necessary for the structural organization of renal epithelial cells (Boletta and Germino, 2003). Further dissection of the role of Varicose at the SJ and the subsequent involvement in tube size regulation may provide insight into the tube-size sensor mechanisms of vertebrate systems and perhaps offer therapeutic ways to relieve tubular defects.

The emergence of multicellular organisms brought about the need for cells to adhere to one another. Cellular junctions developed as the demand for cell-cell adhesion and communication arose. As this change occurred, the necessity of ionic and molecular barriers evolved (Banerjee et al., 2006) and the SJ appeared to maintain homeostasis. The presence of SJs in the most primitive metazoans, (Porifera) (Ledger, 1975) and persistence of SJs across protostomes was indicative of its functional significance. Variations of SJs have also been found among *Coelenterata*, *Annelida*, *Arthropoda* and

Mollusca (Green and Flower, 1980; Wood, 1959; Baskin, 1976; Noirot-Timothee and Noirot, 1980; Gilula et al., 1970). In addition, deuterostomes such as *Echinodermata* and *Chordata* possess SJs (Green, 1981; Banerjee et al., 2006b; Georges, 1979). Invertebrate SJs and vertebrate TJs are proposed to be functionally analogous. TJs not only act as impermeable barriers but select ions based on size and have variable tightness depending on cell type (Tsukita et al., 2001). Among some classes of *Arthropoda*, such as cockroaches (*Periplaneta americana*), both SJs and TJs have been observed in rectal epithelia and in the perineurium of the CNS (Lane, 1979; Lane and Chandler, 1980). In these cases, the TJ is suspected to regulate permeability whereas the role of the SJ is unknown. Both spiders (*Tegenaria domestica*) and moths (*Manduca sexta*) possess TJs in the CNS but not SJs (Lane and Chandler, 1980; Lane et al., 1977). Neither SJs nor TJs have been found in the perineurium of *Drosophila* (Tepass and Hartenstein, 1994). The absence of TJs among *Hydra* and *Drosophila* suggest that in the absence of these junctions, SJs perform the role of permeability barrier. Little evidence suggests that TJs evolved from SJs. Moreover, it is likely that these junctions have evolved separately and the necessity of the SJ in vertebrate systems has been superseded by the TJ (Lane, 1984). Although the paracellular functions of septate and tight junctions are highly similar, the junctional components have diverged. Along the same lines, MAGUK family members have evolved in concert with metazoan lineages (te Velthuis et al., 2007). For example, vertebrate TJ protein ZO-1 has been found to be associated with the plasma membrane of *Hydra*, but is excluded from the SJ (Fei et al., 2000). As members of the animal kingdom have become progressively more complex, the number of MAGUK members has

increased; for example, mammals encode almost four times the number of MAGUKs compared to *Drosophila*. Vari and PALS2 are another example of structural conservation, and evolutionary divergence, demonstrated by limited conservation between junctional expression of these two MAGUKs. It is an intriguing possibility that the septate-like junctions observed in glia of the vertebrate nervous system may be a deuterostome descendent of protostome SJs. For now, we will have to await the discovery of the functional role(s) PALS2 plays in vertebrates. Meanwhile, our investigations have identified a MAGUK member that can be used to enhance our understanding of SJ organization and structure, in addition to dissecting the roles of this junction in barrier permeability in a variety of cell types.

REFERENCES

- Adams, M.D., Sekelsky, J.J., 2002. From sequence to phenotype: reverse genetics in *Drosophila melanogaster*. *Nature Rev.* 3, 189-198.
- Adler, P.N., 2002. Planar signaling and morphogenesis in *Drosophila*. *Dev. Cell* 2, 525-535.
- Aho, S., Arffman, A., Pummi, T. and Uitto, J., 1997. A novel reporter gene *MEL1* for the yeast two-hybrid system. *Anal. Biochem.* 253, 270-272.
- Aihara, H., Nakagawa, T., Yasui, K., Ohta, T., Hirose, S., Dhomae, N., Takio, K., Kaneko, M., Takeshima, Y., Maramatsu, M., Ito, T., 2004. Nucleosomal histone kinase-1 phosphorylates H2A Thr 119 during mitosis in the early *Drosophila* embryo. *Genes Dev.* 18, 877-888.
- Alberts, B., Bray, D., Lewis, J., Raff, M., Roberts, K., Watson, J.D., 1994. *Molecular Biology of the Cell*, Third Edition. U.S.A: Garland Publishing.
- Anderson, R.A., Lovrien, R.E., 1984. Glycophorin is linked by band 4.1 protein to the human erythrocyte membrane skeleton. *Nature* 307, 655-658.
- Araújo, S.J., Aslam, H., Tear, G., and Casanova, J., 2005. mummy/cystic encodes an enzyme required for chitin and glycan synthesis, involved in trachea, embryonic cuticle and CNS development - analysis of its role in *Drosophila* tracheal morphogenesis. *Dev. Biol.* 288, 179-193.
- Arguello, J.R., Chen, Y., Yang, S., Wang, W., Long, M., 2006. Origination of an X-linked testes chimeric gene by illegitimate recombination in *Drosophila*. *PLoS Genetics* 2, e77.
- Arroyo, E.J., Xu, Y.T., Zhou, L., Messing, A., Peles, E., Chiu, S.Y., Scherer, S.S., 1999. Myelinating Schwann cells determine the internodal localization of Kv1.1, Kv1.2, Kvbeta2, and Caspr. *J. Neurocytol.* 28, 333-347.
- Auld, V.J., Fetter, R.D., Broadie, K., Goodman, C.S., 1995. Gliotactin, a novel transmembrane protein on peripheral glia, is required to form the blood-nerve barrier in *Drosophila*. *Cell* 81, 757-767.
- Bachmann, A., Draga, M., Grawe, F., Knust, E., 2008. On the role of the MAGUK proteins encoded by *Drosophila* Varicose during embryonic and postembryonic development. *BMC Dev. Biol.* 8, 55.
- Bachmann, A., Schnelder, M., Thellenberg, E., Grawe, F., and Knust, E., 2001. *Drosophila* Stardust is a partner of Crumbs in the control of epithelial polarity. *Nature* 414, 638-643.
- Bachmann, A., Timmer, M., Sierralta, J., Peitrini, G., Gundelfinger, E.D., Knust, E., Thomas, U., 2004. Cell type-specific recruitment of *Drosophila* Lin-7 to distinct MAGUK-based protein complexes defines novel roles for Sdt and Dlg-S97. *J. Cell Sci.* 117, 1899-1909.
- Balda, M.S., Anderson, J.M., Matter, K., 1996. The SH3 domain of the tight junction protein ZO-1 binds to a serine protein kinase that phosphorylates a region C-terminal to this domain. *FEBS Lett.* 399, 326-332.
- Banerjee, S., Bainton, R.J., Mayer, N., Beckstead, R., and Bhat, M.A., 2008. Septate junctions are required for ommatidial integrity and blood-eye barrier function in *Drosophila*. *Dev. Biol.* 317, 585-99.

- Banerjee, S., Sousa, A.D., Bhat, M.A., 2006. Organization and function of septate junctions. *Cell Biochem. Biophys.* 46, 65-77.
- Banerjee, S., Pillai, A.M., Paik, R., Li, J., Bhat, M.A., 2006b. Axonal ensheathment and septate junction formation in the peripheral nervous system of *Drosophila*. *J. Neurosci.* 26, 3319-3329.
- Baskin, D.G., 1976. The fine structure of Polychaete septate junction. *Cell Tissue Res.* 174, 55-67.
- Baumgartner, S., Littleton, J.T., Broadie, K., Bhat, M.A., Harbecke, R., Lengyel, J.A., Chiquet-Ehrismann, R., Prokop, A., and Bellen, H.J., 1996. A *Drosophila* neurexin is required for septate junction and blood-nerve barrier formation and function. *Cell* 87, 1059-1068.
- Bayraktar, J., Zygmunt, D., Carthew, R.W., 2006. Par-1 kinase establishes cell polarity and functions in Notch signaling in the *Drosophila* embryo. *J. Cell Sci.* 119, 711-721.
- Behr, M., Riedel, D., and Schuh, R., 2003. The claudin-like megatrachea is essential in septate junctions for the epithelial barrier function in *Drosophila*. *Dev. Cell* 5, 611-620.
- Behr, M., Wingen, C., Wolf, C., Schuh, R., Hoch, M., 2007. Wurst is essential for airway clearance and respiratory-tube size control. *Nature Cell Biol.* 9, 847-853.
- Beitel, G.J., and Krasnow, M.A., 2000. Genetic control of epithelial tube size in the *Drosophila* tracheal system. *Development* 127, 3271-3282.
- Bellen, H.J., Lu, Y., Beckstead, R., Bhat, M.A., 1998. NeurexinIV, caspr and paranodin – novel members of the neurexin family: encounters of axons and glia. *Trends Neurosci.* 21, 444-449.
- Benton, R., St Johnston, D., 2003. *Drosophila* Par-1 and 14-3-3 inhibit Bazooka/Par-3 to establish complementary cortical domains in polarized cells. *Cell* 115, 691-704.
- Berger, C., Renner, S., Lüer, K., Technau, G.M., 2007. The commonly used marker ELAV is transiently expressed in neuroblasts and glial cells in the *Drosophila* embryonic CNS. *Dev. Dyn.* 236, 3562-3568.
- Berger, S., Bulgakova, N.A., Grawe, F., Johnson, K., Knust, E., 2007. Unraveling the genetic complexity of *Drosophila* Stardust during photoreceptor morphogenesis and prevention of light-induced degeneration. *Genetics* 176, 2189-2200.
- Betschinger, J., Mechtler, K., Knoblich, J.A., 2003. The Par complex directs asymmetric cell division by phosphorylating the cytoskeleton protein Lgl. *Nature* 422, 326-330.
- Bhat, M.A., Izaddoost, S., Lu, Y., Cho, K.O., Choi, K.W., Bellen, H.J., 1999. Discs Lost, a novel multi-PDZ domain protein, establishes and maintains epithelial polarity. *Cell* 96, 833-845.
- Bieber, A.J., Snow, P.M., Hortsch, M., Patel, N.H., Jacobs, J.R., Traquina, Z.R., Schilling, J., and Goodman, C.S., 1989. *Drosophila* Neuroglian: a member of the immunoglobulin superfamily with extensive homology to the vertebrate neural adhesion molecule L1. *Cell* 59, 447-460.
- Biggs, J., Tripoulas, N., Hersperger, E., Dearolf, C., Shearn, A., 1988. Analysis of the lethal interaction between the prune and killer of prune mutations of *Drosophila*. *Genes Dev.* 2, 1333-1343.
- Bilder, D., 2001. PDZ proteins and polarity: functions from the fly. *Trends Genet.* 17, 511-519.

- Bilder, D., Li, M., Perrimon, N., 2000. Cooperative regulation of cell polarity and growth by *Drosophila* tumor suppressors. *Science* 289, 113-116.
- Bilder, D., Perrimon, N., 2000. Localization of apical epithelial determinant by the basolateral PDZ protein Scribble. *Nature* 403, 676-680.
- Bilder, D., Schober, M., Perrimon, N., 2003. Integrated activity of PDZ protein complexes regulates epithelial polarity. *Nat. Cell Biol.* 5, 53-58.
- Boletta, A., Germino, G.G., 2003. Role of polycystins in renal tubulogenesis. *Trends Cell Biol.* 13, 484-492.
- Bonnon, C., Bel, C., Goutebroze, L., Maigret, B., Girault, J.A., Faivre-Sarrailh, C., 2007. PGY repeats and N-glycans govern the trafficking of Paranodin and its selective association with Contactin and Neurofascin-155. *Mol. Biol. Cell* 18, 229-241.
- Bouley, M., Tian, M.Z., Paisley, K., Shen, Y.C., Malhotra, J.D., Hortsch, M., 2000. The L1-type cell adhesion molecule Neuroglian influences the stability of neural Ankyrin in the *Drosophila* embryo but not its axonal localization. *J. Neurosci.* 20, 4515-4523.
- Brenman, J.E., Topinka, J.R., Cooper, E.C., McGee, A.W., Rosen, J., Milroy, T., Ralston, H.J., Bredt, D.S., 1998. Localization of Postsynaptic Density-93 to dendritic microtubules and interaction with Microtubule-Associate Protein 1A. *J. Neurosci.* 18, 8805-8813.
- Bryant, P.J., 1997. Junction genetics. *Dev. Genetics* 20, 75-90.
- Bulgakova, N.A., Kempkens, Ö., Knust, E., 2008. Multiple domains of Stardust differentially mediate localisation of the Crumbs-Stardust complex during photoreceptor development in *Drosophila*. *J. Cell Sci.* 121, 2018-2026.
- Cabernard, C., Neumann, M., Affolter, M., 2004. Cellular and molecular mechanisms involved in branching morphogenesis of the *Drosophila* tracheal system. *J. Appl. Physiol.* 97, 2347-2353.
- Cao, X., Ding, X., Guo, Z., Zhou, R., Wang, F., Long, F., Wu, F., Bi, F., Wang, Q., Fan, D., Forte, J.G., Teng, M., Yao, X., 2005. PALS1 specifies the localization of Ezrin to the apical membrane of gastric parietal cells. *J. Biol. Chem.* 280, 13584-13592.
- Carlson, S.D., Hilgers, S.L., Juang, J.L., 1997. Ultrastructure of blood-nerve barrier of chordotonal organs in the *Drosophila* embryo. *J. Neurocytol.* 26, 377-288.
- Carlson, S.D., Juang, J.L., Hilgers, S.L., and Garment, M.B., 2000. Blood barriers of the insect. *Annu. Rev. Entomol.* 45, 151-174.
- Carthew, R.W., 2007. Pattern formation in the *Drosophila* eye. *Curr. Opin. Genet. Dev.* 17, 309-313.
- Caruana, G., 2002. Genetic studies define MAGUK proteins as regulators of epithelial cell polarity. *Int. J. Dev. Biol.* 46, 511-518.
- Chen, C.M., Freedman, J.A., Bettler, Jr., D.R., Manning, S.D., Giep, S.N., Steiner, J., Ellis, H.M., 1996. polychaetoid is required to restrict segregation of sensory organ precursors from proneural clusters in *Drosophila*. *Mech. Dev.* 57, 215-227.

- Chen, K., Merino, C., Sigrist, S.J., Featherstone, D.E., 2005. The 4.1 protein Coracle mediates subunit-selective anchoring of *Drosophila* glutamate receptors to the postsynaptic actin cytoskeleton. *J. Neurosci.* 25, 6667-6675.
- Chen, Y.W., Pedersen, J.W., Wandall, H.H., Levery, S.B., Pizette, S., Clausen, H., Cohen, S.M., 2007. Glycosphingolipids with extended sugar chain have specialized functions in development and behavior in *Drosophila*. *Dev. Biol.* 306, 736-749.
- Chien, C.T., Bartel, P.L., Sternglanz, R., Fields, S., 1991. The two-hybrid system: a method to identify and clone genes for proteins that interact with a protein of interest. *Proc. Nat. Acad. Sci. USA* 88, 9578-9582.
- Cho, K.O., Hunt, C.A., Kennedy, M.B., 1992. The rat brain postsynaptic density fraction contains a homolog of the *Drosophila* Discs-large tumor suppressor protein. *Neuron* 9, 929-942.
- Couderic, J.L., Godt, D., Zollman, S., Chen, J., Li, M., Tiong, S., Cramton, S.E., Sahut-Barnola, I., Laski, F.A., 2002. The bric à brac locus consists of two paralogous genes encoding BTB/POZ domain proteins and acts as a homeotic and morphogenetic regulator of imaginal development in *Drosophila*. *Development* 129, 2419-2433.
- Crosby, M.A., Goodman, J.L., Strelets, V.B., Zhang, P., Gelbart, W.M., and FlyBase Consortium, 2007. FlyBase: genomes by the dozen. *Nucleic Acids Res.* 35, D486-D491.
- Cullen, C.F., Brittle, A.L., Ito, T., Ohkura, H., 2005. The conserved kinase NHK-1 is essential for mitotic progression and unifying acentrosomal meiotic spindles in *Drosophila melanogaster*. *J. Cell Biol.* 171, 593-602.
- D'Souza-Schorey, C., 2005. Disassembling adherens junctions: breaking up is hard to do. *Trends Cell Biol.* 15, 19-26.
- Dammai, V., Adryan, B., Lavenburg, K.R., Hsu, T., 2003. *Drosophila* awd, the homolog of human nm23, regulates FGF receptor levels and functions synergistically with shi/dynamin during tracheal development. *Genes Dev.* 17, 2812-2824.
- Denholm, B., Sudarsan, V., Pasalodos-Sanchez, S., Artero, R., Lawrence, P., Maddrell, S., Baylies, M., Skaer, H., 2003. Dual origin of the renal tubules in *Drosophila*: mesodermal cells integrate and polarize to establish secretory function. *Curr. Biol.* 13, 1052-1057.
- Deutsch, W.A., Yacoub, A., Jaruga, P., Zastawny, T.H., Dizdaroglu, M., 1997. Characterization and mechanism of action of *Drosophila* Ribosomal protein S3 glycosylase activity for the removal of oxidatively damaged DNA bases. *J. Biol. Chem.* 272, 32857-32860.
- Dimitratos, S.D., Woods, D.F., Bryant, P.J., 1997. Camguk, Lin-2, and CASK: novel membrane-associated guanylate kinase homologs that also contain CaM kinase domains. *Mech. Dev.* 63, 127-130.
- Dimitratos, S.D., Woods, D.F., Statkakis, D.G., and Bryant, P.J., 1999. Signaling pathways are focused at specialized regions of the plasma membrane by scaffolding proteins of the MAGUK family. *BioEssays* 21, 912-921.
- Dodd, R.B., Drickamer, K., 2001. Lectin-like proteins in model organisms: implications for evolution of carbohydrate-binding activity. *Glycobiology* 11, 71R-79R.

- Doe, C.Q., Chu-LaGraff, Q., Wright, D.M., and Scott, M.P., 1991. The prospero gene specifies cell fates in the *Drosophila* central nervous system. *Cell* 65, 451-464.
- Doerks, T., Bork, P., Kamberov, E., Makarova, O., Muecke, S., Margolis, B., 2000. L27, a novel heterodimerization domain in receptor targeting proteins Lin-2 and Lin-7. *Trends Biochem. Sci.* 25, 317-318.
- Döring, F., Wischmeyer, E., Kühnlein, R.P., Jäckle, H., Karschin, A., 2002. Inwardly rectifying K⁺ (Kir) channels in *Drosophila*. *J. Biol. Chem.* 277, 25554-25561.
- Dubreuil, R.R., Maddux, P.B., Grushko, T.A., and MacVicar, G.R., 1997. Segregation of two spectrin isoforms: polarized membrane-binding sites direct polarized membrane skeleton assembly. *Mol. Biol. Cell* 8, 1933-1942.
- Duffy, J.B., 2002. GAL4 system in *Drosophila* a fly geneticist's Swiss army knife. *Genesis* 34, 1-15.
- Dunlop, J., Morin, X., Corominas, M., Serras, F., and Tear, G., 2004. glaikit is essential for the formation of epithelial polarity and neuronal development. *Curr. Biol.* 14, 2039-2045.
- Dworak, H.A., Charles, M.A., Pellerano, L.B., Sink, H., 2001. Characterization of *Drosophila* hibris, a gene related to human nephrin. *Development* 128, 4265-4276.
- Ebnet, K., 2008. Organization of multiprotein complexes at cell-cell junctions. *Histochem. Cell Biol.* 130, 1-20.
- Egger, B., Boone, J., Stevens, N.R., Brand, A.H., and Doe, C.Q., 2007. Regulation of spindle orientation and neural stem cell fate in the *Drosophila* optic lobe. *Neural Develop.* 2, 1-14.
- Erez, N., Bershadsky, A., and Geiger, B., 2005. Signaling from adherens-type junctions. *Eur. J. Cell Biol.* 84, 235-244.
- Evans, J.M., Allan, A.K., Davies, S.A., Dow, J.A.T., 2005. Sulphonylurea sensitivity and enriched expression implicate inward rectifier K⁺ channels in *Drosophila melanogaster* renal function. *J. Exp. Biol.* 208, 3771-3783.
- Fan, Y., Soller, M., Flister, S., Hollmann, M., Müller, B., Bello, B., Egger, B., White, K., Schäfer, M.A., Reichert, H., 2005. The egghead gene is required for compartmentalization in *Drosophila* optic lobe development. *Dev. Biol.* 287, 61-73.
- Fanning, A.S., Anderson, J.M., 1999. PDZ domains: fundamental building blocks in the organization of protein complexes at the plasma membrane. *J. Clin. Invest.* 103, 67-772.
- Faivre-Sarrailh, C., Banerjee, S., Li, J., Hortsch, M., Laval, M., Bhat, M.A., 2004. *Drosophila* Contactin, a homolog of vertebrate Contactin, is required for septate junction organization and paracellular barrier function. *Development* 131, 4931-4942.
- Fehon, R., 2006. Polarity bites. *Nature* 442, 519-520.
- Fehon, R.G., Dawson, I.A., and Artavanis-Tsakonas, S., 1994. A *Drosophila* homologue of membrane-skeleton protein 4.1 is associated with septate junctions and is encoded by the coracle gene. *Development* 120, 545-557.

- Fei, K., Yan, L., Zhang, J., Sarras Jr., M.P., 2000. Molecular and biological characterization of a zonula occludens-1 homologue in *Hydra vulgaris*, named HZO-1. *Dev Genes Evol.* 210, 611-616.
- Feng, W., Long, J.F., Fan, J.S., Suetake, T., Zhang, M., 2004. The tetrameric L27 domain complex as an organization platform for supramolecular assemblies. *Nat. Struct. Mol. Biol.* 11, 475-480.
- Feng, W., Long, J.F., Zhang, M., 2005. A unified assembly mode revealed by the structures of tetrameric L27 domain complexes formed by mLin-2/mLin-7 and Patj/Pals1 scaffold proteins. *Proc. Natl. Acad. Sci. USA* 102, 6861-6866.
- Fields, S., Song, O., 1989. A novel genetic system to detect protein-protein interactions. *Nature* 340, 245-247.
- Foe, V.E., Alberts, B.M., 1983. Studies of nuclear and cytoplasmic behavior during the five mitotic cycles that precede gastrulation in *Drosophila* embryogenesis. *J. Cell Sci.* 61, 31-70.
- Foe, V.E., Odell, G.M., Edgar, B.A., 1993. Mitosis and morphogenesis in the *Drosophila* embryo. *The Development of Drosophila* (ed. M. Bate and A. Martinez-Arias). Cold Spring Harbor NY: Cold Spring Harbor Laboratory.
- Fristrom, D., 1988. The cellular basis of epithelial morphogenesis. A review. *Tissue Cell* 20, 645-690.
- Fristrom, D.K., 1982. Septate junctions in imaginal disks of *Drosophila*: a model for the redistribution of septa during cell rearrangement. *J. Cell Biol.* 94, 77-87.
- Funke, L., Dakoji, S., and Brecht, D.S., 2005. Membrane-associated guanylate kinases regulate adhesion and plasticity at cell junctions. *Annu. Rev. Biochem.* 74, 219-245.
- Gateff, E., 1978. Malignant neoplasms of genetic origin in *Drosophila melanogaster*. *Science* 200, 1448-1459.
- Genova, J.L., and Fehon, R.G., 2003. Neuroglian, Gliotactin, and the Na⁺K⁺ ATPase are essential for septate junction function in *Drosophila*. *J. Cell. Biol.* 161, 979-989.
- Georges, D., 1979. Gap and tight junctions in Tunicates. Study in conventional and freeze-fracture techniques. *Tissue Cell* 11, 781-792.
- Ghabrial, A., Luschnig, S., Metzstein, M.M., Krasnow, M.A., 2003. Branching morphogenesis of the *Drosophila* tracheal system. *Annu. Rev. Cell Dev. Biol.* 19, 623-647.
- Gibson, M.C., Perrimon, N., 2003. Apicobasal polarization: epithelial form and function. *Curr. Opin. Cell. Biol.* 15, 747-752.
- Gilula, N.B., Branton, D., Satir, P., 1970. The septate junction: A structural basis for intercellular coupling. *Proc. Natl. Acad. Sci. USA* 67, 213-220.

- Giot, L., Bader, J.S., Brouwer, C., Chaudhuri, A., Kuang, B., Li, Y., Hao, L., Ooi, E., Godwin, B., Vitols, E., Vijayadamodar, G., Pochart, P., Machineni, H., Welsh, M., Kong, Y., Zerhusen, B., Malcolm, R., Varrone, Z., Collis, A., Minto, M., Burgess, S., McDaniel, L., Stimpson, E., Spriggs, F., Williams, J., Neurath, K., Ioime, N., Agee, M., Voss, E., Furtak, K., Renzulli, R., Aanensen, N., Carrolla, S., Bickelhaupt, E., Lazovatsky, Y., DaSilva, A., Zhong, J., Stanyon, C.A., Finley Jr., R.L., White, K.P., Braverman, M., Jarvie, T., Gold, S., Leach, M., Knight, J., Shimkets, R.A., McKenna, M.P., Chant, J., Rothberg, J.M., 2003. A protein interaction map of *Drosophila melanogaster*. *Science* 302, 1727-1736.
- Goldstein, L.S.B., and Fyrberg, E.A., 1994. *Drosophila Melanogaster*: Practical uses in cell and molecular biology. Toronto: Academic Press.
- González-Mariscal, L., Betanzos, A., and Ávila-Flores, A., 2000. MAGUK proteins: structure and role in the tight junction. *Cell Dev. Biol.* 11, 315-324.
- Goode, S., Melnick, M., Chou, T.B., Perrimon, N., 1996. The neurogenic genes egghead and brainiac define a novel signaling pathway essential for epithelial morphogenesis during *Drosophila* oogenesis. *Development* 122, 3863-3879.
- Graf, F., Noirot-Timotheé, C., Noirot, C.H., 1982. The specialization of septate junctions of regions of tricellular junctions. I. Smooth septate junctions (=continuous junctions). *J. Ultrastruct. Res.* 78, 136-151.
- Grawe, F., Wodarz, A., Lee, B., Knust, E., Skaer, H., 1996. The *Drosophila* genes crumbs and stardust are involved in the biogenesis of adherens junctions. *Development* 122, 951-959.
- Green, C.R., 1981. Fixation-induced intramembrane particle movement demonstrated in freeze-fracture replicas of a new type of septate junction in *Echinoderm* epithelia. *J. Ultrastruct. Res.* 75, 11-22.
- Green, C.R., Flower, N.E., 1980. Two new septate junctions in the phylum *Coelenterata*. *J. Cell Sci.* 42, 43-59.
- Gurtner, G.C., Werner, S., Barrandon, Y., Longaker, M.T., 2008. Wound repair and regeneration. *Nature* 453, 314-321.
- Harris, B.Z., Venkatasubrahmanyam, S., Lim, W.A., 2002. Coordinated folding and association of the LIN-2, -7 (L27) domain. *J. Biol. Chem.* 277, 34902-34908.
- Harris, T.J.C., Peifer, M., 2005. The positioning and segregation of apical cues during epithelial polarity establishment in *Drosophila*. *J. Cell Biol.* 170, 813-823.
- Harris, T.J.C., Peifer, M., 2004. Adherens junction – dependent and –independent steps in the establishment of epithelial cell polarity in *Drosophila*. *J. Cell Biol.* 167, 135-147.
- Hilgendeldt, S., Eriskens, S., Carthew, R.W., 2008. Physical modeling of cell geometric order in an epithelial tissue. *Proc. Nat. Acad. Sci.* 105, 907-911.
- Hipfner, D.R., Cohen, S.M., 1999. New growth factors for imaginal discs. *BioEssays* 21, 718-720.
- Hodge, J.J., Mullasseril, P., Griffith, L.C., 2006. Activity-dependent gating of CaMKII autonomous activity by *Drosophila* CASK. *Neuron* 51, 327-337.

- Hong, Y., Stronach, B., Perrimon, N., Jan, L.Y., Jan, Y.N., 2001. *Drosophila* Stardust interacts with crumbs to control polarity of epithelia but not neuroblasts. *Nature*. 414, 634-638.
- Hortsch, M., Homer, D., Malhotra, J.D., Chang, S., Frankel, J., Jefford, G., Dubreuil, R.R., 1998. Structural requirements for outside-in and inside-out signaling by *Drosophila* Neuroglian, a member of the L1 family of cell adhesion molecules. *J. Cell Biol.* 142, 251-261.
- Hortsch, M. and Margolis, B., 2003. Septate and paranodal junctions: kissing cousins. *Trends Cell Biol.* 13, 557-561.
- Hortsch, M., Wang, Y.E., Marikar, Y., Bieber, A.J., 1995. The cytoplasmic domain of the *Drosophila* cell adhesion molecule Neuroglian is not essential for its homophilic adhesive properties in S2 cells. *J. Biol. Chem.* 270, 18809-18817.
- Hough, C.D., Woods, D.F., Park, S., Bryant, P.J., Organizing a functional junctional complex requires specific domains of the *Drosophila* MAGUK Discs large. *Genes Dev.* 11, 3242-3253.
- Hrdlicka, L., Gibson, M., Kiger, A., Micchelli, C., Schober, M., Schöck, F., and Perrimon, N., 2002. Analysis of twenty-four gal4 lines in *Drosophila melanogaster*. *Genesis* 34, 51-57.
- Hung, A.Y., Sheng, M., 2002. PDZ domains: structural modules for protein complex assembly. *J. Biol. Chem.* 277, 5699-5702.
- Hurd, T.W., Gao, L., Roh, M.H., Macara, I.G., Margolis, B., 2003. Direct interaction of two polarity complexes implicated in epithelial tight junction assembly. *Nat. Cell Biol.* 5, 137-142.
- Hutterer, A., Betschinger, J., Petronczki, M., Knoblich, J.A., 2004. Sequential roles of Cdc42, Par-6, aPKC, and Lgl in the establishment of epithelial polarity during *Drosophila* embryogenesis. *Dev. Cell* 6, 845-854.
- Ivanovska, I., Khandan, T., Ito, T., Orr-Weaver, T.L., 2005. A histone code in meiosis: the histone kinase, NHK-1, is required for proper chromosomal architecture in *Drosophila* oocytes. *Genes Dev.* 19, 2571-2582.
- Jacobs, J.R. and Goodman, C.S., 1989. Embryonic development of axon pathways in the *Drosophila* CNS. I. A glial scaffold appears before the first growth cones. *J. Neurosci.* 9, 2402-2411.
- James, P., Haliaday, J., Craig, E.A., 1996. Genomic libraries and a host strain designed for highly efficient two-hybrid selection in yeast. *Genetics* 144, 1425-1436.
- Jemth, P., Gianni, S., 2007. PDZ domains: folding and binding. *Biochem.* 46, 8701-8708.
- Jessen, S., Gu, B., Dai, X., 2008. Pygopus and the Wnt signaling pathway: a diverse set of connections. *BioEssays* 30, 448-456.
- Jung, A.C., Ribeiro, C., Michaut, L., Certa, U., Affolter, M., 2006. Polychaetoid/ZO-1 is required for cell specification and rearrangement during *Drosophila* tracheal morphogenesis. *Curr. Biol.* 16, 1224-1231.
- Jürgens, G., Wieschaus, E., Nüsslein-Volhard, C., Lüding, M., 1984. Mutations affecting the pattern of the larval cuticle in *Drosophila melanogaster*. II. Zygotic loci on the third chromosome. *Wil. Roux's Arch.* 193, 283-95.

- Kaech, S.M., Whitfield, C.W., and Kim, S.K., 1998. The LIN-2/LIN-7/LIN-10 complex mediates basolateral membrane localization of the *C.elegans* EGF receptor LET-23 in vulval epithelial cells. *Cell* 94, 761-771.
- Kamberov, E., Makarova, O., Roh, M., Liu, A., Karnak, D., Straight, S., and Margolis, B., 2000. Molecular cloning and characterization of Pals, proteins associated with mlin-7. *J. Biol. Chem.* 275, 11425-11431.
- Katsube, T., Takahisa, M., Ueda, R., Hashimoto, N., Kobayashi, M., Togashi, S., 1998. Cortactin associates with the cell-cell junction protein ZO-1 in both *Drosophila* and mouse. *J. Biol. Chem.* 273, 29672-29677.
- Kawamura, K., Shibata, T., Saget, O., Peel, D., Bryant, P.J., 1999. A new family of growth factors produced by the fat body and active on *Drosophila* imaginal disc cells. *Development* 126, 211-219.
- Kennedy, M.B., 1995. Origin of PDZ (DHR, GLGF) domains. *Trends Biochem. Sci.* 20, 350. Kerman, B.E., Cheshire, A.M., and Andrew, D.J., 2006. From fate to function: the *Drosophila* trachea and salivary gland as models for tubulogenesis. *Differentiation* 74, 326-348.
- Kim, E., Naisbitt, S., Hsueh, Y.P., Rao, A., Rothschild, A., Craig, A.M., Sheng, M., 1997. GKAP, a novel synaptic protein that interacts with the guanylate kinase-like domain of the PSD-95/SAP90 family of channel clustering molecules. *J. Cell Biol.* 136, 669-678.
- Klebes, A., Knust, E., 2000. A conserved motif in Crumbs is required for E-cadherin localization and zonula adherens formation in *Drosophila*. *Curr. Biol.* 10, 76-85.
- Klinge, K., Onichtchouk, D., Jackle, H., 2004. Bällchen is a novel Ser/Thr kinase involved in germ cell development. *A. Dros. Res. Conf.* 45:421A.
- Knust, E. and Bossinger, O., 2002. Composition and formation of intercellular junctions in epithelial cells. *Science* 298, 1955-1959.
- Kocherlakota, K.S., Wu, J.M., McDermott, J., Abmayr, S.M., 2008. Analysis of the cell adhesion molecule Sticks-and-Stones reveals multiple redundant functional domains, protein-interaction motifs and phosphorylated tyrosines that direct myoblast fusion in *Drosophila melanogaster*. *Genetics* 178, 1371-1383.
- Kuchinke, U., Grawe, F., and Knust, E., 1998. Control of spindle orientation in *Drosophila* by the Par-3-related PDZ-domain protein Bazooka. *Curr. Biol.* 8, 1357-1365.
- Kukulies, J., Komnick, H., 1983. Plasma membranes, cell junctions and cuticle of the rectal chloride epithelia of the larval dragonfly *Aeshna cyanea*. *J. Cell Sci.* 59, 159-182.
- Kusunoki, H., Kohno, T., 2007. Structural insight into the interaction between the p55 PDZ domain and glycoporphin C. *Biochem Biophys Res Commun.* 359, 972-978.
- Kyte, J., Doolittle, R.F., 1982. A simple method for displaying the hydropathic character of a protein. *J. Mol. Biol.* 157, 105-132.
- Lamb, R.S., Ward, R.E., Schweizer, L., and Fehon, R.G., 1998. *Drosophila* coracle, a member of the protein 4.1superfamily, has essential structural functions in the septate junctions and developmental functions in embryonic and adult epithelial cells. *Mol. Biol. Cell* 9, 3505-3519.

- Lane, N.J., 1984. A comparison of the construction of intercellular junctions in the CNS of vertebrates and invertebrates. *Trends Neurosci.* 7, 95-99.
- Lane, N.J., 1979. Freeze-fracture and tracer studies on the intercellular junctions of insect rectal tissues. *Tissue Cell* 11, 481-506.
- Lane, N.J., Chandler, H.J., 1980. Definitive evidence for the existence of tight junctions in invertebrates. *J. Cell Biol.* 86, 765-774.
- Lane, N.J., Skaer, H., Swales, L.S., 1977. Intercellular junctions in the central nervous system of insects. *J. Cell Sci.* 26, 175-199.
- Lange, B.M.H., Rebollo, E., Herold, A., González, C., 2002. Cdc37 is essential for chromosome segregation and cytokinesis in higher eukaryotes. *EMBO J.* 21, 5364-5374.
- Laprise, P., Beronja, S., Silva-Gagliardi, N.F., Pellikka, M., Jensen, A.M., McGlade, C.J. Tepass, U., 2006. The FERM protein Yurt is a negative regulatory component of the Crumbs complex that controls epithelial polarity and apical membrane size. *Dev. Cell* 11, 363-374.
- Laval, M., Bel, C., Faivre-Sarrailh, C., 2008. The lateral mobility of cell adhesion molecules is highly restricted at septate junctions in *Drosophila*. *BMC Cell Biol.* 9, 38.
- Le Bivic, A., 2005. E-cadherin-mediated adhesion is not the founding event of epithelial cell polarity in *Drosophila*. *Trends Cell Biol.* 15, 237-240.
- Ledger, P.W., 1975. Septate junctions in the calcareous sponge *Sycon ciliatum*. *Tissue Cell* 7, 13-18.
- Lee, S., Fan, S., Makarova, O., Straight, and Margolis, B., 2002. A novel and conserved protein-protein interaction domain of mammalian Lin-2/CASK binds and recruits SAP97 to the lateral surface of epithelia. *Mol. Cell Biol.* 22, 1778-1791.
- Lee, S., Leung H.T., Kim, E., Jang, J., Lee, E., Baek, K., Pak, W.L., Yoon, J., 2007. Effects of a mutation in the *Drosophila* porin gene encoding mitochondrial voltage-dependent anion channel protein on phototransduction. *Dev. Neurobiol.* 67, 1533-45.
- Leonoudakis, D., Conti, L.R., Radeke, C.M., McGuire, L.M.M., Vandenberg, C.A., 2004a. A multiprotein trafficking complex composed of SAP97, CASK, Veli, and Mint1 is associated with inward rectifier Kir2 potassium channels. *J. Biol. Chem.* 279, 19051-19063.
- Leonoudakis, D., Conti, L.R., Anderson, S., Radeke, C.M., McGuire, L.M.M., Adams, M.E., Froehner, S.C., Yates III, J.R., Vandenberg, C.A., 2004b. Protein trafficking and anchoring complexes revealed by proteomic analysis of inward rectifier potassium channel (Kir2.x)-associated proteins. *J. Biol. Chem.* 279, 22331-22346.
- Leptin, M., 1999. Gastrulation in *Drosophila*: the logic and the cellular mechanisms. *EMBO J.* 18, 3187-3192.
- Li, Y., Karnak, D., Demeler, B., Margolis, B., Lavie, A., 2004. Structural basis for L27 domain-mediated assembly of signaling and cell polarity complexes. *EMBO J.* 23, 2723-2733.
- Lin, H., and Spradling, A.C., 1993. Germline stem cell division and egg chamber development in transplanted *Drosophila* germaria. *Dev. Biol.* 159, 140-152.

- Llimargas, M., Strinini, M., Katidou, M., Karagogeos, D., Casanova, J., 2003. Lachesin is a component of septate junction-based mechanism that controls tube size and epithelial integrity in the *Drosophila* tracheal system. *Development* 131, 181-190.
- Lopes, C., Gassanova, S., Delabar, J.M., Rachidi, M., 2001. The CASK/Lin-2 *Drosophila* homologue, Camguk, could play a role in epithelial patterning and neuronal targeting. *Biochem. Biophys. Res. Commun.* 284, 1001-1010.
- Lu, C.S., Hodge, J.J., Mehren, J., Sun, X.X., Griffith, L.C., 2003. Regulation of the Ca²⁺/CaM-responsive pool of CaMKII by scaffold-dependent autophosphorylation. *Neuron* 40, 1185-1197.
- Lubarsky, B., Krasnow, M.A., 2003. Tube morphogenesis: making and shaping biological tubes. *Cell* 112, 19-28.
- Lundgren, J., Masson, P., Mirzaei, Z., and Young, P., 2005. Identification and characterization of a *Drosophila* proteasome regulatory network. *Mol. Cell. Biol.* 25, 4662-4675.
- Luschnig, S., Batz, T., Armbruster, K., and Krasnow, M.A., 2006. serpentine and vermiform encode matrix proteins with chitin binding and deacetylation domains that limit tracheal tube length in *Drosophila*. *Curr. Biol.* 16, 186-194.
- MacMullin, A., and Jacobs, J.R., 2006. Slit coordinates cardiac morphogenesis in *Drosophila*. *Dev. Biol.* 293, 154-164.
- Manfruelli, P., Arquiere, N., Hanratty, W.P., Sémériva, M., 1996. The tumor suppressor gene, lethal(2)giant larvae (l(2)gl), is required for cell shape change of epithelial cells during *Drosophila* development. *Development* 122, 2282-2294.
- Martin, J.R., Ollo, R., 1996. A new *Drosophila* Ca²⁺/calmodulin-dependent protein kinase (Caki) is localized in the central nervous system and implicated in walking speed. *EMBO J.* 15, 1865-1876.
- Matter, K. and Balda, M.S., 2003. Functional analysis of tight junctions. *Methods* 30, 228-234.
- Matter, K. and Mellman, I., 1994. Mechanisms of cell polarity: sorting and transport in epithelial cells. *Curr. Opin. Cell Biol.* 6, 545-554.
- Maurel, P., Einheber, S., Galinska, J., Thaker, P., Lam, I., Rubin, M.B., Scherer, S.S., Murakami, Y., Gutmann, D.H., Salzer, J.L., 2007. Nectin-like proteins mediate axon-Schwann cell interactions along the internode and are essential for myelination. *J. Cell Biol.* 178, 861-874.
- Mazumdar, A., Mazumdar, M., 2002. How one becomes many: blastoderm cellularization in *Drosophila melanogaster*. *BioEssays* 24, 1012-1022.
- McGee, A.W., Brecht, D.S., 1999. Identification of an intramolecular interaction between the SH3 and guanylate kinase domains of PSD-95. *J. Biol. Chem.* 274, 17431-17436.
- McGee, A.W., Dakoiji, S., Olsen, O., Brecht, D.S., Lim, W.A., 2001. Structure of the SH3-Guanylate kinase module from PSD-95 suggests a mechanism for regulated assembly of MAGUK scaffolding proteins. *Mol. Cell* 8, 1291-1301.

- Médina, E., Williams, J., Klipfell, E., Zarnescu, D., Thomas, G., Le Bivic, A., Crumbs interacts with moesin and β_{Heavy} -spectrin in the apical membrane skeleton of *Drosophila*. *J. Cell Biol.* 158, 941-951.
- Mendoza, C., Olgún, P., Lafferte, G., Thomas, U., Ebisch, S., Gundelfinger, E.D., Kukuljan, M., Sierralta, J., 2003. Novel isoforms of Dlg are fundamental for neuronal development in *Drosophila*. *J. Neurosci.* 23, 2093-2101.
- Miller, J., Stagljar, I., 2004. Using the yeast two-hybrid system to identify interacting proteins. *Methods Mol. Biol.* 261, 247-262.
- Moussian, B., Schwarz, H., Bartoszewski, S., and Nüsslein-Volhard, C., 2005. Involvement of chitin in exoskeleton morphogenesis in *Drosophila melanogaster*. *J. Morphol.* 264, 117-130.
- Moyer, K.E., and Jacobs, J.R., 2006. Senz'aria, a MAGUK family adapter, is required for tracheal morphogenesis. *A. Dros. Res. Conf.* 48, 540C.
- Müller, B.M., Kistner, U., Veh, R.W., Cases-Langhoff, C., Becker, B., Gundelfinger, E.D., Garner, C.C., 1995. Molecular characterization and spatial distribution of SAP97, a novel presynaptic protein homologous to SAP90 and the *Drosophila* Discs-large tumor suppressor proteins. *J. Neurosci.* 15, 2354-2366.
- Müller, H.J., 2000. Genetic control of epithelial cell polarity: Lessons from *Drosophila*. *Dev. Dyn.* 218, 52-67.
- Müller, H.J., Wieschaus, E., 1996. armadillo, bazooka, and stardust are critical for early stages in formation of the zonula adherens and maintenance of the polarized blastoderm epithelium in *Drosophila*. *J. Cell Biol.* 134, 149-163.
- Myat, M.M., 2005. Making tubes in the *Drosophila* embryo. *Dev. Dyn.* 232, 617-632.
- Nallmothu, G., Woolworth, J.A., Dammai, V., Hsu, T., 2008. awd, the homolog of metastasis suppressor gene Nm23, regulates *Drosophila* epithelial cell invasion. *Mol. Cell. Biol.* 28, 1964-1973.
- Nambu, J.R., Franks, R.G., Hu, S., and Crews, S.T., 1990. The single-minded gene of *Drosophila* is required for the expression of genes important for the development of CNS midline cells. *Cell* 63, 63-75.
- Nance, J., 2005. PAR proteins and the establishment of cell polarity during *C. elegans* development. *BioEssays* 27, 126-135.
- Nelson, W.J., 2003. Adaptation of core mechanisms to generate cell polarity. *Nature* 422, 766-774.
- Niessen, C.M., Gottardi, C.J., 2008. Molecular components of the adherens junction. *Biochim. Biophys. Acta* 1778, 562-571.
- Noirot-Timotheé, C., Graf, F., Noirot, C.H., 1982. The specialization of septate junctions of regions of tricellular junctions . II. Pleated septate junctions. *J. Ultrastruct. Res.* 78, 152-165.
- Noirot-Timotheé, C., Noirot, C., 1980. Septate and scalariform junctions in arthropods. *Int. Rev. Cytol.* 63, 97-141.

- Ogita, H., Takai, Y., 2008. Cross-talk among integrin, cadherin, and growth factor receptor: roles of nectin and nectin-like molecule. *Int. Rev. Cytol.* 265, 1-54.
- Ohno, S., 2001. Intercellular junctions and cellular polarity: the PAR-aPKC complex, a conserved core cassette playing fundamental roles in cell polarity. *Curr. Opin. Cell Biol.* 13, 641-648.
- Olsen, O., Brecht, D.S., 2003. Functional analysis of the nucleotide binding domain of membrane-associated guanylate kinases. *J. Biol. Chem.* 278, 6873-6878.
- Olsen, O., Liu, H., Wade, J.B., Merot, J., Welling, P.A., 2002. Basolateral membrane expression of the Kir 2.3 channel is coordinated by PDZ interaction with Lin-7/CASK complex. *Am. J. Physiol. Cell Physiol.* 282, C183-C195.
- Pai, L.M., Kirkpatrick, C., Blanton, J., Oda, H., Takeichi, M., Peifer, M., 1996. *Drosophila* α -catenin and E-cadherin bind to distinct regions of *Drosophila* armadillo. *J. Biol. Chem.* 271, 32411-32420.
- Parker, D.S., Jemison, J., Cadigan, K.M., 2002. Pygopus, a nuclear PHD-finger protein required for Wingless signaling in *Drosophila*. *Development* 129, 2565-2576.
- Parker, R.J. and Auld, V.J., 2006. Roles of glia in the *Drosophila* nervous system. *Cell Dev. Biol.* 17, 66-77.
- Patel, N., 1994. Imaging neuronal subsets and other cell types in whole-mount *Drosophila* embryos and larvae using antibody probes. *Methods Cell Biol.* 44, 445-505.
- Patel, N.H., Snow, P.M., Goodman, C.S., 1987. Characterization and cloning of FasciclinIII: A glycoprotein expressed on a subset of neurons and axon pathways in *Drosophila*. *Cell* 48, 975-988.
- Patthy, L., 1991. Laminin A-related domains in Crb protein of *Drosophila* and their possible role in epithelial polarization. *FEBS Lett.* 289, 99-101.
- Paul, S.M., Ternet, M., Salvaterra, P.M., and Beitel, G.J., 2003. Na⁺/K⁺ ATPase is required for septate junction function and epithelial tube-size control in the *Drosophila* tracheal system. *Development* 130, 4963-4974.
- Payre, F., 2004. Genetic control of epidermis differentiation in *Drosophila*. *Int. J. Dev. Biol.* 48, 207-215.
- Peles, E., Joho, K., Plowman, G.D., Schlessinger, J., 1997a. Close similarity between *Drosophila* Neurexin IV and mammalian Caspr protein suggests a conserved mechanism for cellular interactions. *Cell* 88, 745-746.
- Peles, E., Nativ, M., Lustig, M., Grumet, M., Schilling, J., Martinex, R., Plowman, G.D., Schlessinger, J., 1997b. Identification of a novel contactin-associated transmembrane receptor with multiple domains implicated in protein-protein interactions. *EMBO J.* 16, 978-988.
- Peng, C.Y., Manning, L., Albertson, R., and Doe, C.Q., 2000. The tumour-suppressor genes *lgl* and *dlg* regulate basal protein targeting in *Drosophila* neuroblasts. *Nature* 408, 596-600.
- Perrimon, N., 1988. The maternal effect of *lethal(1)discs-large-1*: A recessive oncogene of *Drosophila melanogaster*. *Dev. Biol.* 127, 392-407.

- Petronczki, M., Knoblich, J.A., 2001. DmPAR-6 directs epithelial polarity and asymmetric cell division of neuroblasts in *Drosophila*. *Nat. Cell Biol.* 3, 43-49.
- Petrosky, K.Y., Ou, H.D., Löhr, F., Dötsch, V., Lim, W.A., 2005. A general model for preferential hetero-oligomerization of Lin-2/7 domains: mechanism underlying directed assembly of supramolecular signaling complexes. *J. Biol. Chem.* 280, 38528-38536.
- Phelan, P., 2005. Innexins: members of an evolutionary conserved family of gap-junction proteins. *Biochim. Biophys. Acta* 1711, 225-245.
- Pilot, F., Philippe, J.M., Lemmers, C., Lecuit, T., 2006. Spatial control of actin organization at adherens junctions by the synaptotagmin-like protein Btsz. *Nature* 442, 580-584.
- Poliak, S., Gollan, L., Martinez, R., Custer, A., Einheber, S., Salzer, J.L., Trimmer, J.S., Shrager, P., Peles, E., 1999. Caspr2, a new member of the neurexin superfamily, is localized at the juxtaparanodes of myelinated axons and associates with K⁺ channels. *Neuron* 24, 1037-1047.
- Poliak, S., Gollan, L., Salomon, D., Berglund, E.O., Ohara, R., Ranscht, B., Peles, E., 2001. Localization of Caspr2 in myelinated nerves depends on axon-glia interactions and the generation of barriers along the axon. *J. Neurosci.* 21, 7568-7575.
- Prochnow, N., Dermietzel, R., 2008. Connexons and cell adhesion: a romantic phase. *Histochem. Cell Biol.* 130, 71-77.
- Prokop, A., Martín-Bermudo, M.D., Bate, M., and Brown, N.H., 1998. Absence of PS integrins or laminin A affects extracellular adhesion, but not intracellular assembly, of hemiadherens and neuromuscular junctions in *Drosophila* embryos. *Dev. Biol.* 198, 58-76.
- Purves, W.K., Orians, G.H., Heller, H.C., Sadava, D., 1998. *Life: The Science of Biology*, Fifth Edition. U.S.A: Sinauer Associates, Inc.
- Reese, M.L., Dakoji, S., Bredt, D., Dötsch, V., 2007. The guanylate kinase domain of the MAGUK PSD-95 binds dynamically to a conserved motif in MAP1a. *Nat. Struct. Mol. Biol.* 14, 155-163.
- Roberts, D.B., 1986. *Drosophila: A practical approach*. Washington D.C: IRL Press, pg 175-197.
- Rodriguez Boulan, E., Nelson, W.J., 1989. Morphogenesis of the polarized epithelial cell phenotype. *Science* 245, 718-725.
- Rodriguez Boulan, E., Sabatini, D.D., 1978. Asymmetric budding of viruses in epithelial monolayers: A model system for study of epithelial polarity. *Proc. Natl. Acad. Sci. USA* 75, 5071-5075.
- Roh, M.H., Makarova, O., Liu, C.J., Shin, K.Y., Lee, S., Laurinec, S., Goyal, M., Wiggins, R., Margolis, B., 2002. The MAGUK protein, Pals1, functions as an adapter, linking mammalian homologues of Crumbs and Discs Lost. *J. Cell Biol.* 157, 161-172.
- Rotin, D., Bar-Sagi, D., O'Brodovich, H., Merilainen, J., Lehto, V.P., Canessa, C.M., Rossier, B.C., Downey, G.P., 1994. An SH3 binding region in the epithelial Na⁺ channel (α ENaC) mediates its location at the apical membrane. *EMBO J.* 13, 4440-4450.
- Sambrook, J., Russell, D.W., 2001. *Molecular Cloning – A laboratory manual*, Third Edition. New York: Cold Springs Harbor Laboratory Press.

- Sato, T., 1967. A modified method for lead staining of thin sections. *J. Electron Microsc.* 16,133.
- Schulte, J., Tepass, U., and Auld, V.J., 2003. Gliotactin, a novel marker of tricellular junctions, is necessary for septate junction development in *Drosophila*. *J. Cell Biol.* 161, 991-1000.
- Schwabe, T., Bainton, R.J., Fetter, R.D., Heberlein, U., Gaul, U. 2005. GPCR signaling is required for blood-brain barrier formation in *Drosophila*. *Cell* 123, 133-144.
- Seppa, M.J., Johnson, R.I., Bao, S., Cagan, R.L., 2008. Polychaetoid controls patterning by modulating adhesion in the *Drosophila* pupal retina. *Dev. Biol.* 318, 1-16.
- Shen, C.P., Jan, L.Y., and Jan, Y.N., 1997. Miranda is required for the asymmetric localization of Prospero during mitosis in *Drosophila*. *Cell* 90, 449-458.
- Shingai, T., Ikeda, W., Kakunaga, S., Morimoto, K., Takekuni, K., Itoh, S., Satoh, K., Takeuchi, M., Imai, T., Monden, M., and Taki, Y., 2003. Implications of Nectin-like Molecule-2/IGSF4/FA175/Sg1GSF/TSLC1/SynCAM1 in cell-cell adhesion and transmembrane protein localization in epithelial cells. *J. Biol. Chem.* 278, 35421-35427.
- Sierralta, J., Mendoza, C., 2004. PDZ-containing proteins: alternative splicing as a source of functional diversity. *Brain Res. Brain Res. Rev.* 47, 105-115.
- Simons, K., Fuller, S.D., 1985. Cell surface polarity in epithelia. *Annu. Rev. Cell Biol.* 1, 243-288.
- Simske, J.S., Kaech, S.M., Harp, S.A., Kim, S.K., 1996. LET-23 receptor localization by the cell junction protein LIN-7 during *C. elegans* vulval induction. *Cell* 85, 195-204.
- Skaer, H.B., Maddrell, S.H.P., Harrison, J.B., 1987. The permeability properties of septate junctions in malpighian tubules of *Rhodnius*. *J. Cell Sci.* 88, 251-265.
- Snustad, D.P., Simmons, M.J., 2000. Principles of Genetics, Second Edition. Toronto: John Wiley and Sons, Inc.
- Sotillos, S., Díaz-Meco, M.T., Caminero, E., Moscat, J., Campuzano, S., 2004. DaPKC-dependent phosphorylation of Crumbs is required for epithelial cell polarity in *Drosophila*. 166, 549-557.
- Staehelin, L.A., 1973. Further observations on the fine structure of freeze-cleaved tight junctions. *J. Cell Sci.* 13, 763-786.
- Stewart, M., Murphy, C., Fristrom, J.W., 1972. The recovery and preliminary characterization of X chromosome mutants affecting imaginal discs of *Drosophila melanogaster*. *Dev. Biol.* 27, 71-83.
- Stork, T., Engelen, D., Krudewig, A., Silies, M., Bainton, R., Klämbt, C., 2008. Organization and function of the blood-brain barrier in *Drosophila*. *J. Neurosci.* 28, 587-597.
- Straight, S.W., Pieczynski, J.N., Whiteman, E.L., Liu, C.J., Margolis, B., 2006. Mammalian Lin-7 stabilizes polarity protein complexes. *J. Biol. Chem.* 281, 37738-37747.
- Strand, D., Jakobs, R., Merdes, G., Neumann, B., Kalmes, A., Heid, H.W., Husmann, I., Mechler, B.M., 1994a. The *Drosophila* lethal(2)giant larvae tumor suppressor protein forms homo-oligomers and is associated with nonmuscle myosin II heavy chain. *J. Cell Biol.* 127, 1361-1373.

- Strand, D., Raska, I., Mechler, B.M., 1994b. The *Drosophila* lethal(2)giant larvae tumor suppressor protein is a component of the cytoskeleton. *J. Cell Biol.* 127, 1345-1360.
- Sudbery, P.E., 1996. The expression of recombinant proteins in yeasts. *Curr. Opin. Biotechnol.* 7, 517-524.
- Susuki, K., Rasband, M.N., 2008. Spectrin and Ankyrin-based cytoskeletons at polarized domains in myelinated axons. *Exp. Biol. Med.* 233, 394-400.
- Swanson, L.E., Beitel, G.J., 2006. Tubulogenesis: An inside job. *Curr. Biol.* 16, R51-R53.
- Takahashi, K., Matsuo, T., Katsube, T., Ueda, R., Yamamoto, D., 1998. Direct binding between two PDZ domain proteins Crumbs and ZO-1 and their roles in regulation of the Jun N-terminal kinase pathway in *Drosophila* morphogenesis. *Mech. Dev.* 78, 97-111.
- Takahisa, M., Togashi, S., Suzuki, T., Kobayashi, M., Maruyama, A., Kondo, K., Miyake, T., Ueda, R., 1996. The *Drosophila* tamou gene, a component of the activating pathway of extramacrochaetae expression, encodes a protein homologous to mammalian cell-cell junction-associated protein ZO-1. *Genes Dev.* 10, 1783-1795.
- Takai, Y., Irie, K., Shimizu, K., Sakisaka, T., Ikeda, W., 2003. Nectins and nectin-like molecules: roles in cell adhesion, migration, and polarization. *Cancer Sci.* 94, 655-667.
- Tanentzapf, G., Tepass, U., 2003. Interactions between the Crumbs, Lethal giant larvae and Bazooka pathways in epithelial polarization. *Nat. Cell Biol.* 5, 46-52.
- Tardent, P., Holstein, T., 1982. Morphology and morphodynamics of the stenotele nematocyst of *Hydra attenuata* Pall. *Cell Tissue Res.* 224, 269-290.
- te Velthuis, A.J.W., Admiraal, J.F., Bagowski, C.P., 2007. Molecular evolution of the MAGUK family in metazoan genomes. *BMC Evol. Biol.* 7, 129.
- Teal, K., 2005. Identification and molecular characterization of dPALS2, the *Drosophila* ortholog of mammalian PALS2. Master of Science Thesis. McMaster University.
- Tepass, U., 2002. Adherens junctions: new insight into assembly, modulation and function. *BioEssays* 24, 690-695.
- Tepass, U., 1997. Epithelial differentiation in *Drosophila*. *BioEssays* 19, 673-682.
- Tepass, U., 1996. Crumbs, a component of the apical membrane, is required for zonula adherens formation in primary epithelia of *Drosophila*. *Dev. Biol.* 177, 217-225.
- Tepass, U., and Hartenstein, V., 1994. The development of cellular junctions in the *Drosophila* embryo. *Dev. Biol.* 161, 563-596.
- Tepass, U., Knust, E., 1993. crumbs and stardust act in a genetic pathway that controls the organization of epithelia in *Drosophila melanogaster*. *Dev. Biol.* 159, 311-326.
- Tepass, U., Tanentzapf, G., Ward, R., and Fehon, R., 2001. Epithelial cell polarity and cell junctions in *Drosophila*. *Annu. Rev. Genet.* 35, 747-784.

- Tepass, U., Theres, C., Knust, E., 1990. crumbs encodes an EGF-like protein expressed on apical membranes of *Drosophila* epithelial cells and required for organization of epithelia. *Cell* 61, 787-799.
- Thompson, B., Townsley, F., Rosin-Arbesfeld, R., Musisi, H., Bienz, M., 2002. A new nuclear component of the Wnt signaling pathway. *Nature Cell Biol.* 4, 367-373.
- Timmons, L., Hersperger, E., Woodhouse, E., Xu, J., Liu, L.Z., Shearn A., 1993. The expression of the *Drosophila* awd gene during normal development and in neoplastic brain tumors caused by lgl mutations. *Dev. Biol.* 158, 364-379.
- Timmons, L., Shearn, A., 2000. Role of AWD/Nucleoside diphosphate kinase in *Drosophila* development. *J. Bioeng. Biomembr.* 32, 293-300.
- Tseng, T.C., Marfatia, S.M., Bryant, P.J., Pack, S., Zhuang, Z., O'Brien, J.E., Lin, L., Hanada, T., Chishti, A.H., 2001. VAM-1: A new member of the MAGUK family binds to human Veli-1 through a conserved domain. *Biochim. Biophys. Acta.* 1518, 249-259.
- Tsukita, S., Furuse, M., and Itoh, M., 2001. Multifunctional strands in tight junctions. *Nat. Rev. Mol. Cell Biol.* 2, 285-293.
- Venema, D.R., Zeev-Ben-Mrdehai, T., and Auld, V.J., 2004. Transient apical polarization of Gliotactin and Coracle is required for parallel alignment of wing hairs in *Drosophila*. *Dev. Biol.* 275, 301-314.
- Venken, K.J.T., Bellen, H.J., 2005. Emerging technologies for gene manipulation in *Drosophila melanogaster*. *Nat. Rev. Genet.* 6, 167-178.
- Wang, Q., Hurd, T.W., and Margolis, B., 2004. Tight junction protein Par6 interacts with an evolutionarily conserved region in the amino terminus of PALS1/Stardust. *J. Biol. Chem.* 279, 30715-30721.
- Wang, S., Jayaram, S.A., Hemphala, J., Senti, K.A., Tsarouhas, V., Jin, H., and Samakovlis, C., 2006. Septate-junction-dependent luminal deposition of chitin deacetylases restricts tube elongation in the *Drosophila* trachea. *Curr. Biol.* 16, 180-185.
- Ward, R.E., Lamb, R.S., and Fehon, R.G., 1998. A conserved functional domain of *Drosophila* Coracle is required for localization at the septate junction and has membrane-organizing activity. *J. Cell Biol.* 140, 1463-1473.
- Wei, X., Ellis, H.M., 2001. Localization of the *Drosophila* MAGUK protein Polychaetoid is controlled by alternative splicing. *Mech. Dev.* 100, 217-231.
- Wieschaus, E., Nüsslein-Volhard, C., Jürgens, G., 1984. Mutations affecting the pattern of the larval cuticle in *Drosophila melanogaster*. III. Zygotic loci on the X-chromosome and fourth chromosome. *Wil. Roux's Arch.* 193, 296-307.
- Willott, E., Balda, M., Fanning, A., Jameson, B., Itallie, C., Anderson, J., 1993. The tight junction protein ZO-1 is homologous to the *Drosophila* Discs-large tumor suppressor protein of septate junctions. *Proc. Natl. Acad. Sci. USA* 90, 7834-7838.
- Wirtz-Peitz, F., Knoblich, J.A., 2006. Lethal giant larvae take on a life of their own. *Trends Cell Biol.* 16, 234-241.

- Wodarz, A., Hinz, U., Engelbert, M., Knust, E., 1995. Expression of crumbs confers apical character on plasma membrane domains of ectodermal epithelia of *Drosophila*. *Cell* 82, 67-76.
- Wodarz, A., Ramrath, A., Grimm, A., Knust, E., 2000. *Drosophila* atypical protein kinase C associates with Bazooka and controls polarity of epithelia and neuroblasts. *J. Cell Biol.* 150, 1361-1374.
- Wood, R.L., 1959. Intercellular attachment in the epithelium of *Hydra* as revealed by electron microscopy. *J. Biophys. Biochem. Cytol.* 6, 343-352.
- Woods, D.F., Bryant, P.J., 1993a. Apical junctions and cell signaling in epithelia. *J. Cell Sci.* 17, 171-181.
- Woods, D.F., Bryant, P.J., 1993b. ZO-1, Dlg-A and PSD-95/SAP90: homologous proteins in tight, septate and synaptic cell junctions. *Mech. Dev.* 44, 85-89.
- Woods, D.F., and Bryant, P.J., 1991. The discs-large tumor suppressor gene of *Drosophila* encodes a guanylate kinase homolog localized at septate junctions. *Cell* 66, 451-464.
- Woods, D.F., Hough, C., Peel, D., Callaini, G., and Bryant, P.J., 1996. Dlg protein is required for junction structure, cell polarity, and proliferation control in *Drosophila* epithelia. *J. Cell Biol.* 134, 1496-1482.
- Woods, D.F., Wu, J., and Bryant, P.J., 1997. Localization of proteins to the apico-lateral junctions of *Drosophila* epithelia. *Dev. Genetics* 20, 111-118.
- Wootton, R., 1992. Functional morphology of insect wings. *Annu Rev Entomol.* 37, 113-140.
- Wong, L.L., and Adler, P.N., 1993. Tissue polarity genes of *Drosophila* regulate the subcellular location for prehair initiation in pupal wing cells. *J. Cell Biol.* 123, 209-221.
- Wu, V.M., Beitel, G.J., 2004. A junctional problem of apical proportions: epithelial tube-size control by septate junctions in the *Drosophila* tracheal system. *Curr. Opin. Cell Biol.* 16, 493-499.
- Wu, V.M., Schulte, J., Hirschi, A., Tepass, U., and Beitel, G.J., 2004. Sinuous is a *Drosophila* claudin required for septate junction organization and epithelial tube size control. *J. Cell Biol.* 164, 313-323.
- Wu, V.M., Yu, M.H., Paik, R., Banerjee, S., Liang, Z., Paul, S.M., Bhat, M.A., and Beitel, G.J., 2007. *Drosophila* Varicose, a member of a new subgroup of basolateral MAGUKs, is required for septate junctions and tracheal morphogenesis. *Development* 134, 999-1009.
- Xiong, W.C., Okano, H., Patel, N.H., Blendy, J.A., and Montell, C., 1994. repo encodes a glial-specific homeo domain protein required in the *Drosophila* nervous system. *Genes Dev.* 8, 981-994.
- Xu, J., Liu, L.Z., Deng, X.F., Timmons, L., Hersperger, E., Steeg, P.S., Veron, M., Shearn, A., 1996. The enzymatic activity of *Drosophila* AWD/NDP kinase is necessary but not sufficient for its biological function. *Dev. Biol.* 177, 544-557.
- Young, K.H., 1998. Yeast two-hybrid: so many interactions, (in) so little time... *Biol. Repro.* 58, 302-311.
- Yu, H., Chen, J.K., Feng, S., Dalgarno, D.C., Brauer, A.W., Schreiber, S.L., 1994. Structural basis for the binding of proline-rich peptides to SH3 domains. *Cell* 76, 933-945.

- Zhang, M., Wang, W., 2003. Organization of signaling complexes by PDZ-domain scaffold proteins. *Acc. Chem. Res.* 36, 530-538.
- Zhu, M.Y., Wilson, R., Leptin, M., 2005. A screen for genes that influence fibroblast growth factor signal transduction in *Drosophila*. *Genetics* 170, 767-777.
- Zhu, Q., Deng, Y., Vanka, P., Brown, S.J., Muthukrishnan, S., Kramer, K.J., 2004. Computational identification of novel chitinase-like proteins in the *Drosophila melanogaster* genome. *Bioinformatics* 20, 161-169.
- Zimmermann, P., 2006. The prevalence and significance of PDZ domain – phosphoinositide interactions. *Biochim Biophys Acta.* 1761, 947-956.
- Zinyk, D.L., McGonnigal, B.G., Dearolf, C.R., 1993. *Drosophila* awd^{K-pn}, a homologue of the metastasis suppressor gene nm23, suppresses the Tum-1 haematopoietic oncogene. *Nature Genetics* 4, 195-201.
- Zordan, M.A., Massironi, M., Ducato, M.G., te Kronnie, G., Costa, R., Reggiani, C., Chagneau, C., Martin, J.R., Megighian, A., 2005. *Drosophila* CAKI/CMG protein, a homologue of human CASK, is essential for regulation of neurotransmitter vesicle release. *J. Neurophysiol.* 94, 1074-1083.

APPENDIX

Appendix A: 5' and 3' RNA Ligase Mediated Rapid Amplification of cDNA Ends

RACE experiments were performed to answer two questions. How many *varicose* transcripts are expressed? Is the L27 domain encoded in a Vari protein product?

Three *varicose* transcripts are computationally predicted, Vari, Vari^{L27B}, and Vari^{L27D} (Crosby et al. 2007). We performed RACE experiments to verify these predictions. During embryonic and adult stages of development, we were able to identify a single predominant transcript. Sequencing verified the expression of transcript Vari. The other transcripts were not detected.

Each predicted transcript encodes a protein possessing PDZ, SH3 and GUK domains. An evolutionary conserved L27 domain is encoded into the 5'UTR of these transcripts however a transcriptional start site upstream of the L27 domain was absent. Our RACE results did not identify a transcriptional start site upstream of the L27 domain. On this basis, we concluded that, for transcript Vari, the L27 domain was not encoded into the protein product.

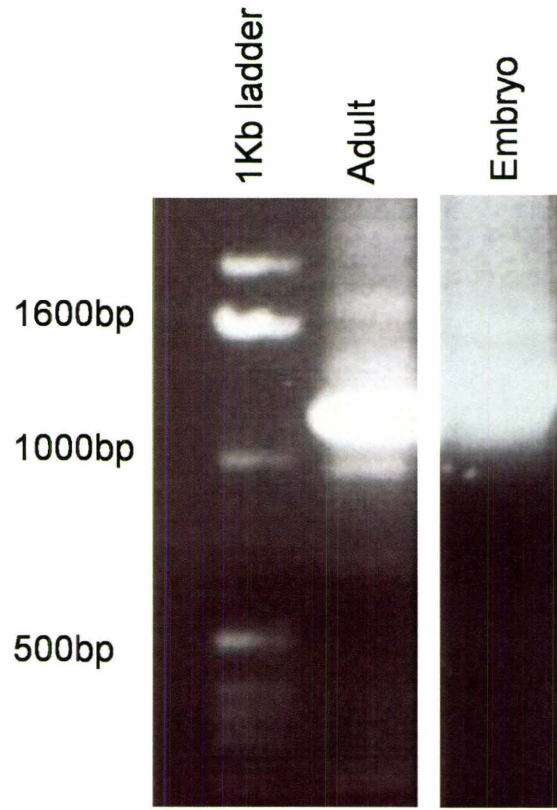
Initially predicted Vari^{L27B} and Vari^{L27D} transcripts also lacked a transcriptional start site upstream of the L27 domain. Revised transcripts corrected a computational error in the intron/exon boundaries within the 5'UTR of transcripts Vari^{L27B} and Vari^{L27D}. The boundary change resulted in a shift in the reading frame upstream of the L27 domain and presented a possible transcriptional start site. Currently, data has not been presented to confirm the expression of a Vari protein product encoding the L27 domain.

Figure A: Varicose is present as one predominant transcript in both adult and embryonic CS-P flies.

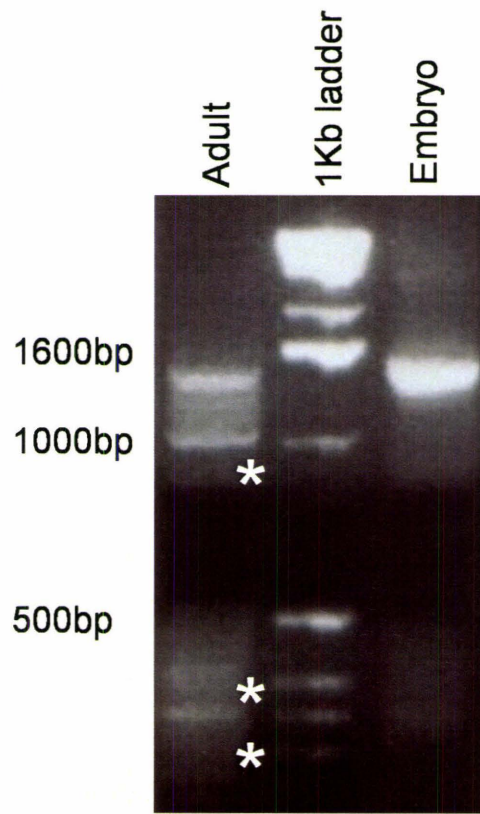
[A] Reverse transcription and PCR amplification of the 5' end of *varicose* transcript(s) from adult and embryonic CS-P flies. The PCR reaction amplified an abundant PCR product of approximately 1200 bp. Sequencing of the PCR product corresponded to the 5' UTR of *varicose* transcript C. A less abundant PCR product is resolved at approximately 1600 bp. Attempts to sequence this product provided inconclusive results.

[B] Reverse transcription and PCR amplification of the 3' end of *varicose* transcript(s) from adult and embryonic CS-P flies. During embryonic development a single PCR product is identified. Sequencing confirmed the predicted 3' UTR sequence shared by all three transcripts. A band of similar size was observed during adult stage. Sequencing of this product confirmed the embryonic results. The presence of additional PCR products (asterisks) during the adult stage is presumed to be the result of non-specific binding during the PCR reaction.

A



B



Appendix B: Imprecise Excision of GE13049

In order to determine a functional role for Varicose during *Drosophila* development, we wanted to generate a *varicose* null allele. We obtained a P-element insertion line, GE13049 and performed standard genetic crosses to excise the element from the genome. This appendix presents the genetic scheme used for creating our *varicose* imprecise excision lines. Additionally, a schematic map of the primers used to map the excision breakpoints is also presented.

Five homozygous lethal alleles were generated, *vari*^{48EP}, *vari*^{B4}, *vari*^{L4}, *vari*^{K4} and *vari*^{B5}. All are embryonic lethal however, *vari*^{K4} appears to have few larval escapers which are lethal by 2nd instar larval stage. All *varicose* alleles fail to complement each other suggesting little to no *varicose* protein is being expressed. To confirm this, each excision allele was immunolabeled with Vari antibody. We were unable to detect Vari expression in any of the ectodermally-derived epithelial tissues suggesting each is a null for *varicose*. Western blot analysis is needed to confirm this result.

Genetic Scheme for Imprecise Excision

Step One:	δ w- ; $\frac{GE13049}{CyO}$; +	X	δ w- ; $\frac{CyO\Delta 2-3}{Bc^1Egfr^{E1}}$; +
F1:	δ w- ; $\frac{GE13049}{CyO\Delta 2-3}$; + orange eyes, curly wings		w- ; $\frac{GE13049}{Bc^1Egfr^{E1}}$; + orange eyes, straight wings
	w- ; $\frac{Bc^1Egfr^{E1}}{CyO}$; + white eyes, curly wings		w- ; $\frac{CyO\Delta 2-3}{CyO}$; + adult lethal
Step Two:	δ yw- ; $\frac{Sco}{CyO}$; +	X	δ w- ; $\frac{GE13049}{CyO\Delta 2-3}$
F1:	w- ; $\frac{GE13049?}{CyO}$; + white eyes, curly wings	w- ; $\frac{GE13049?}{Sco}$; + white eyes, scute	w- ; $\frac{Sco}{CyO\Delta 2-3}$; + white eyes, scute, curly wings
			w- ; $\frac{CyO\Delta 2-3}{CyO}$; + adult lethal
Step Three* :	δ w- ; $\frac{GE13049?}{CyO}$; +	X	δ yw- ; $\frac{Sco}{CyO}$; +
	δ yw- ; $\frac{Sco}{CyO}$; +	X	δ w- ; $\frac{GE13049?}{CyO}$; +
F1:	w- ; $\frac{GE13049?}{CyO}$; + white eyes, curly wings	w- ; $\frac{GE13049?}{Sco}$; + white eyes, scute	w- ; $\frac{Sco}{CyO}$; + white eyes, scute, curly wings
			w- ; $\frac{CyO}{CyO}$; + adult lethal

*crosses set up in pairwise

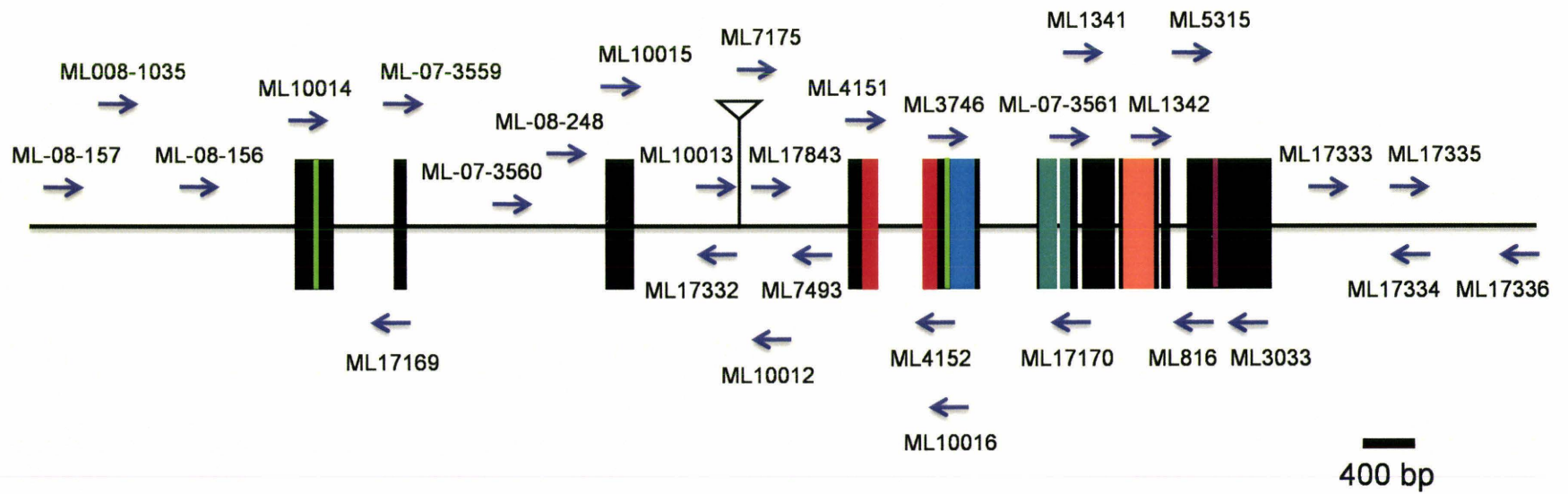
Step Four:	δ w- ; $\frac{GE13049?}{CyO}$; +	X	δ w- ; $\frac{GE13049?}{CyO}$; +
F1:	w- ; $\frac{GE13049?}{GE13049?}$; + *adult lethal	w- ; $\frac{GE13049?}{CyO}$; + ** white eyes, curly wings	w- ; $\frac{CyO}{CyO}$; + adult lethal

*lines selected for complementation test

** δ and δ crossed to establish stock

Figure B.1: Map of primers used during imprecise excision mapping.

The following primers were used in various combinations to map the genomic breakpoints of the *vari* alleles. Homozygous embryos were selected using a balancer marked with GFP and DNA was extracted using single embryo DNA preparation methods (see Chapter 2).



| Start
 | L27
 | PDZ
 | SH3
 | GUK
 | Stop

Table B: Complementation test of *varicose* imprecise excision alleles

Allele	% Viable Adults (n)				
	<i>vari</i> ^{48EP*}	<i>vari</i> ^{B4}	<i>vari</i> ^{K4}	<i>vari</i> ^{L4}	<i>vari</i> ^{B5}
<i>vari</i> ^{48EP}		0% (537)	0% (442)	0% (343)	0% (391)
<i>vari</i> ^{B4}	0% (322)		0% (468)	0% (425)	0% (326)
<i>vari</i> ^{K4}	0% (468)	0% (466)		0% (500)	0% (399)
<i>vari</i> ^{L4}	0% (348)	0% (466)	0% (453)		0% (351)
<i>vari</i> ^{B5}	0% (394)	0% (427)	0% (508)	0% (440)	

All stocks were maintained over CyO, Kruppel-GFP balancers

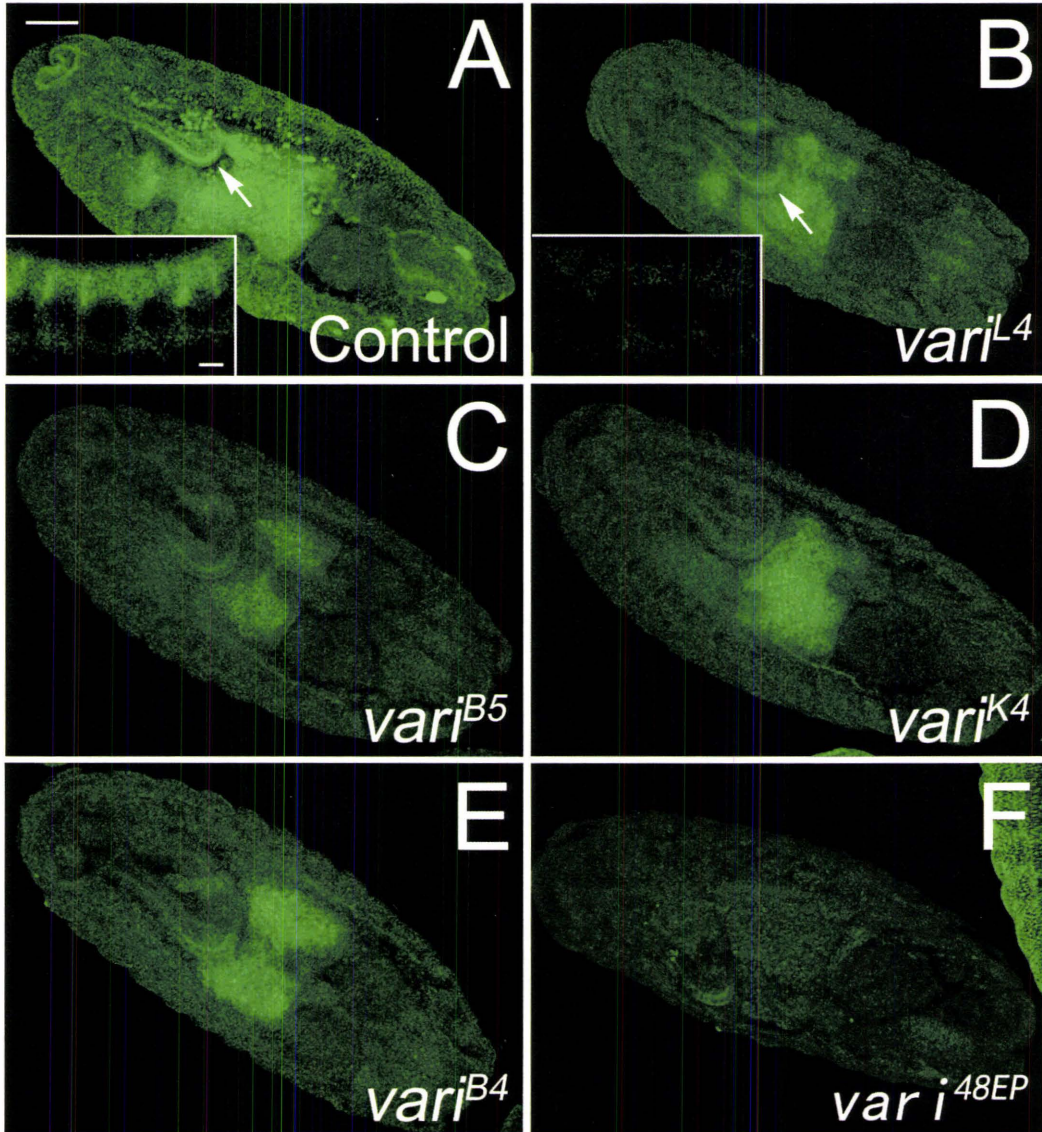
% Viability= number straight wing flies/ [straight wing flies + curly wing flies]x100

n= number of viable adult progeny counted

*females of the column genotype were crossed to males of the row genotype

Figure B.2: Varicose expression is not detected in excision alleles.

[A-F] Whole-mount stage 16 embryos were labeled with Vari antibody and visualized using confocal microscopy. Homozygous embryos were selected by absence of balancer GFP. Unlike control embryos (A) where Varicose is detected in epithelial tissues such as the epidermis, trachea and hindgut (arrow), we do not detect Varicose expression in our *vari* excision alleles (B-F). Typically, Varicose is expressed along the lateral membrane of epithelial cells, more specifically at the septate junction (inset, A). However, in *vari* alleles, expression of *varicose* is reduced to background levels (inset, B) and is not detected at the septate junction. Calibration: 50 μ m, A; 2 μ m, inset A.



Appendix C: Sequence of PCR primers used in the presented thesis

The name and sequence of PCR primers are listed along with introduced restriction sites in bold. Primers beginning with ML were used for excision mapping and can be found on the primer map in Appendix B, Figure B.1. L27FOR and L27REV primers were designed by Kelly Teal.

Primer Name	Forward (F) Reverse (R)	Oligonucleotide Sequence 5'→3'	Restriction Site
5' RACE G.S. outer ML816	R	ACTGCTCCTCGTGGCTCATCTGGTTCGACCGTT	SalI
5' RACE G.S. inner ML817	R	CTGGTAGTCGACATGACCGCTCCGAACCTTGT	SalI
5' Outer Adaptor Region	F	GCTGATGGCGATGAATGAACACTG	
5' Inner Adaptor Region	F	CGCGGATCCGAACACTGCGTTTGCTGGCTTTGATG	
3' RACE G.S. outer ML1341	F	GAGGCGGACTACGTTTACAAGATTGGCATTGCGG	
3' RACE G.S. inner ML1342	F	TGGACCGCGAGGAAATGGAAGAGGCCGTGC	
3' Outer Adaptor Region	R	GCGAGCACAGAATTAATACGACT	
3' Inner Adaptor Region	R	CGCGGATCCGAATTAATACGACTCACTATAGG	
Y2H bait construct ML3746	F	GAGGACGTCCATATGACCAAGATGCCAGT	NdeI
Y2H bait construct	R	GGCGCGTCGACAAAGGGTCCTGGGATTCTAGTA	SalI
T7 Promoter	F	TAATACGACTCACTATAGGG	
T7 Terminator	R	GCTAGTTATTGCTCAGCGG	
AD-insert screening	F	CTATTCGATGATGAAGATACCCACCA	
AD-insert screening	R	GTGAACCTGCGGGGTTTTTCAGTATCTACGA	
UAS-Vari construct ML3596	F	CCGAGGACGTCTCTAGACCAAGATGCCAG	XbaI
UAS-Vari construct ML3033	R	CCCCGGAGGGCGCATCTAGACTTATACAAACATTGC	XbaI
<i>hsp70</i> TATA region ML5220	F	ACAAGCGCAGCTGAACAAGCTAAAC	
Vari ^{L27} Antibody ML16977	F	GGGGGTACCTCATTCCGGTCTGTTA	KpnI
Vari ^{L27} Antibody ML15551	R	TAGATCCAGTCGACAGGCCACCCACT	SalI
M13For	F	GTAACACGACGGCCAGT	
M13Rev	R	CAGGAAACAGCTATGAC	
Plac1 (P-element) ML7175	F	CACCCAAGGCTCTGCTCCCACAAT	
ML7493	R	GTGTGGAGTCTTAGGTCAAAAATTGGGTC	
L27FOR ML4151	F	CGCTCATCTGCAGAACAAGCCCATC	PstI
L27REV ML4152	R	GATCCCCCGGCCGCTTTAAGTC	EagI
ML10012	R	ATATTTGTGGATGAGTAATCCCCGACTGCTT	
ML10013	F	TCACAGCCACAGCCTTCAATATGAAACA	
ML10014	F	AGTTAGCCTCTTTCTCACAAACAAGTCGGT	
ML10015	F	GTAACCTGGCTCACGCGGAGCTTTT	
ML10016	R	TGAGGACGTCTCGGTGAACAGGTA	

Primer Name	Forward (F) Reverse (R)	Oligonucleotide Sequence 5'→3'	Restriction Site
ML17169	R	TCTACTTGCCATCAGTTCCTTGTGGG	
ML17170	R	CCACCAGTTGGGATCCTTTACGTTGATGAT	
ML5315	F	GTCCTGACCTATCCTTAATTACAG	
ML17332	R	TGTTTCATATTCGAAGGCTGTGGCTGTGA	
ML17333	F	CCAGGCATTTAGCAACTTCATTTGCAGGG	
ML17334	R	AAAGAGTTGCCAGTCTGGTTTCTACTACTAC	
ML17335	F	GTAGTGTAGAAACCAGACTGGCAACTCTTT	
ML17336	R	ATCTTCTCGCCCTGAGATCTCCATCT	
ML17843	F	AAGCAGTCGGGATTACTCATCCACAAATAT	
ML-07-3559	F	CCCACAAGGAACTGATGGCAAGTAGA	
ML-07-3560	F	GGCTCATTCGTTTGTGGTTTTCTGCTG	
ML-07-3561	F	ATCATCAACGTAAAGGATCCCAACTGGTGG	
ML-08-156	F	TTACTGCCTGATTTAGTGTACTTTCGCGAA	
ML-08-157	F	TCAATTCAGCTGAGTCTGCCAATAG	
ML-08-248	F	AGATGCTGTTAAGATCACTGAAGTAGTTGG	
ML-08-1035	F	ACAGCAGGACATACAGCAAATCGGACG	

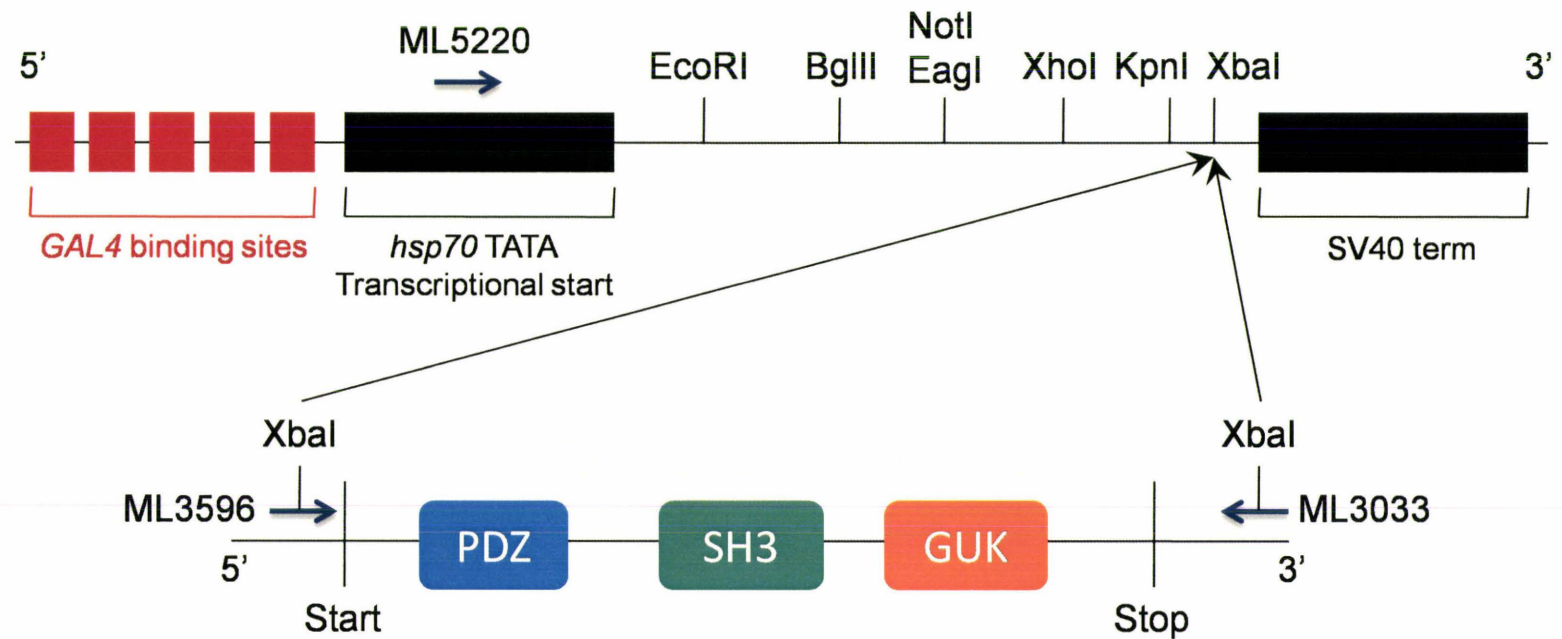
Appendix D: *pUAS-Vari* transgenic construct

To determine the effects of over- and misexpression of *varicose* during *Drosophila* development, we engineered a *UAS-vari* transgenic construct to include the full-length Vari transcript. This construct was microinjected into *yw*- embryos by Xiao-Li Zhao and genomic insertion sites were mapped using the presented genetic scheme.

Overexpression of the *UAS-vari* construct was determined by *heat-shockGAL4* and western blot analysis and verified the expression of an expected 54 kDa protein (Chapter 3, Fig. 10G). Misexpression of the *UAS-vari* construct was determined by *single-mindedGAL4* and immunolabelling with Vari antibody which confirmed *varicose* misexpression in the ventral midline (Chapter 3, Fig. 10E, 10F).

Ubiquitous expression of *UAS-vari* using *daGAL4* was able to rescue adult viability of our *vari*^{48EP} null allele. The absence of the L27 domain from this transgenic construct suggests that this domain is not required for viability.

pUASSt – vari



This construct was sequenced to ensure the PCR insert was error-free and in the proper orientation.

Genetic Scheme for Mapping Transgenic Constructs

Step One*:	(injected)	$\frac{\delta}{+}$ ♂	$yw^- ; + ; +$	X	$\frac{\delta}{+}$ ♂	$yw^- ; + ; +$
F1:		$\frac{\delta}{+}$ ♂	$yw^- ; P[w+(Vari)]$ red/orange eyes			$yw^- ; + ; +$ white eyes
Step Two*:		$\frac{\delta}{+}$ ♂	$yw^- ; P[w+(Vari)]$	X	$\frac{\delta}{+}$ ♂	$yw^- ; + ; +$
F1:		$\frac{\delta}{+}$ ♂	$yw^- ; P[w+(Vari)]$ red/orange eyes			$yw^- ; + ; +$ white eyes

*crosses set up in pairwise tubes

Step Three:		$\frac{\delta}{+}$ ♂	$yw^- ; P[w+(Vari)]$	X	$\frac{\delta}{+}$ ♂	$yw^- ; P[w+(Vari)]$
F1:			$yw^- ; \underline{P[w+(Vari)]}$ + *red/orange eyes			$yw^- ; \underline{P[w+(Vari)]}$ + *red/orange eyes
						$yw^- ; + ; +$ white eyes

*establish stocks

Step Four:		$\frac{\delta}{+}$	$yw^- ; \underline{P[w+(Vari)]}$ + $\underline{P[w(Vari)]}$	X	$\frac{\delta}{+}$	$w^- ; \underline{S}$; \underline{D} CyO TM3
F1:			$w^- ; \underline{P[w+(Vari)]}$; \underline{D} , $\underline{TM3}$ S + + orange eyes, star, dichete (stubble)			$w^- ; \underline{P[w(Vari)]}$; $\underline{TM3}$, \underline{D} CyO + + orange eyes, curly wings, dichete (stubble)
			$w^- ; \underline{CyO}$; \underline{D} , $\underline{TM3}$ + + + white eyes, curly wings, dichete (stubble)			$w^- ; \underline{S}$; \underline{D} , $\underline{TM3}$ + + + white eyes, star, dichete (stubble)
			$w^- ; \underline{S}$, \underline{CyO} ; $\underline{P[w+(Vari)]}$ + + D orange eyes, star (curly wings), dichete			$w^- ; \underline{S}$, \underline{CyO} ; $\underline{P[w+(Vari)]}$ + + TM3 orange eyes, star (curly wings), stubble
			$w^- ; \underline{S}$, \underline{CyO} ; \underline{D} + + + white eyes, star (curly wings), dichete			$w^- ; \underline{S}$, \underline{CyO} ; $\underline{TM3}$ + + + white eyes, star (curly wings), stubble

Step Five:

$$\sigma^{\delta} \frac{w^- ; \underline{P[w+(Vari)]}}{\text{CyO, TM3}} \quad X \quad \frac{\delta}{\dagger} \quad yw^- ; + ; +$$

F1 (if on the 2nd):

$$\frac{w^- ; \underline{P[w+(Vari)]}}{+} ; +$$

*orange eyes

$$\frac{w^- ; \underline{P[w+(Vari)]}}{+} ; \frac{\text{TM3}}{+}$$

orange eyes, stubble

$$\frac{w^- ; \underline{\text{CyO}}}{+} ; +$$

* white eyes, curly wings

$$\frac{w^- ; \underline{\text{CyO}}}{+} ; \frac{\text{TM3}}{+}$$

white eyes, stubble

*cross to generate a balanced stock

F1 (if on the 3rd):

$$\frac{w^- ; + ; \underline{P[w+(Vari)]}}{+}$$

*orange eyes

$$\frac{w^- ; \underline{\text{CyO}}}{+} ; \frac{\underline{P[w+(Vari)]}}{+}$$

orange eyes, curly wings

$$\frac{w^- ; + ; \underline{\text{TM3}}}{+}$$

*white eyes, stubble

$$\frac{w^- ; \underline{\text{CyO}}}{+} ; \frac{\underline{\text{TM3}}}{+}$$

white eyes, curly wings, stubble

*cross to generate a balanced stock

F1 (if on the X or the 4th):

$$\frac{\underline{P[w+(Vari)]}}{yw^-} ; + ; +$$

*orange eyes

$$\frac{\underline{P[w+(Vari)]}}{yw^-} ; \frac{\underline{\text{CyO}}}{+} ; +$$

orange eyes, curly wings

*if on the X, only females will have orange eyes

Appendix E: Knockdown of Varicose expression using *UAS-vari^{RNAi}*

The embryonic lethality phenotype associated with our null *varicose* alleles limits our ability to assess functionality phenotypes of *varicose* during later stages of development. Mosaic analysis is underway, however these experiments require time and fine-tuning. We sought a quicker and simpler method to study *varicose* function and obtained a *UAS-vari^{RNAi}* transgenic line.

Ubiquitous expression of *UAS-vari^{RNAi}* using *daGAL4* resulted in embryonic lethality. *varicose* expression was not detected in ectodermally-derived epithelial tissues and tracheal morphogenesis was disrupted. These results are independent of and comparable to the results observed with our *vari^{48EP}* allele, suggesting the *UAS-vari^{RNAi}* and the associated phenotypes are specific to varicose.

To determine the effects of loss of *varicose* function during later stages of development, we expressed *UAS-vari^{RNAi}* in various tissues using tissue specific drivers. Loss of *varicose* from egg chambers using *nos:VPGAL4* had no phenotypic effect. Immunohistochemical analysis using Vari antibody failed to detect a loss of *varicose* expression in experimental egg chambers compared to the controls. Females were viable and fertile suggesting Varicose does not play a role during oogenesis.

To determine the role of Varicose in optic lobe neuroepithelia, we expressed *UAS-vari^{RNAi}* in the optic lobe using *c855aGAL4*. Although this expression was adult lethal, the levels of *varicose* expression in these neuroepithelial cells was not reduced. The integrity of neuroepithelial cells and developing neuroblasts was unaffected. The role of Varicose in this developing tissue still needs to be resolved.

Figure E.1: Loss of Varicose through RNAi disrupts tracheal morphogenesis

Ubiquitous expression of *UAS-vari^{RNAi}* using *daGAL4* results in late embryonic lethality.

To determine if RNAi knockdown of *vari* results in similar tracheal phenotypes as our *vari* null alleles, embryos were labelled with luminal marker MAb2A12. Stage 15 (A, B), stage 16 (C, D) and stage 17 (E, F) embryos were whole-mounted and visualized using Zeiss Axioskop microscope. Tracheal branches of control embryos [A, C, E] appear uniform in diameter and connections are seen between the dorsal trunk and lateral trunks (asterisk). [B, D, F] Misexpression of *UAS-vari^{RNAi}* by *daGAL4* disrupts the uniformity of the dorsal trunk diameter. Large and irregular dilations appear along the length of the trunk (arrowhead) and lateral trunks appear disconnected from the dorsal trunk (asterisk). In addition, the accumulation of luminal marker 2A12 is greatly reduced in comparison to the control. These results are consistent with results of null *varicose* alleles. Lateral view: anterior to the left, dorsal is up. Calibration: 20µm, A.

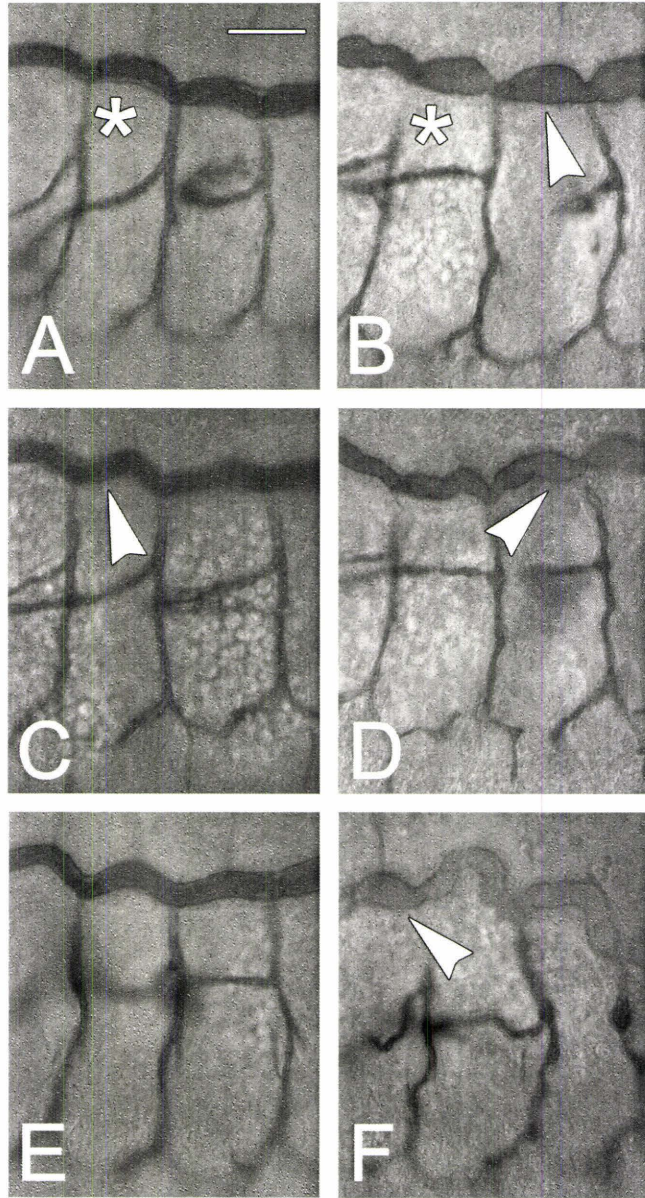


Figure E.2: Varicose does not play a role during oogenesis

To determine the role of Varicose during oogenesis, we misexpressed *UAS-vari^{RNAi}* using *nos:VP16GAL4*. Ovaries were dissected from 3-5 day old females and labelled with Vari (C) or Phosphotyrosine (D) antibodies. As a control, *UAS-CD8gfp* was overexpressed using *nos:VP16GAL4*. Ovaries were dissected and labelled with GFP (A) and Vari (B) antibodies. [A] Verification of the expression pattern of *nos:VP16GAL4*. [C] Immunolabeling of ring canals in the germarium and throughout egg chamber development with phosphotyrosine antibody (Robinson et al., 1994) suggests the overall morphology of egg chambers is unaffected by the absence of *varicose*. [B, D] We were unable to distinguish a difference in *varicose* expression pattern in both the experimental (D) and control egg chambers (B). In addition, females are viable and fertile, suggesting Varicose does not play a role during this process of development. Calibration: 50µm, A.

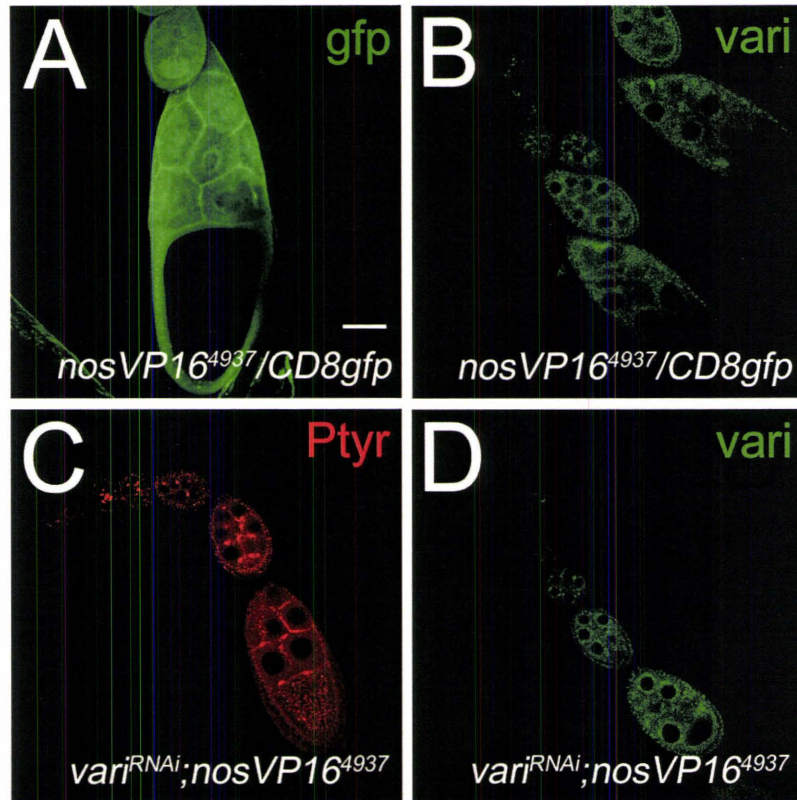


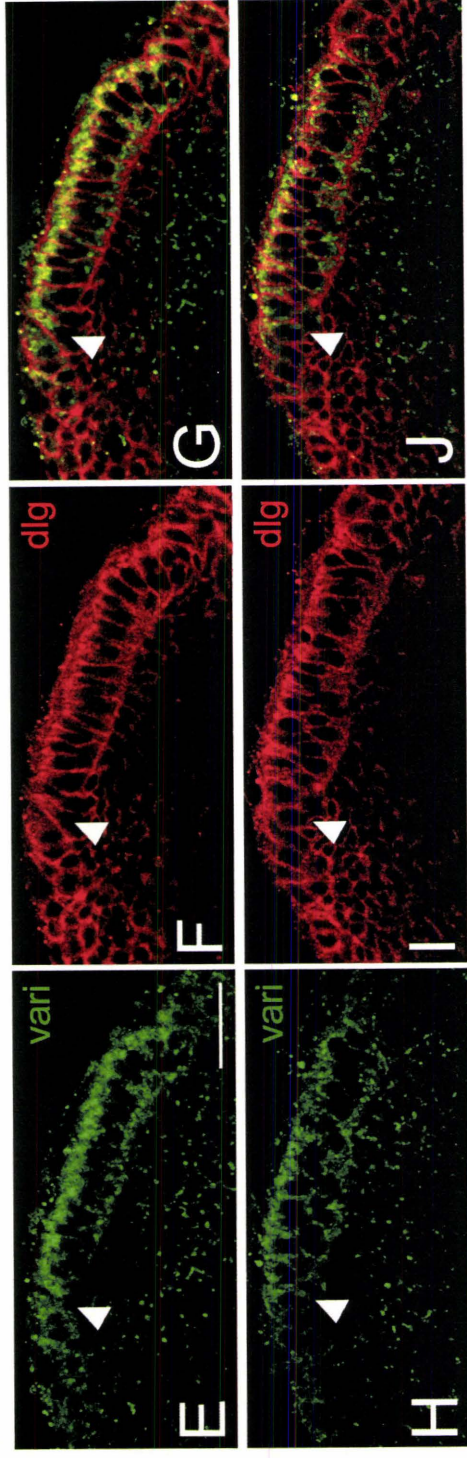
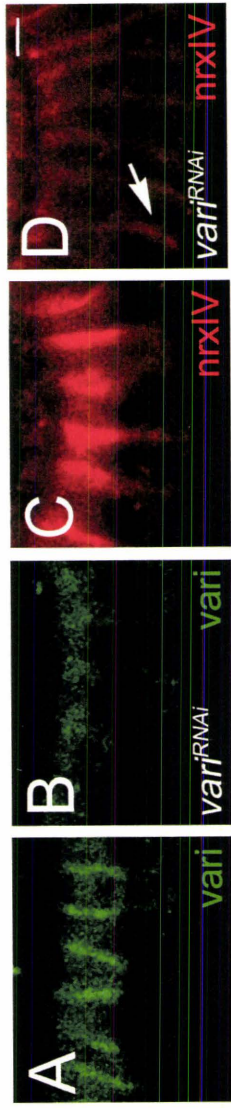
Figure E.3: Neuroepithelial cells are not affected by loss of Varicose

[A, B] Stage 15 embryos ubiquitously expressing *UAS-vari^{RNAi}* using *daGAL4* were immunolabeled with Vari antibody and visualized by confocal microscopy. In control embryos, Varicose expression is observed at the lateral membrane of hindgut epithelial cells (A). However, expression of *UAS-vari^{RNAi}* by *daGAL4* reduces *vari* expression to background levels (B). This observation is consistent with the results obtained with null allele, *vari^{48EP}*. [C, D] Septate junction components are mislocalized in the absence of *vari*. Stage 15 embryos ubiquitously expressing *UAS-vari^{RNAi}* using *daGAL4* were labelled with NrxF antibody. In control embryos (C), the expression of NrxF is restricted to the apicolateral region of hindgut epithelial cells. Reducing *varicose* expression by RNAi disrupts NrxF localization which is localized more basally (arrow, D). These results are also consistent with the phenotypes observed with *vari^{48EP}*. Apical is up. Calibration: 2µm, A-D.

[E-G] Varicose is expressed in the apical region of neuroepithelial cells of 3rd instar larval optic lobes (right of arrowhead, E) but is excluded from the neuroblasts (left of arrowhead, E). Dlg is expressed at the septate junction of neuroepithelial cells and distributed throughout the cortex of developing neuroblasts (right and left of arrowheads, respectively, F). Colocalization of Dlg and Vari are limited along the lateral membrane as Varicose expression appears more cytoplasmic than membrane associated (merge, G).

[H-J] Targeting *UAS-vari^{RNAi}* using *c855aGAL4* results in adult lethality. *c855aGAL4* expression is first detected in the optic lobe at 2nd instar larval stage (Hrdlicka et al.,

2002). Flies expressing both *UAS-vari^{RNAi}* and *c855aGAL4* complete pupation but fail to hatch as viable adults. We assessed the phenotypic effects in the optic lobe by immunolabeling 3rd instar larval brains with Vari (H) and Dlg (I; merge J). When compared to the controls (E-G) we did not detect a reduction in the expression levels of Vari, nor did we see a disruption in the expression pattern of Dlg. Columnar neuroepithelial cells and rounded neuroblasts are still present. All images are a single confocal section. Medial is left. Calibration: 20µm, E-J.



Appendix F: Varicose Antibodies – Vari and Vari^{L27}

All three Varicose proteins possess a PDZ, SH3 and GUK domain. Two proteins, Vari^{L27B} and Vari^{L27D}, possess an additional L27 domain, encoded at the N-terminus. Preliminary western blot experiments with our Vari antibody were unable to identify Vari^{L27B} or Vari^{L27D} protein products. We thought perhaps, that our antibody was unable to recognize these proteins due to a difference in protein conformation. We generated a second antibody designed against the full-length sequence of Vari^{L27B} and named this antibody, Vari^{L27}. Following affinity purification of anti-Vari^{L27}, we tested the specificity of the antibody and present the results in this appendix.

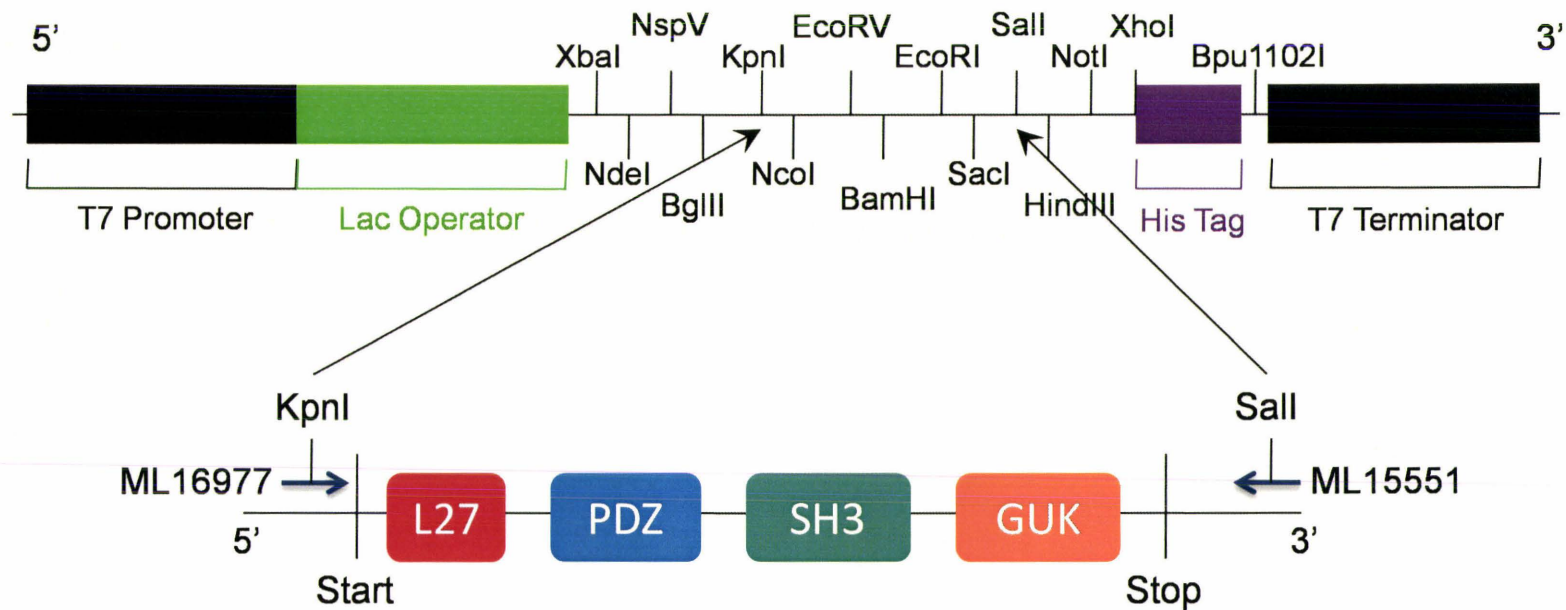
As presented in Chapter 3, our Vari antibody is specific to Varicose. Our Vari^{L27} antibody was unable to detect a similar expression pattern and was therefore not used for immunohistochemistry. This antibody was not tested in larval, pupal or adult tissues.

Neither antibody is able to recognize a 54 kDa or 75 kDa protein product corresponding to Varicose. It is possible that protein levels are below the threshold of detection as overexpression of *UAS-vari* using *heat-shock GAL4* provides ample protein to be detected by western blotting using Vari antibody. These results were inconclusive with Vari^{L27} antibody.

Figure F.1: Outline of the pET29b(+)-Vari^{L27} construct used to generate our Vari^{L27} antibody

For an outline of the construct used for our Vari antibody, please refer to Kelly Teal's Master of Science thesis, Appendix 4, page 108.

pET29b(+)-Vari^{L27}



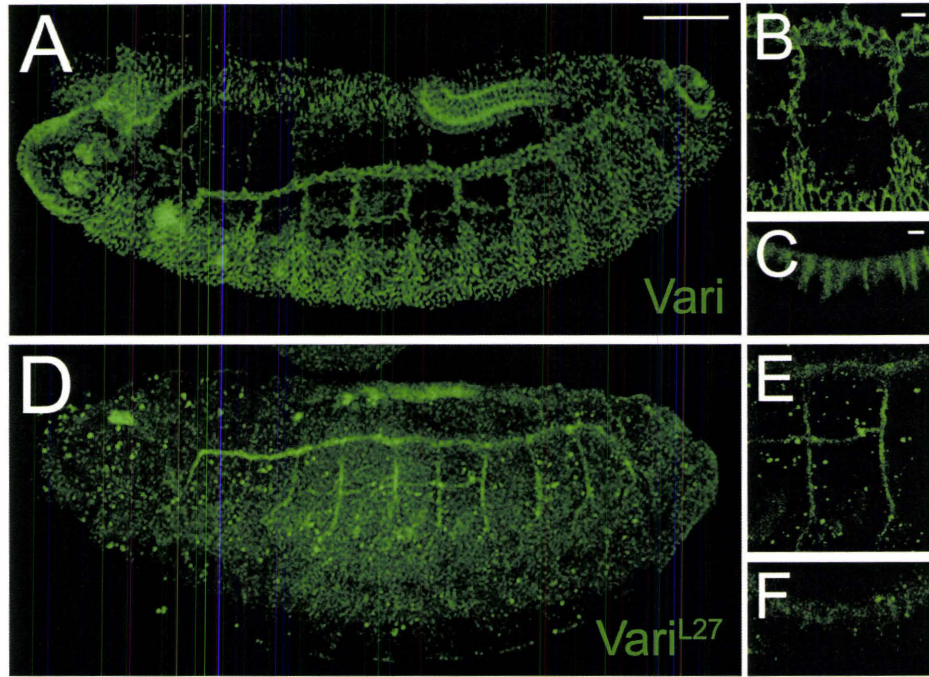
This construct was sequenced using T7 Promoter and T7 Terminator primers to ensure the PCR insert was error-free and in frame with the His Tag.

Figure F.2: Comparison of Vari Antibodies, Vari and Vari^{L27}

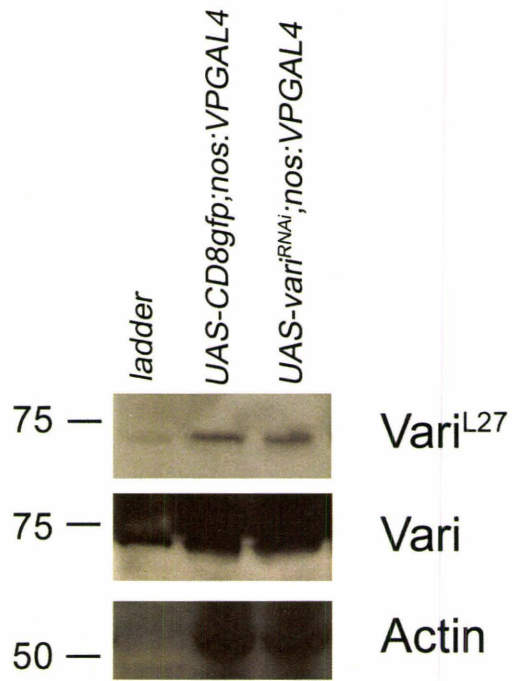
[I] Unlike immunolabelling experiments using anti-Vari (A-C), we were unable to detect Varicose expression using anti-Vari^{L27} (D-F). Wildtype expression of Varicose is detected along the lateral membrane of epithelial tissues such as the trachea (B), hindgut (C) and epidermis (not shown). Vari^{L27} is unable to recognize these epithelial tissues (D) and fails to detect lateral membrane expression in the trachea (E) and hindgut (F). This antibody was not tested for Varicose expression during larval or pupal stages. As a result, all immunohistochemical experiments performed in this thesis were completed using our Vari antibody. Calibration: 50µm, A, D; 5µm, B, E; 2µm, C, F.

[II] Preliminary western blot data using anti-Vari^{L27} suggested Vari^{L27B/L27D}, a 75 kDa protein, was expressed in abundance during oogenesis. To test the specificity of anti-Vari^{L27}, we reduced the expression of *varicose* in the ovary by *UAS-vari^{RNAi}* using *nos:VP16GAL4* and performed western blot techniques using both Vari and Vari^{L27} antibodies and actin as a loading control. As an additional control, *UAS-CD8gfp* was expressed using *nos:VP16GAL4*. Unfortunately, in the presence and absence of *UAS-vari^{RNAi}*, we were able to detect a protein product corresponding to the weight of Vari^{L27B/L27D} suggesting our Vari^{L27} antibody is not specific to Varicose. As a result of background interference with our Vari antibody, results remain inconclusive. In addition, neither antibody recognizes a protein product corresponding to the weight of Vari, a 54 kDa protein.

I



II



Appendix G: Yeast two-hybrid positive interacting clones

A yeast-two-hybrid screen was employed to screen an adult cDNA library for interacting partners of Varicose. The screen identified 142 putative positive colonies which were replica plated to remove multiple library plasmids. To sort the colonies and eliminate duplicates, potential interacting clones were screened by PCR. The library plasmid inserts were amplified by PCR using screening primers (Appendix C) and analyzed by gel electrophoresis. The resulting data are presented in this Appendix. Each insert clone was then restriction digested with *Hae* III to eliminate duplicate clones. The remaining clones were rescued via transformation of *E. coli* and the interaction with Varicose was reverified.

Figure G: PCR amplification of putative positive clones from the yeast two-hybrid adult library screen using Varicose as bait. DNA was isolated from positive clones identified from the adult cDNA library yeast two-hybrid screen. Each clone insert was PCR amplified using screening primers designed to the outlying regions of the multicloning site of the library vector pACT2. Products were separated by gel electrophoresis and insert size was estimated by comparison to a 1 Kb DNA ladder (blue, 2036 bp; yellow, 1636 bp; green, 1018 bp; red, 506 bp). PCR products were digested with *Hae* III and duplicate clones were eliminated. Unique clones were rescued by transformation of *E. coli* and reverified for an interaction with Varicose.

